University of Cape Town

Faculty of Engineering and the Built Environment

Influence of Mix Design Parameters on Restrained Shrinkage Cracking in Non-Structural Concrete Patch Repair Mortars

Philemon Arito

Supervisors

Prof. Hans Beushausen

Emeritus Prof. Mark Alexander

Thesis Presented for the Degree of

DOCTOR OF PHILOSOPHY

in the Department of Civil Engineering

UNIVERSITY OF CAPE TOWN

January 2018

Declaration

I, Philemon Abuti Arito, hereby declare that this Thesis is my own, unaided work. All the work in this document, save for that which is properly acknowledged, is my own. It is being submitted for the degree of DOCTOR OF PHILOSOPHY at the University of Cape Town. It has not been submitted before for any degree or examination in any other University.

Signed by candidate

Signed: Signature Removed

Date: 29^{th} January 2018

Abstract

There is a dearth of clear and consistent information on the effects of mix design parameters, and their corresponding interactions, on restrained shrinkage cracking in non-structural concrete patch repair mortars (PRMs). This dearth of information makes the design and development of PRMs with improved resistance to cracking challenging. The problem is further compounded by the fact that the existing code of practice for concrete repair - the EN 1504-3:2005 - specifies many material properties such as chloride ion content, compressive strength, bond strength, skid resistance and capillary absorption. Some of these material properties, such as skid resistance and chloride ion content, are not relevant to cracking. Also, empirical analytical models for predicting stresses and the age at cracking in PRMs need improvement to accommodate recent developments in materials such as admixtures and additives. Accurate prediction models help design engineers make informed choices during the selection of PRMs.

The principal objective of this study was to generate new knowledge that would inform the design of non-structural PRMs and the development of performance requirements for these PRMs. This was accomplished through an investigation into the influence of multiple mix design parameters and crack-determining material properties on restrained shrinkage cracking, involving a critical review of literature and a comprehensive laboratory experimental programme. The experimental work was organised into two phases. Phase one entailed an investigation into the effect of water content, binder content, binder type, curing type, shrinkage reducing admixture (SRA) dosage, polymer type and polymer content on cracking. A 2^5 full factorial experiment approach with three replicates was used in this phase. 32 mixes were studied. The sensitivity of cracking to the listed mix design parameters was determined with respect to the age at cracking in ring specimens made in accordance with ASTM C 1581. A trend analysis of the investigated mix design parameters and cracking was also done.

The trends identified in phase one informed the development of a reference mix in phase two. The reference mix was further modified to improve its cracking resistance using the information gleaned from a trend analysis of the test results

from phase one. The modification of the reference mix comprised: the adjustment of water- and binder contents and the addition of two redispersible polymers - ethylene vinyl acetate (EVA) and styrene acrylate (SA) - at polymer contents of 10%, 15% and 20% by mass of binder. Eight mixes were investigated. The material properties investigated in phase two comprised: flow, compressive and direct tensile strength, static modulus of elasticity in compression, drying shrinkage, tensile relaxation, age at cracking and durability indexes. Mixes in this study were made in accordance with the EN 1504-3:2005 performance requirements for non-structural PRMs. The test results were also used to evaluate the accuracy and adequacy of an existing deterministic empirical analytical model to predict tensile stresses and the age at cracking in non-structural PRMs.

Cracking in non-structural PRMs was observed to be sensitive to the investigated mix design parameters in the following order of decreasing sensitivity: SRA dosage, binder content, binder type, curing method and water content. The experimental work showed that a delay in cracking could be achieved by: increasing the SRA dosage, reducing the binder content, using 100% PC instead of 50/50 PC/GGBS, curing using a combination of superabsorbent polymers (SAPs) and wet hessian and reducing water content. The modification of the PRM mixes using ethylene vinyl acetate (EVA) and styrene acrylate (SA) polymers resulted in the following effects: an increase in flow, a reduction in compressive and direct tensile strength, a reduction in elastic modulus, an increase in drying shrinkage, a delay in cracking, a reduction in surface crack widths, an increase in tensile relaxation and a reduction in water sorptivity index (WSI). The magnitude of the effects of polymer-modification increased with an increase in polymer content. Also, an analysis of the interrelationships between cracking and the investigated crack-determining material properties challenged the common misconception in literature on the contribution of strength (direct tensile and compressive), elastic modulus and drying shrinkage to cracking. Specifically, the cracking resistance of the non-structural PRMs under investigation can be improved by reducing their strength (direct tensile and compressive) and elastic modulus.

A critical analysis of the performance requirements for non-structural PRMs in EN 1504-3:2005 led to the conclusion that adherence to the specifications in this code might not produce non-structural PRMs with an improved resistance to cracking in service. To ensure crack-free or crack resistant PRMs in service, the existing performance requirements should be revised and a new set of requirements more relevant to cracking developed. The EN 1504-3:2005 ought to include performance

requirements for crack-determining material properties such as tensile strength, elastic modulus, tensile relaxation and shrinkage strains. To ensure durability in PRMs in service, the resistivity of the PRMs and their transport properties ought to be specified. The code also ought to recommend the use of more robust standard test procedures such as the ring test and avoid the use of visual inspection to assess the coefficient of thermal expansion.

The predicted age at cracking using an existing empirical deterministic analytical model yielded mixed results. The predicted age at cracking in PRM mixes without polymers was higher than the actual age at cracking by a factor that ranged between 1.33 and 2.15. The predicted age at cracking in polymer-modified mixes was lower than the actual age at cracking by a factor that ranged between 0.75 and 0.98. Also, it was observed that the existing empirical analytical model was not sensitive to the changes in mix design parameters. The existing model also could not quantify the relative contribution of crack-determining material properties to cracking. From the predicted results, it was concluded that the accuracy of the existing empirical analytical model in predicting cracking, especially in the mixes without polymers, was poor.

To overcome the challenges of the existing empirical model, two deterministic empirical analytical models were proposed to predict tensile stresses and the age at cracking in mixes with and without polymers. The proposed models were an improvement of the existing model and were of the following general form - $\sigma = \mu \times E(t)^a \times (1 - \frac{\varphi\ (t)}{100})^b \times \varepsilon\ (t)^c$. The exponents a, b and c in the proposed model were determined using results from experiments. The proposed model was able to capture the relative contribution of crack-determining material properties to cracking. Also, from the proposed model, it was observed that tensile relaxation and shrinkage have a significant contribution to cracking in comparison to the elastic modulus. The extent to which tensile relaxation and shrinkage affect cracking, however, depends on the type of mix - i.e., whether it was modified with polymers or not. Strains due to shrinkage had the greatest contribution to the cracking performance in specimens cast without polymer. However, tensile relaxation had the greatest contribution to cracking in polymer-modified mixes. To improve the accuracy and sensitivity of the proposed model, it was recommended that the real-time development of tensile stresses within the PRMs ought to be monitored in future studies.

Acknowledgements

An undertaking of this magnitude cannot take place successfully with the unilateral efforts of one individual. Thus, I would like to acknowledge the following:
The Almighty God, for His guidance, sustenance and never-ending mercies and Grace throughout the entire duration of my research at the University of Cape Town.
My supervisors: Prof. Hans Beushausen and Emeritus Prof. Mark Gavin Alexander for their support, guidance and constructive criticisms while undertaking this research.
I would also wish to acknowledge with gratitude the following for financial support and materials for this research: The Cement and Concrete Institute, The National Research Foundation (NRF), Chryso SA, PPC, AfriSam, Sika (SA) Pty Ltd., SNF Floerger (France), The Concrete Manufacturers Association, The Tertiary Education Support Programme (TESP) of ESKOM, the Water Research Commission (WRC), the University of Cape Town (in the form of a Research Associateship award) and The Carnegie Corporation of New York.
I would also like to express my appreciation to my family members - Mrs Cecilia Arito, Mr Timothy Arito, Mrs Ruth Arito, Mr Hosea Arito, Mr. Ezekiel Arito, Ms Bilhah Arito and Mr Samuel Arito for their prayers, sacrifice and support throughout the duration of my studies. I would also like to thank Ms Beryl Onyango for being the ever-constant and caring friend in times of need. The many FaceTime calls, chats and visits to Cape Town gave me the strength to soldier on in good and bad times. I would also like to thank my adopted family in Cape Town - the Abutos, the Bandas, the Nyamwanges, Karen, Joshua, Albert, Billy, Joan, Lydia, Terry, Robert, Sandra, Janet and Prof. Himonga for the wonderful moments we spent encouraging each other and engaging in intellectually and spiritually stimulating talks. The moments we shared together during fellowship and 'swallowship' have been engraved in my heart. I also like to take this opportunity to thank the boys - Richard, Simba, Bryan, Mkhonzeni, Armstrong, Prosper and Robin for the special moments we spent together in the form of chats, debates, watching and playing soccer and other social gatherings. You made my stay in Cape Town enjoyable.
I would also like to thank Prof. Billy Boshoff and Mr Stefan from Stellenbosch University for granting me an opportunity to use the facilities at their laboratory. I would like to thank Dr. Mike Otieno for his constructive criticisms and

critique regarding this thesis. I also wish to thank my research colleagues within the Department of Civil Engineering - especially Messrs. Kabani Matongo, John Okedi, Philbert Habimana, Brian Abala and Nosakhare Enoma - the laboratory technicians and personnel - especially Messrs. Charles May, Christopher Caesar, Elvino Witbooi, Nooredien Hassen, Taahir Mukaddam - and non-academic staff within the Department of Civil Engineering for their assistance or otherwise. May God bless you all.

Contents

List of Tables

List of Figures

Abbreviations

a/b	Aggregate:binder ratio
ACI	American Concrete Institute
ASR	Alkali Silica Reaction
Avg.	Average
BRE	Building Research Establishment (UK)
C&CI	Cement and Concrete Institute
CBD	Compacted Bulk Density
CCI	Chloride Conductivity Index
CSF	Condensed Silica Fume
CSH	Calcium Silicate Hydrate
CTE	Coefficient of Thermal Expansion
DI	Durability Index
EVA	Ethylene Vinyl Acetate
F.M	Fineness Modulus
FA	Fly Ash
FHWA	Federal Highway Administration (USA)
Fig.	Figure
GGBS	Ground Granulated Blastfurnace Slag
GNP	Gross National Product
HCP	Hardened Cement Paste
ICRI	International Concrete Repair Institute
ITZ	Interfacial Transition Zone
LWA	lightweight Aggregates
n/a	Not Applicable

NaOH	Sodium Hydroxide
OPC	Ordinary Portland Cement
OPI	Oxygen Permeability Index
PMM	Polymer Modified Mix or Polymer Modified Mortar
PRM	Patch Repair Mortar
RC	Reinforced Concrete
RH	Relative Humidity
SA	Styrene Acrylate
SABS	South African Bureau of Standards
SANS	South African National Standards
SAP	Super Absorbent Polymer
SA:V	Surface are:volume ratio
SCM	Supplementary Cementitious Material
SF	Silica Fume
SLWA	Saturated Lightweight Aggregates
SP	Superplasticiser
SRA	Shrinkage Reducing Admixture
UCT	University of Cape Town
vs.	versus
w/b	Water-to-binder ratio or water:binder ratio
WSI	Water Sorptivity Index

Symbols

σ	Stress	(MPa)
μ	Degree of restraint	(no unit)
ψ	Tensile relaxation	(%)
E	Elastic modulus	(MPa)
ε	Shrinkage strain	(microstrains)

List of peer-reviewed publications

The following peer-reviewed articles have been published from this study.

i. Arito, P.A., Beushausen, H and Alexander, M.G. (2016). Barriers to the realisation of effectiveness in the cracking performance of concrete patch repair mortars in service. Proceedings of the fib symposium in Cape Town, 21^{st} - 23^{rd} November 2016. (Article in press, accepted for publication).

ii. Arito, P.A., Beushausen, H., and Alexander, M.G. (2016). An experimental investigation into the effects of water and binder-related parameters on restrained shrinkage cracking in concrete patch repair mortars. Concrete Solutions, Taylor and Francis, Pp. 247-252.

iii. Ngassam, I.L.T., Arito, P., and Beushausen, H. (2016). Rethinking the formulation of (patch) repair mortars. 2^{nd} International Conference on Advances in Cement and Concrete Technology in Africa, Schmidt and Msinjili (Eds), BAM Federal Institute for Materials Research and Testing, Pp. 517-524.

iv. Arito, P.A., Beushausen, H., and Alexander, M.G. (2016). Towards improved cracking resistance in concrete patch repair mortars. International Conference on Concrete Repair, Rehabilitation and Retrofitting IV - Dehn et al. (Eds), Taylor and Francis Group, London, Pp. 657-662.

"Our great future progress in Science may lie in the hands of men who are willing and able to ignore the artificial classifications which we have erected, men who will readily criss-cross these fields in the pursuit of an idea."

Melvyn Calvin, Nobel Laureate in Chemistry in 1963

Chapter 1

INTRODUCTION

This chapter contains the introduction and background to the study and the study problem. The research objectives, significance, hypothesis, key questions, scope and limitations and the conceptual framework are discussed.

1.1 General introduction

Concrete is the most preferred construction material worldwide (Acker and Ulm, 2001; Baldwin and King, 2003; Nehdi and Sumner, 2002). It is the material of choice in most modern-day buildings, bridges, dams, pavements and other components of infrastructure. Abdelkader et al. (2010) attributes the success of concrete as a construction material and its preference over other construction materials to its versatility, good structural properties, ease of manufacturing, inherent durability and relatively low production costs. While most concrete structures provide satisfactory performance over an acceptably long service life, it is common knowledge that the concrete and the structures themselves deteriorate during their service life. This deterioration may result in a reduction in service life. Thus, unless the causes of deterioration are identified correctly and appropriate interventions are made properly and in good time, many concrete structures will continue to deteriorate and fail to realise their design service life.

The protection, repair and maintenance of aging infrastructure and deteriorating concrete structures is an economically important and scientifically interesting field (Morgan, 1996; Raupach, 2008). This is because many concrete structures worldwide are either approaching the end of their service life or deteriorating rapidly and need periodic repairs (Ghezal and Assaf, 2014; Masuku et al., 2008; Naderi et al., 1986; Nehdi and Sumner, 2002). The premature failure and poor performance of repairs in service in some repaired structures is a worldwide problem (Al-Ostaz et al., 2010; Banthia and Gupta, 2009; Bissonnette et al., 2008; Brandt, 2009; Concrete-Society, 2003b; Luković, 2016; Matthews, 2007; Matthews

and Morlidge, 2008; Radlińska and Weiss, 2012; Tilly and Jacobs, 2007; Vaysburd and Emmons, 2000).

The principal objective of investing in the repair of structures is to restore their performance during their service life (Baldwin and King, 2003; Luković, 2016; Vaysburd et al., 2008). Nevertheless, the choice of an appropriate repair method is a complex process that must consider many factors such as: the history of the structure and its importance, the availability of manpower and repair materials, the desired service life, the cost of the repair and the compatibility between the repair materials and the underlying concrete substrate. The effectiveness and appropriateness of a repair refers to its ability to realise its purpose while in service. The need for durable and effective repairs has facilitated the development of many repair methods that vary from one structure to another depending on the extent and type of deterioration, the specific condition of the structure (Beushausen and Alexander, 2009), the readiness with which the technique can be executed and the exposure environment. Common concrete repair methods comprise bonded overlays and electrochemical repair methods among others. The bonded overlay is the most economical and commonly used repair method. It involves the removal of a layer of surface concrete from a concrete substrate and its subsequent replacement with a layer of fresh concrete or cementitious material - the overlay. Despite being a common repair method, bonded overlays often fail prematurely because of their tendency to crack and/or debond.

The differential shrinkage between a bonded overlay and the concrete substrate affects its performance in service (Bernard and Brühwiler, 2002; Beushausen and Alexander, 2009,0; Fowler, 2011; Ghezal and Assaf, 2014; Masuku et al., 2008). Differential shrinkage deformations generate tensile stresses within an overlay. Cracking and/or debonding of an overlay from its substrate occurs when the developed tensile stresses exceed the tensile strength of the overlay (Amba et al., 2010; Baluch et al., 2002; Beushausen and Alexander, 2006; Bissonnette et al., 1999; Denarié et al., 2011; Mauroux et al., 2012). Cracking in bonded overlays can be reduced considerably if an overlay is engineered such that it has sufficient strain capacity and tensile relaxation to counteract the effects of the tensile stresses that result from differential shrinkage.

Cracking in overlays has initiated extensive scientific research into: the causes and mechanisms of overlay failure, durability, crack control and mitigation methods, cracking mechanics, the interaction between repair materials and the concrete substrate and analytical and numerical modelling. Previous and on-going research has facilitated the development of non-standard test methods (BRE-DME-D62, 2003) and the new materials. Research on bonded overlays has also facilitated the modification of the properties of repair materials through nanotechnology and new

admixtures and additives (Raupach, 2008). Several researchers have developed innovative repair solutions such as: electrodeposition (Otsuki and Ryu, 2001), engineered cementitious composites (Boshoff and van Zijl, 2007; Zhou et al., 2008), rubberised aggregates (Ho et al., 2008), expanding agents (Pistolesi et al., 2008), polymer-modified and epoxy-modified mortars (Bhutta et al., 2008; Kardon, 1997; Ohama, 1995) and internal curing agents (Beushausen and Gillmer, 2014).
Past research has also informed remarkable developments in admixtures and additives. These developments have resulted in a paradigm shift in the way concrete is designed, produced, handled and placed as well as its performance in service. Whereas modern research has taken cognisance of these developments and subsequently investigated their individual effects on the properties of cementitious materials, a holistic investigation into the combined effect these developments on cracking in patch repair mortars (abbreviated as PRMs hereafter) has not been reported. There exists a dearth of information on how the developments in admixtures and additives can be integrated simultaneously to inform the development of PRMs that are durable and with an improved crack resistance.

1.2 Background of study

The premature deterioration of repaired structures and their associated repairs has continued to raise concerns about the functionality and safety of the aging infrastructure globally. Repair failure analysis shows that repair materials are underperforming despite significant advancements in the understanding of various chemical and physical phenomena responsible for their failure (Arito et al., 2016b; Bagheri and Hashemi, 2006; Ghezal and Assaf, 2014; Tilly and Jacobs, 2007; Vaysburd et al., 2008). A study on the performance of concrete repair materials in 215 case histories in the UK by the Building Research Establishment (BRE), for example, reports that only 50% of the repair projects are successful (Vaysburd et al., 2008). Tilly (2006), Matthews (2007), Tilly and Jacobs (2007) and Matthews and Morlidge (2008) - while studying 230 repair cases in Europe - report that 20% of the repairs under study failed within 5 years, 55% failed within 10 years and 90% failed within 25 years of service. Cracking and debonding were identified as the most common mechanism of repair failure in the reported studies. Tilly and Jacobs (2007) further report that cracking was responsible for 30% of the failure in the patch repairs under investigation. Luković (2016) also reports that the failure of repairs in The Netherlands follows trends that are similar to those observed in the greater Europe region. The premature failure of repairs has also been reported by the US Army Corp of Engineers and other organisations

and researchers (Luković, 2016; MDoT, 1996; Radlińska and Weiss, 2012; Tilly and Jacobs, 2007; Vaysburd et al., 2008).
The failure of most repair materials and systems in service has been attributed to incorrect diagnosis of the original cause of deterioration of the structure, incorrect and/or inappropriate design of the intervention works, inappropriate specification, choice and selection of materials, environmental influences, curing procedures or the lack thereof, time-dependent material properties and generally poor workmanship (Beushausen and Alexander, 2009; Concrete-Society, 2003b; Luković, 2016; Matthews, 2007; Matthews and Morlidge, 2008; Tilly, 2006; Tilly and Jacobs, 2007; Vaysburd et al., 2008). Deterioration impacts the functionality of concrete structures negatively. It also results in massive socio-economic losses and marginal returns on investments. The spalling of large pieces of deteriorated concrete in elevated structures could cause accidents, injuries and/or death. The partial or prolonged closure of structures of national importance such as bridges, nuclear power plants, wharfs, harbours and airports during repairs could result in financial losses and reduction in national revenue. It is evident, from the negative effects of deterioration, that there is an urgent need to design, develop and adopt concrete repair strategies and products that are durable, economical and technically sound. Concrete patch repair is one such technique.

1.3 Problem statement

While it is evident that a large amount of resources and research effort has been expended into addressing the problem of cement-based non-structural patch repair mortars (referred to as PRMs hereafter) failure through cracking - as discussed in the previous sections - the positive results of these efforts are yet to be seen in repaired concrete structures in service. There is a need, therefore, to develop strategies, products and systems that would help reconcile the mismatch between the rate at which PRMs in service are deteriorating prematurely and the amount of resources spent addressing this plight. An informed manipulation of multiple mix design constituents (referred to as mix design parameters hereafter) simultaneously during the design of PRM mixes, for example, could be one such a strategy.
It has been posited that an informed manipulation of mix design parameters simultaneously can help to engineer the crack-determining material properties of PRMs for optimal performance with respect to cracking resistance. However, the extent to which the veracity of this claim can be validated has not yet been determined. The design and development of PRMs that are effective with respect to cracking resistance entails the multi-objective optimisation of competing and interacting mix design parameters and material properties (Arito et al., 2016a).

The fact that several desirable crack-determining material properties cannot be achieved simultaneously presents a challenge in determining the extent to which the above proposition can be validated. A study on the influence of mix design parameters on cracking and crack-determining material properties, the nature of the interactions that exist among them and the relative levels of sensitivity of cracking to these parameters is, thus, necessary. Furthermore, a review of literature reveals that there is a dearth of clear and consistent information on the nature of the interrelationships that exist among mix design parameters and crack-determining material properties (Arito et al., 2016c). Thus, there is a need for an in-depth study on the nature of these interrelationships. Such a study has the potential to unlock the barriers to achieving durable and effective PRMs in service by providing crucial knowledge to manufacturers of repair materials and design engineers involved in repair projects.

Currently, the design of PRMs is guided by the EN 1504 series of standards. Prior to the introduction of these standards, there were no readily available, clear, coordinated and well-established standard procedures that would guide the design of crack resistant PRMs. Mangat and Limbachiya (1997), BRE-DME-D62 (2003), Mangat and O'Flaherty (2000), Beushausen (2005) and Mallat and Alliche (2006) specifically report that the design of PRMs over the past was crude and relied heavily on the experience of specialist contractors and engineering judgement which was either done on an ad hoc basis or informed by material properties such as compressive strength, bond strength, early-age plastic shrinkage/expansion and past experience. Whereas the mentioned material properties are important; it is postulated, based on reports on the widespread failure of PRMs in past repairs, that their continued use and over-reliance by specialist contractors might have contributed to their widespread failure in service in the past. Existing design recommendations do not incorporate new construction materials - such as admixtures and additives - which are increasingly gaining importance in concrete repair. There is a need, therefore, to reconsider and challenge the previous and current concepts, approaches and performance requirements used to design PRMs.

A careful analysis of the EN 1504-3:2005, shows that strict compliance to its performance specifications would not necessarily result in the realisation of cracking resistance in PRMs (Arito et al., 2016b). The EN 1504, though published recently, does not deviate drastically from the predominating paradigm of specifying material properties (such as skid resistance and compressive strength) that do not have a direct correlation with durability and cracking resistance in PRMs. The EN 1504-3:2005, therefore, should specify material properties that are more relevant and critical to the cracking resistance of PRMs in service. These material properties comprise elastic modulus, thermal and hygral deformations, creep and

relaxation.

There is also a need to investigate and improve an existing deterministic empirical analytical model - $\sigma = \mu \times E\ (t) \times (1 - \frac{\varphi\ (t)}{100}) \times \varepsilon\ (t)$ - that has been frequently used to predict stresses due to restrained shrinkage deformations and the time to crack. This model was developed for cement-based materials cast using conventional materials - i.e., cement, water and normal aggregates. Recent developments in admixtures and additives, however, necessitates the need to investigate and consequently improve the accuracy of this model in predicting stresses and the time to crack in modern PRM mixes that are cast with new admixtures. It can be postulated that admixtures and other recently developed materials affect the crack-determining material properties that serve as input parameters to the analytical model significantly to such an extent that they will affect its accuracy. An accurate analytical model would help design engineers and repair contractors to accurately predict stresses and the age at cracking and to inform the selection of appropriate PRMs.

From the above discussions and illustrations, it is evident that a holistic and fundamental research into the salient interrelationships that exist among mix design parameters, crack-determining material properties and cracking in PRMs is necessary. Also, there is a need to critically evaluate the current performance requirements for PRMs with respect to cracking resistance. Finally, the accuracy of an existing deterministic empirical analytical model (referred to as existing empirical model hereafter) that has been used to predict stresses and the age at cracking in PRMs cast using recent admixtures needs to be investigated and improved.

1.4 Research objectives

The principal objective of this study was to generate new knowledge that would inform the design and development of non-structural PRMs and the future development of performance requirements for these PRMs through an investigation into the influence of mix design parameters on restrained shrinkage cracking. This study also aimed to achieve the following sub-objectives:

i. To investigate the influence of mix design parameters on crack-determining material properties and cracking in non-structural PRMs.

ii. To establish the relative sensitivity of cracking in non-structural PRMs to mix design parameters.

iii. To evaluate the contribution of the EN 1504-3:2005 performance specifications towards the realisation of non-structural PRMs with an improved resistance to cracking in service.

iv. To improve the accuracy of an existing deterministic empirical analytical model to predict the age at cracking in ethylene vinyl acetate and styrene acrylate polymer-modified mortars.

1.5 Key research questions

The key questions that this study intends to address are:

i. What defines a good non-structural PRM? Is a 'good non-structural PRM' an omnibus term that applies to a specific 'one-fits-it-all' repair product that can be used in all patch repair scenarios or is it based on a material that meets specific predefined performance requirements?

ii. What are the key performance requirements for non-structural PRMs that ought to be considered to render them effective with respect to resistance to cracking?

iii. Must all non-structural PRMs meet the performance requirements specified in the BS EN 1504-3:2005 to be deemed effective?

iv. Does compliance to the performance requirements specified in the EN 1504-3:2005 for non-structural PRMs provide effectiveness with respect to resistance to cracking? If not, how can these performance requirements be modified and/or improved to provide effectiveness with respect to resistance to cracking?

v. Can recent developments in admixtures assist in improving the performance of non-structural PRMs with respect to resistance to cracking in service? If so, how and to what extent can these developments improve the resistance to cracking in PRMs?

vi. What is the relative sensitivity of cracking in non-structural PRMs to mix design parameters? What criteria and methods, if any, could be employed to establish the levels of sensitivity?

vii. Is it possible to develop a crack-resistant non-structural PRM?

viii. Is the existing empirical deterministic analytical model accurate enough to predict stresses and the age at cracking in non-structural PRMs made using ethylene vinyl acetate and styrene acrylate redispersible polymers? If yes, how accurate is it? If no, how can it be improved?

1.6 Conceptual research framework

Cracking in PRMs results from the tensile stresses that develop from restrained volume changes (ACI224, 2003; Beushausen and Alexander, 2007; Beushausen et al., 2012; Bissonnette and Pigeon, 1995; Byard et al., 2012; Carlswärd, 2006; Concrete-Society, 2003b; He and Li, 2005; ICRI, 2003; Mauroux et al., 2012; Nguyen et al., 2012; Rixom and Mailvaganam, 1999; Taylor, 2014). To address cracking, a proper understanding of the principal causes of deformations and volume changes in cement-based materials and its influencing factors is necessary. In addition, a proper understanding of the mechanics of cement-based materials (e.g., elasticity, fracture mechanics and viscoelasticity) would assist in understanding their time-dependent stress-strain relationships.

Cement-based materials such as PRMs are viscoelastic. The relationship between tensile stresses and restrained deformation is time-dependent and can be described by the following empirical deterministic analytical model (Beushausen and Bester, 2016; Beushausen and Chilwesa, 2013; Beushausen and Gillmer, 2014; Byard et al., 2012; Dittmer and Beushausen, 2014; Ngassam et al., 2016):

$$\sigma\ (t) = \mu \times E\ (t) \times (1 - \frac{\varphi\ (t)}{100}) \times \varepsilon\ (t) \tag{1.1}$$

where: $\sigma(t)$ refers to stress at time t; μ refers to the degree of restraint; E(t) refers to the modulus of elasticity at time t; $\varphi\ (t)$ refers to tensile relaxation at time t and $\varepsilon\ (t)$ refers to the free strain at time t. From Equation 1.1, it is evident that the magnitude of induced tensile stress (σ) depends on the degree of restraint (μ) and two time-dependent material properties, namely: strain (ε) and the stiffness of the material (κ). The stiffness of the material is further dependent on the modulus of elasticity (E), creep and/or relaxation (φ). Cracks result when the tensile stresses developed within the PRM exceed its tensile strength. Stress relief mechanisms such as tensile relaxation, however, reduce the magnitude of the induced tensile stresses - consequently delaying the time to cracking (Atrushi, 2003; Baluch et al., 2002; Beushausen and Bester, 2016; Beushausen and Chilwesa, 2013; Byard et al., 2012; Dittmer and Beushausen, 2014; Ghezal and Assaf, 2014; Hotta and Takiguchi, 1995; Luković, 2016; Ngassam et al., 2016; Nossoni and Harichandran, 2010; Radlińska and Weiss, 2012; Wittmann, 2008; Yuan et al., 2003; Zhang et al., 2014; Zhou et al., 2014). A diagrammatic representation of the relationship between the state of stress in a PRM and the time taken to crack is shown in Figure 1.1.

Cracking in PRMs can be minimised through the manipulation of their time-dependent material properties in a manner that constantly ensures that induced tensile stresses are lower than the tensile strength of the PRMs at any given

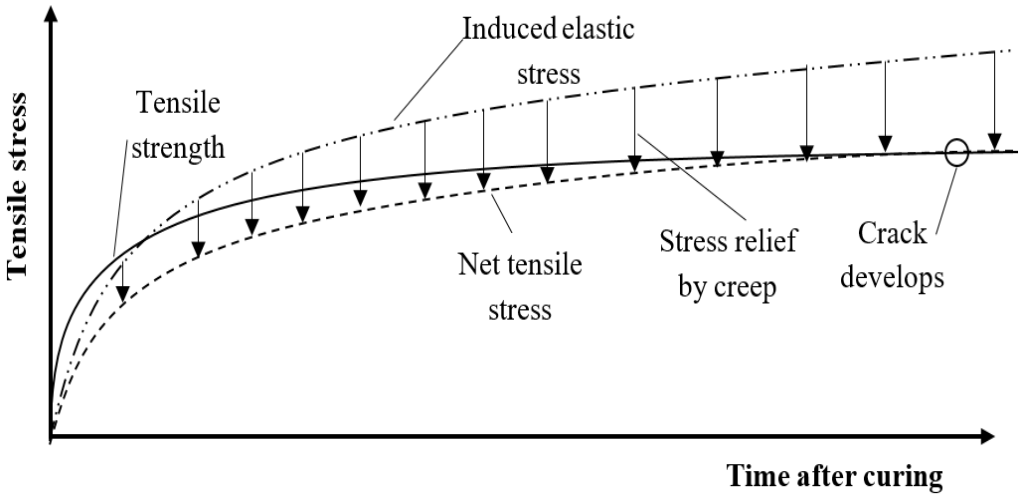

FIGURE 1.1: Schematic pattern of crack development under tensile stresses due to restrained shrinkage - adapted from Neville (1995)

time. To achieve this, the following key material properties could be manipulated: reducing the modulus of elasticity, increasing the tensile relaxation/creep, increasing the tensile strain capacity, minimising the amount of strain induced in the PRM (mainly by reducing thermal and shrinkage-induced strains), increasing the tensile strength, and by reducing the degree of restraint (Atrushi, 2003; Bagheri and Hashemi, 2006; Beushausen and Chilwesa, 2013; Bissonnette and Pigeon, 1995; Carlswärd, 2006; He and Li, 2005; Mallows, 1985; Nguyen et al., 2010; Taylor, 2014; Turatsinze et al., 2005; Vaysburd and Emmons, 2000; Yuan et al., 2003). These crack-determining properties, except for the tensile strain capacity at failure, depend on mix design parameters. An informed selection of mix design parameters, therefore, would assist in minimising, or eliminating cracking in PRMs.

1.7 Research hypothesis

This study hypothesises that cracking in PRMs can be reduced significantly through an informed mix design approach that optimises mix design parameters and crack-determining material properties simultaneously.

1.8 Research significance

This study will:

i. Provide a platform and a rationale for the design and development of PRMs that exhibit an improved resistance to cracking.

ii. Provide a methodology that could be used to optimise mix design parameters simultaneously with the intention of improving their resistance to cracking.

Further to these, this study will contribute to knowledge in the following ways:

i. Generate information regarding the influence of mix design parameters, crack-determining material properties, and their corresponding interactions, on cracking in PRMs.

ii. Generate information regarding the relative sensitivity of cracking in PRMs to mix design parameters, and their corresponding interactions.

iii. Generate information that would inform the development of new and/or the modification of the existing performance requirements for PRMs with an improved resistance to cracking.

iv. Generate information that would help in improving the accuracy of an existing empirical deterministic analytical model to predict stresses and the age at cracking in PRM mixes cast using ethylene vinyl acetate and styrene acrylate redispersible polymers.

1.9 Scope and limitations of study

This study was limited to:

i. Cement-based non-structural PRM specimens exposed to a controlled laboratory environment.

ii. Experimental investigation of restrained shrinkage in ring specimens made in accordance with ASTM-C1581.

iii. Laboratory-made non-structural PRMs for application on horizontal surfaces in accordance with Principle 3 and Method 3.1 as specified in the EN 1504 series of standards.

1.10 Thesis layout

This thesis comprises six chapters, a list of references and an appendix. A summary of the content in each chapter is hereby provided:

i. Chapter 1 contains the general introduction and background to the research problem. The research problem statement, objectives, key research questions, conceptual research framework, research hypothesis, significance, scope and limitations of this study are presented.

ii. Chapter 2 provides additional background information to the research problem through a critical review of literature on deformation and volume changes in cement-based materials. This chapter also discusses the microstructure of the cement paste and its influence on paste properties, the mechanics of cement-based materials and cracking in concrete and cement-based materials are discussed. The chapter ends with discussions on the effects of cracking in cement-based materials and commonly used crack control and remediation techniques.

iii. Chapter 3 is a critical review of literature that pertains to the actual research problem. This chapter introduces the concept of concrete repair. It also covers the factors that govern the effectiveness in the performance of PRMs and their performance requirements. The influence of various mix design parameters on cracking in PRMs is presented.

iv. Chapter 4 provides information pertaining to the experimental work. The testing philosophy, the experimental design method and the experimental variables are presented. The test methods and standards that were used during the testing have also been presented.

v. Chapter 5 presents the experimental results and an analysis and discussion of the test results.

vi. Chapter 6 presents the conclusions that have been arrived at during this study and the recommendations for further research work.

vii. The final portions of this thesis comprises a list of references that were reviewed in this study. The test materials, test results, test standards and the standard test methods followed during this study are contained in the appendix.

Chapter 2

CEMENTITIOUS MATERIALS: STRUCTURE, MECHANICS OF CRACKING AND SHRINKAGE

This chapter provides a critical review of literature on cracking and shrinkage in cement-based materials. Aspects such as the microstructure of the cement paste and its influence on paste properties, shrinkage and the mechanics of cracking in cement-based materials are presented. Finally, the effects of cracking in cement-based materials and common techniques used to control and/or remediate cracking in structures are presented.

2.1 Introduction

Hardening and hardened cement-based materials - such as concrete and PRMs - are prone to time-dependent deformations. These deformations can be attributed to simultaneously operating processes, mechanisms and influences. Deformation and volume changes in cement-based materials are of considerable importance in practice because they are usually restrained. The partial or complete restraint of these movements induces tensile stresses which result in cracking. The most common causes of deformations in cement-based materials are: stress-dependent deformations/viscoelastic response (e.g., elastic strains, creep) and stress-independent/viscoelastic response (e.g., shrinkage) (Neville, 1995).

2.2 The structure of the cement paste and its influence on paste properties

Brandt (2009) defines a multiphase material as a heterogeneous medium composed of two or more materials or phases which occupy separate regions in space. A typical cement-based material, at the macroscopic level, is a multi-phase material comprising three phases: the hardened cement paste (abbreviated as HCP hereafter), the aggregate phase and an interfacial transition zone (referred to as ITZ hereafter) (Alexander and Beushausen, 2009; Bezerra et al., 2011; Brandt, 2009; Neubauer et al., 1996; Ramesh et al., 1998; Rao and Prasad, 2004,0; Xu et al., 2011). Brandt (2009) further reports that there are different types of interfaces, namely: between small grains of aggregates and cement paste, between the matrix itself and grains of coarse aggregates from various materials, between matrix and reinforcement and between similar composite materials but of different age or quality.

The HCP is a relatively rigid and strong solid of high porosity and internal surface area (Taylor, 1997). It imparts strength and cohesion. Its hygrometric instability, however, renders it susceptible to deformations. Aggregates impart bulk, rigidity and dimensional stability. The properties of an aggregate also govern other mechanical properties such as elastic modulus. The ITZ influences the elastic modulus and shrinkage. The microstructure of the ITZ is different from that of the HCP (Elsharief et al., 2003). It depends on the properties of the HCP and the aggregate phase and on the conditions of mixing, hydration, the composition of the binder, curing and ageing of the material (Brandt, 2009; Ramesh et al., 1998). Compared to the bulk paste, the ITZ has a higher porosity, a lower density and a lower content of unhydrated cement grains. The ITZ affects the elastic modulus by partially de-coupling the paste and aggregate to varying degrees, thus influencing the interaction between these two components (Alexander and Beushausen, 2009; Brandt, 2009; Neubauer et al., 1996; Ramesh et al., 1998). The ITZ further influences the transfer of stresses between the HCP and aggregate phases (Bezerra et al., 2011; Brandt, 2009).

The susceptibility of the HCP to undergo deformations can be understood from its microstructure. At the microscopic level, the HCP is predominantly made up of unreacted cement, water and a hydration product - the calcium silicate hydrate gel (abbreviated as CSH hereafter). The CSH is a precipitated colloid with a high surface area. It is made up of interlayer spaces which vary in size depending on the w/b and the degree of hydration of the cement (Diamond, 2004). The interlayer spaces within the HCP facilitate the movement of water during drying and rewetting. This movement of water results in creep, shrinkage and

swelling of the HCP. The movement of water within the pores of the HCP, and its corresponding effects on the cement paste, provides a basis for understanding the viscoelasticity of the HCP (Jennings, 2004).

2.3 Mechanics of cement-based materials

The crack behaviour of cement-based materials can be understood from their mechanical characteristics. While it can be acknowledged that the mechanical characteristics of any material is a broad term that encompasses various parameters; this section will briefly discuss the following parameters: elasticity, viscoelasticity and fracture mechanics.

2.3.1 Elasticity

Elastic modulus is the ratio between an applied uniaxial stress and the resultant axial strain within an assumed limit of proportionality. It is a measure of the stiffness of a material to an imposed stress. It is quantified in terms of an elastic modulus. There are various types of elastic moduli, namely: static modulus, dynamic modulus and flexural modulus. Details pertaining to these moduli and their corresponding measurements will not be discussed within this thesis. The stress-strain behaviour of cement-based materials is shown in Figure 2.1. It can be observed, from Figure 2.1, that the stress-strain behaviour of concrete is non-linear and complex. The strain on a concrete specimen under instantaneous loading is neither directly proportional to the applied stress nor fully recovered upon unloading. The non-linearity in behaviour under a compressive load is attributed to the non-linear stress strain responses of the paste and the ITZ, creep and plastic deformations and microcracking in the matrix under various levels of compressive stress (Alexander and Beushausen, 2009; Mehta and Monteiro, 2006; Neville, 1995; Uys, 1983; van Breugel, 1980).

The elastic properties of heterogeneous, multiphase materials such as PRMs depends on intrinsic and extrinsic factors. Intrinsic factors comprise: the mix proportions, porosity, age, strength (and related to that, the stiffness) of the paste phase, the volume fraction, type, shape, porosity and stiffness of the embedded aggregates, the properties of the cement, the characteristics of the ITZ, the density and modulus of elasticity of the principal constituents, the level of compaction of the mix and the presence of microcracks (Alexander and Beushausen, 2009; Gilbert, 1988; Mehta and Monteiro, 2006; Schutter, 2002; Taylor, 2014; Uys, 1983; Yurtdas et al., 2004). Extrinsic factors comprise: the testing conditions i.e., temperature and relative humidity at the time of test, rate of loading, size and moisture

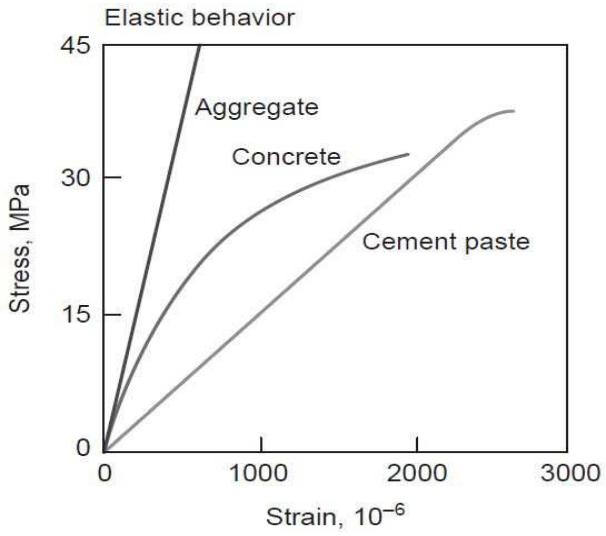

FIGURE 2.1: Typical stress-strain behaviour of cement paste, aggregate and concrete - adopted from Mehta and Monteiro (2006)

condition of specimen - (Atrushi, 2003; Gilbert, 1988; Mehta and Monteiro, 2006; Taylor, 1997; Uys, 1983). The exact nature of the relationship between each of these factors and elasticity will not be discussed. The cited references, nevertheless, can be consulted for additional information.

The elastic properties of repair materials are critical to their restrained shrinkage deformation. A review of literature on elasticity and its influence on cracking reveals that at least two distinct viewpoints exist. On the one hand, Mangat and O'Flaherty (2000) report that effective repairs are achieved when the elastic modulus of a repair material is greater than that of the substrate. This viewpoint is premised on the fact that a stiffer repair material achieves a better strain transfer to the substrate during the shrinkage and therefore reduces restrained shrinkage tension in the repair material. The second viewpoint, on the other hand, is premised on the fact that material that are more elastic experience lower induced stresses from restrained deformations; thereby prolonging their time to first cracking. It is important to note that an increase in elastic modulus, with all other factors held constant, results in an increase in induced tensile stresses and consequently an increase in the susceptibility to cracking.

2.3.2 Viscoelasticity

Cement-based materials are aging viscoelastic materials. Their mechanical properties and deformations depend on the duration of the applied load and their age at the time of loading. The one-dimensional viscoelastic behaviour of cement-based

materials can be characterised by two parameters: creep (the increase in strain with time under a constant stress) and relaxation (the decrease in stress with time under a constant strain).

2.3.2.1 Creep

Creep is the time-dependent increase in strain of a solid body under a constant sustained stress (Alexander and Beushausen, 2009; Atrushi, 2003; Brandt, 2009; Gilbert, 1988; Neville, 1995; van Breugel, 1980). It is distinct from the time-dependent strains that occur in other materials because it occurs at all stress levels and at ordinary temperatures. Under sustained loads, creep continues for an indefinite time although proceeding at a continuously diminishing rate (Uys, 1983).

Creep deformations were discovered by Hatt in 1907 (Jaufeerally, 2001) and are thought to originate from the HCP. However, van Breugel (1980) and Atrushi (2003) report that the origin of creep is not well understood. van Breugel (1980) specifically reports that there is a lack of clear understanding on whether the origin of creep can be attributed to purely mechanical, physical or chemical processes. The inability of researchers to clearly identify the specific processes - chemical, physical or mechanical - that describe the origin of creep has facilitated the emergence of diverse theories and mechanisms that have been postulated to explain it. These theories are characterised by an inherent shortcoming of their inability to account for all observed creep phenomena (Atrushi, 2003). None of these theories can explain, in a unified way, the creep behaviour of concrete under different environmental conditions and various stress states.

The predominant creep theories comprise, but are not limited to, the following (ACI209, 2005; Acker, 2004; Alexander and Beushausen, 2009; Atrushi, 2003; Brandt, 2009; Gilbert, 1988; Jaufeerally, 2001; Jennings, 2004; Mallows, 1985; Rossi et al., 2013):

i. Sliding (or shear) of the colloidal sheets in the cement gel between the layers of absorbed water (viscous flow);

ii. The expulsion and decomposition of the interlayer water within the cement gel (seepage);

iii. Elastic deformation of the aggregate and the gel crystals as viscous flow and seepage occur within the cement gel (delayed elasticity);

iv. Local fracture of the cement gel involving the breakdown (and formation) of physical bonds (microcracking);

v. Diffusion of water from areas of hindered to unhindered adsorption which reduces swelling pressure leading to a reduction in interparticle spacing;

vi. Diffusion of water from high to low pressure areas causing gradual load transfer from liquid to solid phase (thus a delayed elastic-type strain);

vii. Formation of new bonds when particles are brought into close contact for the first time;

viii. Microcracking evolution;

ix. The rearrangement of globules.

The magnitude of creep and its rate of development are influenced by the intrinsic properties of the mix and the environmental and loading conditions. Creep is affected by: moisture content, water content, aggregate properties (e.g., modulus of elasticity, grading, content, size and shape, shrinkage, porosity, petrological and mineralogical characteristics and stiffness), w/b, aggregate:paste ratio, stress/strength ratio, curing, characteristics of the cement paste binder (e.g., cement type, volume and composition), degree of honeycombing, the presence of fibres, the strength and age at the time of loading, the duration and type of loading, microcracking within the system, environmental conditions (e.g., relative humidity, drying conditions and ambient and/or curing temperature), the geometry and size of the member and the degree of hydration (Acker, 1993; Acker and Ulm, 2001; Alexander and Beushausen, 2009; Atrushi, 2003; Bissonnette and Pigeon, 1995; Brandt, 2009; Carlswärd, 2006; Gilbert, 1988; Igarashi et al., 2000a; Jennings, 2004; Mallows, 1985; Neville, 1995; Østergaard et al., 2001; Rüsch et al., 1983; Schutter, 2002; Taylor, 1997, 2014; Uys, 1983; van Breugel, 1980). Details pertaining to the extent to which each of these parameters affects creep will not be covered within this thesis; but can be consulted from the cited references.
Creep can be broadly categorised into recoverable creep and irrecoverable creep. Recoverable creep is referred to as the delayed elastic strain and is thought to be caused by the elastic aggregate acting on the viscous cement paste after the applied stress is removed (Gilbert, 1988). Most creep strain is irrecoverable and is often referred to as flow. The flow component of creep is further subdivided into rapid initial flow, which occurs in the first 24 hours after loading, and the remaining flow which develops gradually with time. The rapid initial flow is irrecoverable and highly dependent on the age at first loading. The remaining flow which occurs after the first day under load depends on the relative humidity and may be divided into a basic flow component and a drying flow component (Alexander and Beushausen, 2009; Gilbert, 1988; Rüsch et al., 1983; Taylor, 2014).

Basic flow refers to the creep experienced by a material which has previously been brought into hygral equilibrium with its environment (Alexander and Beushausen, 2009; Atrushi, 2003; Carlswärd, 2006; Rüsch et al., 1983). The predominant cause of basic flow is viewed as a property of delayed elasticity and the viscous deformations of the hydrated cement gel. Drying creep (or Pickett effect) is usually ascribed to an accelerated movement of water molecules within the pore system of the HCP caused by the external load (Atrushi, 2003; Rüsch et al., 1983; Taylor, 2014; Uys, 1983). Basic flow depends on: mix composition (aggregate type, size and quantity, strength), w/b, content of cement paste, moisture content and the age at the time of loading. Drying flow depends on the moisture content and gradient, dimensions (size and shape) of the member and the tensile stress induced in the outer part of a concrete specimen with resultant cracking (Atrushi, 2003; Gilbert, 1988; Rüsch et al., 1983; Uys, 1983).
The effects of creep can either be beneficial or detrimental. Creep, for example, imparts a degree of ductility which is desirable from the point of view of structural behaviour. It also results in a relief of stresses due to differential structural movement and restrained shrinkage, which is of importance to the behaviours of PRMs subjected to restrained deformations. Creep can be detrimental on structures by producing effects such as: increased deflections which can result in cracking, reduction in the stiffness of structural members, loss of prestress, and creep buckling of long columns (Alexander and Beushausen, 2009; Atrushi, 2003; Brandt, 2009; Carlswärd, 2006; Gilbert, 1988; Igarashi et al., 2000a; Jaufeerally, 2001; Taylor, 2014).

2.3.2.2 Relaxation

Relaxation is the gradual, time-dependent decrease in stress in a body under a sustained strain. It originates from the cement paste and contributes to the reduction in self-induced stresses. The main mechanisms of tensile relaxation, as reported by Gillmer (2012), are viscous shear and microcracking within the cement paste. Atrushi (2003), Beushausen and Alexander (2006), Alexander and Beushausen (2009), Masuku et al. (2008), Beushausen et al. (2012) and Beushausen and Chilwesa (2013), while referring to their own study and studies by other researchers, further report that tensile relaxation in concrete and other cement-based materials can reduce the initial tensile stresses levels in concrete and mortar by values as high as 50% to 67% at the age of 28 days depending on the type of material and its mix design parameters. It is, therefore, evident that stress relief - due to tensile relaxation - in restrained members would contribute to an improvement in overlay performance.

The factors that influence tensile relaxation comprise: w/b, moisture content, elastic modulus, specimen dimensions, compressive strength, creep coefficient, aggregate properties (content, size and stiffness), properties of the cement paste (e.g., paste strength), age at loading, maturity, temperature, relative humidity and the stress level above certain limits (Atrushi, 2003; Beddoe and Lippok, 1999; Beushausen and Alexander, 2006; Beushausen and Chilwesa, 2013; Beushausen et al., 2012; Denarié et al., 2011; Dittmer, 2013; Gillmer, 2012; Masuku, 2009; Masuku et al., 2008). Additional details pertaining to the extent to which each of these parameters affects tensile relaxation will not be covered within this thesis but can be obtained from the cited references.

2.3.3 Fracture mechanics

The fracture behaviour of brittle cement-based materials can be altered by manipulating their microstructure. The toughness of a brittle cementitious matrix can be increased through the incorporation of aggregates particles which act as bridges - i.e., they inhibit the separation of crack-faces by anchoring the cement matrix (Merchant et al., 2001; Wittmann, 2002). An in-depth knowledge of the mechanisms through which cracks intercept aggregates is crucial to the understanding of toughening cementitious materials. More specifically, the nature of the ITZ between an aggregate and the cement matrix affects the mechanisms through which cracks intercept aggregates.

A full-bond between an aggregate and the matrix, for example, does not increase toughness. The formation of a bridge that would hinder the separation of crack faces could result from a crack that detaches from an aggregate early. Also, bridging does not occur in relatively weak aggregates. Cracks may propagate through relatively weak aggregates consequently inhibiting bridging. Spherical aggregates - whether bonded or unbonded - do not toughen the cement matrix because they do not have 'pinning points' due to their lack of irregularity. The mechanism of crack propagation is different when no appreciable bond exists between the matrix and the aggregates. Cracks - in materials with no appreciable bond - appear to interact with inclusion-shaped holes. Thus, the crack would pass through the region of inclusion consequently creating opportunities for crack bridging. The propagation of cracks will depend on the aggregate or the crack bridge breaking through the obstructing portion of matrix. The additional energy requirement dissipates crack energy and slows it down (Merchant et al., 2001; Wittmann, 2002).

The interfacial bond between the matrix and aggregates restrains the expansion of the matrix in cement-based systems containing dimensionally stable aggregates bonded to an expansive matrix. In such systems, the aggregate is usually subjected to tensile forces while the matrix is in hoop compression around the aggregate.

These residual stresses lead to metastability such that an approaching macrocrack may release these stresses resulting in an 'active' debonding of the matrix from the aggregate. The debonding of the matrix from the aggregate could result in either of the following scenarios (Merchant et al., 2001):

i. The crack being attracted towards the aggregate. This results in an improvement in toughening due to aggregate bridging.

ii. The relaxation of the expansive matrix results in a net compression from the matrix towards the main crack faces consequently resulting in crack closure.

2.4 Mechanisms and causes of cracking in cement-based materials

A crack, in the context of the mechanics of solids, is defined as a plane two-dimensional discontinuity in a solid body with its two dimensions much larger than the third one (Brandt, 2009). Beushausen (2005) and Beushausen and Alexander (2007) report that the mechanisms of crack-formation in cement-based systems depend on their material parameters, environmental influences and the degree of restraint governed by the structural characteristics of the system. There are two hypotheses that have been posited to explain the cause of cracking. These hypotheses are premised on two distinct material properties, namely: tensile strength and tensile strain capacity. The tensile strength hypothesis is the most popular. It posits that cracking occurs when the net tensile stress in a restrained material exceeds its inherent tensile strength. The tensile strain capacity hypothesis posits that cracks form when the induced tensile strains exceed the inherent tensile strain capacity of the restrained material (Brandt, 2009; Concrete-Society, 2003a; Li et al., 2012; Radlińska and Weiss, 2012; Taylor, 2014; Uys, 1983).
The loss and/or movement of moisture within a cement-based material implies that cracks can form in the plastic or hardened state (ACI224, 2003). Other effects such as temperature variations and external loads (e.g., differential settlement, overloading) also result in cracking. The rate at which cracks develop depends on: w/b (through its influence on the porosity of the HCP thus the hygral stress), material composition and mixture proportions, the rate of heat development during hydration, shrinkage rate, stress or creep relaxation, degree of structural restraint and production procedures, relative humidity (Beddoe and Lippok, 1999; Brandt, 2009; He and Li, 2005; Uys, 1983). The tensile stresses that cause cracking in cement-based materials can be generated through shrinkage, corrosion and ASR among other causes. These tensile stress generators are discussed in the subsequent sub-sections.

2.4.1 Shrinkage in cement-based materials

Shrinkage is the time-dependent strain that a material undergoes at constant temperature without any external strains. It can also be defined as the reduction in volume of an unloaded specimen at a constant temperature (ACI209, 2005; Brandt, 2009; Rüsch et al., 1983; Uys, 1983; Wittmann, 2008). Shrinkage is attributed to the drying process that has been reported by Carlswärd (2006) as the main generator of tensile stresses that cause cracking in overlays. The most important characteristic of shrinkage - as reported by Gilbert (1988), Atrushi (2003), Alexander and Beushausen (2009) - is that it is independent of stress.
The cement paste phase is prone to shrink. The susceptibility of the paste to shrink can be attributed to the evaporation of the mixing water or the removal of the physically adsorbed water from within the layers of the CSH gel. The movement of water within the cement paste phase results in volumetric changes which, if restrained, result in the development of tensile stresses (Abbasnia et al., 2005; Banthia et al., 1996; Beddoe and Lippok, 1999; Filho et al., 2005; He and Li, 2005). The magnitude of these tensile stresses dictate the susceptibility to cracking. The magnitude and rate of shrinkage is governed by the nature of the CSH, the pore structure (size and distribution) and the nature and quantity of water associated with the paste and the amount of internal restraint (Alexander and Beushausen, 2009; Thomas and Jennings, 2003). Other factors that influence shrinkage include: the shape and dimensions of the structural element, temperature, water content, the composition of the material and the degree of hydration at the onset of initial cracking, the structure of the paste, cement composition and fineness, relative humidity of the ambient air, the content and stiffness of the aggregates (Alexander and Beushausen, 2009; Brandt, 2009; Masuku, 2009; Rüsch et al., 1983). Details regarding how each of these factors relate to shrinkage will not be discussed in this thesis but can be obtained from the cited references. Shrinkage can be categorised into: chemical (and autogenous), plastic, drying, carbonation and thermal shrinkage. These sub-categories of shrinkage are subsequently discussed.

2.4.1.1 Chemical and autogenous shrinkage

Chemical shrinkage (also known as Le Chatelier contraction or hardening shrinkage) is the volume reduction resulting from the hydration of cement and the internal consumption of water (Mechtcherine and Dudziak, 2011; Soliman and Nehdi, 2013). It is an intrinsic property of portland cement, corresponding to a reduction of 6 ml per 100g of reacted cement, or approximately 7 to 10% of the volume of the hydrating portland cement products as shown in Figure 2.2 (Bouasker et al., 2008; Gagné et al., 1999; Henkensiefken et al., 2009; Jensen and Hansen, 2001a,0;

Mechtcherine and Dudziak, 2011; van Breugel, 2001). Mechtcherine and Dudziak (2011) report that chemical shrinkage in cement-based materials containing silica fume (referred to as SF hereafter) equals 22 ml per 100g of SF that has reacted.

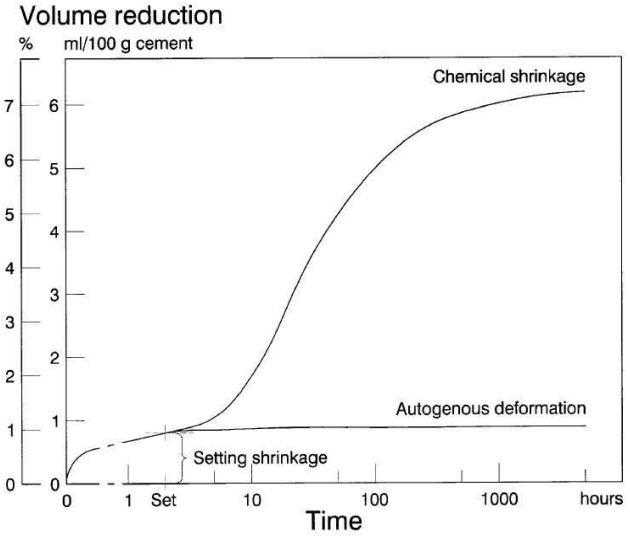

FIGURE 2.2: Schematic development of volume changes that take place in a sealed cement paste system - adopted from Jensen and Hansen (2001a)

The formation of hydration products that have lesser volume than the sum of the volumes of the original components causes the cement-plus-water system to contract as hydration proceeds. Chemical shrinkage does not have a significant detrimental effect on the micro- and macrostructure of cement-based materials even though it plays a significant role in their deformation. The reason behind the absence of significant detrimental effects of chemical shrinkage, according to Gillmer (2012), can be attributed to the fact that it occurs when a material is in the plastic state. Gillmer (2012), while referring to other studies, reports that most chemical shrinkage translates into internal voids within the HCP.

The internal consumption of water during hydration, called self-desiccation, can lead to autogenous shrinkage (Alexander and Beushausen, 2009; Atrushi, 2003; Bentz, 2008; Brandt, 2009; Craeye et al., 2011; Kovler and Jensen, 2005). Autogenous shrinkage is a macroscopic reduction in length under constant temperature and without any moisture migration to or from the cementitious material (Byard et al., 2012; Li et al., 2012; Mechtcherine and Dudziak, 2011; Tazawa and Miyazawa, 1995; Tazawa et al., 1995). It is mainly driven by chemical shrinkage, with the two i.e., autogenous and chemical shrinkage - being roughly equal when a material is in a fluid state (Byard et al., 2012; Mechtcherine and Dudziak, 2011; Soliman and Nehdi, 2013). It is critical in high performance concretes with low

w/b and develops rapidly after setting; with 40% of this shrinkage taking place within the first 24 hours after casting. Autogenous shrinkage results in a high risk of early-age cracking because it takes place when the tensile strain capacity of a material is low (Alexander and Beushausen, 2009; Igarashi and Kawamura, 2002; Mechtcherine and Dudziak, 2011; Soliman and Nehdi, 2013).

The magnitude of autogenous shrinkage increases linearly with a decrease in w/b and accounts for 50% and 40% of the shrinkage in concrete with w/b of 0.3 and 0.4 respectively. Gopinath (2010) reports that autogenous shrinkage accounts for 100% of the total shrinkage in concrete with w/b of 0.17 at a constant temperature. Kovler and Jensen (2005) report that autogenous shrinkage could account for approximately 50% of the shrinkage in mixes with w/b of 0.30. Gillmer (2012), while referring to other studies, attributes the increase in autogenous shrinkage with a reduction in w/b to the finer porosity associated with low w/b. The fine porosity coupled with low relative humidity results in a greater radius of curvature of the water meniscus within the pores, consequently resulting in large compressive stresses on the pore walls. These stresses pull the pore walls inwards and result in greater autogenous shrinkage.

A critical analysis of literature reveals the lack of a clearly defined w/b that would initiate autogenous shrinkage. On the one hand, Bentz (2008) reports that autogenous shrinkage increases dramatically as the w/b is lowered below 0.35 in portland cement systems; with further dramatic increases being observed in systems containing SF and slag additions. Jensen and Hansen (2001a), on the other hand, report that autogenous shrinkage is prone to mixes with w/b less than 0.40-0.45. Carlswärd (2006) reports that autogenous shrinkage is negligible in mixes with w/b exceeding 0.5. Byard et al. (2012), while referring to other studies, report that autogenous shrinkage and stress development are not a concern when the w/b exceeds 0.42. Carlswärd (2006) further confounds the problem of the lack of a definitive w/b by reporting that autogenous shrinkage has been observed in mixes with w/b of 0.55 and 0.6.

Autogenous shrinkage deformations are influenced by: w/b, cement type, composition and fineness, volume of aggregate, temperature of exposure environment (Brandt, 2009; Jensen and Hansen, 2001a; Li et al., 2012; Mechtcherine and Dudziak, 2011; Taylor, 2014; Zhang et al., 2014). Autogenous shrinkage cracks can neither be prevented using mixes that have a low w/b nor controlled by traditional curing procedures because it is internally- and chemically-initiated in nature. The effects of autogenous shrinkage can be mitigated by SRAs (Carlswärd, 2006) and active moist curing. Saturated light-weight aggregates (SLWAs) also minimise autogenous shrinkage. SLWAs prevent the reduction in relative humidity in cementitious materials by acting as internal water reservoirs (Alexander and Beushausen,

2009; Atrushi, 2003; Bentur et al., 2001; Jensen and Hansen, 2001a). Condensed silica fume (referred to as CSF hereafter) increases autogenous shrinkage slightly (Alexander and Beushausen, 2009; Igarashi et al., 2000a; Igarashi and Kawamura, 2002; Igarashi et al., 2000b; Mechtcherine and Dudziak, 2011). Gopinath (2010) and Mechtcherine and Dudziak (2011) attribute the slight increase in autogenous shrinkage, due to the use of CSF, to increased capillary stresses that result from a fine pore structure. Igarashi and Kawamura (2002), further, report that the effect of CSF on autogenous shrinkage depends on the property of the cement paste matrix, w/b, curing temperatures and coarse aggregate content.
The magnitude of the various forms of chemical and autogenous shrinkage depends on the degree of hydration (Gagné et al., 1999), the availability of free water in the pores (Uys, 1983), w/b, cement content and the presence of admixtures and additives (Atrushi, 2003; Tazawa et al., 1995; van Breugel, 2001), the temperature history of the mortar (Atrushi, 2003; Loukili et al., 2000), the density of the microstructure (Igarashi et al., 2000a; Tazawa et al., 1995) and the type and chemical composition of the cement and its fineness (Beltzung, 2001; Carlswärd, 2006; Gopinath, 2010).

2.4.1.2 Plastic shrinkage

Plastic shrinkage, also known as capillary shrinkage, results when the rate of loss of water from the surface exceeds the rate at which the bleed water is appearing. It takes place during the first hours of the life of a cementitious material depending on the relative humidity, temperature, wind velocity, exposed surface area, spaces between solid particles at the surface of the material and permeability (ACI224, 2003; Atrushi, 2003; Banthia and Gupta, 2009; Bentz, 2008; Carlswärd, 2006; Concrete-Society, 2003a; Gopinath, 2010; Kronlöf et al., 1995; Mechtcherine and Dudziak, 2011; van Breugel, 1980). Plastic shrinkage is commonly attributed to four driving forces, namely: rapid evaporation of water that creates menisci and high tensile stresses in the capillary water near the surface, differential settlement, thermal gradients and autogenous shrinkage that occurs during the plastic phase (Gopinath, 2010). Plastic shrinkage cracks develop when the material near the surface becomes too stiff to move while not yet strong enough to withstand the tensile stresses caused by restrained shrinkage (ACI224, 2003; Concrete-Society, 2003b; Mehta and Monteiro, 2006). These cracks are commonly observed in elements with a high surface area:volume ratio (abbreviated as SA:V hereafter) and with varying depths.
Plastic shrinkage is mainly caused by: bleeding or sedimentation, absorption of water by subgrade or forms or aggregate, rapid water loss by evaporation, reduction in the volume of the cement-water system, and bulging or settlement of the

formwork. The susceptibility of materials to undergo plastic shrinkage cracking is increased by high temperatures and wind velocity, low humidity, presence of microsilica and a high amount of superplasticiser or retarding additives. Plastic shrinkage can be controlled by: moistening the subgrade and forms, moistening the aggregates that are dry and absorptive, erecting temporary windbreaks to reduce wind velocity over the surface, erecting temporary sunshades to reduce the surface temperature, keeping the temperature of the fresh material low by cooling the aggregate and mixing water, protecting the material with temporary coverings, using fog nozzles to saturate the air above the surface, using plastic sheeting to cover the surface between finishing operations, or by scheduling flat work after the wind breaks have been erected, early curing, using SRAs, good mix design and curing procedures, good site practice (ACI224, 2003; ACI546, 2003; Banthia and Gupta, 2009; Carlswärd, 2006; Concrete-Society, 2003a; Gillmer, 2012; Mehta and Monteiro, 2006; Taylor, 2014).

2.4.1.3 Drying shrinkage

Drying shrinkage is a time-dependent reduction in volume due to the loss of moisture from a material to its environment. It is usually non-uniform throughout the section of a material; thus, resulting in warping and cracking (Juenger and Jennings, 2002). Drying shrinkage originates from the HCP and is caused by the removal of adsorbed water from HCP stored in unsaturated air (Mehta and Monteiro, 2006; Neville, 1995). Drying shrinkage is mainly attributed to the contraction of the CSH gel within the HCP. The magnitude of drying shrinkage is rapid in the initial stages; thereafter decreasing with an increase in the age of the material (Gillmer, 2012). The ACI224 (2003) quantifies the magnitude of drying shrinkage as 0.06% and 1% of the total volume of a cementitious material with and without aggregates respectively; with the lower magnitude being attributed to the internal restraint provided by the presence of aggregates. The three common mechanisms through which the loss of water causes volume changes are capillary stress, disjoining pressure and surface tension (Alexander and Beushausen, 2009; Brandt, 2009; Hua et al., 1995; Hubert et al., 2003; Mehta and Monteiro, 2006).
Drying shrinkage comprises two components: reversible and irreversible shrinkage. Reversible shrinkage refers to the component of total shrinkage that is reproducible on wet-cycles while irreversible shrinkage is the component of total shrinkage on first drying that cannot be reproduced on subsequent wet cycles. These components of shrinkage are shown in Figure 2.3.
Drying shrinkage is influenced by many parameters, namely: material and mix proportions (e.g. grading, maximum size, density, texture, stiffness, type and volume fraction of aggregates), time (age), ambient temperature and relative humidity,

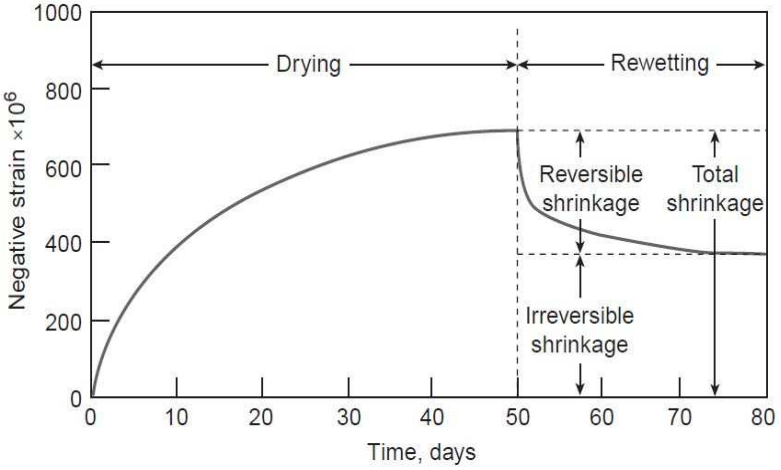

FIGURE 2.3: Reversibility of drying shrinkage - adopted from Mehta and Monteiro (2006)

drying conditions, admixtures, amount and composition of the cement paste, water content, temperature history, degree of hydration, curing methods, ratio of volume to exposed surface area, w/b and the geometry of the element (ACI209, 2005; ACI224, 2003; Amba et al., 2010; Bisschop and van Mier, 2002; Bissonnette et al., 1999; Brandt, 2009; Carlswärd, 2006; Concrete-Society, 2003a; Coussy et al., 2004; Gutsch, 2002; Hubert et al., 2003; Juenger and Jennings, 2002; Mehta and Monteiro, 2006; Park et al., 2009; Rao, 2001a; Saliba et al., 2011; Topçu and Bilir, 2010; Uys, 1983).

Drying shrinkage manifests itself in the form of cracks. The extent to which these cracks are formed depends on the properties of the material (tensile strength and tensile strain capacity), the degree of restraint, the provision of reinforcement and joints and reinforcement detailing (Concrete-Society, 2003a; Nossoni and Harichandran, 2010; Park et al., 2009). Drying shrinkage cracks vary from one structure to another in terms of size, location, spacing and orientation/pattern. The Concrete-Society (2003a), ACI224 (2003), Carlswärd (2006), Gopinath (2010) and Taylor (2014) report that drying shrinkage can be reduced by: increasing the amount of aggregate, reducing the water content of a mix, proper detailing, using contraction joints, using shrinkage compensating cement and SRAs, using expanding agents, adding fibres and reduction/minimising substrate restraint.

2.4.1.4 Carbonation shrinkage

The chemical reaction between carbon dioxide from the atmosphere and the constituents of the HCP results in a reduction in volume called carbonation shrinkage.

This shrinkage occurs later in the life of hardened concrete structures that are exposed to carbon dioxide from the atmosphere (Brandt, 2009). Beushausen and Alexander (2009) and Gopinath (2010) report that carbonation shrinkage occurs over a long period; with its magnitude, in some cases, exceeding that of drying shrinkage. The humidity of the material during exposure to carbon dioxide is the major factor influencing carbonation shrinkage; with carbonation shrinkage being greatest at intermediate humidities.
Masuku (2009), Gopinath (2010) and Gillmer (2012), while referring to other studies, report that the ideal range of relative humidity for carbonation shrinkage lies between 40% and 80%. Neville (1995), Alexander and Beushausen (2009) and Gopinath (2010) further report that carbonation shrinkage reduces at either higher or lower humidities and is greatest when carbonation occurs subsequent to drying. The magnitude of the relative humidity below which carbonation would not proceed, however, is not specific as reported in literature. On the one hand, Gopinath (2010) reports a lower limit value of 25% while Masuku (2009) and Gillmer (2012), on the other hand, report a lower limit value of 40%.
The reduction in carbonation with a decrease in relative humidity (i.e., lower than 25%) has been attributed to insufficient water in the pores for carbonation to take place. Similarly, the reduction in carbonation with an increase in relative humidity (greater than 80%) has been attributed to the slow diffusion of carbon dioxide through the pores that are filled with water and the clogging of surface pores through the precipitation of calcium carbonate. Carbonation results in adverse effects such as: reduction in the level of protection provided to the reinforcing steel - by the lowering of the pH and cracking at the surface of the material - reduction in strength, increase in deflection, an increase in the mass of the HCP which consequently translates into an increase in the mass of the material (ACI224, 2003; Gillmer, 2012; Gopinath, 2010; Uys, 1983).

2.4.1.5 Thermal shrinkage

Thermal shrinkage (or thermal dilation) is a temperature-dependent volume change (Atrushi, 2003). It is a property of concern in the stress analysis of cementitious materials at early ages. Rao (2001a) and The Concrete-Society (2003b) attribute thermal shrinkage to the high temperatures that develop from the time of setting. Atrushi (2003) and Zhou et al. (2014) attribute this deformation to the temperature changes that take place due to the heat of hydration and environmental conditions.
Thermal shrinkage results from the combination of the heat produced during cement hydration and the relatively poor heat dissipation that could result in a

large rise in temperature within a few days after placement. The subsequent cooling of the material to the ambient temperature results in cracking. The ACI224 (2003), ACI546 (2003), the Concrete-Society (2003a), Concrete-Society (2003b), Gopinath (2010) and Taylor (2014) have further reported that the thermal gradient within thick members results in cracking. When the surface layer cools and contracts, movement is restrained by the core of the member which is still at a higher temperature, and thus cracks may form on the surface. When the temperature through the member eventually becomes uniform, the surface cracks close. The tensile stresses resulting from thermal shrinkage are proportional to the temperature differential, the coefficient of thermal expansion (abbreviated as CTE hereafter), the effective modulus of elasticity and the degree of restraint (ACI224, 2003; Wyrzykowski and Lura, 2013).
The factors that affect thermal movements and stresses are: moisture content, aggregate properties (type, volume, CTE), tensile strain capacity, degree of restraint, temperature change, cement properties (type, content and fineness), ambient temperature conditions, the geometry of the member, w/b, moisture content of the saturated phase, admixtures and curing conditions - through their influence on the heat capacity - (Atrushi, 2003; Bentz, 2008; Brandt, 2009; Concrete-Society, 2003a,0; Mehta and Monteiro, 2006). The temperature rise in massive patch repairs and concrete structures can be controlled through proper selection of materials, mix proportions, curing conditions and construction practices such as limiting the time between pours so that the temperature history between adjacent pours are as similar as possible (Concrete-Society, 2003a). The use of slag and fly ash can significantly reduce the heat of hydration, thereby reducing the possibility of thermal-induced cracking.

2.4.2 Other causes of cracking

Cracking can result from the corrosion of steel. The expansive products of corrosion have been reported to generate tensile stresses that result in cracks. Structural and environmental loads and actions such as overloading (DANSK-Standard, 2004; Tilly and Jacobs, 2007), impact loads and loss of prestress could also result in cracks. Cracking could also result from the tearing of the surface due to late finishing operations, construction movement, settlement and poor construction practice (ACI224, 2003; ACI546, 2003; Concrete-Society, 2003a; Raupach and Büttner, 2014; Tilly and Jacobs, 2007; Uys, 1983). Details on these types of cracks will not be discussed in this thesis but can be obtained from the cited references.

2.5 Effects of cracking

Cracking results in negative effects with respect to aesthetics and functionality, durability, and socio-economic aspects. These effects are discussed in the subsequent subsections.

2.5.1 Aesthetics and functionality

The ingress of dirt in cracks and the presence of random cracks at unexpected locations makes the affected structures aesthetically unappealing. Cracks also compromise the water tightness, appearance, functionality and sound transmission of structures (Carlswärd, 2006; Concrete-Society, 2003a; Neville, 1995). Cracks of appreciable sizes and depths in liquid-retaining structures can result in leakage which would render these structures useless. Cracks enhance the initiation and corrosion of steel in RC structures. Igarashi et al. (2000b), Concrete-Society (2003b), Carlswärd (2006), Brandt (2009) and Zhang et al. (2014) further report that cracks reduce the stiffness of a section and its load-bearing and shear capacity. A reduction in stiffness results in an increase in deformations.

2.5.2 Socio-economic

The costs associated with the demolition and consequent rebuilding, or the repair and rehabilitation, of deteriorating structures are very high (Beushausen et al., 2017; Radlińska and Weiss, 2012). The inability of structures, e.g. water-retaining structures, to realise their functionality inconveniences the public. The closure of bridges, dams and water tanks due to cracks or during repairs, for example, denies communities access to water and other essential services which play a vital life in their well-being. The fact that governments spend much money to repair deteriorating concrete structures implies that funding for other equally critical sectors of the economy such as education, food security and healthcare will be reduced. The reduced funding to other critical sectors of the economy results in stunted economic development, with more negative consequences being experienced in developing countries.

2.5.3 Durability

Cracking of cement-based materials results in high permeability and consequently the lack of durability (Akhavan et al., 2012; Banthia and Gupta, 2009; Bissonnette et al., 1999; Vaysburd and Emmons, 2000; Yuan et al., 2003). Cracks modify the transport properties of cement-based materials (Gérard and Marchand, 2000). Cracks can open later and provide an easy passage for aggressive chemical

species into concrete. The ingress of chemical species increases the susceptibility of the embedded reinforcement to corrode due to attack by chlorides and carbon dioxide (Alahmad et al., 2009; Alexander and Beushausen, 2009; Baluch et al., 2002; Beushausen, 2005; Brandt, 2009; Carlswärd, 2006; Juenger and Jennings, 2002; Kim and Weiss, 2003; Mehta and Monteiro, 2006; Neville, 1995; Topçu and Bilir, 2010; Zhang et al., 2014). Corrosion-induced cracking affects durability; consequently resulting in a reduction in service life (Al-Gahtani and Khan, 2003; Carlswärd, 2006; Concrete-Society, 2003a,0; Grondin et al., 2012; Ranaivomanana et al., 2013; Vaysburd and Emmons, 2000). Brandt (2009) further reports that the danger with which cracks affect the durability of materials adversely is proportional to their width, is strongly related to their connectivity and depends on the environmental conditions and the location of the crack.

2.6 Crack control and remediation techniques

There is an important need to control cracking in cement-based materials. Common crack control and remediation techniques comprise, but are not limited to, the use of SRAs, expansive cements, fibre reinforcements, rubberised aggregates and polymer-modified materials. Details pertaining to these techniques are discussed in the subsequent subsections.

2.6.1 Shrinkage reducing admixtures

Shrinkage reducing admixtures (abbreviated as SRAs hereafter) are anionic surface-active agents, whose molecular structure comprises hydrophobic and hydrophilic groups bonded covalently (such compounds are termed as amphiphilic). When dissolved in water, amphiphiles are attracted to non-polar interfaces (such as water-air or water-oil interfaces). The adsorption of such a surfactant at interfaces causes a reduction in the interfacial energy, which is responsible for the reduction of surface tension of the water-air (i.e., liquid-vapour) interface. The reduction in surface tension results in a reduction in shrinkage (Gopinath, 2010; Ribeiro et al., 2011; Rixom and Mailvaganam, 1999). The magnitude with which the surface tension is reduced depends on the dosage of the SRA as shown in Figure 2.4. The concept of the reduction in shrinkage due to a reduction in surface tension has been challenged. Wittmann (2008), for example, reports that a significant reduction in surface tension has hardly any influence on shrinkage.

SRAs affect fresh and hardened properties like workability and setting time. Incorporating SRAs in mortars could also reduce compressive strength and introduce

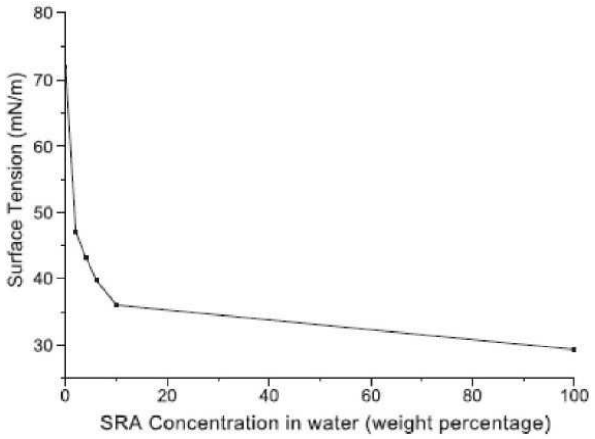

FIGURE 2.4: Reduction in surface tension of water due to SRA addition - adopted from Gopinath (2010)

a superplasticising effect. Ribeiro et al. (2011) reports that the reduction in compressive strength, due to the incorporation of SRA, is more pronounced in the early ages and is highly dependent on the type of SRA that has been used. The superplasticising effect of SRAs could be used to reduce water content and/or superplasticiser dosage and slump; therefore, resulting in an improvement in mechanical and durability performance. An increase in SRA dosage increases setting time. In the case of high strength materials, there can be a further increase in setting time due to the combined effect of the SRA and superplasticiser (Gopinath, 2010; Ribeiro et al., 2011; Rixom and Mailvaganam, 1999). Gopinath (2010), while referring to other studies, reports that the addition of SRAs retards temperature development and reduces the compressive, splitting tensile and flexural strength. The reduction in compressive and flexural strength has been attributed to the delay in hydration resulting from the use of SRAs.

SRAs reduce evaporation from fresh concrete, thus reducing the susceptibility to plastic shrinkage cracking. This phenomenon can be attributed to the low capillary pressure in the drying mortar when the surface tension of water is reduced by SRAs. SRAs also result in fewer and narrower cracks under restrained plastic shrinkage. Gopinath (2010) - while referring to other studies - reports that SRAs reduce (and can eliminate) autogenous shrinkage. Gopinath (2010) further reports that a combination of SRAs and proper curing is effective in reducing shrinkage; with SRAs reducing drying shrinkage by values ranging between 25% and 60%. Baluch et al. (2002), while referring to other studies, reports a 50% reduction in drying shrinkage due to the incorporation of 2% SRA by weight of cement. The reported reduction in drying shrinkage was observed to be more within the RH range of 20% and 45% than at higher relative humidities. Ribeiro et al.

(2011) also report that the effect of SRA on shrinkage is influenced by cement type. Gopinath (2010), while referring to other studies, further reports that SRA reduces the chloride content and the rapid chloride permeability coefficient of concrete. Additional details pertaining to the use and role of SRAs in reducing shrinkage-induced cracking are provided in Section 3.4.5.2.

2.6.2 Expansive cements and agents

Expansive cements, also called shrinkage-compensating cements, are cements that, on hydration, counteract the deformation induced by shrinkage by expanding by an amount equal to or slightly greater than the anticipated drying shrinkage. Cement-based materials containing expansive cement expand during the first few days after casting, and a form of prestress is obtained by restraining this expansion. Because of the restraint, compressive stresses are induced in the material during expansion. Subsequent shrinkage of the material would reduce the magnitude of the compressive stresses as shown in Figure 2.5. Ideally, a residual compression will remain in the material, eliminating the risk of shrinkage cracking (Mehta and Monteiro, 2006; Neville, 1995).

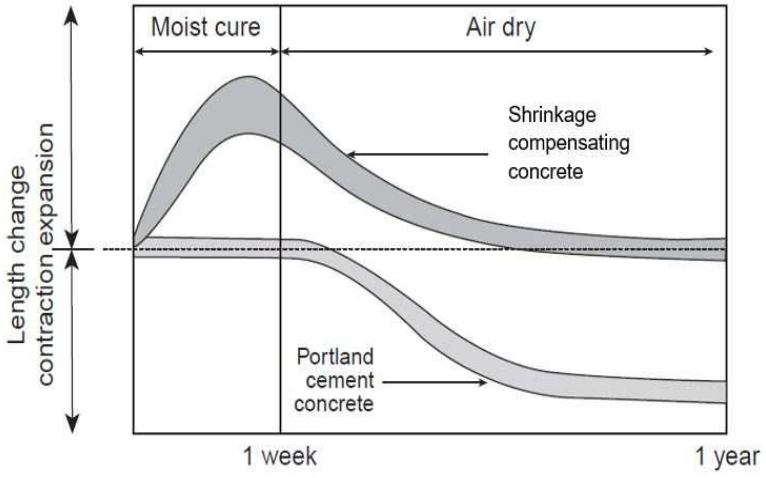

FIGURE 2.5: Length change characteristics between shrinkage-compensating and portland cement concretes - adapted from Mehta and Monteiro (2006)

The most commonly used expansive agents are sulphoaluminates and lime. These agents achieve the same purpose through different mechanisms. Sulphoaluminates are generally used in normal strength concrete where a gradual strength attainment is desired whereas lime-based expansive agents are used in the case of concrete which attains strength at early ages because of the quicker expansive rate of lime.

Gopinath (2010), while referring to other studies, reports that the combination of SRA and an expansive admixture results in a reduction in compressive strength. The efficacy of expanding agents is influenced by the conditioning of cementitious materials immediately after casting. When humid curing is not ensured, the expanding effect fails to occur and shrinkage cannot be efficiently compensated by the expanding action (Pistolesi et al., 2008). Sahamitmongkol and Kishi (2011) report that the age of the material and restraint affect the tensile properties of an expansive mortar.

2.6.3 Fibre reinforcements

Fibre reinforcements are produced from steel, plastic, glass, asbestos and natural/organic materials such as sisal, vegetables and coconut. They come in various sizes and shapes. Fibres improve flexural strength, impact strength, tensile strength, bond strength, abrasion resistance, ductility and flexural toughness, reduce shrinkage, delay the age of first crack and reduce crack widths (Baluch et al., 2002; Brandt, 2009; Filho and Sanjuán, 1999; Huang, 2001; Kim and Weiss, 2003; Luković, 2016; Ma et al., 2002; Mehta and Monteiro, 2006; Nossoni and Harichandran, 2010; Sanjuán and Filho, 1998; Theodorakopoulos, 1995; Topçu and Bilir, 2010; Xu et al., 2011). The reduction in crack widths due to the incorporation of fibres can be attributed to the fact that fibres act as crack-arrestors when cracks occur; consequently controlling their propagation (Brandt, 2009; Luković, 2016). The Concrete-Society (2003a), Gopinath (2010) and Gillmer (2012) further report that most fibres reduce the risk of plastic shrinkage cracks; with the Concrete-Society (2003a) attributing the reduction in the risk to cracking to an increase in the tensile strain capacity by a factor of 2 or 3. The properties of fibre-reinforced materials that are important for shrinkage-induced cracking and crack-determining material properties comprise: type of fibre, aspect ratio, strength and bond to the matrix, their distribution within the matrix, geometric shape and their volume fraction (Brandt, 2009; Filho et al., 2005; Ma et al., 2004; Mehta and Monteiro, 2006). The effect of the volume fraction of fibres on modulus of rupture and tensile strength is shown in Figure 2.6.

Low volume fibre fraction - less than 1% - for example, are used to reduce shrinkage cracking (Banthia et al., 1996; Mehta and Monteiro, 2006). Kronlöf et al. (1995), Beushausen and Alexander (2009), Nguyen et al. (2010) and Dawood and Ramli (2011) report that adding fibre reinforcement in patch repairs and overlays enhances their: crack resistance and bond durability, compressive strength, modulus of elasticity, flexural strength, toughness and strain capacity. Huang (2001), while studying the effects of polypropylene fibres on grouts containing fly ash, found out that fibres reduce compressive and flexural strength. The observed reduction in

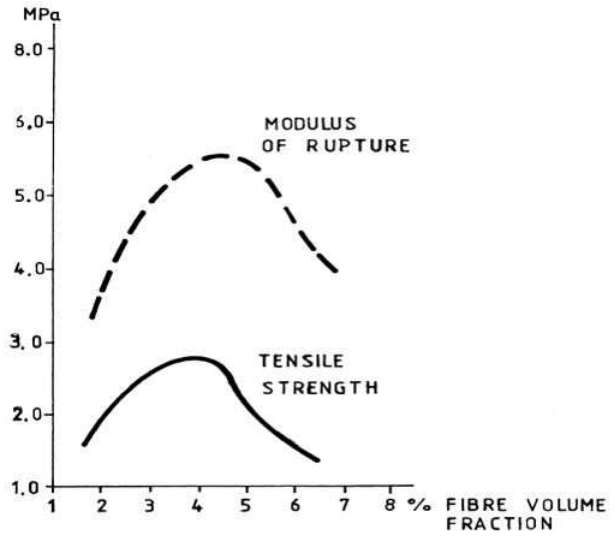

FIGURE 2.6: Effect of fibre content on tensile strength and modulus of rupture of composite elements - adopted from Brandt (2009)

compressive strength was attributed to the redistribution of the void structure of the grout due to the inclusion of fibre and the presence of weak interfacial bonds between the fibre and the cement-fly ash grains. Kronlöf et al. (1995) and Filho et al. (2005) report that fibres reduce plastic shrinkage; with Kronlöf et al. (1995) reporting on a 30% reduction in the magnitude of plastic shrinkage. Filho et al. (2005) report that a high volume of vegetable fibres increases drying shrinkage. They attribute the increase in drying shrinkage to an increase in the porosity of the cement matrix. The distribution and orientation of steel fibres within a cement matrix, the cleanliness of their surface and their anchorage to the matrix would determine their efficiency (Brandt, 2009).

2.6.4 Polymer modification

Polymer-modified concrete and mortar are not new. The first set of patents for polymer hydraulic cements and mortars were issued in the 1920s (Kardon, 1997; Miller, 2005; Ohama, 1998, 2011; Ramli and Tabassi, 2012b). Polymers are incorporated into cementitious materials in several ways, namely: by direct addition as part of the gauging liquid (latex emulsion) or pre-blended into the cementitious material (redispersible polymer powders). Alternatively, they can be added as fibres of the desired resin into the hardened composite (Miller, 2005; Ohama, 1997, 2011). Polymer-modified systems have been used for various construction applications, namely: deck coverings for motorway bridges and bridge repairs,

paving, floorings, waterproofing, lining manholes, finishing and repair works, anti-corrosives and adhesives (Chorinsky, 1986; Kardon, 1997; Miller, 2005; Ohama, 1996; Ohama et al., 1986; Peier, 1986; Ramli and Tabassi, 2012a).
Polymer-modified systems are reported to possess the following superior properties in comparison to ordinary cement concrete and mortars: high flexural, compressive and tensile strengths, better chemical, impact, abrasion and corrosion resistance, improved adhesion and adhesive bond strength to different substrates, waterproofness, airtightness, resistance to cycles of freezing and thawing, durability, a reduced risk of cracking, reduced bleeding and segregation, increased flexibility and an improved fracture toughness (ACI546, 2003; Bezerra et al., 2011; Boyd and Smith, 2007; Brandt, 2009; Chorinsky, 1986; Gao et al., 2002; Jingang et al., 2005; MDoT, 1996; Miller, 2005; Ohama, 1998; Ramli and Tabassi, 2012a; Reis and Jurumenha, 2013; Schulze and Killermann, 2001; Soshiroda et al., 1986).
The material properties and overall performance of polymer-modified cementitious materials depend on the type and nature of polymer used, the ratio of polymer to cement content by weight, the temperature and environment (external and internal) in which curing takes place (Miller, 2005; Ohama, 1998; Rixom and Mailvaganam, 1999). In comparison to polyester and acrylic mortars, ACI 546 (2003) reports that epoxy mortars experience less shrinkage. Mehta and Monteiro (2006) also report that polymer-modified mortars made using a hardener-free epoxy resin have a self-healing or self-repairing function for microcracks. A study by Mallat and Alliche (2006) observed that fibre-reinforced polymer-modified and fibre-reinforced ordinary mortar exhibited greater shrinkage in comparison to plain mortar. They further reported that fibres and polymers are incapable of modifying the nature of the cement hydration products even if the polymer slowed down the kinetics of the reaction. Additional details regarding the contribution of polymer-modified systems to shrinkage-induced cracking in PRMs are provided in Section 3.4.7.

2.6.5 Rubber aggregates

Ordinary cement-based materials have a low tensile strength and a poor strain capacity regardless of their compressive strength. They are also brittle (Topçu, 1997; Turatsinze et al., 2006; Zhang et al., 2014). This brittleness increases their susceptibility to cracking. Studies by Topçu (1995),Topçu (1997), Toutanji (1996), Topçu and Avcular (1997a), Topçu and Avcular (1997b), Segre and Joekes (2000), Turatsinze et al. (2006), Turatsinze et al. (2007), Ho et al. (2008), Topçu and Bilir (2010), Corinaldesi et al. (2011), Nguyen et al. (2012) and Zhang et al. (2014) report that the incorporation of rubber aggregates in mortars improves their strain capacity before macrocrack localisation, deformation ability, toughness, impact

resistance and reduces their potential for restrained shrinkage cracking. Turki et al. (2012) and Zhang et al. (2014) further report that the incorporation of rubber particles in cement-based materials reduces internal stresses within their matrix. Zhang et al. (2014) attribute this reduction in internal stresses to the stress relaxation effect due to the low modulus of elasticity in rubberised materials.
Topçu (1995), Topçu (1997), Segre and Joekes (2000), Turatsinze et al. (2005) and Corinaldesi et al. (2011) further report that the incorporation of rubber reduces the unit weight, thermal conductivity, Schmidt hardness value, ultrasound velocity and tensile deformation modulus of the material. Topçu (1995), Toutanji (1996), Topçu (1997), Segre and Joekes (2000), Turatsinze et al. (2005), Turatsinze et al. (2006), Turatsinze et al. (2007), Corinaldesi et al. (2011) and Turki et al. (2012) report that the incorporation of rubber in cement-based materials is detrimental to their compressive, flexural and tensile strength; with Toutanji (1996) observing greater reduction in compressive strength than in flexural strength. The reduction in the compressive strength due to the incorporation of rubber is shown in Figure 2.7; and has been attributed to the low compactness due to the addition of rubber and an increase in matrix porosity.

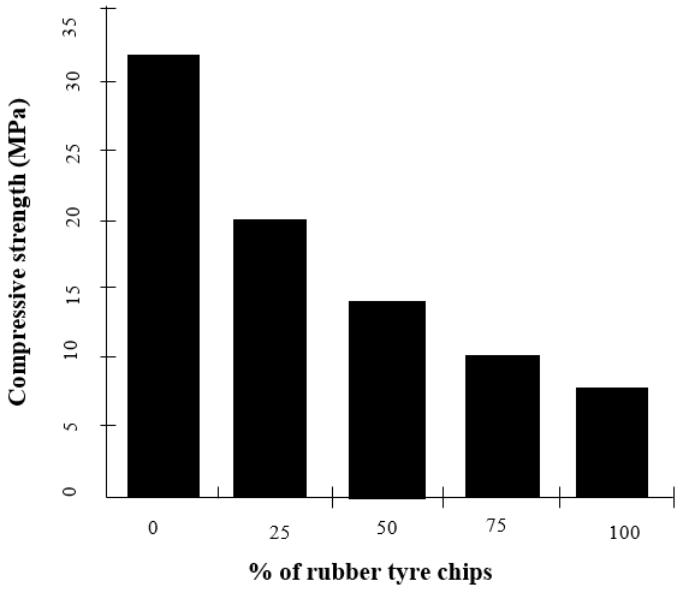

FIGURE 2.7: Compressive strength as a function of percentage of rubber tyre chips - adapted from Toutanji (1996)

Topçu (1997) attributed the reduction in compressive strength to the reduction in the quantity of solid load-carrying material and to stress concentrations in the paste at the boundaries of the rubber aggregate. Turatsinze et al. (2005), while referring to other studies, attribute the reduction in strength with an increase in

rubber content to the high compressibility of rubber particles which consequently generates local stresses and bonding problems between the rubber and the cement matrix. Turki et al. (2012) attribute the loss in mechanical properties to the low density of rubber compared to the sand that has been substituted. Segre and Joekes (2000) report that treating rubber particles with a solution of sodium hydroxide (NaOH) before incorporating them in cement-based mixes improves their bonding to the cement paste; consequently resulting in relatively higher compressive strength than in untreated rubberised cementitious composites.

Turatsinze et al. (2006) and Turatsinze et al. (2007) report that rubberised composites exhibit a reduced elastic modulus. Increasing the volume fraction of rubber aggregates in mortars increases their strain capacity. Turatsinze et al. (2006) reports that the strain capacity in rubberised mortars increases by a factor of 2.5. This increase has been attributed to the effect of the rubber aggregates on cracking kinetics that is where the rubber decreases the stress concentration and removes the geometric singularity caused by the crack tip. Thus, when the first microcracks run into the rubber-matrix interface, the resulting stress relaxation prevents further propagation and delays microcrack coalescence. Turatsinze et al. (2006), Turatsinze et al. (2007) and Nguyen et al. (2012) also report that incorporating rubber aggregates in cement composites delays shrinkage-induced cracking and results in multiple cracks with thin crack openings. Turatsinze et al. (2007) and Nguyen et al. (2012), further report that the presence of rubber in cementitious composites increases free shrinkage as shown in Figure 2.8. In Figure 2.8, the notations M30, M20 and M0 refer to specimens with rubber contents of 30%, 20% and 0% respectively.

The combination of rubber aggregates and fibre reinforcements increases the deformation capacity before macrocrack formation and enhances ductility (Nguyen et al., 2012; Turatsinze et al., 2005). Turatsinze et al. (2005) suggest that when strength is not a high priority, such behaviour is an asset that improves material durability.

2.7 Closure

The causes of deformation and volume changes in cement-based materials and the theories that explain them have been presented within this chapter. From this chapter, it is evident that the micro- and macrostructure of the HCP play a significant role in deformations and volume changes. It is thus important that the structure of the paste be understood.

The mechanics of cement-based materials play a critical role in the understanding of the cracking phenomenon. A proper understanding of elasticity, viscoelasticity

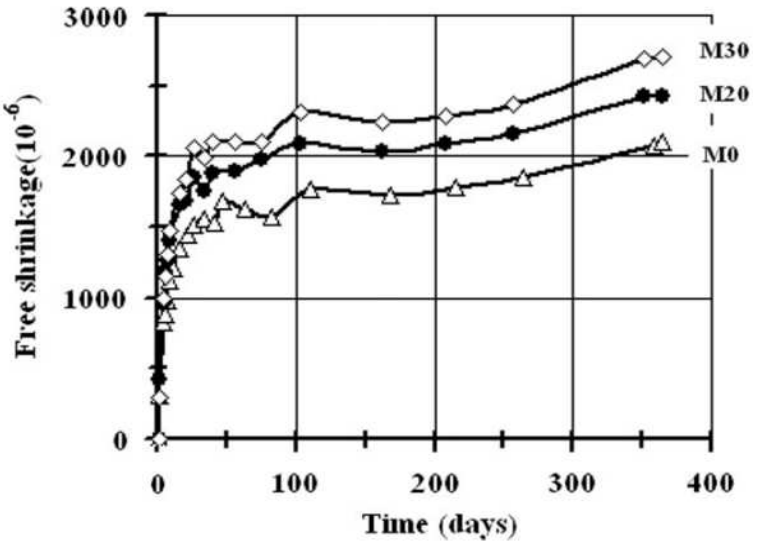

FIGURE 2.8: Free shrinkage vs. time in cementitious composites with rubber aggregate substitution - adopted from Turatsinze et al. (2007)

and fracture mechanics helps in the understanding of crack initiation and propagation as well as in the development of methods that could be used to minimise cracking significantly. The mechanics of cement-based materials are influenced by multiple mix design parameters. The exact nature of the influence of mix design parameters on the elasticity, viscoelasticity and fracture mechanics has been discussed.

Two hypotheses have been formulated by previous researchers to explain the mechanisms of cracking in cement-based materials. These hypotheses are based on two material properties: tensile strength and tensile strain capacity. These hypotheses postulate that cracking will initiate when either the induced tensile strength or strain exceeds the inherent tensile strength or tensile strain capacity of the material.

Cracking in cement-based material is mainly attributed to the tensile stresses generated from the volume changes that result from the movement or loss of water (and/or moisture) from the material to the environment or within the material itself. These stresses can also be generated from other phenomena, namely: alkali silica reaction (ASR), temperature variations and external loading. Restrained shrinkage is the main generator of tensile stresses that result in cracking in cement-based materials. Shrinkage generally manifests itself in the form of: chemical, autogenous, drying, thermal and carbonation shrinkage. Each of these shrinkage mechanisms requires a specific set of conditions to initiate and propagate. The susceptibility and the magnitude of shrinkage in any cement-based material depends

on its mix design parameters.

Cracking in cement-based materials is undesirable. It results in negative socio-economic, aesthetic, functionality, structural and durability effects. However, the negative effects of cracking can be controlled and/or mitigated by using SRAs, expansive cements and agents, fibre reinforcements, polymers and rubber aggregates. Furthermore, the review of literature in this chapter reveals that there is a need for further studies on the critical w/b below which autogenous shrinkage initiates. Also, there is a need to study the relationship between surface tension and shrinkage in the cement matrix. Whereas one group of researchers ascribe a reduction in cracking to a reduction in surface tension, a second group of researchers report that the effect of surface tension on cracking is insignificant.

Chapter 3

CONCRETE PATCH REPAIR MORTARS

This chapter provides a critical review of literature pertaining to PRMs and their cracking. The factors that govern the effectiveness in the performance of PRMs in service as well as their performance requirements are discussed. Finally, the influence of selected mix design parameters on cracking in PRMs are presented.

3.1 Introduction to concrete repair, repair materials and systems

A bonded overlay refers to a layer of cementitious mortar or concrete placed on top of an existing concrete substrate to which a bond develops. Bonded overlays used for repairs that have a relatively small surface area are referred to as patch repairs. Patch repairs are generally used to replace deteriorating and/or contaminated concrete as well as repairing damage due to corrosion at various levels of their evolution (Soufi et al., 2016). The primary objective of repairing deteriorating concrete structures is to increase their service life by restoring structural continuity. Baldwin and King (2003) report that repairs are executed to achieve one or a combination of the following: restore structural integrity, arrest deterioration, prevent future deterioration, restore original profile, restore integrity of sealed systems and aesthetic appearance. Concrete repair is an extensive, complex and challenging process. It is expected to address the conflicting demands and expectations of the client, the repair expert and the contractor. Prior to the execution of a repair, there is a need to understand the underlying causes of the deterioration, assess the deteriorating structure and predict the future rate and extent of deterioration (ACI546, 2003; Baldwin and King, 2003; Cleland et al., 1986; Concrete-Society, 2003b; ICRI, 2003; Jacobs, 2006; Raupach and Büttner, 2014).

Thereafter, informed decisions that address the conflicting needs of the client, the repair experts and the contractors can be initiated. Davies (2003), Maage (2003), Matthews and Morlidge (2006b) and Raupach and Büttner (2014) report the that following options ought to be considered while deciding on the appropriate action to meet the future requirement for the remaining service life of a deteriorating structure:

i. Do nothing for a specific time;

ii. Re-analyse the structural capacity;

iii. Prevent or reduce further deterioration;

iv. Improve, strengthen or refurbish all or part of the structure;

v. Replace all or part of the structure;

vi. Demolish the structure completely or partially.

The use of products, techniques and procedures that are appropriate for the specific deterioration mechanisms, environmental conditions and structural circumstances can help realise the durability of repairs in the structure under consideration (ACI546, 2003; BRE-DME-D53, 2003; Lambe, 1988; Matthews and Morlidge, 2006a). The selection of appropriate materials for surface repairs is a complex process that must be guided by the following criteria: constructability, serviceability, aesthetics and an understanding of the owners (users) concept and the engineering requirements (ICRI, 2003; MDoT, 1996). The selection of materials can only be made after the above criteria have been defined and the required material properties identified. Often, more than one material or system of materials will satisfy the established requirements. The final selection of materials is based on the relationship between cost, performance, health and safety and the environment (Baldwin and King, 2003; ICRI, 2003; Tilly and Jacobs, 2007). The process of selecting repair materials is summarised in the flow chart in Figure 3.1.
The repair of concrete structures prior to 1997 was governed by numerous national standards and guidelines that varied from one locality to another (Arito et al., 2016b; Jacobs, 2006). The challenges associated with the wide variability in standards and guidelines necessitated the need to draft and adopt a more generalised standard of practice that could assist in creating harmony, especially in repair projects that involved the sourcing of materials and experts from different localities (Arito et al., 2016b). Attempts to harmonise the repair of concrete structures facilitated the drafting and eventual publication of the EN 1504 series of standards and other standards that address specific forms of repairs such as realkalisation, cathodic protection and electrochemical chloride extraction.

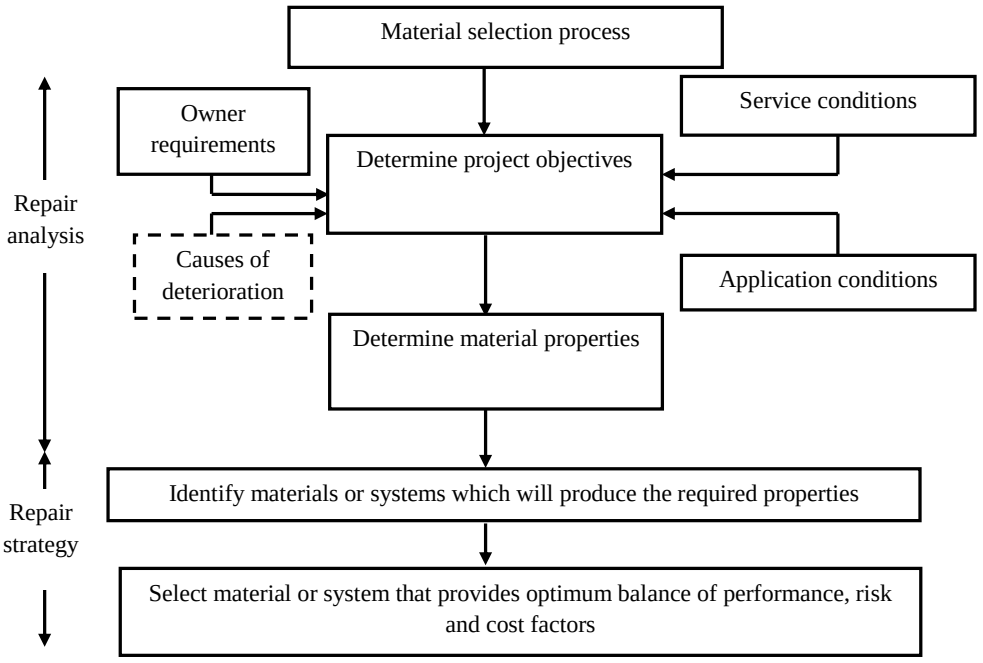

FIGURE 3.1: Flow chart of the material selection process for concrete repair - adopted from ICRI (2003)

The EN 1504 series of standards '*Products and systems for the protection and repair of concrete structures*' comprises 10 parts. It includes test methods for specific properties, minimum performance requirements, the general principles for repair work and a standard for site execution (Davies and Robery, 2006; Tilly and Jacobs, 2007). This series of standards deals with all the phases of a repair project, starting at the awareness of a problem up to the maintenance and inspection after the repair work is done. Table 3.1 summarises the parts of the EN 1504 series and its corresponding section titles and dates of publication and revision. The numbers in brackets in Table 3.1 refer to the year of revision of the specific standard.
Despite the attempt to develop a universal, harmonised and comprehensive series of standards that addresses concrete repair at various stages, there are many challenges that are yet to be addressed by the EN 1504. The EN 1504, despite its comprehensiveness, fails to address other types of concrete damage - a challenge that has also been reported by Davies and Robery (2006), Jacobs (2006) and Tilly and Jacobs (2007). The DANSK-Standard (2004), Jacobs (2006) and Tilly and Jacobs (2007) also report that the EN 1504 does not cover the repair of concrete structures that have been damaged by fire, the repair of defects in existing post-tensioned systems or repair materials and systems that would be used for purposes other than rehabilitation of concrete structures (e.g., improving the aesthetic appearance or a change in the primary use of a concrete structure). Should the repair of deteriorating concrete structures fail to fit into any of the categories highlighted

TABLE 3.1: European standards related to concrete repair products and systems - adopted from DANSK-Standard (2004); Davies and Robery (2006); Jacobs (2006); Tilly and Jacobs (2007)

Number	**Year of publication**	**Title**
EN 1504-1	1998 (2006)	Part 1: Definitions
EN 1504-2	1998 (2006)	Part 2: Surface protection systems for concretes
EN 1504-3	2006	Part 3: Structural and non-structural repair
EN 1504-4	2005	Part 4: Structural bonding
EN 1504-5	2004 (2013)	Part 5: Concrete injection
EN 1504-6	2006	Part 6: Anchoring of reinforcing steel bar
EN 1504-7	2006	Part 7: Reinforcement corrosion protection
EN 1504-8	2004	Part 8: Quality control and evaluation of conformity
EN 1504-9	1997 (2009)	Part 9: General principles for use of products and systems
EN 1504-10	2004	Part 10: Site application of products and systems and quality control of the works

in the EN 1504; The DANSK-Standard (2004) recommends that supplementary considerations be made.

It is evident, therefore, that the attempt to address the repair of concrete structures in an 'omnibus' document, though commendable, is still unsatisfactory. The current series of standards is far from addressing the challenges that hinder the realisation of durable and effective concrete repairs in service. The failure of the EN 1504 to recognise various forms of concrete deterioration - some of which are still emerging - implies that it must undergo continuous and drastic modifications and revisions in future. These modification and revisions could pose serious challenges within the concrete repair industry - especially in repairing structures that were previously repaired using a standard different to that in use at the material time. The existing standard also creates a potential for conflict with other standards and guidelines are more problem-, material- and environment-specific.

Although the EN 1504 has attempted to provide performance requirements for non-structural PRMs, there is an inherent need to expand their scope and, in some instances, interrogate the relevance of some its performance specifications. The lack of specifications for elastic modulus and tensile relaxation, for example, demonstrates the lack of an understanding of the role of these important material properties in cracking. There is a need, therefore, for a proper understanding of the role of tailored performance requirements that are informed by the intended use of the repair material. This need has also been highlighted by Mangat and Limbachiya (1997). There is also a need to identify and specify material properties that directly contribute to the realisation of durable and effective repairs. An analysis of trends in existing literature reveals that the design of concrete patch

repairs would continue to be done on an ad hoc basis (Mangat and O'Flaherty, 2000) or by over-relying on the experience and knowledge of specialist contractors - as reported by Mangat and Limbachiya (1997) and the BRE-DME-D62 (2003). To overcome this impending challenge, it is necessary that drastic amendments to the EN 1504 and other repair guidelines be effected soon.

3.2 Factors that govern the effectiveness in performance of PRMs in service

The effectiveness in the performance of PRMs in service is defined by its ability to achieve the performance it was originally intended for (Baldwin and King, 2003). Effectiveness involves factors that are relevant to the preparation and application of repair materials in addition to the realisation of their long-term performance. An assessment of effectiveness is, therefore, governed by many parameters. These parameters comprise, but are not limited to: durability, quality of workmanship, compatibility and interactions between the patch repair with the existing concrete substrate and the environment, quality and properties of its constituent materials, curing methods, edge conditioning, interface properties (roughness, cleanliness), substrate properties, substrate preparation, bond strength, access restrictions, strain capacity, health and safety aspects, workmanship and the handling and storage of repair materials prior to their use (Bester, 2015; Beushausen and Alexander, 2009; Beushausen et al., 2017; Cardon and Hiel, 1986; Concrete-Society, 2003b; Crosswell, 2009; Czarnecki, 2008; DANSK-Standard, 2004; Luković, 2016; Mangat and Limbachiya, 1997; Morgan, 1996; Perez et al., 2008; Raupach and Büttner, 2014; Silfwerbrand et al., 2011; Vassie, 1989). Baldwin and King (2003), Matthews (2007) and Tilly and Jacobs (2007) also report that durable and effective repairs can be realised through good supervision of works. Some of the factors that have been enlisted will be discussed in the subsequent paragraphs and subsections within this chapter.

The materials used in any PRM dictate, to a large extent, its effectiveness in performance while in service (Chen et al., 2011). The workability and compaction of a freshly-placed PRM influences its ability to fill open cavities and voids on the concrete substrate. A relatively fluid PRM enhances capillary suction in the substrate and therefore improves physical anchorage in the surface pores and cavities within the substrate. Curing prevents the rapid loss of moisture to the environment; thus, controlling stress development by reducing early-age shrinkage when the bond strength is still low (Beushausen and Alexander, 2009; Beushausen and Bester, 2016). The cleanliness and surface preparation of the substrate determines

the effectiveness of a given PRM and its longevity regardless of its cost, complexity, quality and method of application (ACI546, 2003; Baldwin and King, 2003; Beushausen and Alexander, 2009; Cardon and Hiel, 1986; DANSK-Standard, 2004; Lambe, 1988; Morgan, 1996; Raupach and Büttner, 2014; Sahmaran et al., 2014; Vaysburd et al., 2011). The removal of unsound, poor quality and deteriorated concrete substrate and any bond-inhibiting foreign materials such as dirt, oil and grease to the greatest possible extent helps guarantee good and durable patch repairs. The surface of the substrate needs to be free from microcracks because microcracks constitute a zone of weakness; consequently, making them prone to bond failure. The amount of microcracking depends on the method of concrete removal. Mechanical methods such as blasting and jackhammers are likely to introduce microcracking (ACI546, 2003; Beushausen and Alexander, 2009; Cleland et al., 1986; DANSK-Standard, 2004; Morgan, 1996). Silfwerbrand (1986) and Beushausen and Alexander (2009) report that water jetting or sandblasting produces sound substrate surfaces with sufficient roughness for bonding.
The substrate moisture condition, and its corresponding temperature, influences bond strength significantly (Beushausen et al., 2017; Luković, 2016; Morgan, 1996). A dry, "thirsty" concrete surface tends to suck water from the fresh PRM. This results in a weak interfacial layer and low bond strength. A surface that is too wet tends to dilute the repair material at the interface and increases the localised w/b at the interface. The increased localised w/b leads to low material strength, increased shrinkage and low bond strength. The presence of water in open pores prevents the interlocking effect (Beushausen and Alexander, 2009; Beushausen et al., 2017; Chorinsky, 1986; Morgan, 1996; Silfwerbrand et al., 2011; Vaysburd et al., 2011). According to Chorinsky (1986), a substrate that would be repaired ought to have sufficient compressive strength and not contain any water-repelling agents which could diminish the absorptive properties on the substrate and the adherence properties of the repair materials. Beushausen et al. (2017) further reports that the pre-wetting of a concrete substrate prior to the application of an overlay does not result in an added benefit with respect an increase in bond strength.

3.3 Performance requirements for non-structural PRMs

Performance requirements refer to a specific set of mechanical, physical and chemical properties for products and systems that would guarantee durability and stability for the repaired concrete and the structure. Performance requirements are

usually accompanied by a specific set of tests that ought to be done in accordance to a predefined test standard on a given material to directly verify its required properties (Maage, 2003). The test methods to be used are usually given, and requirements stated, in terms of a threshold value or as a pass/fail criterion. According to ICRI (2003), Matthews (2007) and Nossoni and Harichandran (2010), the specification of repair materials only ought to be done after the material properties that will best satisfy the overall objectives of a specific repair project are determined, identified and prioritised. The selection of materials for surface repair ought to be based on specific performance criteria. The EN 1504-3:2005 recommends specific performance characteristics that ought to be considered and specified in non-structural PRMs. A summary of the recommended performance characteristics and their corresponding supplementary information is presented in Table 3.2.2.

Table 3.2: Performance characteristics for non-structural PRMs for various fields of application - adopted from BS EN 1504-3:2005

Performance characteristics	**Test method**	**Field of application**	
		Concrete restoration	**Preserving or restoring passivity**
Compressive strength	EN 12190	AIU*	AIU
Chloride ion content	EN 101517	AIU	AIU
Adhesive bond	EN 1542	AIU	AIU
Restrained shrinkage /expansion	EN 126174	AIU	AIU
Durability: a)Carbonation resistance	EN 13295	AIU	AIU
Durability: b) Thermal compatibility (part 1 or Part 2 or Part 4 of EN 13687)	EN 13687-1-2-4	CIU*	CIU
Elastic modulus	EN 13412	CIU	CIU
Skid resistance	EN 130364	CIU	CIU
Coefficient of thermal expansion	EN 1770	CIU	CIU
Capillary absorption	EN 13057	CIU	CIU

* Note: AIU denotes all intended uses; CIU denotes certain intended uses

The EN 1504-3:2005 classifies patch repair products into two categories: structural and non-structural. The role of structural repairs, according to the DANSK-Standard (2004) and Soufi et al. (2016), is to restore the durability and load-carrying capacity of deteriorating structures whereas that of non-structural repairs is to restore durability, maintain aesthetics and to fill cavities. Structural and non-structural mortars are further

categorised into two classes based on their compressive strengths: R1 and R2 (for non-structural repairs) and classes R3 and R4 (for structural repair). A summary of the performance requirements for non-structural PRMs according to the EN 1504-3:2005 is presented in Table 3.3. Additional information regarding the values in Table 3.3 can be obtained in the EN 1504-3:2005. The performance requirements in Table 3.3 will be discussed in the subsequent subsections.

3.3.1 Shrinkage

Shrinkage mainly results from the movement of water within a porous material and its environment as explained in Section 2.4.1. The movement of water takes place throughout the life of the PRM. Restrained shrinkage results in the development of contraction forces which generate high tensile stresses which result in cracking and debonding (ICRI, 2003; Radlińska and Weiss, 2012; Silfwerbrand et al., 2011). For PRMs to be effective in service with respect to resistance to cracking; they ought to have a low shrinkage potential.

The relative dimensional changes between a surface repair material and an existing substrate affects bond, ability to carry loads, durability and appearance. The ACI (2003) also reports that repair materials are generally expected to be shrinkage-free or capable of shrinking without losing bond. ICRI (2003), however, reports that the chances of finding a patch repair material that can fill a repair cavity without shrinking - while having properties that are identical to the substrate in response to loads and changes in temperature and moisture - is unlikely. Baluch et al. (2002) - while analysing various test standards that have been in use in Hong Kong, USA, The Netherlands and Australia - report that there is a lack of standardisation of specifications addressing measurable and tolerable limits of free shrinkage strain. They further report the lack of standardisation as a contributing factor to cracking in PRMs in service. The performance requirements for shrinkage in non-structural PRMs as per the EN 1504-3:2005 are based on tests for restrained shrinkage done in accordance with the EN 12617-4. The EN 1504-3:2005 has not specified shrinkage requirements for class R1 non-structural PRMs. The EN 1504-3:2005 recommends a bond strength greater than 0.8 MPa after testing the repair product on a concrete substrate cast using w/b of 0.4 in R2 mortars.

3.3.2 Bond strength

Bond refers to the adhesion of an applied product or system to the concrete substrate. It is an important material property. Its importance is attributed to the need for repairs to: ensure that appropriate transmission of forces between the old and new material - in structural applications (Brandt, 2009; Cardon and Hiel, 1986) - or to adhere well to the existing concrete substrate - in structural and non-structural applications. A major objective of patch repair is to ensure the monolithic action between the repair

TABLE 3.3: Performance requirements for non-structural repair products - adapted from BSI (2005)

Performance characteristic	**Reference substrate**	**Test method**	**Non-structural requirements**	
			Class R1	**Class R2**
Compressive strength	None	EN 12190	$\geq$ 10 MPa	$\geq$ 15 MPa
Chloride ion content	None	EN 101517	$\leq$ 0.05%	
Adhesive bond	MC (0.40)	EN 1542	$\geq$ 0.8 MPa	
Restrained shrinkage/ expansion	MC (0.40)	EN 126174	No requirement	Bond strength after test $\geq$ 0.8 MPa
Carbonation resistance	None	EN 13295	No requirement	
Elastic modulus	None	EN 13412	No requirement	
Thermal compatibility: Part 1: freeze-thaw	MC (0.40)	EN 13687-1	Visual inspection after 50 cycles	Bond strength after 50 cycles $\geq$ 0.8 MPa
Thermal compatibility: Part 2 thunder shower	MC (0.40)	EN 13687-2	Visual inspection after 30 cycles	Bond strength after 30 cycles $\geq$ 0.8 MPa
Thermal compatibility: Part 4: Dry cycling	MC (0.40)	EN 13687-4	Visual inspection after 30 cycles	Bond strength after 30 cycles $\geq$ 0.8 MPa
Skid resistance	None	EN 13036-4	Class I: >40 units wet tested; Class II: >40 units dry tested; Class III: >55 units wet tested.	
CTE	None	EN 1770	Not required if tests 7, 8 or 9 are carried out, otherwise declared value	
Capillary absorption	None	EN 13057	No requirement	$\leq$ 0.5 kg.m^2.h$^{0.5}$

material and the concrete substrate. Sufficient bond between the concrete substrate and the PRM is, thus, a prerequisite for monolithic action and a primary requirement for successful repair (ACI546, 2003; Gillmer, 2012; ICRI, 2003; Lambe, 1988; Mallat and Alliche, 2006; Silfwerbrand, 1986; Silfwerbrand et al., 2011; Turatsinze et al., 2011).
Bond strength is broadly defined as the amount of stress required to separate an overlay from its substrate. It can be used as a quantitative measure of the bonding of a

repair material to an existing concrete substrate. There is no standard definition of bond strength - a challenge that has been highlighted by Naderi et al. (1986). The definition of bond strength depends on the state of stress that a structure is subjected to while in service. Thus, bond stress could either refer to the shear stress parallel to the interface or the tensile stress perpendicular to the interface (Gillmer, 2012). The lack of a clear definition of bond strength and a standard test method for bond strength makes it difficult to compare bond strengths that have been determined using various test methods. Naderi et al. (1986) report that the mere magnitude of bond strength obtained in, say tension, ought not be compared with the one from shear tests since the stress mechanisms that cause failure are different in both methods; and that the quoted tensile bond strength is the average, while the shear bond strength is the maximum shear stress obtained in torsion.

Adhesion is defined as the adherence of two materials in contact. It is a significant material property because PRMs ought to adhere to an existing substrate. The adhesion between a repair material and a substrate affects its service life, reliability and durability (Beushausen, 2005; Brandt, 2009; Czarnecki, 2008; Gillmer, 2012; Granju, 2001; Morgan, 1996; Sahmaran et al., 2014). The adhesion of a PRM to an existing substrate is a complex phenomenon. It involves different types of bond, namely: chemical bond (chemical reaction between the substrate and the repair material), mechanical bond (associated with the interpenetration of the repair material into the roughness and porosity of the substrate, resulting in mechanical anchorage) and physical bond (associated with the van der Waals and surface tension forces) (Bissonnette et al., 2008; Courard, 2000; Czarnecki, 2008).

The effectiveness of adhesion and bond strength between a PRM and the concrete substrate is dictated by: substrate properties (e.g., surface geometry and roughness, laitance layer, moisture condition, mechanical integrity and strength, microcracks, temperature at the time of application of the PRM, porosity, dampness, impurities), dimensions of the repair material, rheology of the repair material (viscosity, wetting/surface tension), interface factors (surface roughness, cleanliness and soundness, curing method, bond adhesive, humidity conditions), overlay compaction, method of testing, curing, age of the material, exposure environment, physical, mechanical and chemical properties of the repair material (tensile strength, modulus of elasticity, setting shrinkage, CTE and creep), type of repair material, the presence of bonding agents and workmanship (Al-Ostaz et al., 2010; Beushausen and Alexander, 2009; Beushausen et al., 2017; Bissonnette et al., 2008; Brandt, 2009; Cardon and Hiel, 1986; Carlswärd, 2006; Chorinsky, 1986; Cleland et al., 1986; Courard, 2000; Crosswell, 2009; Czarnecki, 2008; Hayakawa and Soshiroda, 1986; Luković, 2016; Mallat and Alliche, 2006; Morgan, 1996; Naderi et al., 1986; Ohama et al., 1986; Peier, 1986; Perez et al., 2008; Sahmaran et al., 2014; Silfwerbrand et al., 2011; Vaysburd et al., 2011). Information on how each of the listed parameters affects adhesion and bond strength can be found in the references cited.

Many tests and test procedures have been developed to assist in testing for bond strength directly or indirectly in concrete repairs. These tests comprise, but are not limited

to: direct tensile test, direct shear strength test, slant shear test, splitting prism test, three-point bending test, tensile pull-off test, push-out/push-off test and guillotine test (Al-Ostaz et al., 2010; ICRI, 2003; Mallat and Alliche, 2006; Sahmaran et al., 2014; Wall et al., 1986). Although some of the listed methods are less common in practice, Sahmaran et al. (2014) report that the splitting prism and slant shear test are used frequently because: they are easy to set up and perform, have a wide range of applications, are inexpensive and offer a greater reliability of results. The choice of any of these tests is generally informed by the availability of equipment and the information being sought. Care ought to be taken while comparing the test results from any of these methods without a thorough understanding of their strengths, weaknesses, assumptions and operating conditions. Carlswärd (2006) and Gillmer (2012), for example, report that bond strengths that have been measured using two different methods on the same specimen could differ by a factor of eight. Ohama et al. (1986) also report that the selection of an appropriate test method for adhesion ought to be informed by the ability of the test method to successfully reproduce the service conditions that the material under investigation would be subjected to.

The ACI503 (1993) recommends a pull-off value of 0.7 MPa for bond strength (subject to a revised limit which depends on the actual substrate conditions) as a minimum requirement. This minimum bond strength value is based on field experience, whereby, it was established that bond strengths that are lower than 0.7 MPa are a clear indication of serious problems that would require careful consideration (ACI503, 1993; ICRI, 2003). ICRI (2003) also reports that many specifiers recommend minimum bond strengths that range between 0.86 MPa and 1.2 MPa depending on specific project conditions. The test method that was used to determine the reported bond strengths, has been described within the ACI503 (1993). The EN 1504-3:2005 recommends that non-structural patch repairs ought to achieve an adhesive bond strength that is greater than 0.8 MPa. This bond strength ought to be tested in accordance with the EN 1542. The EN 1504-3:2005 further reports that the minimum bond strength of 0.8 MPa is not required where cohesive failure occurs in the repair material. Instead, the code requires that a minimum tensile strength of 0.5 MPa be achieved if cohesive failure occurs. Bond strength has also been used in the EN 1504-3:2005 as a proxy requirement of other performance characteristics such as: restrained shrinkage/expansion and thermal compatibility due to freeze-thaw, thunder shower and dry cycling.

3.3.3 Compatibility

Compatibility is defined as the balance of physical, chemical, aesthetic and electrochemical properties and dimensions between the repair and existing substrate. This balance is necessary for the optimal performance of repairs because repairs ought to withstand the stresses and strains induced by the total load envelope without distress or deterioration in a specified environment over a designated period (Brandt, 2009; ICRI, 2003; Luković, 2016; Morgan, 1996). It is important to note that compatibility is not the same

as the similarity in properties. According to Luković (2016), compatibility refers to the well-designed interactions that exist between the repair material and the substrate under different loading and exposure conditions. Material incompatibility is a major course of repair failure (Bagheri and Hashemi, 2006; Baluch et al., 2002; ICRI, 2003; Lambe, 1988; Mangat and O'Flaherty, 2000). Brandt (2009) suggests that the compatibility of repair materials with their existing substrates ought to be investigated analytically and thereafter verified experimentally in the laboratory and in situ. Compatibility of repairs comprise various aspects, namely: thermal, chemical, physical/dimensional and electrochemical.

Thermal compatibility is the property of a repair product or system, when bonded onto a prepared concrete substrate, to accommodate cyclic changes in temperature (BSI, 2005; Vaysburd et al., 2008). It is particularly important in large patches. A large difference between the thermal properties of a repair material and the concrete substrate results in significant stress build-up due to changes in temperature; consequently, resulting in failure either at the interface or within the material of lower strength (ACI546, 2003; ICRI, 2003). Two suggestions have been postulated towards achieving thermal compatibility. Fowler and Treviño (2011), on the one hand, suggest that to achieve thermal compatibility, the CTE of the repair material ought to be lower than that of the concrete substrate. The ACI546 (2003), on the other hand, suggests that thermal compatibility can be achieved when the CTE of the repair material is similar to that of the concrete substrate. The author believes that the reasons that underpin any of these two distinct suggestions are based on the purpose of the repair material within the structure i.e., whether the repair is structural or not.

Chemical compatibility entails the selection of repair materials in a manner that ensures that they do not have any adverse effects on the repaired component or structure. Electrochemical compatibility relates to the ability of a repair system to inhibit subsequent corrosion of reinforcement within the repair and in the substrate. Vaysburd and Emmons (2000) report that electrochemical incompatibility is responsible for the 'ever-present' risk of corrosion in concrete repairs. Electrochemical compatibility is determined by properties such as resistivity (or conductivity) and differences in electrical potential. Morgan (1996) defines dimensional compatibility as the ability of a material to withstand volume changes without loss of bond and delamination. Dimensional compatibility also includes the ability of a material to transfer its proportion of applied load without distress. It includes material aspects such as drying shrinkage, thermal expansion, creep and modulus of elasticity (Luković, 2016). The dimensional compatibility of PRMs relative to their substrate is important because differential volume changes between PRMs and their concrete substrates results in cracking. The lack of dimensional compatibility is manifested in the form of excessive deformations - due to shrinkage or thermal actions. Dimensional compatibility is influenced by: the size, shape and thickness of the area being repaired, the amount of reinforcing and anchorage (if any), modulus of elasticity, strain capacity and creep of the repair material (Morgan, 1996). The ideal compatibility requirements for repair materials are summarised in Table 3.4.

TABLE 3.4: Ideal compatibility requirements for repair materials - adopted from BRE-DME-D53 (2003); Luković (2016); Morgan (1996)

Property	**Ideal relationship of repair material to concrete substrate**
Curing and long-term shrinkage	Higher
Shrinkage strain	Lower
Fatigue performance	Higher
Creep coefficient (for repairs in compression)	Lower
Creep coefficient (for repairs in tension)	Higher
Strain capacity	Higher
CTE	Same
Elastic modulus in compression, tension and flexure (structural mortars)	Same
Elastic modulus (non-structural mortars)	Lower
Poissons ratio	Same
Tensile, Compression and Flexural strength	Higher
Adhesion in tension and shear	Higher
Porosity and resistivity	Same
Chemical reactivity	Lower

It is important to note, from Table 3.4, that the compatibility requirements for creep depend on whether creep causes desirable or undesirable effects. Other aspects of compatibility that are critical to the performance of a repair system comprise: bond compatibility (the development of a satisfactory level of bond between the substrate and the repair material), permeability compatibility and structural and mechanical compatibility. Specific details regarding these aspects of compatibility can be obtained from Morgan (1996), Brandt (2009) and Luković (2016). The EN 1504-3:2005 only addresses the performance requirements for thermal compatibility with respect to freeze thaw, thunder shower and dry cycling in non-structural patch repair products. Specific values of these performance requirements and their supplementary information have been provided in Table 3.3. Owing to the diverse nature of compatibility and the seemingly contradictory requirements that are needed to realise them in repairs in service, Morgan (1996) advises that a holistic approach ought to be undertaken while evaluating the suitability of a specific repair material for service.

3.3.4 Strength

Strength is a broad term that refers to the ability of a material to resist stresses emanating from compressive, tensile and flexural forces. It can be categorised into bond strength, tensile strength, flexural strength and compressive strength. Tensile strength is the ability of a material to withstand tensile stresses (ICRI, 2003). Repair materials ought to possess a high tensile and flexural strength and adequate compressive strength depending on the part of the structure where they will be used. Ghezal and Assaf (2014), while investigating the effects of different binder types on their corresponding properties

on the susceptibility of self-compacting concrete to cracking, report that a high tensile strength does not always translate into a high resistance to shrinkage cracking. Flexural strength measures the ability of a repair material to resist bending. It, therefore, ought to be specified when a material is likely to be subjected to bending (ICRI, 2003).
The compressive strength of a repair material is a basic measure of its ability to resist compressive forces (ICRI, 2003). Although it is an important and commonly used material property, Silfwerbrand et al. (2011) report that compressive strength has a negligible influence on important material properties such as bond strength. Compressive strength can only become a critical factor if a PRM is used for structural purposes because structural mortars are intended to be load-bearing. Non-structural PRMs are generally intended to restore the surface profile and durability of the substrate. Their compressive strength is, thus, not very relevant. Baldwin and King (2003), further report that the compressive strength of non-structural mortars is usually specified in the form of a minimum strength requirement; with this requirement being used as a crude approximation of durability. The EN 1504-3:2005 performance requirements for the compressive strength of non-structural class R1 and class R2 PRMs are 10 MPa and 15 MPa respectively. These strengths ought to be tested in accordance with the EN 12190.

3.3.5 Miscellaneous

Non-structural PRMs ought to possess the following properties: high cracking resistance (or low cracking tendency), adequate setting time, trowelability and workability, low modulus of elasticity, high tensile relaxation and good durability. The workability of PRMs, for example, determines the ease with which it is mixed, placed, consolidated and finished to a homogeneous condition (Baldwin and King, 2003; Kellerman and Crosswell, 2009; Mehta and Monteiro, 2006; Taylor, 1997). Whereas a quantitative assessment of the aesthetics of a repair is subjective and indeterminate; it ought to be considered. Baldwin and King (2003) report that repairs ought to be finished to be flush with the surrounding concrete surface and, when overcoated, their presence should not be detectable.
ICRI (2003) and ACI546 (2003) report that the modulus of elasticity of a structural repair material ought to be similar to that of the concrete substrate so that uniform load transfer can be achieved across the repaired section. Morgan (1996) reports that the likelihood of achieving a modulus of elasticity that is similar to the substrate is higher in portland cement-based repair materials than in polymer-modified repair materials. Repair materials with a high modulus of elasticity, as reported by Morgan (1996) and the DANSK-Standard (2004), ought to be avoided as they may cause the repaired area to attract undue load. ICRI (2003) advises that a low modulus of elasticity ought to be specified for non-structural PRMs. Materials with a low modulus of elasticity, with all other factors held constant, have a reduced potential for cracking and delamination. ICRI (2003) further reports that the creep of repair materials, in structural repairs, ought to be like that of the concrete substrate. Higher creep, however, is advantageous

for protective repairs. Scaling refers to the flaking or peeling away of the near-surface portion of hardened concrete or mortar as a result of the hydraulic and osmotic pressure caused by freezing. Scaling resistance ought to be specified when a likelihood of the repair material being subjected to de-icing salt exists. ICRI (2003) recommends that the scaling resistance of a repair material ought to be less than 0.5 kg/m^2 loss at 50 cycles when the tests are conducted according to ASTM C 672.
Sulphate attack causes chemical decomposition of certain binder compounds in the HCP. The resistance to sulphate ions ought to be specified for materials exposed to the following environments: decaying organic matter, chemical processes effluent, agricultural runoff and waste water treatment, piers, dams, bridge columns, buried concrete pipes, waste water treatment facilities, transmission tower footings and highway pavements. The ASTM subcommittee which developed the ASTM C 1012 recommends the adoption of the following performance criteria for sulphate resistance: moderate sulphate resistance - 0.10% maximum expansion at 6 months and high sulphate resistance - 0.05% maximum expansion at 6 months ICRI (2003). There are no clearly defined performance requirements for non-structural PRMs with respect to the South African durability index (DI) testing method. Nevertheless, the information in Table 3.5 could help inform the development of performance requirements for non-structural PRMs.

Table 3.5: Durability classification based on the UCT DI prediction tests - adopted from Gillmer (2012)

Durability class	**OPI (log scale)**	**Sorptivity (mm/hr0.5)**	**Conductivity (mS/cm)**
Excellent	>10	<6	<0.75
Good	9.5 - 10.0	6 - 10	0.75 - 1.50
Poor	9.0 - 9.5	10 - 15	1.50 - 2.50
Very poor	<9.0	>15	>2.50

3.4 The influence of mix design parameters on cracking of PRMs

PRMs are intended to extend the service life of deteriorating concrete structures. To achieve this, they ought to possess a range of properties such as cracking resistance, durability and aesthetics, among other performance requirements (Arito et al., 2016c). These performance requirements are influenced by mix design parameters. The selection of mix design parameters for PRM mixes, however, is a complex process that must be informed by the aspects discussed in Section 3.1.
Owing to the complexity of the mix design process and the need to address various, and sometimes conflicting needs and requirements from many stakeholders; it is crucial that this process is done carefully. The selection of mix design parameters ought to be founded on a solid understanding of the influence of multiple mix design parameters

and their corresponding interactions, on the desired performance requirements. The interactions that exist among mix design parameters complex and poorly understood (Arito et al., 2016c; Kellerman and Crosswell, 2009; Mehta and Monteiro, 2006). The subsequent subsections will attempt to elucidate the current state of knowledge from literature regarding the individual influence of selected mix design parameters - binder-related parameters, water content, w/b, aggregates, chemical admixtures and curing - on cracking and crack-determining material properties of PRMs.

3.4.1 Binder-related parameters

Binder-related parameters play a critical role in the cracking performance of PRMs. Aspects of binder-related parameters that will be discussed comprise: binder content, binder type, binder composition/chemistry and other miscellaneous binder properties.

3.4.1.1 Binder content

Cement content affects shrinkage (Mehta and Monteiro, 2006; Neville, 1995). Increasing the cement content, at a constant w/b, results in a corresponding increase in shrinkage. However, at a given workability, which approximately means a constant water content, shrinkage is unaffected by an increase in the cement content, or may even decrease, because the w/b is reduced and the material is, therefore, more capable of resisting shrinkage (Neville, 1995). A reduction in cement content results in a corresponding reduction in heat of hydration and shrinkage (Fowler and Treviño, 2011). Also, an increase in cement content increases flexural strength (Braga et al., 2014; Schulze, 1999).

3.4.1.2 Binder type

The type of binder and its particle size influences crack-determining material parameters such as water requirement and water demand (Gallias et al., 2000; Yurdakul et al., 2014), creep (Atrushi, 2003), tensile strength, tensile relaxation, creep and shrinkage (Ghezal and Assaf, 2014). Thus, the type of binder used to make a PRM dictates its susceptibility to cracking. The Concrete-Society (2003a) reports that cement type and composition have a minimal influence on long-term drying shrinkage. The Concrete-Society (2003a) also acknowledges that the type of cement is important as far as it affects the water content of a specific mix. Tazawa and Miyazawa (1995) report that alumina cements and high early-strength cements exhibit early autogenous shrinkage which ultimately lead to large shrinkage. Pane and Hansen (2002) report that tensile creep is reduced in cement-based materials made using blended cements. Mallows (1985) reports that creep in cementitious materials increases with the type of cement in the following order: alumina, rapid hardening, ordinary portland, portland blast furnace, low-heat and portland pozzolan. Al-Gahtani and Khan (2003), while comparing shrinkage in cementitious materials made from blended and portland cement, report that greater early-age drying shrinkage is experienced in specimens made from blended cement than those made from

portland cement. The tendency of blended cements to undergo early-age cracking is highly sensitive to the curing period.

Supplementary cementitious materials (abbreviated as SCMs hereafter) such as FA, SF and slag, have been used to make PRMs. Their use is associated with energy conservation, cost reduction and environmental sustainability. SCMs modify the kinetics of hydration (Choi et al., 2012; Jaufeerally, 2001; Lawrence et al., 2003; Ortega et al., 2012; Sakai et al., 2005; Toutanji et al., 2004), minimise shrinkage and the heat of hydration, improve workability, durability, mechanical strength, elastic modulus, tensile strength, creep and relaxation to varying degrees as well as reduce the tendency to bleed and segregate (Carrasco et al., 2005; Concrete-Society, 2003a; Khan et al., 2000; Kovler et al., 1999b; Langan et al., 2002; Li et al., 2012; Marchand et al., 1996; Pane and Hansen, 2008a,0; Poppe and Schutter, 2005; Taylor, 2014; Uys, 1983; Yurdakul et al., 2014). Yurdakul et al. (2014) report that the incorporation of large quantities of a single type of SCM (binary mixtures) may extend setting time. Limestone fillers accelerate chemical shrinkage and hydration (Bouasker et al., 2008; Nepomuceno et al., 2012); thus, their incorporation into PRM mixes could increase their susceptibility to cracking.

a) Fly ash

The use of fly ash (hereafter referred to as FA) and slag results in: reduction in the amount of water required to achieve a given consistency, improved workability, reduced porosity and improved durability (Bouzoubaâ and Fournier, 2003; Langan et al., 2002; Mehta and Monteiro, 2006; Ortega et al., 2012; Taylor, 2014; Toutanji et al., 2004; Uys, 1983; Yurdakul et al., 2014). The reduction in the volume of water required to achieve a given consistence could further reduce the propensity to drying shrinkage (Al-Gahtani and Khan, 2003; Kanna et al., 1998; Neville, 1995; Pane and Hansen, 2002). The reduction in the volume of water for a given consistence, however, is not clearly defined. It depends on the method of mix design and the quality and quantity of FA (Uys, 1983). The volume of FA in a mix dictates the magnitude of drying shrinkage that would be experienced in a material using the mix in its hardened state. Autogenous and drying shrinkage are reduced when FA is used in correct quantities; and is increased when excessive amounts are used (Banthia and Gupta, 2009; Li et al., 2012; Uys, 1983). Brandt (2009) reports that FA increases drying shrinkage. Banthia and Gupta (2009), however, report that the exact relationship between the amount of FA in a mix and shrinkage is elusive.

While there lacks a clear definition of the 'the correct quantity' of FA that could be used in a mix; Uys (1983) and Lam et al. (1998) report that the optimum proportions of FA that can be used to replace cement is informed by: the pozzolanic activity of the FA, the richness of the mix, the grading of the aggregates, the w/b and the material properties that the FA is intended to improve. Banthia and Gupta (2009) and Brandt (2009) report that mixes with FA are more susceptible to cracking in comparison with plain cement mixes. They attribute the increased tendency to crack in FA-incorporated

mixes to their low initial matrix strength and the higher amount of water available for evaporation.

FA reduces the rate and heat of hydration, autogenous shrinkage, tensile strength, the rate of strength gain, drying shrinkage, wetting expansion, thermal volume changes and contraction cracking (Bentz, 2008; Brandt, 2009; Choi et al., 2012; Fowler and Treviño, 2011; Langan et al., 2002; Lawrence et al., 2003; Li et al., 2012; Pane and Hansen, 2002; Sakai et al., 2005; Taylor, 2014; Toutanji et al., 2004; Uys, 1983). The reduction in the rise in temperature during hydration depends on the fineness of the FA and its volume. Choi et al. (2012) reports that the rise in temperature decreases with an increase in the volume of FA in the mix. The effect of the fineness of FA at various replacement levels on the heat of hydration is shown in Figure 3.2. Note: R refers to the amount of replacement of cement with FA.

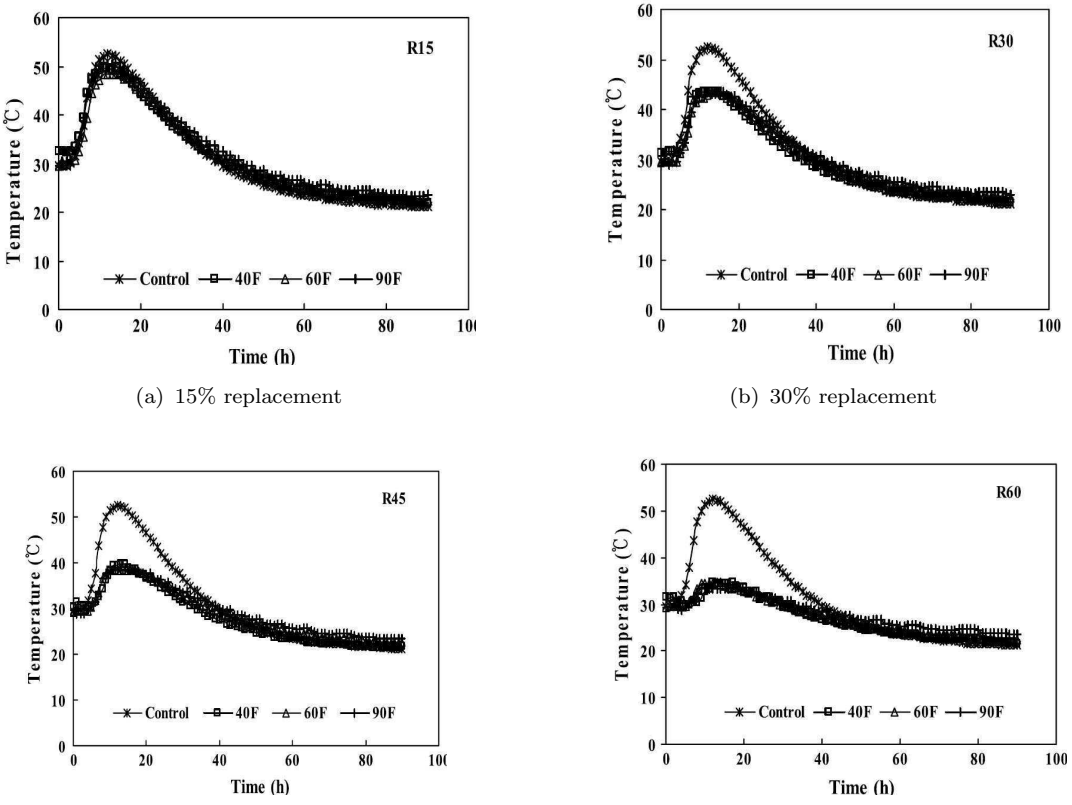

(a) 15% replacement

(b) 30% replacement

(c) 45% replacement

(d) 60% replacement

FIGURE 3.2: Temperature rise vs. FA fineness at various replacement levels - adopted from Choi et al. (2012)

Choi et al. (2012) attributes the reduction in temperature rise during hydration in FA mixes to the dilution of the cement and the slow pozzolanic reaction between FA and calcium hydroxide from the hydrating cement. Reducing the rise in heat of hydration is desirable because it reduces the susceptibility to cracking from thermally-induced

stresses. A reduction in tensile strength due to the addition of FA is undesirable because PRMs need sufficient tensile strength to resist the tensile stresses associated with restrained shrinkage deformations. Lam et al. (1998), while investigating the effect of the volumetric proportion of FA and SF on concrete properties, found out that the FA increases the splitting tensile strength of cylindrical concrete specimens vis-á-vis those made from plain portland cement. An increase in tensile strength, due to the use of FA, has also been reported by Uys (1983). Choi et al. (2012) while investigating the effect of FA fineness on tensile strength reports that the tensile and compressive strength increases with an increase in FA fineness. They attributed the increase in strength with FA fineness to its reactiveness and its packing effect in the small voids in the mortar which improves the interfacial bond between the cement paste and aggregates.

Uys (1983), Toutanji et al. (2004) and Choi et al. (2012) further report that FA increases compressive strength at later ages. Uys (1983) attributes the increase in strength to the additional cementitious material provided by the FA during hydration. Choi et al. (2012) attribute the delay in early strength development to the relatively low surface area of FA which affects the pozzolanic reaction during hydration. Uys (1983) and the Concrete-Society (2003a) have also reported that the use of GGBS and FA simultaneously produces concrete with a high modulus of elasticity and reduced creep properties at later ages. The high modulus of elasticity and reduced creep properties are undesirable in PRMs. They offset the benefit of reduced water content and shrinkage. The Concrete-Society (2003a) reports that the magnitude of these negative effects due to the use of FA are clearly insignificant when compared to other factors that govern cracking due to long-term drying shrinkage.

Wong et al. (1999) while studying the effects of cement-FA replacement levels on various mortar mixes found that replacing cement with 15 to 25% FA did not affect flexural strength and fracture toughness at 28 days and 90 days significantly. Their study also showed that high FA replacement levels (i.e., 45% and 55%) reduced flexural strength and fracture toughness. Whereas the observations by Wong et al. (1999) support those of Choi et al. (2012), they seem to contradict that of Uys (1983), who reported that FA increases flexural strength. Rao and Prasad (2002), while investigating the effect of various concentrations of FA and SF on the properties of mortars and cement pastes, observed that the addition of 15% FA improved interfacial bond strength at 28 days. The improvement in bond strength has also been reported by Uys (1983), Tanyildizi et al. (2006) and Sahmaran et al. (2014). The improvement in interfacial bond strength has been attributed to either an improvement in microstructure (due to the microfiller effect) or the ability of FA to hinder the growth of calcium hydrate crystals. Banthia and Gupta (2009) have also reported that replacing cement with Class C FA in the range of 0% and 15% increases the susceptibility to cracking. Their study also observed that there was a threshold cement replacement rate (around 20%) at which the beneficial effects of FA addition on shrinkage cracking occurred.

b) Condensed silica fume

Silica fume (SF), when added to cement, acts as a chemical inert filler by improving its structure; and as a pozzolan by reacting chemically with calcium hydroxide formed during the hydration of cement (Rao, 2003; Rao and Prasad, 2002; Zelić et al., 2000). While SCMs like CSF and FA have been clearly understood to contribute to an enhanced durability in cementitious materials; there is a lack of a common understanding of the role of these SCMs on other important crack-determining material properties such as tensile strength. There are contradictory reports on the contribution of CSF to tensile strength - an observation that has also been reported by Toutanji et al. (1999). Whereas Lam et al. (1998), Gao et al. (2002), Atrushi (2003) and Bhanja and Sengupta (2005) - while undertaking various unrelated studies - report that the incorporation of CSF in cementitious mixes, with all other factors held constant, improves tensile, split tensile and flexural strengths. Toutanji et al. (1999) and Abdelkader et al. (2010) report that the contribution of CSF to tensile strength improvement is negative and insignificant respectively. Lam et al. (1998) attributed the increase in tensile strength with the addition of CSF to an improved interfacial bond between the paste and the aggregate. Toutanji et al. (1999) investigated the effect of CSF content on the mechanical properties of high strength cement pastes and mortars. Their study concluded that the addition of CSF decreases the tensile strength of cement pastes and mortars; with the decrease in strength being greater in cement pastes than in the mortar as shown in Figure 3.3.

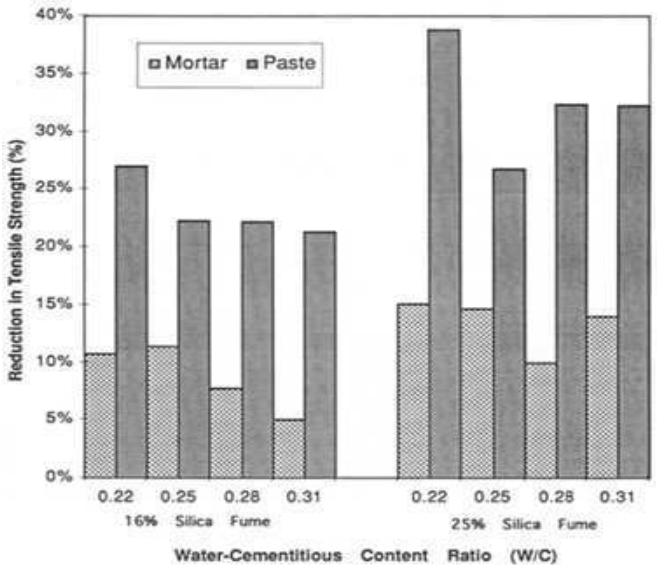

FIGURE 3.3: Percentage reduction in tensile strength vs. the percentage of SF in cement paste and mortar - adopted from Toutanji et al. (1999)

The reduction in tensile strength due to an increase in the quantity of CSF was attributed to an increase in microcracking that results from autogenous shrinkage - a

phenomenon that mainly affects the tensile and flexural strengths in high strength cementitious materials. Toutanji and El-Korchi (1995) and Igarashi et al. (2000b) have, in two separate and unrelated studies, also reported that CSF do not strengthen cement pastes and mortars with low w/b. Igarashi et al. (2000b) specifically reports that the addition of CSF in mortars with extremely low w/b - 0.24 and 0.3 - does not always result in an increase in strength; but a reduction in strength - a phenomenon that could be attributed to reduction in the quantity of water available for the pozzolanic reaction due to self-desiccation. The incorporation of CSF in mortars with moderate to relatively high w/b increases compressive strength. This improvement in strength can be attributed to the formation of an improved aggregate matrix bond which results in an improved interlock between the paste and the aggregates and the formation of a less porous interfacial zone (Toutanji and El-Korchi, 1995).

Rao and Prasad (2002) and Toutanji et al. (2004), while investigating the effect of CSF content on material properties in two different and independent studies, observed that the replacement of cement by 8% CSF resulted in the highest improvement in tensile and compressive strength. They attributed this improvement in tensile strength to a more discontinuous and impermeable pore structure that results from CSF addition and the improvement in bond between the hydrated cement matrix and the aggregate.

The densification of the microstructure through the addition of CSF reduces the rate of moisture loss (Alexander and Beushausen, 2009; Neville, 1995). This densification of the paste implies that drying shrinkage takes place at a slower rate in CSF mixes. However, it has been observed that there is no substantial difference between the magnitude of the final shrinkage in specimens made using CSF and other binders. Baluch et al. (2002), Atrushi (2003), Brandt (2009) and Li et al. (2012) report that the addition of CSF increases free plastic shrinkage and autogenous shrinkage. Atrushi (2003), further reports that the increase in autogenous shrinkage would be observed clearly when autogenous shrinkage is recorded immediately after casting - i.e., when the cementitious mix has no measurable elastic modulus. However, in instances where autogenous shrinkage is measured after 24 hours from the time of casting, the addition of CSF results in a reduction in autogenous shrinkage. Brandt (2009) attributes the increased autogenous shrinkage to pore refinement.

Baluch et al. (2002) also report that the incorporation of CSF reduces the time to crack and increases crack widths. The increase in crack widths is directly proportional to the volume of CSF substituted into a cementitious mix. Kovler et al. (1999a) and Igarashi and Kawamura (2002) have further reported that the effects of the densification of the microstructure, due to the addition of CSF, depend on the age of the paste. This observation, could thus explain the seemingly contradictory observations between some of the reported studies. Igarashi et al. (2000b) reports that CSF increases crack widths in mortar specimens with extremely low w/b. Toutanji and El-Korchi (1995), Rao (2001a), Hammer (2001), Pane and Hansen (2002), Al-Gahtani and Khan (2003) and Rao (2003) report that increasing the content of CSF in a mix results in a corresponding increase in water demand, autogenous, plastic and drying shrinkage. Alexander and Beushausen

(2009), however, report that the effect of CSF content in a mix on shrinkage is little - especially when the volume of CSF is less than 10% by mass of cement. This view has also been supported by results from the study by Atrushi (2003).
The densification of the paste - through the addition of CSF - improves compressive strength, modulus of elasticity, bonding, durability and resistance to corrosion of reinforcing steel (Atrushi, 2003; Khan et al., 2000; Toutanji and El-Korchi, 1995). The improvement in durability can be attributed to the reduced permeability (Rao, 2003; Taylor, 2014; Toutanji and El-Korchi, 1995). An increase in CSF content above 8% results in a drastic reduction in durability (Toutanji et al., 2004). Increasing the content of CSF in a paste decreases its air content and workability (Rao, 2003; Toutanji and El-Korchi, 1995). The decrease in workability has been attributed to the higher specific surface of CSF which needs more water for complete hydration and workability. Increasing the content of CSF in a mix - up to a replacement level of 10% - increases its compressive strength. The increase in compressive strength could be attributed to the transformation of large pores into finer pores due to the pozzolanic reaction. A reduction in compressive strength is experienced when the quantity of cement replaced with CSF exceeds 10% (Rao, 2003; Toutanji et al., 2004). Baluch et al. (2002) and Atrushi (2003) report that the creep of CSF concrete is generally smaller than that of plain concrete with equal w/b if the load is applied when the concretes are well matured. CSF, however, increases tensile creep at early ages (Atrushi, 2003).

c) Ground granulated blastfurnace slag

Cementitious materials cast using blast furnace slag cements are characterised by high workability, reduced heat of hydration, increased rate of bleeding (at replacement levels that are greater than 60%), slow rate of setting, large shrinkage, increased tensile creep and low cracking sensitivity (under isothermal and restrained conditions) (Brandt, 2009; Concrete-Society, 2003a; Darquennes et al., 2011b; Jaufeerally, 2001; Kanna et al., 1998; Neto et al., 2008). Luković (2016) reports that slag reduces the tensile strength at the interface between a repair material and the concrete substrate at 28 days. Brandt (2009) reports that slag improves long term strength if proper curing is ensured. The fineness of blast furnace slag influences the magnitude of early age shrinkage (Jaufeerally, 2001; Tazawa and Miyazawa, 1995); with Tazawa et al. (1989) attributing the rate of drying of slag to its specific surface and the type of slag. At shorter curing times, an increase in specific surface area of slag in concrete results in a decrease in drying shrinkage and vice versa. Slag mortars with a high specific surface experience large drying shrinkage. Tazawa and Miyazawa (1995) have also reported that the magnitude of autogenous shrinkage increases proportionally with an increase in the percentage of cement that has been replaced by blast furnace slag up to 90%. Darquennes et al. (2011a) attributes this phenomenon to the slow hydration and high capillary porosity of materials made using blast furnace slag. Tazawa et al. (1989), while studying shrinkage in concrete made using w/b of 0.5, observed that the drying shrinkage of concrete containing slag was nearly

equal to that of concrete without slag at shorter drying times. The drying shrinkage has been observed to be lower in slag concrete that in the one without slag at longer curing times. Luković (2016) reports that the finer pore structure that results from the addition of slag in cement-based materials leads to a higher autogenous shrinkage in comparison to OPC. An increase in autogenous shrinkage would translate into a higher probability of cracking in a repair system. Thus, it can be inferred that the beneficial effect of a fine microstructure can easily be outweighed by the higher stresses induced by autogenous shrinkage.

Ground granulated blastfurnace slag (abbreviated as GGBS hereafter) improves durability. Luo et al. (2003), Toutanji et al. (2004) and Brandt (2009) report that replacing portland cement with GGBS results in: an improvement in pore structure, an increase in chloride binding capacity, a decrease in chloride diffusion coefficient and resistance to degradation by magnesium brine. The improvement in chloride binding capacity can be attributed to the fact that GGBS forms more calcium chloroaluminate hydrate (Friedels salt) which can bind more chloride ions. Slag also produces mortars that have low early-age compressive and tensile strengths and a high compressive strength at later ages (Carrasco et al., 2005; Concrete-Society, 2003a; Taylor, 2014; Tazawa et al., 1989; Toutanji et al., 2004). The low early age strength could be attributed to the slow hydration reaction of slag. Brandt (2009) further reports that slag reduces the rate of heat evolution as shown in Figure 3.4.

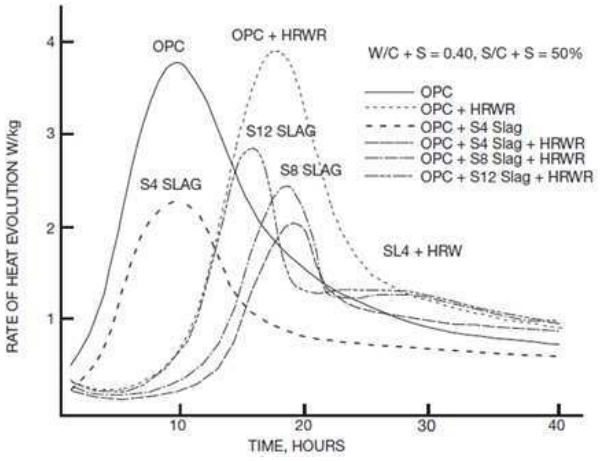

FIGURE 3.4: Rate of hydration heat as a function of time for various concrete mixes - adopted from Brandt (2009)

Concrete-Society (2003a) further reports that the magnitude of the reduction in tensile strength, due to the replacement of cement with slag, exceeds the benefit gained from the reduction in temperature due to the slow rate of hydration. Concrete made using slag creeps less than non-slag concrete (Tazawa et al., 1989). A study by Carrasco et al. (2005) on specimens made from ternary cement mixes containing slag and limestone fillers reports that the addition of slag - up to 22% - increases flexural strength.

3.4.1.3 Cement fineness

The effect of the composition and fineness of cement on shrinkage has been characterised by many contradicting views; an observation that has also been made by The Concrete-Society (2003a). On the one hand, Uys (1983), Tazawa and Miyazawa (1995), Mehta and Monteiro (2006), Neville (1995) and Bentz et al. (2008) report that the fineness and composition of cement, within limits, influences shrinkage; with cements with finer grains experiencing high shrinkage from an early age. Uys (1983) further reports that an increase in the fineness of cement from 300 to 500 kg/m^2, for example, increases shrinkage by approximately 15%. The Concrete-Society (2003a) and Alexander and Beushausen (2009), on the other hand, report that the influence of the fineness of cement on shrinkage is insignificant. This contrary view is premised on the fact that as the fineness of cement is increased, its tendency to shrink more (which is significant only at early age) is offset by the faster development of tensile strain capacity to resist shrinkage. Mallows (1985) further reports that fine portland cements exhibit high creep. The high creep in fine cements, however, is complicated by the fact that fine cements develop strength faster due to an increase in hydration rate; thus, the effect, although present, may be hidden. Fine cements have an increased heat release rate and a corresponding temperature rise in semi-adiabatic experimental conditions as shown in Figure 3.5. Fine cements can, thus, lead to large temperature rises within and large temperature gradients, both of which increase the risk of early age cracking (Bentz et al., 2008).

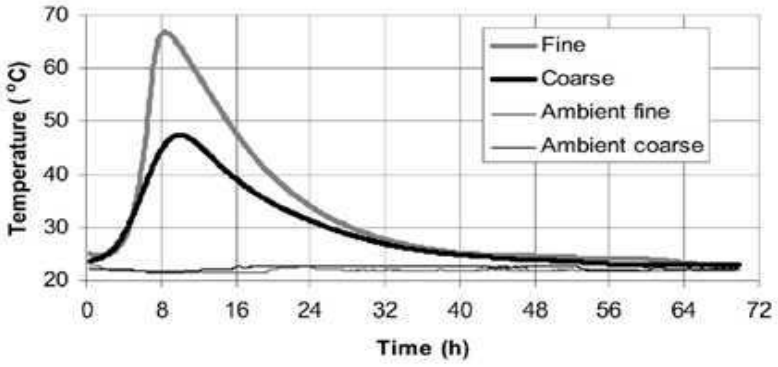

FIGURE 3.5: Semi-adiabatic temperature rise for w/c = 0.35 cement pastes - adopted from Bentz et al. (2008)

3.4.1.4 Chemical composition

There are equally conflicting views regarding the influence of the chemical composition of cement on shrinkage - an observation that has also been reported by Smaoui et al. (2005). He and Li (2005), Smaoui et al. (2005), Alexander and Beushausen (2009), Wittmann (2008) and Fowler and Treviño (2011), on the one hand, assert that cements with high alkali contents are susceptible to high shrinkage. He and Li (2005) further report that the

form, amount and type of alkali influence early hydration reactions and microstructure development of cement-based material significantly. Smaoui et al. (2005) - while referring to a research on 53-year old concrete and cement paste specimens - and Wittmann (2008) also report that the amount of drying shrinkage cracking in cement pastes and mortars is directly proportional to the alkali content in the cement. Cements with a high alkali content produces mortars and pastes with: a high dynamic modulus of elasticity, low flexural strength (modulus of rapture), low modulus of elasticity under compression, reduced tensile strength, low splitting and direct tensile strength, accelerated hydration, accelerated strength development in the short term, increased early-age strength and low compressive strength after 28 days (He and Li, 2005; Smaoui et al., 2005). In the case of concretes, high alkali contents result in a reduction in drying shrinkage (Smaoui et al., 2005). The low compressive strength characterised with high alkali contents can be attributed to the less dense microstructure due to a weaker (reticular) and porous microtexture that is characteristic of high alkali cement pastes (Smaoui et al., 2005). The effect of alkalis on cracking time and flexural strength of mortar specimens is presented in Figure 3.6 and Figure 3.7 respectively.

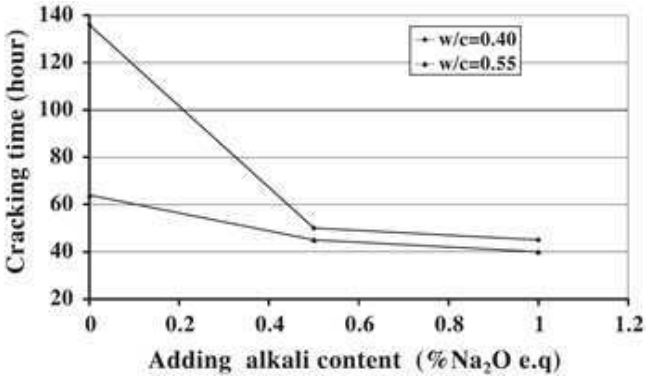

FIGURE 3.6: Effect of NaOH content and w/c on initial cracking time of mortars - adopted from He and Li (2005)

Neville (1995), on the other hand, reports that the chemical composition of cement does not affect shrinkage. Neville (1995), further asserts that cements that are deficient in gypsum exhibit a greatly increased shrinkage because the initial framework established in setting determines the subsequent structure of the paste and thus influence the gel/space ratio, strength and creep. From a review of literature, it is evident that there is a lack of common understanding on the exact influence of various binder-related parameters on most crack-determining material properties. While much effort has been expended in the understanding of binder-related parameters; there are many contradictory observations that have been postulated and reported by many studies - a fact that has also been observed and acknowledged by Uys (1983). It is, thus, important that fundamental research is undertaken to clarify some of these contradictions that have been highlighted

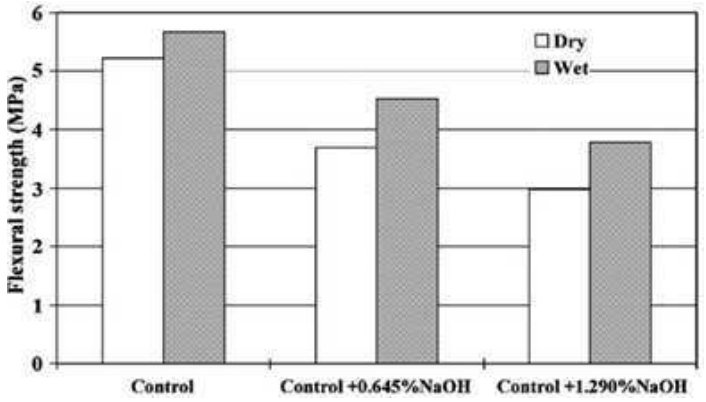

FIGURE 3.7: Flexural strength of mortars at the age of initial cracking - adopted from He and Li (2005)

and provide reliable information that would guide the choice of binder-related parameters for effectives PRMs.

3.4.2 Water content

The water requirement of a mix is the quantity of water required to obtain a neat cement paste of standard consistency. It is an important mix design parameter in cement-based materials; and depends on the properties of materials used in a mix such as the specific surface area, cement type, aggregate morphology, size and packing and the volumetric proportion of fine material (Gallias et al., 2000). Water content affects shrinkage as far as it reduces the volume of the restraining aggregate. Water content would, therefore, qualitatively indicate the order of drying shrinkage to be expected (Alexander and Beushausen, 2009; Neville, 1995). For given materials and conditions, the higher the water content, the higher the susceptibility to drying shrinkage and the greater the tendency to crack (Crosswell, 2009). Increasing the free water content above the amount required to achieve the required rheological properties further increases the susceptibility to segregate and bleed. High water contents also increase the porosity of the hardened material, reduce the mechanical properties and durability, reduce resistance to permeation and increase shrinkage and creep deformations (Acker and Ulm, 2001; Mechtcherine, 2011).

3.4.3 Water:binder ratio

The HCP is the major source of shrinkage and relaxation in cement-based materials. It plays an important role as far as shrinkage-induced cracking is concerned. The water:binder ratio (also referred to as the w/b hereafter) is directly related to the pore system of the paste (Popovics and Ujhelyi, 2008). The porosity of the paste, and its associated interconnectivity, influences important crack-determining material properties

such as tensile strength, elastic modulus and permeability (Abdelkader et al., 2010; Bester, 2015; Yurdakul et al., 2014; Yurtdas et al., 2006). The w/b also influences creep and shrinkage; and has been reported by Rixom and Mailvaganam (1999), Banthia and Gupta (2009) and Bentz et al. (2008) as one of the most important factors affecting shrinkage cracking. While the relationship between the w/b and compressive strength, as described by Abrams formula, is direct and well-established (Bentz et al., 2009; Nagaraj et al., 1990; Popovics and Ujhelyi, 2008; Rao, 2001b); its relationship with cracking is quite complex and incorporates other factors inter alia.

Uys (1983) reports that increasing the w/b increases the potential for shrinkage; with the effect being more pronounced with a decrease in aggregate content by volume. Atrushi (2003) - while referring to other studies - reports that low w/b lead to more pronounced volume reduction, earlier build-up of internal tensile stresses and greater sensitivity to early cracking. Banthia and Gupta (2009) - while investigating the effect of w/b, sand:cement ratio and other parameters on cracking in cementitious materials - report that increasing the w/b decreases the total amount of heat evolved, increases the rate of evaporation and delays the occurrence of first crack. They also report that lower w/b result in low crack areas and small crack widths. The movement of water within the porous paste sets up tensile and hygral stresses which are a function of w/b (Beddoe and Lippok, 1999; Yurtdas et al., 2006). These stresses result in volumetric changes within the paste. A reduction in the w/b, for example, would reduce creep - because it produces materials that are strong and stiff (Taylor, 1997) - and with a high tensile strength (Kovler et al., 1999b; Schulze, 1999). A high tensile strength is desirable because it increase the capability of a material to resist the tensile stresses responsible for cracking. Pastes with high w/b contain more free water and are therefore more susceptible to drying shrinkage (He and Li, 2005). The susceptibility of the paste to shrinkage-induced cracking can, thus, be reduced by lowering its w/b (Neville, 1995). The extent to which w/b can be reduced, however, ought to be considered carefully vis-á-vis the susceptibility of a material to undergo autogenous shrinkage resulting from mixes with low w/b (Tazawa and Miyazawa, 1995) and the high tensile stresses induced in a material due to the corresponding high elastic modulus. Bentz et al. (2009) reports that the w/b influences the thermal properties at early age; with changes in w/b resulting in distinct influences on the semi-adiabatic temperature curves. Decreasing the w/b increases the peak temperature achieved during semi-adiabatic hydration except for w/b less than approximately 0.38, where the reduced degree of achievable hydration limits the heat release and consequent temperature rise. A decrease in w/b increases the magnitude of autogenous stresses and autogenous shrinkage of mortars cured under sealed conditions. Bentz et al. (2009) attribute the increased autogenous stresses to the menisci in the partially water-filled pores that exist between the closely-spaced cement particles. Wall et al. (1986) report that very low w/b reduces bond strength.

3.4.4 Aggregates

Aggregate refers to a system of grains of various materials, forms and dimensions. They can be coarse or fine. Brandt (2009) describes coarse aggregates as a discontinuous phase of a composite where each grain is an inclusion in the matrix. The grains of fine aggregate are made of natural sand in most kinds of concrete-like materials and are considered as a matrix when mixed with cement and water. Fine aggregates could also be considered as inclusions causing microcracks in the cement paste. The fine grain fraction may be composed of other materials such as non-hydrated cement particles and FA. The aggregate phase is significant in the cracking-performance of cement-based materials. It plays an integral part with respect to the following material properties: rheology, elastic modulus, wear resistance, strength, stiffness, and dimensional/volumetric stability (Alexander and Mindess, 2005; Dittmer and Beushausen, 2014; Mehta and Monteiro, 2006; Westerholm et al., 2008). Important aggregate properties that influence cracking comprise: aggregate type and content, grading, size, shape and surface texture, stiffness, porosity, moisture absorption, bulk density and crushing strength (Alexander and Beushausen, 2009; Kellerman and Crosswell, 2009; Mehta and Monteiro, 2006). These properties are discussed in the subsequent subsections.

3.4.4.1 Content, grading, stiffness and type

Aggregates affect the shrinkage of the cement paste through two distinct mechanisms: dilution and restraint. Dilution, on the one hand, refers to the reduction in paste volume (and consequently shrinkage) through an increase in aggregate content. This relationship is shown in Figure 3.8. Restraint, on the other hand, refers to the reduction in shrinkage through an increase in aggregate stiffness (Alexander and Beushausen, 2009; Neville, 1995).

Aggregates restrain the movement of the paste because they are generally dimensionally stable (Mallows, 1985; Maruyama and Sasano, 2013; Zhang et al., 2014). The amount of restraint provided by aggregates depends on their content, size, grading, texture and stiffness and/or elastic modulus. Aggregates with a large maximum size are effective in reducing shrinkage (Alexander and Mindess, 2005). The grading of aggregates influences the water and cement paste requirements for a given consistency and creep (Alexander and Beushausen, 2009; Kellerman and Crosswell, 2009; Mallows, 1985; Mehta and Monteiro, 2006).

The stiffness of the aggregate phase dictates the susceptibility of a cementitious material to crack because of shrinkage. An increase in the elastic modulus results in a reduction in shrinkage. Stiff aggregates restrain the shrinkage of the cement paste (Alexander and Beushausen, 2009; Rüsch et al., 1983). Aggregates with a high elastic modulus also restrain the creep of the paste. Dittmer (2013) and Dittmer and Beushausen (2014), while investigating the effect of various aggregate contents (0%, 25%, 35% and 45%) at two w/b on tensile strength, observed an increase in 7-day tensile strength due to an increase in aggregate content in concretes with w/b of 0.6. At similar mixes with a lower

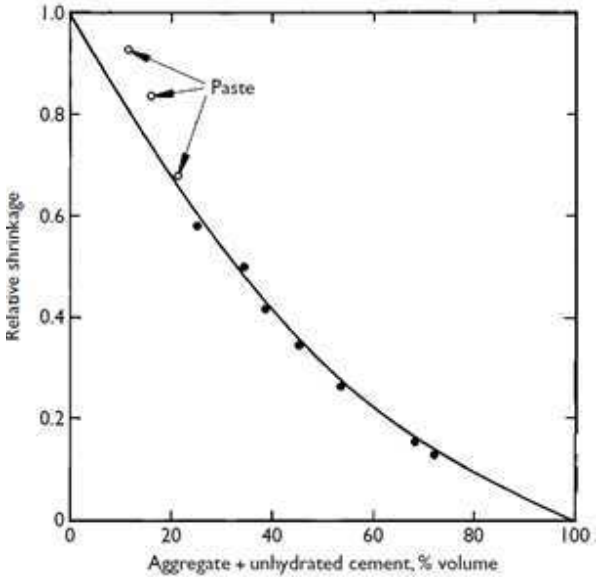

FIGURE 3.8: Effect of aggregate on reducing shrinkage of pure paste - adopted from Alexander and Mindess (2005)

w/b, the effect of aggregate on tensile strength was found to be minimal. Dittmer and Beushausen (2014) further report that an increase in the volume of coarse aggregates delays cracking - with the impact being great at higher w/b than at lower w/b - decreases drying shrinkage and increases elastic modulus. Banthia and Gupta (2009) - while investigating the effect of coarse aggregates content on crack area, average and maximum crack widths - report that the addition of a very small volume of coarse aggregates can provide significant internal restraint reducing the shrinkage of the cement paste of concrete.

The type of aggregate affects cracking in many ways. Recycled aggregates, for example, produce cementitious materials with low compressive and flexural strengths, low modulus of elasticity, low CTE, low thermal diffusivity and low autogenous shrinkage (Braga et al., 2014; Corinaldesi and Moriconi, 2009; Taylor, 2014) and high porosity. Braga et al. (2014), further, report that the low flexural/tensile strength of mortars made from recycled demolition rubble can be improved by using polypropylene or stainless-steel fibres. Studies by Etxeberria et al. (2007), however, contradict the findings of Corinaldesi and Moriconi (2009) and Braga et al. (2014) by reporting that recycled aggregates produce materials with a high tensile strength. Cementitious materials with a high porosity are more susceptible to cracking owing to their high magnitude of creep and drying shrinkage (Achtemichuk et al., 2009). Topçu and Bilir (2010) also report that recycled aggregates increase drying shrinkage. The increase in drying shrinkage has been attributed to the reduction in the modulus of elasticity and the increase in fine aggregate content. Atrushi (2003) also reports that the CTE of a cementitious mix depends on the type of aggregate. Cement-based materials cast using quartz-rich aggregates have

a high CTE in comparison to those made from limestone-rich aggregates. Mixes with a high CTE exhibit high thermal strains. Increasing the magnitude of thermal strains, with all factors held constant, increases the susceptibility to cracking.
The use of finely ground waste glass as aggregate in mortars densifies their microstructure and improves their mechanical performance specifically by increasing their compressive and flexural strengths (Corinaldesi et al., 2005). The use of glass sand as replacement for normal sand, at replacement levels greater than 25%, reduces compressive strength, splitting tensile strength, modulus of elasticity and flexural strength (Tan and Du, 2013). The reduced compressive strength is due to the weak bond strength formed at the ITZ between glass particles and the cement matrix because of their smooth surface and sharper edges. The reduction in flexural strength is due to the reduction in adhesive strength at the glass particle surface and microcracking. Replacing natural sand with glass sand - with replacement levels that are less than 100% - improves their dimensional stability. Tan and Du (2013) specifically report that drying shrinkage reduces with an increase in glass content. The reduction in drying shrinkage has been attributed to: negligible water absorption capacity of glass particles, higher aspect ratio of glass, the irregular shape of glass particles and the relatively higher volume fraction of fine aggregates.
The use of waste tyres as aggregates in cementitious materials increases cracking and fracture resistance (Li et al., 2004). Li et al. (2004), while referring to other studies, report that crumb rubber-filled mortars have higher flexural and impact strengths in comparison to conventional portland cement and latex-modified mortars. Crumb rubber-filled concretes and mortars also have low stiffness, modulus of elasticity, split tensile strength and compressive strength. Lightweight aggregates (referred to as LWA hereafter) improve the microstructure of the ITZ, the transport properties and durability of mortar (Elsharief et al., 2005). The dense ITZ and microstructure of LWA increases their resistance to penetration by aggressive chemical species. Etxeberria et al. (2007) report that the use of a high content of recycled aggregates - up to 100% - in mortars reduces their compressive strength, elastic modulus and flexural strength. Additional details on the effect of rubber aggregates on crack-determining material properties can be found in Section 2.6.5.

3.4.4.2 Size

The size of an aggregate in a mix affects shrinkage indirectly through its effect on water requirement (Alexander and Beushausen, 2009; Brandt, 2009; Kellerman and Crosswell, 2009; Mehta and Monteiro, 2006; Westerholm et al., 2008). Single-sized sands contribute to excessive bleeding, poor finishing and may increase water demand (Kellerman and Crosswell, 2009). Very fine or angular sands require more water to achieve a given consistency. The extra water required by fine sands could increase drying shrinkage. Wittmann (2002) reports that an increase in the size of aggregates increases specific fracture energy as shown in Figure 3.9.

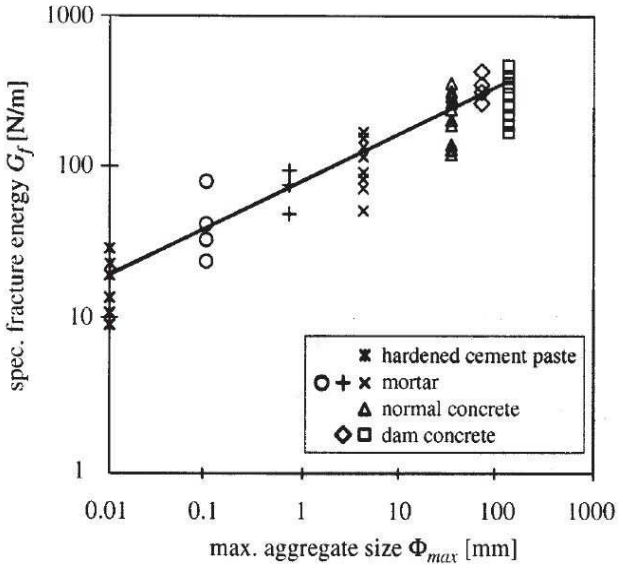

FIGURE 3.9: Specific fracture energy of cement-based materials as a function of maximum aggregate size - adopted from Wittmann (2002)

Dittmer (2013) and Dittmer and Beushausen (2014), while studying the influence of 9.5 mm and 19 mm Greywacke coarse aggregates on the properties of concrete (w/b = 0.6), did not observe any notable differences in the tensile strength of concrete specimens at 7 days. However, there was a notable difference in tensile strength at a later age (28 days); with the aggregates with a smaller size (9.5 mm) exhibiting tensile strengths that are approximately 30% higher than those in mixes made using larger sizes (19 mm). Similar observations have also been reported by Zhang et al. (2005) and have been attributed to an increase in the number of aggregates that can effectively bridge the propagation of cracks which increase as the aggregate particle size decreases. This proposition needs further research. Dittmer (2013) also observed that a reduction in the size of coarse aggregates resulted in an increase in drying shrinkage at younger and older ages (7-day and 56 days respectively). This observation can be attributed to the fact that larger-sized aggregate particles provide better restraint for the shrinking cement paste consequently reducing the magnitude of drying shrinkage in concrete. Similarly, larger coarse aggregates exhibit higher tensile relaxation, higher elastic modulus and stiffness and reduction in crack intensity.

3.4.4.3 Shape and surface texture

The shape and surface texture of aggregates influences the properties of a mix in its fresh state more than in its hardened state. The surface texture of an aggregate determines the workability and water requirement (Taylor, 2014; Uys, 1983). An increase in water requirement increases the susceptibility of a mix to crack due to drying shrinkage. The surface texture of an aggregate affects the matrix-aggregate bond strength (Brandt, 2009;

Dittmer, 2013). The matrix-aggregate bond strength influences other crack-determining material properties like tensile strength. Sands that are very fine increase the water requirement; consequently, increasing the cement requirement for any given w/b.

3.4.4.4 Miscellaneous

Densely packed aggregates produce mortars with less voids. Such mortars require less paste (Schutter and Poppe, 2004). A reduction in paste content, with all other factors held constant, reduces shrinkage. Also, densely packed aggregates have a high elastic modulus. The apparent dry density of sand dictates the susceptibility of a mix to crack owing to its influence on water demand. Crushed aggregates require high cement contents to achieve a given workability (Westerholm et al., 2008). Increasing the cement content increases the susceptibility to crack as discussed in Section 3.4.1.

The porosity of an aggregate affects its stiffness, elastic modulus and density (and strength). Porous aggregates produce materials with low density, elastic modulus and strength and an increased permeability to fluids and deleterious chemical species - especially if their pores are interconnected. Porous aggregates that are not fully saturated at the time of mixing can withdraw water from the mix resulting in a porous ITZ and weak interfacial bond. They may adversely affect the resistance of concrete to freeze-thaw conditions (Alexander and Mindess, 2005). The porosity, or absorption, of an aggregate also affects the creep by influencing the transfer of moisture within the system (Mallows, 1985). The stiffness of the aggregate influences the susceptibility to cracking because stiffness determines the ability of a material to restrain the strain from the cement matrix.

The mineralogical nature of the aggregates, affects the properties of the ITZ (Xu et al., 2000). The presence of clay materials around an aggregate affects the bond at the aggregate-paste interface (Brandt, 2009) and the creep of the concrete (Mallows, 1985). The presence of clay minerals on aggregate surfaces reduces the strength of the bond between the aggregate and the paste. The chemical properties of an aggregate also dictate its susceptibility to crack due to alkali-aggregate reaction (Brandt, 2009). It is recommended that inert aggregates are used in cement-based PRMs. Hannawi et al. (2013), while investigating the effect of plastic waste aggregates on mortar properties in the fresh and hardened states, observed that the incorporation of plastic aggregates in the form of polyethylene terephthalate (PTE): decreased compressive strength, splitting tensile strength, modulus of elasticity and ultrasonic pulse velocity, sensitivity to cracking while increasing free shrinkage, straining capacity and tenacity. These aggregates also delayed the appearance of cracks and limited their opening. The reduction in splitting tensile strength was due to the addition of plastic was attributed to the poor bond between the cement matrix and the plastic aggregates while the increase in free shrinkage was be attributed to the low stiffness of plastic aggregates and to the poor bond between the matrix and the plastic that offers less opposition to shrinkage.

3.4.5 Chemical admixtures

Chemical admixtures are materials other than water, aggregates, hydraulic cement, SCMs, and fibre reinforcement, that are used as ingredients in cementitious mixtures to modify their freshly mixed, setting, or hardened properties and are added to a batch before or during mixing (ACI, 2003; Brandt, 2009; Marais, 2009; Mehta and Monteiro, 2006). They play a crucial role in controlling the fresh and hardened properties of cement-based materials in modern construction applications (Capener, 2008; Neville, 1995). The extent to which an admixture affects shrinkage in a cementitious material depends on its intended use. An admixture may either increase or decrease drying shrinkage and creep slightly if it is used to effect a saving in cement by reducing the water and cement content while maintaining workability and minimal strength in a mix. Admixtures could also be used to increase strength by reducing the water content while maintaining the same cement content and workability. This use results in effects that are similar to the first category of use; except that the magnitudes would be slightly reduced because of small reductions in paste content. In the second category of use, Uys (1983) reports that there is no significant influence on creep if the increase in strength afforded by the admixture is considered when testing all the cementitious materials at the nominal stress/strength ratio.
Even though the effect of admixtures on many cement-based material properties are well-established, Uys (1983) and The Concrete-Society (2003a) report that it is difficult to predict their influence on the creep of a given mix. This difficulty is premised on the fact that the influence of an admixture on creep is highly specific and depends on many factors namely: method of proportioning, cement type, admixture composition, age at loading and the environment before and after loading. Also, the complexity in understanding the exact effect of an admixture on the properties of a mix are due to the fact that the influence of a specific admixture depends on the length of the drying period. Thus, there is no single admixture that can produce mixes of optimum quality under all conditions. It is necessary, therefore, that the influence of various admixtures on crack-determining material properties be investigated. The effect of selected admixtures on crack-determining material properties are hereby discussed.

3.4.5.1 Plasticisers and superplasticisers

Plasticisers and superplasticisers are also called water-reducing admixtures and high-range water-reducing admixtures respectively. Their incorporation in a mix is normally intended to result in any, or a combination, of the following effects: reduce the water requirement of a mix for a given slump, produce a mix with a high strength, obtain a specified strength at lower cement contents, or increase the slump of a given mix without a corresponding increase in water content. They are also used to improve the properties of a mix containing aggregates that are harsh, poorly graded, or both, or in mixes that are placed under difficult conditions. Superplasticisers reduce the water requirement of

a mix by more than 30%, without the side effect of excessive retardation (ACI, 2003; Mehta and Monteiro, 2006; Rixom and Mailvaganam, 1999).
The influence of water reducing admixtures on shrinkage is not defined clearly; consequently, rendering it to many contradictory views. On the one hand, Neville (1995) reports that plasticisers increase shrinkage slightly - by 10% to 20%. Neville (1995) also acknowledges that the effect of plasticisers on shrinkage is indirect because their use may result in a change in the water content or in the cement content of the mix, or in both, and it is the combined action of these changes that influences shrinkage. Tazawa and Miyazawa (1995), on the other hand, report that superplasticisers reduce shrinkage; and have attributed this phenomenon to the effect of the superplasticisers on the rate of hydration.

3.4.5.2 Shrinkage reducing admixtures (SRAs)

Drying shrinkage is the principal cause of cracking in concrete structures (Baluch et al., 2002; Sugiyama, 2003). SRAs reduce the surface tension of the mix water in the capillary pores. The reduction in surface tension in capillary pores reduces tension stresses/forces within the matrix of the material that would lead to drying shrinkage (ACI, 2003; Bentz, 2008; Gopinath, 2010). The extent to which SRAs reduce shrinkage depends on the internal relative humidity of the material and the porosity of the paste, amongst other factors (Saliba et al., 2011). SRAs reduce the rate and the overall magnitude of shrinkage; with the reduction in drying shrinkage ranging between 50% and 56% as reported by Baluch et al. (2002) and Saliba et al. (2011).
An increase in SRA dosage reduces slump and compressive strength, increases flow by 5% and 15% and decreases macro-porosity (Gopinath, 2010; Sugiyama, 2003; Topçu and Bilir, 2010). Gopinath (2010) reports that the combination of SRAs and multifunctional admixtures has a retarding effect on cement mortars. Generally, SRAs do not result in significant changes in flexural strength. However, they increase tensile strength at 28 days (Gopinath, 2010). Carlswärd (2006), Banthia and Gupta (2009) and Gopinath (2010) also report that SRAs reduce the potential for mortars to crack and delay their time to first crack. This phenomenon could be attributed to the lowering of the rate of tensile stress development within the mortar specimens by SRAs. SRAs also reduce autogenous shrinkage Gopinath (2010). Additional information regarding the influence of SRAs on important crack-determining material properties has been discussed in Section 2.6.1.

3.4.5.3 Other admixtures

Other admixtures that influence the crack-determining properties of PRMs are drying shrinkage inhibitors (Tazawa and Miyazawa, 1995) and retarding admixtures. Retarding admixtures are water-soluble chemicals that reduce the rate of hydration of hydraulic cement without affecting their strength gain characteristics significantly once the cementitious material has taken its final set (Marais, 2009; Uys, 1983). They may allow

more shrinkage to be accommodated in the form of plastic shrinkage and increase the extensibility of concrete; therefore, reducing their susceptibility to crack (Neville, 1995). Accelerating admixtures increase the long-term drying shrinkage of cementitious materials (Concrete-Society, 2003a; Uys, 1983). Brandt (2009), also reports that accelerating admixtures that contain calcium chloride exhibit increased drying shrinkage; thus, increasing the susceptibility to cracking. Lignosulphate admixtures increase creep significantly, particularly in a dry environment (Uys, 1983). Other admixtures that influence cracking in PRMs comprise (Brandt, 2009): admixtures that initiate volume expansion during hydration and hardening to compensate natural drying shrinkage of portland cement and admixtures that increase bonding. Ghezal and Assaf (2014) while investigating the effect of admixtures and binder types on SCC made using ternary blends of cement report that viscosity modifying admixtures influence cracking potential.

3.4.6 Curing

Curing is the process of maintaining a satisfactory moisture content and a favourable temperature in cement-based materials during the period immediately following their placement so that the hydration of cement may continue until the desired properties are developed to a sufficient degree to meet the requirements of service (Bester, 2015; Concrete-Society, 2003a; Perrie, 1994; Taylor, 2014). The two main objectives of curing are: to prevent excessive loss of moisture and to control the temperature for a period sufficient to achieve the desired requirements of service (Fowler and Treviño, 2011; Kovler and Jensen, 2005; Mehta and Monteiro, 2006; Perrie, 1994; Wasserman and Bentur, 2013). Curing is essential to the production of high quality cement-based materials. The benefits of adequate curing comprise: improved durability, increased tensile strain capacity, improved impermeability, increased strength, volume stability, abrasion resistance, resistance to weathering, de-icing salts, freezing and thawing and chemical attack (Beushausen and Bester, 2016; Concrete-Society, 2003a; Fowler and Treviño, 2011; Perrie, 1994; Silfwerbrand et al., 2011; Taylor, 2014). Adequate moist curing delays the advent of shrinkage and increases tensile strength (Alexander and Beushausen, 2009; Beushausen and Bester, 2016; Kronlöf et al., 1995; Masuku, 2009; Neville, 1995). Kovler et al. (1999b) reports that the effect of curing is more pronounced on tensile strength than on compressive strength. Beushausen and Bester (2016) also report that the influence of curing on tensile strength is greater for cement-based materials with higher w/b, which have a higher initial porosity, than in those with lower w/b. Common curing techniques comprise: super absorbent polymers (SAPs), curing compounds, covering with wet geo-textile fabrics, water ponding, wet burlap and plastic sheeting.

3.4.6.1 Lightweight aggregates (LWA)

Internal curing entails the use of saturated lightweight aggregates (referred to as SLWA hereafter), superabsorbent polymers (SAPs), water-saturated wood products or other water-filled inclusions that can provide curing water throughout the cross section of a

material. It is very different from conventional water curing where water is provided after placement, and applied on the surface of the member (Castro et al., 2012; Sikora and Klemm, 2014; Siriwatwechakul et al., 2012). Internal curing is effective in reducing autogenous shrinkage and autogenous shrinkage cracking, reducing the likelihood of thermal cracking, delaying cracking and reducing the likelihood of plastic shrinkage cracking (Bentz, 2009; Brandt, 2009; Byard et al., 2012; Castro et al., 2012; Craeye et al., 2011; de Sensale and Goncalves, 2014; Henkensiefken et al., 2009; Jensen and Hansen, 2001b; Kovler and Jensen, 2005; Sakulich and Bentz, 2013; Siriwatwechakul et al., 2012; Taylor, 2014). Gillmer (2012) reports that the water retained by internal curing compounds maintains a relative humidity within the cement-based material that is close to 100%. The high internal relative humidity reduces drying and autogenous shrinkage.

The design of cement-based materials for internal curing requires that enough water is provided to aid in hydration and to overcome the effects of self-desiccation. The provision of adequate water for internal curing, therefore, requires much caution. Providing water above the minimum amount ought to be done with care because excess water prevents the development of a full bond between the cement paste and the aggregate surface. A poor bond at the ITZ compromises the performance and durability of the resulting material due to its high porosity. Two approaches have been postulated to inform the determination of the amount of water for internal curing. They are: Bentz and Snyder Approach and the Jensen and Hansen Approach. These approaches are summarised in Figure 3.10. Specific details regarding these two approaches can be obtained in Castro et al. (2012).

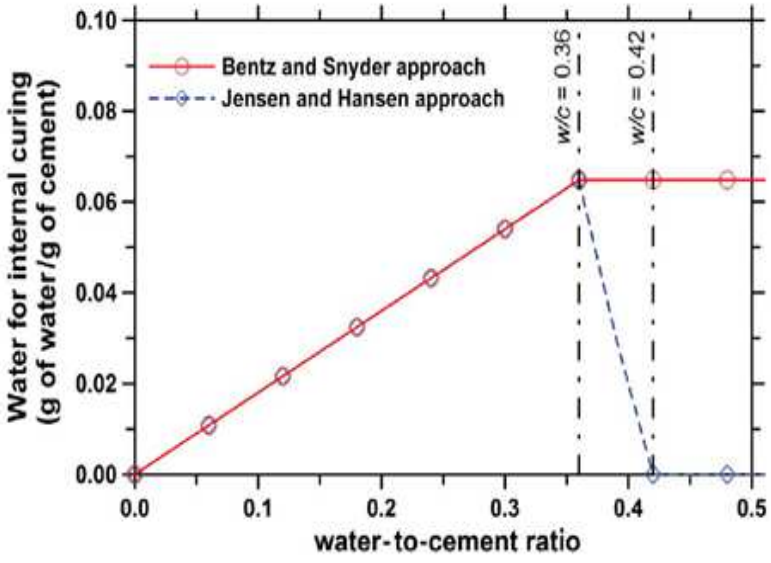

FIGURE 3.10: Water for internal curing required to maintain saturated condition in cement paste - adopted from Castro et al. (2012)

Internal curing using LWA entails substituting a portion of normal aggregates within a mix with SLWA. These aggregates have a vast network of internal voids or capillaries which allow them to absorb and store water. The stored water allows for early age expansion of the material, thereby reducing the adverse effects of shrinkage. Gillmer (2012) reports that autogenous shrinkage can be eliminated without the need for external curing if the size and porosity of the LWA is carefully controlled. SLWA also decrease the likelihood of thermal shrinkage by reducing the heat of hydration and absorbing excess bleed water. The absorption of excess bleed water decreases porosity.
There are two contradictory views regarding the influence of LWA on strength - an observation that has been indirectly made by Byard et al. (2012). On the one hand, some studies show that LWA reduce strength. They attribute the reduction in strength to the fact that LWA are inherently weaker than normal aggregates; thus, their incorporation in a mix reduces strength. On the other hand, other studies show that SLWA increase the long-term compressive strength of cement-based materials. The increase in compressive strength is attributed to increased hydration (Gillmer, 2012). Aggregate stiffness affects the modulus of elasticity. The increased porosity in PRMs with LWA, thus, results in lower modulus of elasticity when compared with those made with normal aggregates. Byard et al. (2012) report that LWA particles are more porous and angular than normal weight aggregates. The porosity and angularity of LWAs improves their ITZ and their tensile bond.

3.4.6.2 Super absorbent polymers (SAPs)

Super absorbent polymers (SAPs) refer to a group of polymeric materials that can absorb a significant amount of liquid from their surroundings and consequently retaining the liquid within their structure without dissolving (de Sensale and Goncalves, 2014; Filho et al., 2011; Gillmer, 2012; Jensen and Hansen, 2001b; Kovler and Jensen, 2005; Lura et al., 2011; Mechtcherine et al., 2013; Sikora and Klemm, 2014). Chemically, SAPs are cross-linked polyelectrolytes that swell upon contact with water or aqueous solutions resulting in the formation of a hydrogel. A gram of SAP can absorb up to 1500 grams of water. Kovler and Jensen (2005) further report that the theoretical maximum water absorption of SAPs is about 5000 times it self-weight. The main driving force for the swelling of SAPs is the osmotic pressure which is proportional to the concentration of ions in the aqueous solution Friedrich (2011). Lura et al. (2011), Reinhardt et al. (2011) and de Sensale and Goncalves (2014) report that the kinetics of absorption and the amount of fluid absorbed by the SAP depends on the nature of the SAP and the cement paste or concrete, on the pore solution composition.
SAPs change the rheology of a fresh mix (Cusson et al., 2011; Filho et al., 2011) and the microstructure of a hardened cementitious material (Ye et al., 2012). SAP particles absorb water which is entrained into their structure. This water is consumed during hydration while some is lost to drying shrinkage. The consumption of entrained water results in empty pores (Lura et al., 2011; Ye et al., 2012). SAPs produce geometrically

predesigned macropore inclusions at the expense of finer, irregular and partly connected capillary pores; thus, resulting in a reduction in permeability (Beushausen and Gillmer, 2014; Reinhardt and Assmann, 2011). Reinhardt and Assmann (2011) attribute the reduction in permeability to the extension in curing. SAPs also increase the air content and decrease the density of fresh high strength mortar mixes (Filho et al., 2011).
SAPs reduce the magnitude of autogenous shrinkage - as shown in Figure 3.11 - drying shrinkage, coefficient of thermal expansion and capillary pressure as well as increase tensile relaxation (Beushausen and Gillmer, 2014; Cusson et al., 2011; de Sensale and Goncalves, 2014; Mechtcherine, 2011; Mechtcherine and Dudziak, 2011; Sikora and Klemm, 2014; Wyrzykowski and Lura, 2013; Ye et al., 2012); and can even cause swelling at early ages (Gillmer, 2012; Mechtcherine and Dudziak, 2011; Mechtcherine et al., 2013; Sikora and Klemm, 2014). The additional water which is entrained in SAPs is responsible for the reduction in autogenous shrinkage. The entrained water prevents self-desiccation (Ye et al., 2012). Gillmer (2012), while studying the effect of SAPs on the properties of cement-based materials, observed that SAPs increase the magnitude of drying shrinkage; even though the total shrinkage at later ages was lower than in specimens without SAPs.

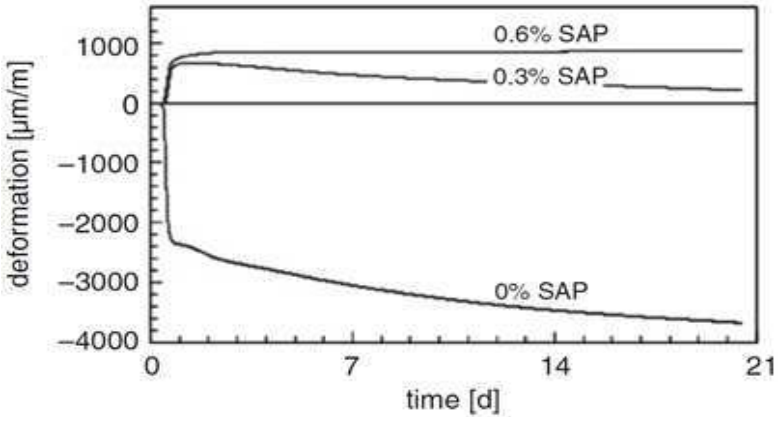

FIGURE 3.11: Autogenous deformations in setting cement pastes with different amounts of SAP by mass of cement in mixes with a basic w/c of 0.3 at 20^{o}C - adopted from Mechtcherine and Dudziak (2011)

The observations by Gillmer (2012) have also been reported by Mechtcherine and Dudziak (2011). Gillmer (2012) attributed the low total shrinkage, due to the incorporation of SAPs, to the significant reduction in autogenous shrinkage at early ages. Gillmer (2012), while referring to other studies, reports that the optimum SAP content that results in maximum reduction in total shrinkage ranges from 0.35% to 0.40% by mass of binder. Nevertheless, Jensen and Hansen (2002) and Mechtcherine et al. (2013) report that the effectiveness of SAPs in reducing shrinkage depends on their amount, particle size and chemistry. SAPs can potentially influence the setting time and hydration development

of cement due to the leaching of extraneous substances (Jensen and Hansen, 2002). Depending on their type, SAP can either accelerate or retard hydration.
Mechtcherine and Dudziak (2011), while investigating the effect of SAPs on the properties of concrete and mortar, report that SAPs reduce stresses due to restraint. They also observed that tensile stresses in test specimens, due to autogenous shrinkage, were not generated when 0.70% SAP (by mass of binder) was added to a mix; and that that the addition of SAP was effective in counteracting the build-up of stresses in restrained ring specimens. The build-up of stresses was counteracted partly in specimens with 0.3% SAP addition and almost fully in specimens with 0.6% SAP addition. Gillmer (2012), while investigating the influence of SAPs on the mechanical properties of concrete, reports that the extent to which SAPs influence compressive strength and durability depends on the w/b and the type of binder. The addition of SAPs, for example, affected compressive strength, Oxygen Permeability Index (OPI), and Chloride Conductivity Index (CCI) of specimens with w/b of 0.45 adversely while improving their sorptivity and porosity. The same SAPs, however, did not impact the OPI and CCI of specimens with w/b of 0.55. The observations by Gillmer (2012) on durability contradict those of Jensen and Hansen (2001b) who report that SAPs generally improve durability; an observation that they attribute to the increase in the degree of hydration and the creation of spherical macropores. Ye et al. (2012) also report that SAPs increase the degree of hydration of cement as shown in Figure 3.12; thus, corroborating the observations of Jensen and Hansen (2001b). Mechtcherine and Dudziak (2011), while investigating the effect of SAP content on autogenous shrinkage in cement pastes, report that doubling the SAP content prevented autogenous shrinkage completely in pastes made using w/b of 0.25; yet failed to completely prevent autogenous shrinkage at w/b of 0.33. A plausible reason for this observation could not be given based on the obtained data.

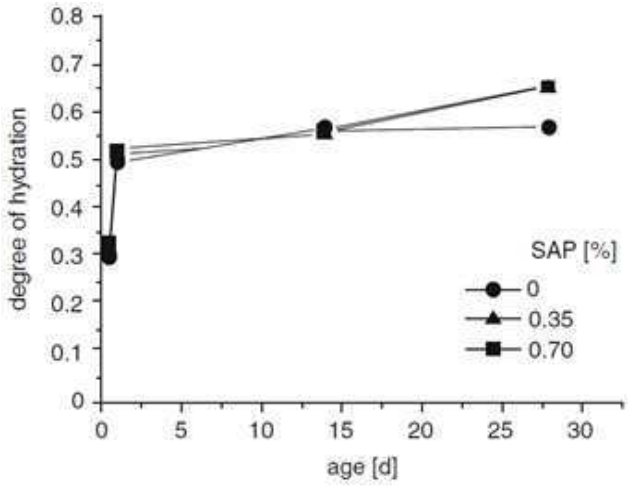

FIGURE 3.12: Degree of hydration in cement pastes with SAP (w/c = 0.25) - adopted from Ye et al. (2012)

Increasing SAP content increases creep, tensile splitting strength and tensile relaxation and a delay in the age at first cracking (Gillmer, 2012). Craeye et al. (2011) also reports that increasing the amount of SAP results in higher basic creep and a reduction in tensile strength - an observation that confirms and contradicts the conclusions of Gillmer (2012) simultaneously. Increasing the tensile relaxation due to the addition of SAPs is beneficial because it contributes towards the development of low tensile stresses; which would consequently minimise the susceptibility to cracking. The increase in tensile strength, as observed by Gillmer (2012), has been attributed to an increase in CSH. The denser microstructure - due to the formation of more CSH and the reduced porosity within the material could also explain the increase in tensile strength. SAPs reduce elastic modulus and flexural strength (Craeye et al., 2011; Gillmer, 2012; Mechtcherine et al., 2013).

The influence of SAPs on compressive strength is subject to contradictory views. Jensen and Hansen (2002), Craeye et al. (2011), Gillmer (2012), Mechtcherine et al. (2013) and Taylor (2014) report that increasing the quantity of SAPs in a mix decreases compressive strength. Jensen and Hansen (2001b), Kovler and Jensen (2005), however, report that SAPs increase compressive strength. Kovler (2011) further reports that incorporating SAPs in mixes results in moderate strength reduction in the early ages and higher strength and elastic modulus values at later ages. They attribute the moderately low strength at early ages to the higher porosity and moisture in mixes made using SAPs. The higher strength and elastic modulus at later ages is attributed to enhanced cement hydration which compensates strength reduction caused by slightly higher porosity. The effect of SAP on strength depends on curing conditions, age and material composition (Kovler, 2011).

Kovler (2011) while referring to other studies, reports that the addition of SAPs to pastes and mortars with and without SF had almost no influence on the compressive strength of high performance mortars, while the compressive strength of cement pastes was reduced by 20% at early ages and by 10% at later ages. The different effect of SAP in cement pastes and mortars was explained by different largest defect size present in the solid matrix of these materials. In cement pastes, for example, the voids left by the largest SAP particles are the largest defects. The largest defects in mortars are paste-aggregate interfaces and weak or pre-cracked aggregates. These defects are usually of the size of the aggregates (which was up to 2 mm in their research), i.e., significantly larger than the size of SAP particles. This may explain why no influence of the SAP on compressive strength of the mortars could be detected. It may also explain the lower strength of the mortars compared to the cement pastes. The authors concluded that since aggregate or ITZs, and not cement paste, are the limiting factor for mortar strength, the influence of SAP on strength of mortar and concrete should be negligible. Kovler (2011), while referring to other studies, further reports that the interpretation of the effect of SAP addition on the compressive strength is not straight forward. On the one hand, a reduction in the strength of the concrete matrix can be generally expected for mixtures with SAP and extra water. This results from the formation of entraining pores, initially filled

with curing water and subsequently dried out. Such voids affect strength negatively. On the other hand, due to the reduction of the autogenous shrinkage of the cement paste, the internal stresses resulting from the hindrance of shrinkage deformations by stiff aggregates must be considerably lower in the case of specimens with SAP. This is positive from the standpoint of concrete strength.
Similarly, there are other contradicting views regarding the effect of SAPs on tensile strength. While Gillmer (2012) report that SAPs increase the tensile strength, Kovler (2011) reports that SAPs reduce tensile strength. Kovler (2011), while referring to other studies, also reports that the addition of SAPs reduces the modulus of elasticity slightly. The addition of SAPs to aluminate cement pastes increase their modulus of elasticity. The influence of SAP on tensile strength is not necessarily the same as that on compressive strength. There are indications that the use of SAP can improve tensile strength at mature ages, more than compressive strength. This phenomenon can be related to the fact that tensile strength is very sensitive to cracking; thus, any improvement in cracking resistance by means of self-desiccation/shrinkage mitigation is expected to be beneficial in terms of tensile properties. The strength of SAP-containing cementitious materials depends on external curing conditions. The most severe reductions occur under water curing Kovler (2011).

3.4.6.3 Other curing techniques

A study by Wasserman and Bentur (2013) on the effectiveness of different curing technologies - curing compounds and use of wet fabrics - reports that water curing is the most efficient curing method with respect to achieving durability-related parameters such as air permeability, capillary absorption and carbonation. Wasserman and Bentur (2013) also observed that water curing and wet fabric were more effective with respect to strength improvement in comparison to curing compounds and curing using plastic sheets. Beushausen and Bester (2016), while comparing the effect of different curing methods on selected crack-determining material properties, observed that curing compounds - in comparison to other methods - resulted in the greatest increase in cracking resistance. Wasserman and Bentur (2013) further observed that wet fabrics are less effective in enhancing the penetration characteristics of cement-based materials. The use of curing compounds - in comparison to moist/water curing - does not provide a very effective sealing of the surface towards the loss of moisture to the environment. The lack of an effective sealing results in relatively inferior material properties (e.g., lower strengths, higher penetration and carbonation values). Wasserman and Bentur (2013) further report that curing affects durability more than it affects strength. Beushausen and Bester (2016), while comparing the effect of different curing methods on selected material properties observed that wet cloth curing outperformed curing using plastic sheet by delaying shrinkage strains and by increasing tensile strength.

3.4.6.4 Duration of curing

The influence of the duration of curing on crack-determining material properties has attracted many contradictory views (Arito et al., 2016c; Mehta and Monteiro, 2006). Neville (1995), for example, reports that the duration of curing is not an important parameter as far as shrinkage is concerned. Other studies, however, report that prolonged curing, with all other factors held constant, increases shrinkage; with the increase in shrinkage resulting from the reduction in volume of the unhydrated cement particles - which restrain shrinkage. Rao (2001a) reports that an increase in the duration of curing decreases the ultimate drying shrinkage. This observation has been premised on the understanding that HCP can restrain a large fraction of shrinkage without cracking because they are strong; with their strength resulting from the little water contained within their matrix. Topçu and Bilir (2010) also report that longer curing, in conjunction with low w/b, decreases drying shrinkage in high performance ready-mixed concrete.
The duration of curing affects the interfacial bond strength. Wong et al. (1999) report that the interfacial bond strength of high volume FA increases proportionately with an increase in curing age. Beushausen and Bester (2016) report that an increase in the duration of curing resulted in an increase in tensile strength, elastic modulus and age at cracking as well as a reduction in tensile relaxation. Research by Beushausen and Chilwesa (2013) on bonded mortar overlays cured at 2 and 7 days reports that the duration of curation does not influence the cracking behaviour significantly. This observation was premised on the effect of prolonged curing on material properties. One the one hand, a long duration of curing is postulated to produce materials with high tensile strength at the onset of stress development; consequently, improving their ability to withstand high induced tensile stresses. On the other hand, a long duration of curing causes potentially higher stresses as it results in less relaxation and a high elastic modulus.

3.4.7 Miscellaneous

The use of fibre reinforcement in repair mortars enhances their resistance to cracking, bond durability and flexural strength and a reduction in their rate of bleeding (Beushausen and Alexander, 2009; Carlswärd, 2006; Concrete-Society, 2003a; Corinaldesi et al., 2002). Fibres also delay the onset of cracking and reduce crack widths as shown in Figure 3.13 (Brandt, 2009; Carlswärd, 2006). The amount of fibres that would be effective in preventing crack formation depends on their type and bond characteristics (Fowler and Treviño, 2011).
Materials that are commonly used as fibres include: sisal (Filho et al., 2005), steel, polypropylene and polyvinyl alcohol. Polypropylene fibres are hydrophobic. Their incorporation in mixes lowers the capillary pressure of water that causes plastic shrinkage; consequently reducing the shrinkage period (Kronlöf et al., 1995). Brandt (2009), while analysing the results from various studies, observed that reinforcing a cementitious matrix with different kinds of fibres does not modify their shrinkage significantly.

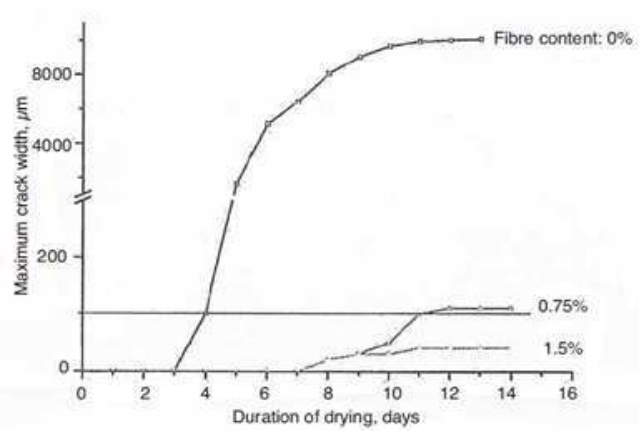

FIGURE 3.13: Influence of fibre reinforcement on the maximum crack widths - adopted from Brandt (2009)

Brandt (2009), nevertheless, reports that fibres with a high youngs modulus not only improve crack resistance greatly but also reduce the maximum crack widths and shrinkage-induced cracks. Studies on fibre-reinforced cementitious composites have shown that the inclusion of steel fibres reduces creep. Boshoff and van Zijl (2007) report that concrete specimens that have been reinforced with small amounts of steel and polypropylene fibres exhibit creep strains that are consistently higher than those in specimens without fibres. Additional information on the role and importance of fibres on crack-determining material properties has been discussed in Section 2.6.3.

The effect of polymer-modification on cracking and crack-determining material properties has been reported comprehensively by Ohama (1995), Ohama (1998), Ohama (2011), Kardon (1997) and Miller (2005) and summarised in Section 2.6.4. Miller (2005) reports that ethylene vinyl acetate polymers affect the following crack-determining properties: hydration rate, elastic modulus, toughness, permeability and bond strength to various substrates in cement and mortars. The incorporation of polymers in the mortars and concretes improves their adhesion to various substrates depending on the polymer:cement ratio and the properties of the substrate (Bezerra et al., 2011; Miller, 2005; Ohama, 1995,9). The relationship between the adhesion in tension and flexure of latex-modified mortars under different concrete substrates is represented in Figure 3.14.

The improvement in the adhesion of polymers to their substrate is attributed to the high adhesion of the polymers. Ohama (1995) further reports that the adhesion of polymer-modified systems in tension, flexure and direct compressive shear increases with a rise in polymer:cement ratio regardless of the polymer type and test method. Ayyar and Joshi (1986) further report that polymers undergo a considerable amount of creep at high temperatures. The high creep of polymers improves their resistance to cracking. The incorporation of polymers into cementitious mixtures reduces their risk of cracking,

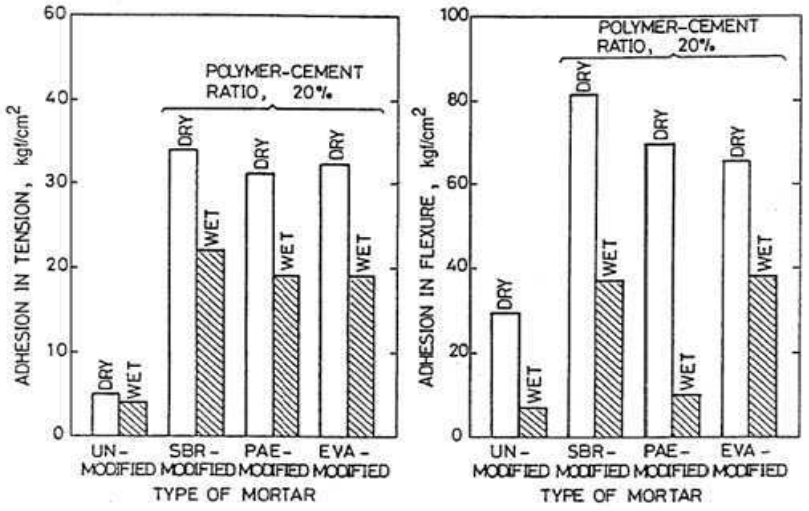

FIGURE 3.14: Effect of water absorption on adhesions in tension and flexure of latex-modified mortars - adopted from Ohama (1995)

water demand and drying shrinkage and improves workability and increases their adhesion, tensile and flexural strengths, modulus of elasticity and flexibility (Miller, 2005; Ohama, 1998, 2011; Ramli and Tabassi, 2012a). Ohama (1998), Miller (2005) and Ramli and Tabassi (2012a) further report that the overall performance of a polymer-modified cementitious material depends on the nature of the polymer, the ratio of polymer to cement by weight, temperature at which the curing occurs and the environment in which curing takes place.

3.5 Closure

A general introduction to concrete repair has been presented. A critical review of literature on the factors that govern the effectiveness in the performance of non-structural PRMs in service and their corresponding performance requirements has also been presented. From the presented discussions and literature review, it can be inferred that concrete repair is a complex and challenging process that ought to address multiple, and sometimes conflicting, demands from the clients, designers and contractors.

PRMs are classified into two groups based on their compressive strength: structural and non-structural. Whereas structural PRMs are meant to restore the durability and load-bearing capacity of deteriorating structures; non-structural PRMs are meant for aesthetics as well as the restoration of durability, passivity and the surface profile of repaired structures amongst other uses. Non-structural PRMs are further classified into R1 ($F_{cu} \geq 10$ MPa) and R2 ($F_{cu} \geq 15$ MPa). The performance requirements for each of these two PRM categories differ. PRMs have generally failed to realise their effectiveness

in service due to premature cracking. The effectiveness in the performance of non-structural PRMs in service depends on: durability, quality of workmanship, interactions between the PRM the substrate and the environment, the properties of the constituent materials, edge conditioning, curing methods, interface properties, substrate properties and health and safety amongst other factors. A detailed discussion of the listed factors has been provided in this chapter. The listed factors must be considered during the design and/or specification of repairs and repair materials.

Currently, the repair of concrete is done in accordance with the EN 1504 series of standards. This standard '*Products and Systems for the Protection and Repair of Concrete Structures*' is comprehensive. It comprises ten parts which are intended to address the different phases of a repair project, starting from the awareness of the problem to the maintenance and inspection of the executed repairs. Part 3 of this series of standards, EN 1504-3:2005, lists the performance requirements for non-structural PRMs. These performance requirements have been discussed in detail in Section 3.3. According to the EN 1504-3:2005, the following material properties ought to be specified for any PRM regardless of their application: compressive strength, chloride ion content, adhesive bond, restrained shrinkage/expansion and carbonation. A critical analysis of the EN 1504-3:2005 performance requirements for non-structural PRMs reveals that strict compliance to the provisions therein would not guarantee their effectiveness with respect to durability and cracking resistance - an observation that has also been reported by Arito et al. (2016b). The EN 1504-3:2005 performance requirements for non-structural PRMs are deficient in the following ways:

i. They do not specify material properties that have been reported to be critical to cracking. These material properties comprise tensile relaxation, creep and elastic modulus.

ii. The code does not specify any shrinkage requirements for R1 PRMs.

iii. They do not specify material properties that are critical to ensuring durability in the performance of PRMs. These material properties pertain to the penetrability of the PRM.

iv. Whereas the code acknowledges the existence of hand-applied PRMs, it does not provide performance requirements for their workability.

Generally, the EN 1504 is also deficient. It does not address other types of concrete damage, e.g., fire damage. These deficiencies have been discussed in detail in the relevant sections in this chapter. It can be inferred that these standards the EN 1504, in general, and the EN 1504-3:2005 in particular will need modifications and/or revisions to make them more responsive to the realisation of effectiveness with respect to durability and cracking resistance in service.

There are numerous other guidelines that specify performance requirements for PRMs. These guidelines existed before the introduction of the EN 1504 series of standards in

1997. The performance specifications from these guidelines have been observed to differ greatly from those in the EN 1504; thereby creating a potential for confusion and conflicts in practice. Most guidelines and standards specify properties that differ from each other. The most common material properties that were observed to differ among the guidelines comprise shrinkage, strength and bond strength. There is a need to resolve the differences in the performance specifications among the existing guidelines and standards so that the potential conflicts and confusion in the specification of performance requirements in practice are avoided. A general critique of the performance specification for PRMs, as inferred from the reviewed literature, is hereby provided:

i. The recommendations by some guidelines are not practically feasible. The ACI224 (2003), for example, suggests that a repair material ought to be shrinkage-free or ought to shrink without losing bond. It is impossible to find a cement-based material that does not experience shrinkage.

ii. There is a lack of standardisation of specifications addressing the measurable and tolerable limits of shrinkage. This problem has been reported by Baluch et al. (2002) to contribute to cracking.

iii. There is no standard definition of bond strength - a situation that makes it difficult to compare test results from various methods. Bond strength ought to be specified vis-á-vis the state of stress that a PRM will be subjected to in service.

Whereas compatibility has been reported to be necessary for the realisation of effective repairs, there is a need to rethink the entire philosophy behind compatibility especially in terms of their practicality. It is impossible to achieve the reviewed compatibility requirements for PRMs in practice. Most of the reviewed ideal compatibility requirements are mutually exclusive. Also, there is a need to rethink the role and contribution of compressive strength in the realisation of cracking resistance in non-structural PRMs. The tendency to correlate compressive strength and durability - as reported by Baldwin and King (2003) - ought to be avoided. A direct correlation between durability and compressive strength does not exist.

The success in performance of non-structural PRMs in service depends on its constituent materials. Thus, it can be inferred that the selection of mix design parameters is crucial to the realisation of effective of non-structural PRMs in service. A review of selected mix design parameters - binder-related parameters, water content, w/b, aggregate properties, chemical admixtures and curing - revealed that these parameters affect cracking through their direct and indirect influence on crack-determining material properties such as elastic modulus, shrinkage, creep and tensile relaxation. It is important, therefore, that the role of mix design parameters, and their corresponding interactions, on cracking and crack-determining material properties is understood.

A review of literature on the influence of mix design parameters on cracking revealed that no research, to the knowledge of the author, has been undertaken on the relationships and interactions that exist among multiple mix design parameters on cracking and

crack-determining material properties. Also, several contradictions and inconsistencies were observed in literature regarding the influence of the reviewed mix design parameters on cracking and crack-determining material properties. These inconsistencies and contradictions have also been highlighted by Arito et al. (2016c) and have been discussed in detail within this chapter. They comprise:

i. The effect of FA replacement levels on flexural strength.

ii. The effect of CSF on tensile strength and drying shrinkage.

iii. The effect of cement fineness and chemical composition on shrinkage.

iv. The effect of recycled aggregates on tensile strength.

v. The effect of superplasticiser on shrinkage.

vi. The effect of LWA on strength.

vii. The effect of SAPs on durability, tensile strength and compressive strength.

viii. The effect of the duration of curing on shrinkage.

Chapter 4

EXPERIMENTAL METHODOLOGY

This chapter provides information pertaining to the experimental work, the testing philosophy, experimental design and the experimental variables. The test methods and standards that were used are also discussed.

4.1 Testing philosophy and experimental design

Important time-dependent material properties that dictate the susceptibility of PRMs to undergo cracking failure have been reviewed in the previous chapters. They comprise: tensile relaxation, tensile strength, heat of hydration, elastic modulus and thermal and hygral deformations. These material properties depend on mix design constituents and parameters. A review of the influence of individual mix design parameters on cracking and crack-determining material properties (referred to as material properties hereafter) has been presented in Chapter 3. Considering the discussions in Section 3.4, it can be hypothesised that the resistance of PRMs to cracking can be improved through the optimisation of mix design parameters and material properties simultaneously.
The optimisation of mix design parameters and material properties for cracking resistance is a difficult process. This difficulty is partly attributed to the fact that there are many interactions among various mix design parameters and material properties whose effects have neither been investigated nor understood, on the one hand; and the dearth of accurate and 'easy-to-use' design tools and analytical models at the disposal of concrete repair manufacturers and design engineers on the other hand. The rapid developments in admixtures, additives and other construction materials also present challenges to the manufacturers of repair materials and design engineers who need to continuously stay abreast in their trade by striving to understand the behaviour and performance of these materials and developments and by updating the existing techniques and prediction models. This study was limited to non-structural PRMs due to the following reasons:

i. Most PRMs are non-structural as the mortar is simply required to 'fill the cavity'.

ii. The dead load is commonly not introduced into the patch unless special construction procedures are designed and executed to achieve this.

iii. Even though a patch would initially contribute to the load-bearing behaviour, shrinkage-induced edge-debonding, as well as excessive creep in the mortar, can be expected to significantly reduce any structural contribution of the mortar with time.

The experimental methodology comprised the use of the 2^n full factorial design of experiment approach. The design of experiments and the analysis of test results entailed the use of two computer software: MINITAB 16 and MS Excel. The experimental work was divided into two phases. Phase one comprised the determination of the mix design parameters for the reference mix. The reference mix was developed using the information synthesised from a trend analysis of the test results from phase one. Phase two comprised the characterisation of the reference mix developed in phase one and its subsequent modification with redispersible polymers for an improved cracking performance. The 2^5 full factorial experiment with three replicates was set up in phase one. A description of the factorial experimental design method is presented in Section 4.7.3. Five mix design parameters (also referred to as factors interchangeably) were varied simultaneously in a random manner. These factors were identified as those that had the greatest contribution to cracking as presented in the literature review in Section 3.4. They have been discussed in the subsequent paragraphs within this subsection. The properties of the constituent materials (e.g., grading of sand, bulk density, fineness modulus, specific gravity) were also determined. Factor screening experiments were done using a set of 32 different trial mixes. Screening experiments were used to determine the sensitivity of cracking to the selected mix design parameters. The age at cracking and the initial crack widths were monitored and recorded. The relationships that exist among the listed mix design parameters and the age at cracking were investigated. The sensitivity of cracking to the mix design parameters was also analysed. Throughout the experimental investigations, the material property that was used to evaluate the suitability of a specific mix for further testing was the age at cracking as specified in ASTM-C1581.
The information gleaned from the trends in phase one was used to cast a reference mix. The reference mix was characterised and subsequently modified to improve its resistance to cracking by redispersible polymers - ethylene vinyl acetate (EVA) and styrene acrylate (SA) - and by adjusting its water- and binder contents. Adjustments in water- and binder contents was also informed by the trends identified from the analysis of the factorial experiment using the mixes in phase one. Eight mixes were investigated in phase two. A diagrammatic summary of the experimental work is shown in Figure 4.1. The water and binder contents of the reference mix were varied at three levels consequently resulting in Mixes C230_P0, C210_P0 and C225_P0 as shown in Figure 4.1. Specific information regarding these mixes has been provided in Figure 4.1. Mix C225_P0 was chosen to assist in investigating the nature of the relationship between w/b and the age at cracking within the domain that had not been captured in phase one.

Thereafter, the mix with the best performance with respect to age at cracking was selected among the four listed mixes and modified with polymers (EVA and SA) at a polymer concentration of 10% polymer by mass of cement. The choice of an initial polymer concentration of 10% was informed by the lack of a significant change in material properties, in comparison to the reference mix, in trial mixes cast using polymer concentrations that were less than 10%. The polymer concentration of the specific type of polymer in the polymer-modified specimens that took relatively long to crack - from either of mixes C250_P1-10 and C250_P2-10 - was thereafter increased to 15% and 20%. The justification for the selected range of polymer concentrations have been provided in subsequent paragraphs within this subsection. The material properties that were investigated comprised: slump (phase one), flow (phase two), compressive strength (phase one and phase two), direct tensile strength (phase two), tensile relaxation (phase two), static elastic modulus in compression (phase two), age at cracking and initial crack widths (phase one and phase two), durability indexes (phase two) and unrestrained drying shrinkage (phase two). These tests are discussed in Section 4.7.2 and Appendix B.

The choice of factorial experiments for phase one was informed by their time- and cost-effectiveness and their ability to optimise multiple mix design parameters simultaneously while exposing and quantifying the levels and magnitude of interactions among various experimental variables. Factorial analysis of mix design parameters also eased the quantification of the levels of sensitivity of two qualitative factors - binder type and curing method - and their corresponding interactions. The inherent advantages of the factorial experimental design technique - as reported by Filho and Sanjuán (1999), Nehdi and Sumner (2002) and Carrasco et al. (2005) - comprise: saving of time and costs by limiting the total number of specimens to be investigated, the significance of experimental variables and their interactions are highlighted and it has a predictive capability for the responses of other experimental points located within the experimental domain. Montgomery (2001) also reports that factorial designs allow the effects of a factor to be estimated at several levels of the other factors, yielding conclusions that are valid over a range of experimental conditions. The availability of a commercial design of experiment statistics software (MINITAB 16) which assisted in analysing data further contributed to the adoption of this approach. Additional information regarding the details, advantages, disadvantages and the robustness of designed experiments can be found in Montgomery (2001), Lin et al. (2004), Montgomery and Runger (2003) and Ryan (2007).

The PRM mixes used in phase one were cast using two (2) binder types - CEM II B-M (L) 42.5 N and GGBS - at two (2) binder combinations - 100% CEM II B-M (L) and 50/50 GGBS/CEM II B-M (L). The choice of these binders is informed by the contribution of GGBS towards an enhanced durability. GGBS has also been reported to reduce the heat of hydration and delay the rate of early-age strength development (Concrete-Society, 2003a). GGBS has other advantageous, though indirect, effects on many crack-determining material properties as discussed in Section 3.4.1.

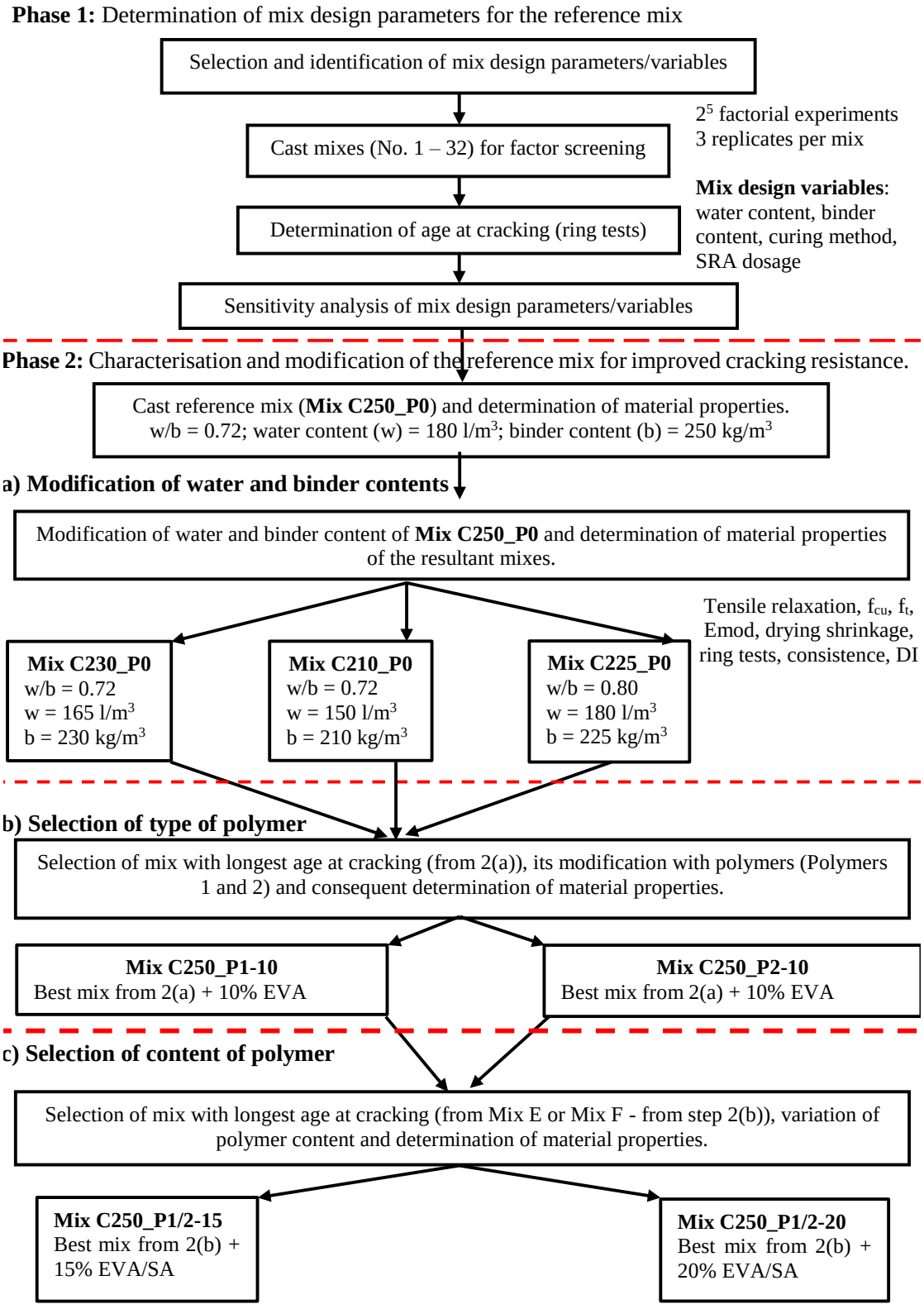

FIGURE 4.1: Flow chart of experimental programme

The choice of CEM II B-M (L), 42.5 N was informed by the fact that it was the only normal hardening cement that was readily available locally in the South African cement

market when this research begun. This cement also had the potential to contribute towards meeting the objectives of this research considering the information presented in Section 3.4.1. The PRMs that were studied were intended to be non-structural; thus, it is preferential that either slow or normal hardening cements are used. Vaysburd and Emmons (2000) and Carlswärd (2006) also report that a rapid gain in stiffness, due to rapid hardening, lowers important crack-determining properties like creep and tensile relaxation; thereby increasing their susceptibility to cracking. Bentz et al. (2008) further report that high early-strength cements contribute to early-age cracking due to their high thermal and autogenous shrinkage deformations. PC/GGBS mixes were only used in phase one.

The w/b is an important parameter and has been discussed in Section 3.4. The effect of w/b was investigated by varying the individual water and binder contents in the mixes simultaneously. The upper and lower limits of binder content of the mixes in phase one were set at 250 kg/m^3 and 450 kg/m^3 respectively while the upper and lower limits for water content were set at 180 l/m^3 and 230 l/m^3 respectively. The choice of the upper and lower limit values of experimental variables in factorial experiments is crucial. More specifically, a narrow range of variable values tends to pick up 'noise' while a very wide range results in non-linearity which could mislead the analysis and interpretation of test results. The chosen range of experimental variables, thus, helped ensure that the effects of noise and non-linearity are eliminated. Furthermore, the water and binder contents were selected such that they were high enough to ensure that effects of autogenous shrinkage were eliminated. ACI209 (2005), Kovler and Jensen (2005), Masuku (2009) and Byard et al. (2012) report that the susceptibility of a cementitious material to autogenous shrinkage can be minimised by limiting its w/b to values that are greater than 0.40 and 0.42 respectively. Also, since the PRMs under investigation were intended for non-structural applications, high strength - which can be achieved using low w/b - was not desired.

Two redispersible polymers - ethylene vinyl acetate (EVA) and Styrene Acrylate (SA) - at contents of 10%, 15% and 20% (by mass of cement) were used. These polymer contents lie within the range that is widely used in research and practice as reported by Ohama (1995), Rixom and Mailvaganam (1999), Miller (2005) and Raupach and Büttner (2014). According to literature, the common content of redispersible polymers in practice that would not affect important material properties - such as tensile strength, bond strength, drying shrinkage - adversely vary between 5% and 20% by mass of cement. The adopted low polymer contents also helped in lowering the cost of producing the specimens. The use of redispersible polymers was restricted to phase two.

Super-absorbent polymers (SAPs) were used in phase one. The dosage of the SAP was set at 0.4% by mass of binder. The choice of this value was informed by the research of Gillmer (2012). Also, Ye et al. (2012), while referring to other studies, reports that an increase in SAP dosage above 0.35% of the mass of cement does not improve the degree of hydration of the cement. Ye et al. (2012) further reports that SAPs increase porosity. An increase in porosity, especially when pores are interconnected, could compromise

durability thereby rendering the PRMs under investigation unable to achieve their long-term role. Ring specimens were cured using wet hessian for 7 days. The hessian was wetted three times a day by soaking it in water and wrapping it around the specimens. Furthermore, curing using wet hessian was informed by the need to simulate a curing practice that closely resembles good site practice.

Environmental exposure conditions are critical to the effective performance of PRMs (Luković, 2016). Ortega et al. (2012), for example, report that a high relative humidity improves the durability and mechanical properties of mortars. This improvement could be attributed to the presence of water which favours cement hydration. Atrushi (2003) also reports that temperature influences the rate of cement hydration, the cracking risk, durability and the time development of the mechanical properties of cementitious materials. The specimens in this study were exposed to a controlled laboratory environment (Temperature: $23^oC \pm 2^o$C; Relative humidity $50\% \pm 4\%$). Temperature and relative humidity was controlled through air conditioning. The chosen range of temperature and relative humidity is also consistent with the requirements for various tests - e.g., tests for drying and restrained shrinkage. The environmental conditions in some tests such as compressive strength deviated from the specified laboratory environment based on compliance to their respective test standards. Temperature and relative humidity were continuously monitored using a Rotronic Hygropalm data logger. A graph of the variation of the mean temperature and relative humidity in the laboratory during the entire duration of testing is presented in Figure 4.2.

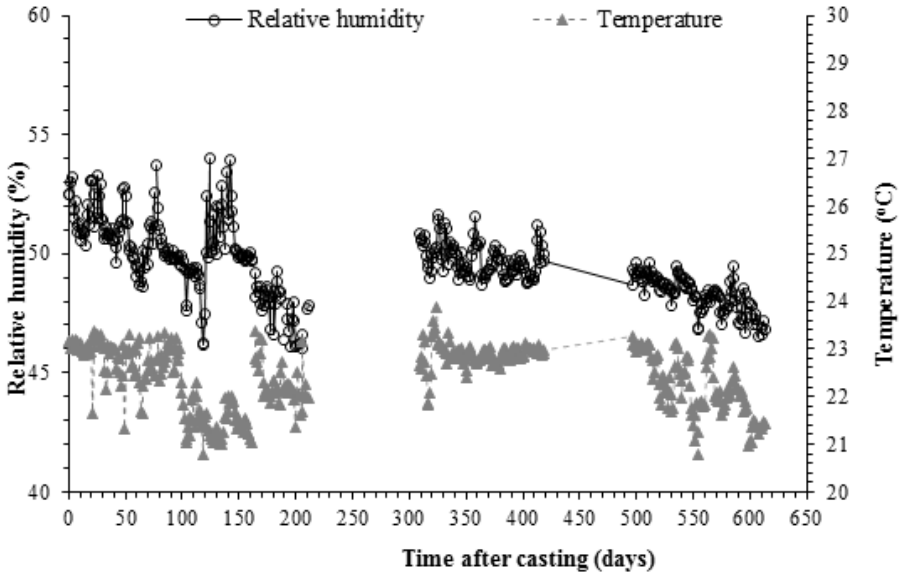

FIGURE 4.2: Variation of mean temperature and relative humidity over the duration of testing

4.2 Specimen types and sizes

The specimens under study comprised standard cubes, cylinders, prisms, rings, and dog-bone specimens whose dimensions conformed to the standard sizes specified in the test standards that have been cited in Section 4.7.2 and Appendix B. Most tests had three replicates each except for specimens that were tested for tensile relaxation and drying shrinkage which had two and four replicates respectively. The use of two specimens for tensile relaxation tests was due to limitations in the number of available equipment to conduct the relaxation tests simultaneously and the general availability of the test equipment in the laboratory. The use of four replicates for drying shrinkage was informed by the need to cater for the large variability in testing.

4.3 Experimental variables

The experimental variables for the first phase of testing comprised the following:

i. Binder content: the minimum and maximum binder contents were 250 kg/m^3 and 450 kg/m^3 respectively.

ii. Binder type: 100% CEM II B-M (L), 42.5 N and a blend of 50/50 CEM II B-M (L), 42.5 N/GGBS.

iii. Water content: the minimum and maximum water contents were 180 l/m^3 and 230 l/m^3 respectively.

iv. Curing: SAPs and wet hessian were used. Specimens for other tests were water-cured in accordance to the respective test standard for the property under consideration.

v. SRA was used. The dosages were 0% and 3% of the total mass of binder. The upper dosage was the specified maximum dosage as per the manufacturers product catalogue.

The following experimental variables were used in the second phase of testing:

i. Water content decreased in the following order: 180 l/m^3, 165 l/m^3 and 150 l/m^3.

ii. Binder content decreased in the following order: 250 kg/m^3, 230 kg/m^3 and 210 kg/m^3.

iii. Redispersible polymer type was varied as follows: Ethylene Vinyl Acetate (hereafter referred to as EVA) and Styrene Acrylate, SA (hereafter referred to as SA).

iv. Polymer content, by mass of cement, was increased in the following order: 10%, 15% and 20%.

4.4 Test equipment

The following equipment were used:

i. 50-litre concrete pan mixer and slump cone: fresh concrete production and testing.

ii. Amsler hydraulic testing machine: compressive strength and static modulus of elasticity under compression.

iii. LVDTs with a data acquisition system: elastic strains under compression stresses.

iv. Strain extensometer (BAM Setzdehnungsmesser): drying shrinkage.

v. Zwick Roell Z020 machine: tensile relaxation and direct tensile strength.

vi. Steel rings: restrained shrinkage cracking.

vii. DI test equipment: Durability Indexes (OPI and WSI).

viii. Electronic scales: mass determination of various specimens and raw materials.

ix. Sieves and mechanical shaker: aggregate sieve analysis.

x. Drying ovens: drying wet materials before casting (100 ± 5^{o}C) and specimen preparation for DI testing (50 ± 2^{o}C).

xi. Tamping rod: manual compaction of specimens and slump testing.

xii. Cylindrical metallic measure with a handle: determination of the density of sand samples.

xiii. Crack meter: crack width measurements.

xiv. Flow table: flow test.

xv. Calliper: measuring diameter.

xvi. Trowel: levelling the surface of freshly cast specimens.

4.5 Test materials

The materials that were used in this study comprise:

i. CEM II B-M (L), 42.5 N (referred to as CEM II hereafter), with a limestone content of 20% and a clinker content of 80%, supplied by AfriSam - density = 2790 kg/m^3. Additional information regarding this material is provided in Appendix A.1.

ii. Ground Granulated Blastfurnace Slag (referred to as GGBS hereafter), supplied by AfriSam density = 2890 kg/m^3. Additional information regarding this material is provided in Appendix A.2.

iii. Philippi/Dune sand (hereafter referred to as dune sand) - Fineness Modulus = 1.88 ± 0.06, loose bulk density = 1560 ± 10 kg/m^3, compacted bulk density = 1670 kg/m^3. Sieve analysis results are in Appendix A.3.1.

iv. Greywacke crusher sand (hereafter referred to as crusher sand) - Fineness Modulus = 3.09 ± 0.07, loose bulk density = 1660 ± 10 kg/m^3, compacted bulk density = 1890 ± 10 kg/m^3. Sieve analysis results are in Appendix A.3.2.

v. Superplasticisers: lignosulphonate type - (referred to as SP hereafter) supplied by Chryso SA in liquid form - density = 1.20 ± 0.02 g/cm^3 (at 20^oC). Plasticising admixture was used to ensure that the desired slump of 80 ± 20 mm is achieved. This slump was assumed to be suitable for non-structural PRMs. The superplasticiser dosage was varied, depending on the mix, to achieve the desired slump. Additional information regarding this material is provided in Appendix A.5.

vi. SAP: supplied by SNF Floerger from Andrzieux Cedex, France. Approximate bulk density = 0.8 - 0.9 g/cm^3. Additional information regarding this material is provided in Appendix A.6.

vii. SRAs: supplied by Chryso SA in liquid form. Density = 0.930 ± 0.020 g/cm^3 (at 20^oC). Additional information regarding this material is provided in Appendix A.7.

viii. Paraffin wax: used to seal specimens while testing for tensile relaxation and restrained shrinkage cracking.

ix. Redispersible polymers: an Ethylene Vinyl Acetate polymer (abbreviated as EVA hereafter) and a Styrene Acrylate polymer (abbreviated as SA hereafter) supplied by Akzo Nobel Chemicals AG from Switzerland. Additional information regarding these materials are provided in Appendix A.8.

4.6 Materials characterisation

The properties of the constituent materials for the PRM mixes were determined beforehand. The dune and crusher sand were dried in an oven at a temperature of 105 ± 5^oC for a period of 24 hours. Oven drying helped to remove any moisture that could have been in the sand. Thereafter, the properties of the oven-dried sand were determined. These properties comprise: sieve analysis, loose bulk density, compacted bulk density, voids, specific gravity and absorption and water requirement (according to ASTM-C29 - see Appendix A.3 and Appendix B.1 for additional details on testing and test results). The gradation of sands is important because it helps in the determination of water demand (Schutter and Poppe, 2004) and drawing indirect inferences on their likely effect on workability and other material properties like shrinkage, creep, tensile relaxation, tensile strength and other plastic properties (Dittmer, 2013). Dune sand from the South

African Cape Flats has a limited grading (Grieve, 2009). It contains a large proportion of fine particles which would increase the water demand. An increase in water demand would increase the susceptibility to cracking as discussed in Section 3.4.2. Owing to the need to maintain a low water demand - which would consequently reduce the susceptibility of mortars to cracking; dune sand was blended with 50% crusher sand to improve the overall grading of the fine aggregates. The grading curve for the blend of dune and crusher sands is presented in Figure 4.3. The individual grading curves for the dune and crusher sands and their corresponding sieve analysis test results are presented in Appendix A.3.

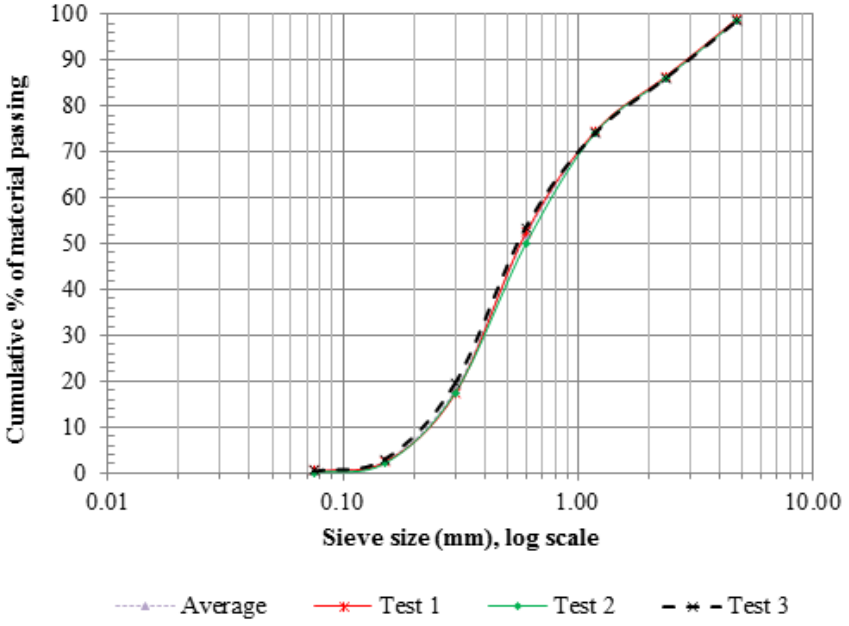

FIGURE 4.3: Grading curves for a 50/50 dune/crusher sand blend

4.7 Overview of testing procedure

The following testing regime and sequence was adopted throughout this study:

i. Determining the properties of the constituent mix materials, namely: sieve analysis, compacted bulk density, relative density, void content, fineness modulus, water demand and absorption. The results of these tests are presented in Appendix A.

ii. Batching and mixing materials for the initial 32 trial mortar mixes (factor screening experiments).

iii. Casting and compacting trial cube and ring specimens made using the mixes in (ii) above. The consistence of the fresh mortar mix was measured using the slump test

and flow test as specified in ASTM-C143 and ASTM-C1437 respectively. These tests have been described in Appendix B.3. A vibrating table was used to compact the freshly cast specimens. Results from slump and flow tests are presented in Appendix C.1.

iv. The freshly cast and compacted cubes and ring specimens were covered with a plastic sheet for 24 hours. Ring specimens were demoulded and thereafter coated with wax on their top outer surface in the radial direction. They were then transferred to a controlled laboratory environment maintained at 23 ± 2^{o}C and a relative humidity of $50 \pm 4\%$ as specified in ASTM-C1581A. Cube specimens were tested for compressive strength after 3, 7 and 28 days of water curing in a bath maintained at a temperature of 23 ± 2^{o}C in accordance with SANS 5863:2006a. Results for compressive strength tests are provided in Appendix C.2.

v. The crack widths and age at cracking of each ring specimen was monitored. The details of the testing and the test results are provided in Section 4.7.2, Appendix B.9 and Appendix C.7 respectively.

vi. A reference mix (C250_P0) was cast using the information from the trends gleaned from screening experiments in phase one. Freshly cast specimens, from the reference mix, were compacted and cured as described in (iv).

vii. The freshly cast specimens referred to in (vi) were tested and monitored for the following properties: age at cracking, crack widths, tensile relaxation, direct tensile strength, elastic modulus in compression, compressive strength (at 3, 7 and 28 days), durability indexes, and drying shrinkage. The results for these tests are in Appendix C.

viii. The reference mix was further modified by adjusting its w/b (through the modification of the water and binder contents) considering the trends identified from the results in step (v). Thereafter, two types of redispersible polymers (EVA and SA) at three different contents (10%, 15% and 20% by mass of binder) were added to the mix at various stages as presented in Figure 4.1.

ix. The effect of the addition of redispersible polymers, at various concentrations, on the age at cracking and crack-determining material properties was investigated. The results of the effect of polymer-modification are presented in Appendix C.

4.7.1 Mix design, casting and curing

The mixes under study were designed to meet the performance requirements for non-structural PRMs as specified in the EN 1504-3:2005 - see Section 3.3 and Table 3.3 for a summary of performance requirements for non-structural PRMs. The design, casting and curing of test mixes varied with the phase of the experimental programme - see Section 4.1 and Figure 4.1 for the various experimental phases of this study. Specific details regarding these phases have been discussed in the subsequent subsections.

4.7.1.1 Phase one

Owing to the large number of experimental variables that ought to be investigated and the need to develop mixes that would eventually produce PRMs that satisfy the material properties discussed earlier, a factorial experimental design approach was adopted as described in Section 4.1. A summary of the experimental variables within the factor screening phase is presented in Table 4.1.

Table 4.1: Variables for factor screening experiments (Phase one)

Factors/experimental variables	**Levels of variation**	
	-1 (low)	**+1 (high)**
Binder type	100% CEM II B-M (L)	50/50 CEM II B-M (L)/GGBS
Water content (l/m^3)	180	230
Binder content (kg/m^3)	250	450
Curing method	Wet hessian	0.4% SAP + wet hessian
SRA dosage	0%	3%

The individual mix designs of the 32 No. trial mixes are summarised in Table 4.2 and Table 4.3. It is important to note that the label of the mixes in the trial experiments were randomly generated using the design of the factorial experiments using the statistical experimental design and analysis software.

Table 4.2: Mix designs for trial mixes with 100% CEM II B-M (L)

Mix ID	**Unit content (kg/m^3)**					
	Water content	**CEM II B-M (L)**	**Dune sand**	**Crusher sand**	**SRA**	**SAP**
15	180	250	620	699	0	0
28			613	691	7.5	0
13			619	698	0	1.0
19			612	690	7.5	1.0
30		450	566	639	0	0
21			554	625	7.5	0
27			565	637	0	1.8
17			552	623	7.5	1.8
25	230	250	578	652	0	0
12			571	644	7.5	0
1			577	651	0	1.0
26			570	643	7.5	1.0
9		450	524	592	0	0
11			512	578	7.5	0
31			523	590	0	1.8
10			511	576	7.5	1.8

The need to provide additional water while using SAPs - especially with respect to achieving hydration, workability requirements and reduction in self-desiccation, plastic deformations and capillary pressure, has been reported by Castro et al. (2012), Mechtcherine and Dudziak (2011), Ye et al. (2012), Mechtcherine et al. (2013) and Sikora and Klemm (2014). Whereas Castro et al. (2012) have presented on two generalised and simple approaches that can be used to calculate the amount of water required

TABLE 4.3: Mix designs for trial mixes with 50/50 CEM II B-M (L)/GGBS

Mix ID	**Unit content (kg/m^3)**						
	Water content	**GGBS**	**CEM II B-M (L)**	**Dune sand**	**Crusher sand**	**SRA**	**SAP**
20	180	75	175	620	699	0	0
16				613	691	7.5	0
32				619	698	0	1.0
18				612	690	7.5	1.0
22		135	315	566	639	0	0
6				554	625	7.5	0
2				565	637	0	1.8
8				552	623	7.5	1.8
24	230	75	175	578	652	0	0
29				571	644	7.5	0
14				577	651	0	1.0
7				570	643	7.5	1.0
3		135	315	524	592	0	0
23				512	578	7.5	0
4				523	590	0	1.8
5				511	576	7.5	1.8

to determine the water needed for internal curing, Sikora and Klemm (2014) report that the careful selection of an SAP with desorption characteristics that are compatible with the hydration process is critical. More specifically, the diversity in types of commercially available cements leads to differences in kinetics of the hydration process which translate into differences in water requirements.

Since water absorption capacity and the rate of water uptake and release depend on the SAP type, the adjustment of water content for the SAPs and the cement used in this study would not only have been very complex, but would have also been inconsistent with the objectives of this study, especially while taking the constraints of time into consideration. Additional water to compensate for the water consumed by SAPs was not provided. The lack of readily available, clear and scientifically-supported guidelines regarding the amount of additional water that ought to be added for this specific type of SAP and binder discouraged the addition of extra water. Also, the limited quantity of SAP that was available for use in this research implied that further tests that would require additional SAPs to determine the amount of additional water needed for each mix under investigation could not be done. The fact that superplasticisers were used to achieve the target range of slump was an antithesis to the provision of additional water. Unsaturated SAPs - at a content of 0.4% by mass of binder - were thus added appropriately in the initial set of mixes during casting.

The consistence of the initial 32 mortar mixes was assessed using the slump test as specified in ASTM-C143. The test procedure for consistence has been described in Appendix B.3. The slump of the initial mixes (in phase one) ranged from 60 mm to a collapse (in some instances) based on the mix design parameters of individual mixes. The measured slump of each mix is presented in Appendix C.1. Slump tests were limited to phase one and were primarily chosen to help determine the quantity of superplasticisers

that would be added to the mix water in the mixes developed in Phase 2. 100 mm cube specimens were tested for compressive strength. The cubes were moist cured in a water tank maintained at a temperature of 23 ± 2^{o}C for a duration of 3, 7 and 28 days. The duration of curing depended on the age at which the compressive strength of the specific mix was needed. Mortar ring specimens were cured using wet hessian in a controlled environmental room for seven days. Figure 4.4 shows a ring specimen being cured using wet hessian.

FIGURE 4.4: Curing of a ring specimen using wet hessian

4.7.1.2 Phase two

Phase two comprised the modification of the original mix designs using the information gleaned from trends that were observed after the analysis of test results from phase one - see the discussions in Section 4.1. The mix designs for the reference mix and the modified mixes are summarised in Table 4.4.

TABLE 4.4: Mix designs for modified mixes (Phase two)

Mix component	**Mix ID**							
	C250_ P0	C230_ P0	C210_ P0	C225_ P0	C250_ P1-10	C250_ P2-10	C250_ P1-15	C250_ P1-20
Cement (kg/m^3)	250	230	210	225	250	250	250	250
Water (l/m^3)	180	165	150	180	180	180	180	180
Dune sand (kg/m^3)	605	605	605	613	605	605	605	605
Crusher sand (kg/m^3)	682	682	682	691	682	682	682	682
EVA (kg/m^3)	0	0	0	0	25	0	37.5	50
SA (kg/m^3)	0	0	0	0	0	25	0	0
SRA (kg/m^3)	7.50	6.90	6.30	6.75	7.50	7.50	7.50	7.50
w/b	0.72	0.72	0.72	0.80	0.72	0.72	0.72	0.72
Sand:binder ratio	5.15	5.60	6.13	5.80	5.15	5.15	5.15	5.15

The reason behind the choice of the mix design parameters presented in Table 4.4 are provided in Section 4.1. The method of batching, mixing and casting the modified

mixes was similar to the one used to cast the initial trial mixes in phase one. Each of the weighed redispersible polymer powder was batched into the mixer together with the cement in their dry state. The dry mortar mix constituents in the mixer were mixed for two minutes and water with SRA and superplasticisers added to the mix continuously as recommended by Ohama (1998) and Rixom and Mailvaganam (1999). Wet mixing was done for three minutes. The consistence of the freshly cast mortar mixes in phase two was determined using the flow test in accordance with the ASTM-C1437. The flow test results are presented in Appendix B.3.2. Figure 4.5 shows the flow testing of a mortar mix.

FIGURE 4.5: Testing a mortar mix for flow

The freshly cast mix was thereafter placed in various moulds to produce test specimens with standard dimensions and distinct shapes in the form of cubes, cylinders, prisms, rings and dog bones as per the material property to be investigated. Moulds containing the freshly cast specimens were thereafter compacted using a vibrating table in accordance with the ASTM-C192. Specific details regarding the compaction of the mortar mixes has been provided in Appendix B.4. The test specimens cast in phase two, except for the ring specimens, were water-cured in a bath. Specific details regarding how the curing was done has been described in Section 4.7.

Whereas Ohama (1995) and Rixom and Mailvaganam (1999) report that the moist curing of polymer-modified systems is detrimental to the development of their properties, the

author of this study chose to use wet-curing throughout the testing. To ensure that a sound basis upon which the effect of polymer-modification on the cracking-performance of the developed PRMs could be compared vis-á-vis that of unmodified mortars and limit the number of experimental variables to a reasonable minimum; it was crucial that the two sets of specimens be subjected to similar curing conditions. Water curing also improves durability by reducing the penetrability of the mortars to carbon dioxide, chlorides and moisture. The impenetrability of mortars further contributes to their long-term durability in service. It was, thus, counter-intuitive to cure mortars in a manner that would not improve their resistance to the ingress of aggressive chemical species on the one hand, yet expect them to be durable and effective while in service on the other hand.
Curing the polymer-modified specimen differently from the initial plain cement mixes would have, thus, confounded the comparison of the performance of these two systems. It is also important to note that most studies that report on the effects of polymers of material properties do not report on whether the mix designs were adjusted to achieve a specific slump upon which their corresponding conclusions were made or otherwise. Nevertheless, had such an action been made, there is a high likelihood that a fairly accurate analysis between polymer-modified and unmodified modified mortar was not arrived at based on the lack of a well-defined reference point. This observation has also been highlighted by Kardon (1997).

4.7.2 Cracking performance assessment of PRM mixes

The EN 1504-3:2005 performance requirements for non-structural PRMs have been discussed in Section 3.3. A critical analysis of the existing performance requirements for non-structural PRMs vis-á-vis their role has led to the conclusion that the EN 1504-3:2005 has not defined important material properties that directly relate to the cracking. It was important, therefore, that the PRMs under investigation be characterised and their cracking performance be monitored vis-á-vis the crack-determining material properties that serve as input parameters in the existing empirical analytical model discussed in Section 1.6. The PRMs under investigation were also expected to fulfil their requirements in accordance with Principle 3 and Method 3.1 in the EN 1504 series of standards. The following material properties were investigated:

i. Compressive strength (as a general material characteristic);

ii. Tensile strength in direct tension;

iii. Static modulus of elasticity in compression;

iv. Drying shrinkage;

v. Restrained shrinkage cracking (age at cracking and crack widths);

vi. Tensile relaxation;

vii. Durability Index (DI) tests (to obtain durability-related properties of the PRMs).

A detailed discussion of the above tests is presented in the subsequent subsections.

4.7.2.1 Compressive and tensile strength

Compressive strength is the most studied material property in mature and young concrete (Atrushi, 2003). The reasons for testing the compressive strength of the PRMs under investigation were to characterise them, monitor their strength development and provide input data for tests for the static modulus of elastic in compression. Compressive strength was also used to assess whether the developed PRMs met the performance requirements for strength - as specified in the EN 1504-3:2005. These tests were done on 100 mm cubes according to SANS 5863:2006a.

Compressive strength is one of the easiest material properties to determine. Atrushi (2003) reports that compressive strength provides a good picture of the general quality of the concrete; and that for a specific concrete, a correlation exists between compressive strength and other properties such as tensile strength, modulus of elasticity, deformation properties and durability. Baldwin and King (2003) also report that compressive strength can be used as a crude approximation for durability. The author, however, does not agree with the claims by Baldwin and King (2003) in totality and some components of the claims by Atrushi (2003) - specifically on the nexus between compressive strength and durability. The author believes that factors that influence compressive strength do not necessarily influence durability. Thus, an attempt to correlate compressive strength and durability could be misleading.

The test for compressive strength entailed the application of a compressive axial load continuously to cube specimens at a uniform rate of 0.3 ± 0.1 MPa/s until failure using an Amsler hydraulic compression testing machine with a load capacity of 3000 kN. The compressive load was applied through square steel platens. Compressive strength was calculated by dividing the maximum load attained during the test by the cross-sectional area of the specimen. The complete test procedure is described in Appendix B.6. Compressive strength tests were done at 3, 7 and 28 days from the date of casting. Three specimens were tested from each mix and the mean of the three compressive strength results was recorded as the compressive strength of the specific mix at a given age. The compressive strength test results of all the mixes are presented in Appendix C.2. Figure 4.6 shows a specimen being tested for compressive strength.

Cracking in cement-based materials results from the tensile stresses that develop within the material as discussed in the previous chapters. It is, thus, important that the tensile strength development of the PRM mixes be monitored to assess their susceptibility to cracking. Uys (1983), Perrie (2009) and Dittmer (2013) report that the tensile strength of a PRM is affected, among other factors, by the following parameters: w/b, binder type, binder content, void content, curing conditions, size and shape of the specimen, type and size of aggregate and the direction and rate of application of load.

FIGURE 4.6: Compressive strength testing of mortar (100 mm cube)

The tensile strength of a cement-based material can be tested in different ways, namely: the direct tensile strength, the flexural strength (or modulus of rapture), the ring/hoop tension test and the splitting tensile strength (also known as the Brazilian test) (Atrushi, 2003; Carlswärd, 2006; Dittmer, 2013; Uys, 1983; Yao and Wei, 2014). Each of these tests has its unique advantages and disadvantages that would render it appropriate for use in specific applications. The measurement of direct tensile strength in cement-based materials, though important for crack assessment purposes, has been reported to be complex, time-consuming and challenging. The difficulties that characterise direct tensile strength tests comprise the fixation of a specimen to the testing equipment and environmental factors (Atrushi, 2003; Carlswärd, 2006; Ranaivomanana et al., 2013; Uys, 1983; Yao and Wei, 2014). Considering the highlighted difficulties, Uys (1983) reports that direct tensile strength tests are not recommended for routine laboratory and field use. Swaddiwudhipong et al. (2003) and Ranaivomanana et al. (2013), however, report that direct tensile strength tests are more rational and reliable.

In contrast, indirect tensile strength test methods, such as the splitting tensile strength are simple to conduct. When compared to direct tensile strength tests, the splitting tensile test has results in strengths whose magnitude are consistently higher than those from direct tensile tests by 5% to 15% as shown in Figure 4.7 (Dittmer, 2013; Neville, 1995; Uys, 1983; Yao and Wei, 2014). Yao and Wei (2014) report that the magnitude of direct tensile strengths are lower than those obtained from splitting tensile strengths at early ages (up to 3 days) with the difference between the two tests narrowing with an increase in the age of test specimens. Uys (1983) reports that strengths obtained from the splitting tensile test are closer to the direct tensile strength when compared to those obtained from the modulus of rapture tests. Thus, it can be inferred that indirect methods for determining tensile strength tend to overestimate strengths at early ages -

i.e., the ages when cement-based materials are more susceptible to crack. The fact that indirect tensile strength tests overestimate tensile strength implies that they might not be an ideal source of input properties for the modelling and prediction of cracking in PRMs.

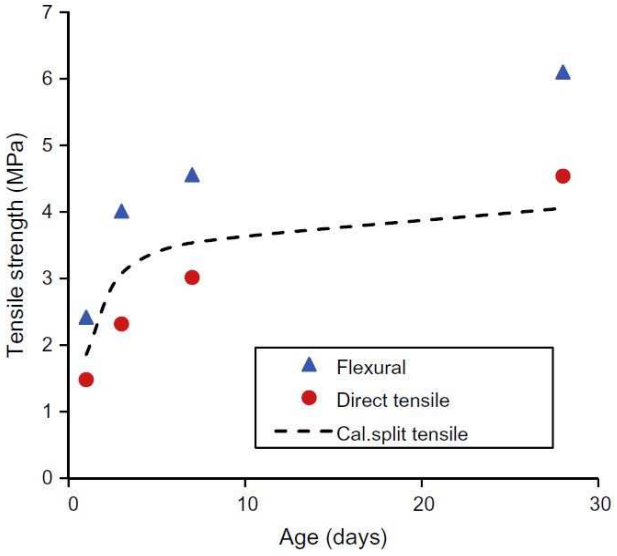

FIGURE 4.7: Comparison of tensile strengths of cementitious materials at various ages using various test methods - adopted from Yao and Wei (2014)

Owing to the need for an accurate understanding, assessment and prediction of the cracking performance of the developed PRMs in the current and future studies, and the need to overcome the limitations of indirect testing for tensile strength as mentioned above, direct tensile strength tests were conducted. These tests were done at 3, 7 and 28 days. Uniaxial direct tensile strength was obtained from notched dog-bone specimens (see Figure 4.8). Notches were created by protrusions on the sides of the mould used to cast the specimens. The concentration of stresses within the notched cross-sections helped to localise failure at the notch. The dimensions of the notched dog-bone specimens are provided in Figure 4.8.

A Zwick Roell Z020 Universal Testing Machine (UTM) (hereafter referred to as the Zwick) with a maximum load capacity of 20 kN was used to test for direct tensile strength. The remote and flared ends of notched dog-bone specimen were clamped into the cavity within the aluminium loading platens of the Zwick. Thereafter, a direct tensile load was applied on the machine at a constant rate within set limits (0.2 mm/minute or approximately 1.2 microstrain per minute) (Arito et al., 2016a; Masuku, 2009) until the specimen failed. The loading rates that were used are also recommended in SANS 863-5:1994 which specifies a time envelope of between three to ten minutes for concrete material tests. The tensile strength of the PRM was calculated as the load at failure divided by the effective cross-sectional area of the specimen. The effective cross-sectional

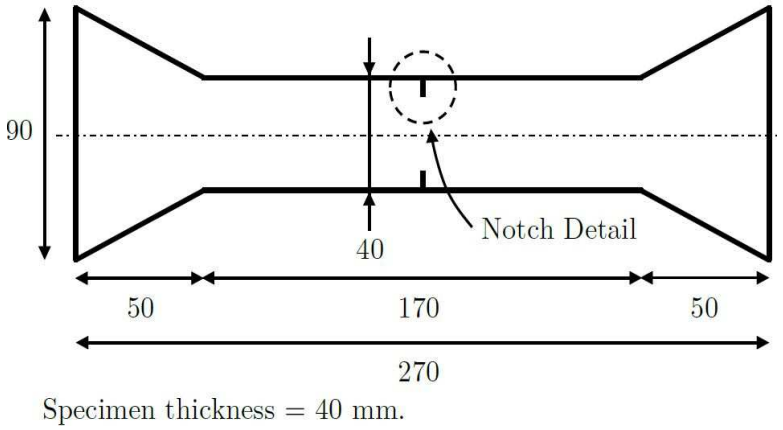

(a) Dog bone specimen configuration

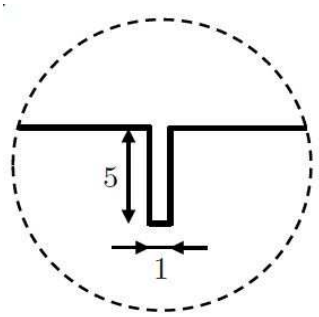

(b) Notch detail

FIGURE 4.8: Dimensions of a notched dog-bone specimen - all dimensions in mm

area of the specimen was 30×40 mm (i.e. after deducting the notch dimensions). Three specimens were tested. The reported mean tensile strengths is the average of three test results of a specific mix at a specific age. These tests were done in an environmental room maintained at a temperature of 21 ± 1^{o}C and relative humidity of $55 \pm 5\%$. The direct tensile strength test results are presented in Appendix C.3. Figure 4.9 shows a specimen being tested for direct tensile strength.

4.7.2.2 Static modulus of elasticity

The elastic modulus (abbreviated as E modulus or E mod) is also known as the young‘s modulus or modulus of elasticity. The elastic modulus of cementitious materials and their corresponding performance requirements has been discussed in detail in previous chapters. The static modulus of elasticity is an important material parameter. It can be determined in many ways, namely: by non-destructive tests, e.g., using ultrasonic pulse velocity (Nilsen et al., 1995), or by destructive tests, e.g., by compressing standard cylindrical specimens or through splitting cubes.

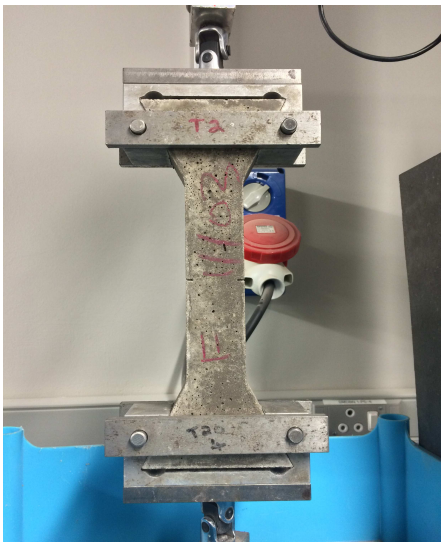

FIGURE 4.9: A dog-bone specimen under direct tensile strength test

Whereas the importance of the elastic modulus to cracking in cementitious materials such as PRMs is clear, there is a need to understand the type of elastic modulus that would be relevant to cracking; and as such, could be used to develop accurate crack prediction models for cracking. Cracking in PRMs is attributed to tensile stresses. It is logical, therefore, that the tensile elastic modulus would be a more appropriate parameter to assess the susceptibility of a PRM to cracking instead of the compressive elastic modulus. Yao and Wei (2014) report that the magnitude of the direct tensile elastic modulus is greater than the compressive elastic modulus; with the ratio of the former to the latter being 1.17 at very early ages, and around 0.97 - 1.07 at other ages. Other studies also report that the ratios of direct tensile to compressive elastic modulus range between 1.11 and 1.2. The relationship between elastic modulus in tension and compression is shown in Figure 4.10.

Atrushi (2003), while referring to other studies, reports that the difference between the results obtained from testing for elastic modulus in tension or compression is not significant. Atrushi (2003) further reports that the elastic modulus determined in tension after 28 days is approximately 15% higher than the one determined in compression; and attributes these differences to: differences in the stress-strain relation in tension and compression beyond the initial tangent relation; differences in the magnitude of loads imposed on the material in the different directions and differences in testing procedures. Yao and Wei (2014) also report that elastic modulus obtained from instantaneous elastic deformation measurements in tensile creep tests are less than those that have been obtained from direct measurement at very early age with the difference diminishing at the age of 7 days. From the discussions above, it is evident that there exists a difference, albeit small in magnitude, between direct tensile elastic modulus and compressive elastic modulus.

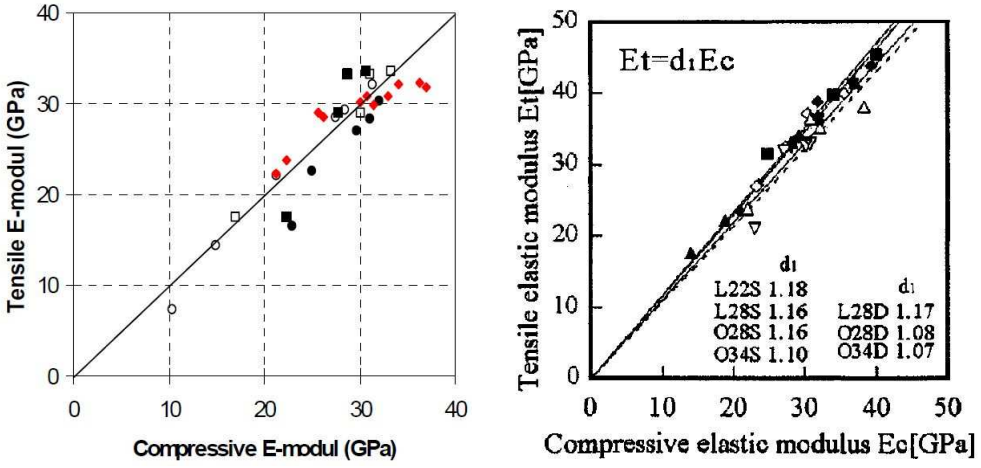

(a) (b)

FIGURE 4.10: Relation between the modulus of elasticity in tension and compression - at 30% loading from two different studies - adopted from Atrushi (2003)

The need to accurately assess the cracking-performance of the PRMs in this study and to create a platform for future research that would facilitate the analytical modelling of cracking demanded that the tensile elastic modulus be measured. However, the absence of a test standard that could guide these tests and the lack of appropriate test equipment that could guarantee accurate and synchronised measurements of tensile stress and their corresponding strains posed a major challenge. The compressive static modulus of elasticity was, therefore, determined at 7 and 28 days according to BS 1881: Part 121:1983. Cylindrical specimens with a diameter of 100 mm and a height of 200 mm were used. A hydraulic compression testing machine equipped with LVDTs and a data acquisition system were used. The loading capacity of the compression testing machine was 3000 kN. Specimens were loaded at a rate of 0.6 ± 0.4 MPa/s until the stress equal to one-third of the compressive strength of the mortar mix was reached. Loading cement-based specimens at stress levels above 30% has been reported by Brandt (2009) to result in a significant loss in the linearity in the stress-strain relationship; consequently, introducing heterogeneities such as microcracks. A significant deviation in linearity eventually results in erroneous elastic modulus test results. Brandt (2009), however, reports that the stress value of 30% is an approximate value which varies in large limits depending on material properties and the type of testing machine. Details regarding this test are provided in Appendix B.7.

The deformations that correspond to each load increment were automatically measured using LVDTs attached to a data acquisition system. The test results - compressive loads and their corresponding displacements - were downloaded from a computer attached to the machine in the form of an MS Excel file and thereafter analysed. The static modulus

of elasticity was calculated from the gradient of the secant modulus of the plotted stress-strain curves as specified in the formula in the BS 1881: Part 121: 1983. For each mix, three specimens were tested for elastic modulus. The mean of the three measurements was reported as the elastic modulus of specimens from that specific mix. The test results for compressive modulus of elasticity are presented in Appendix C.4. Figure 4.11 shows the testing of a cylindrical mortar specimen for elastic modulus under compression.

FIGURE 4.11: Compressive elastic modulus testing using a cylindrical specimen (cylinder with 100 mm diameter and 200 mm height)

4.7.2.3 Drying shrinkage

The test for drying shrinkage entails the determination of length changes produced by causes other than externally applied forces and temperature changes in prismatic mortar specimens made in the laboratory and exposed to controlled temperature and moisture conditions. The dimensions of a patch repair - specifically the area and thickness - affect its performance in service (Baluch et al., 2002; Luković, 2016). Luković (2016) reports that repairs covering a large area are more prone to cracking than those that cover a small area. However, there is no conclusive evidence on the nature of the relationship between the thickness of a repair and its susceptibility to cracking. Studies on this relationship - as reported by Luković (2016) - have reported contradicting results. Nevertheless, it was crucial that the size of the specimen for drying shrinkage tests be carefully considered. Drying shrinkage tests were conducted in accordance with the SANS 6085:2006. Prism specimens, 100 × 100 × 300 mm in dimension, were used. The dimensions of these specimens were carefully chosen to ensure that the surface area to volume ratio (SA:V) between these specimens and those that were used to cast the ring specimens were as close as possible. Consistency in SA:V would make comparisons between various material properties and cracking easy. A constant SA:V also provided a basis upon which research on the modelling cracking in the studied mixes could be done - using

the shrinkage measurements as input parameters in analytical models for cracking and stress prediction.

Drying shrinkage was calculated by dividing the change in length between a set of targets - measured using a strain extensometer - over the duration of measurement by the gauge length of the targets (100 mm). The complete test procedure for this test is described in Appendix B.8. Four specimens were tested for each mix. Drying shrinkage was monitored daily over a period of 56 days from the date of casting. The duration of testing corresponded to the longest time taken by a specific specimen to crack. The mean of the four shrinkage measurements of a specific mix was reported as its shrinkage. Shrinkage results are presented in Appendix C.5. Figure 4.12 shows typical drying shrinkage test specimens.

FIGURE 4.12: Drying shrinkage test specimens (300 mm height, gauge length 100 mm)

4.7.2.4 Restrained shrinkage cracking

Restraint refers to all mechanical effects that prevent the deformation of a given body (Denarié et al., 2011). They can be internal (i.e., provided by the aggregate and unhydrated cement particles, moisture) or external (because of frictional forces between the PRM and the substrate, reinforcement bars and dowels). Although free shrinkage data are useful in comparing different mix proportions, they do not provide sufficient information to determine how cementitious materials will crack in service (Zhou et al., 2014). It is, therefore, necessary that the cracking tendency of a cement-based material be evaluated under restrained conditions by qualitative means through a range of cracking tests. Many test methods have been developed to measure restrained shrinkage cracking. These tests can be broadly categorised into the following: ring tests with a restraining core, longitudinal tests where the restraint is at the edge of the specimen, panel tests in which the restraint is along the circumference, and tests in which the restraint is offered by the substrate. The shape of the rings could either be elliptical (He

and Li, 2005; Zhou et al., 2014) or circular. Further details regarding these tests can be found in Lambe (1988), Bentur and Kovler (2003), Banthia and Gupta (2009) and Zhou et al. (2014).

Darquennes et al. (2011b) further report that the risk of cracking cannot be quantified entirely based on free/drying shrinkage tests because these tests do not consider all the factors that affect the stress development inside a material such as the degree of restraint, stress relaxation and the evolution of tensile strength. It is imperative, therefore, that a test that closely simulates the condition of stresses in PRMs in service is used to estimate the risk of cracking. The ring test is the most commonly used test for estimating the sensitivity of repair mortars to cracking and their cracking potential (Bentur and Kovler, 2003; Carlswärd, 2006; Gopinath, 2010; Hannawi et al., 2013; Nguyen et al., 2012; Turatsinze et al., 2006). This test involves casting a mortar or concrete annulus around a steel ring which restrains its shrinkage due to circumferential drying. This restraint results in the development of tensile stresses and consequently cracking. The progress of cracks, according to Brandt (2009), reflects the influence of material composition, structure and curing on the resistance to cracking. In the ring test, the degree of restraint to the repair mortars depends on the thickness of the steel ring (Zhou et al., 2014). It has been reported that a thicker restraining steel ring provides more restraint in comparison to a thinner one.

Lambe (1988), Hossain and Weiss (2006) and Topçu and Bilir (2010) report that the ring test is advantageous because of the following reasons: its results can be easily correlated with the tendency of a material to show cracking, it is economical, simple to perform and does not pose difficulties in performing end restraint. The ring test has also been used to evaluate autogenous shrinkage (Grondin et al., 2012), the effects of alkalis on the cracking of cementitious materials (Zhou et al., 2014), plastic shrinkage cracking of fresh concrete and the shrinkage cracking of hardened concrete. The simplicity and economy of ring tests has contributed to its widespread use and adoption in various test standards around the world (Carlswärd, 2006; Gopinath, 2010). Despite its widespread use, Banthia et al. (1996), Abbasnia et al. (2005), Mauroux et al. (2012) and Beushausen and Chilwesa (2013) argue that ring tests fail to simulate the real restraint condition of the substrate. Thus, it is crucial that ring tests are complemented by tests on actual substrates should the need to predict the age at cracking of an actual overlay arise. The other disadvantage of ring tests is that uninstrumented rings generally provide qualitative comparisons of shrinkage cracking between mixtures; consequently, limiting the amount of information that can be obtained from such tests.

Tests for restrained shrinkage cracking were done in accordance to ASTM-C1581; but with some modifications owing to the lack of equipment - especially the strain gauges and their accompanying data acquisition systems. The dimensions of the rings that were used in this study are as follows: outer diameter = 406 mm, inner diameter = 330 mm, height = 150 mm. The thickness of the inner steel ring was 12.5 mm. A sample of freshly mixed mortar was compacted in a circular mould around the steel ring using a vibrating table. The resistance of the mortar to cracking was indicated by the age at

cracking. The average width of the cracks on each specimen was measured immediately after opening using a crack meter. The crack meter was capable of measuring widths of up to 4.0 mm with an accuracy of 0.02 mm. The complete test procedure for this test is described in Appendix B.9. Three specimens were tested from each mix. The mean of the three different measurements - age at cracking and crack width - were reported as the mean age at cracking and crack width. The test results from this test are presented in Appendix C.7. Figure 4.13 shows a typical ring specimen.

FIGURE 4.13: Restrained shrinkage specimen (length and width of the wooden base is 450 mm)

4.7.2.5 Tensile relaxation

Tests for tensile relaxation comprised the use of dog-bone specimens. These dog-bone specimens, however, were not notched like the ones used for direct tensile strength testing because they were not loaded to failure. The geometry of the specimens for tensile relaxation were designed and chosen to eliminate errors while testing. Specifically, the specimens and the gripping jaws within the Zwick machine were also designed to avoid the effects of shear failure, torsion and bending moments - which could arise owing to eccentricity - by using a swivel head. The gripping jaws of the Zwick machine were braced to mitigate the effects of deformation and jaw widening. Each relaxation specimen was loaded up to 80% of its ultimate direct tensile strength at the beginning of the test using a Zwick Universal Testing Machine (UTM). The loading at 80% of the ultimate direct tensile strength has been reported by Beushausen et al. (2012) to be more realistic in simulating the behaviour of bonded overlays under service conditions or members that are close to cracking. Furthermore, Atrushi (2003) - while referring to other studies - reports that an initial stress/strength ratio of up to 90% does not exert a very significant influence on tensile relaxation.

Prior to testing for tensile relaxation, each specimen was removed from the curing tank and sealed with paraffin wax on all surfaces to ensure that they could not undergo

additional stress build-up due to drying shrinkage during testing. The sealed specimens were fitted within the gripping jaws of the Zwick testing machine in readiness for testing. Atrushi (2003) - while referring to other studies - reports that the most important parts of the creep, and relaxation, spectra are the first three days after load application. Thus, it was necessary that the relaxation of the test specimens is investigated within this critical period. However, limitations in the number and availability of tensile relaxation testing machines forced the author to conduct these tests over a duration of 48 hours from the time of loading.
Tensile relaxation was determined at 3, 7 and 28 days from the date of casting using two Zwick UTM machines with two different capacities of their loading frame: 20 kN and 100 kN. Whereas Beushausen et al. (2012) report that mature specimens undergo less relaxation at later ages - i.e., ages greater than 7 days, therefore raising an important question on the need for 28-day tensile relaxation - the authors choice for testing for relaxation at later ages were underpinned by the following reasons:

i. The 28-day relaxation test results provided a basis upon which they could be easily compared to other crack-determining material properties that are usually determined at 28-days.

ii. The long-term time development of relaxation would help to assess the effect of mix modification on long-term relaxation - especially with respect to specimens which took long to crack.

iii. To align the test results to the industry practice where material properties are specified using their 28-day properties.

iv. A longer relaxation time could also help in providing input parameters in further studies on analytical modelling of cracking in these mixes - especially in instances where material properties at 28-days are used as input parameters.

The procedure for testing for the tensile relaxation is hereby described:

i. The remote and flared ends of a sealed dog-bone specimen were clamped into the cavity within the loading platens of the Zwick machine.

ii. The data acquisition software on the Zwick was started and a uniaxial tensile force applied on the specimen. Each dog-bone specimen was loaded to a stress level that is equivalent to 80% of its ultimate direct tensile strength. This stress level was informed by prior research done by Masuku (2009) and Beushausen et al. (2012).

iii. Stress relaxation in the specimen was monitored and recorded continuously using the data acquisition software.

iv. The test was terminated after a period of 48 hours from the time of application of the initial uniaxial tensile force.

The mean of the tensile relaxation readings - obtained from two specimens per mix - was reported as the relaxation value of the given mix. The testing environment was maintained at a temperature of 21 ± 1^{o}C and relative humidity of $55 \pm 5\%$. Results from relaxation tests are presented in Appendix C.6. Figure 4.14 shows the testing of a specimen for tensile relaxation.

FIGURE 4.14: Tensile relaxation testing using a Zwick UTM

4.7.2.6 Durability Indexes (DIs)

Durability is the ability of a building and its parts to perform its required function over a specific time despite the influence of agents that cause deterioration. The permeability of a PRM is an important feature of the general performance of materials. It ought to be considered in the design, selection and execution of brittle matrix composites as materials for building and civil engineering structures (Brandt, 2009). Tests for penetrability can be used to predict whether a PRM will prevent the ingress of aggressive chemical species which would lead to further degradation and corrosion of reinforcing steel. The Durability Index (DI) tests were used to test for penetrability and to characterise the PRMs. The Oxygen Permeability Index and Water Sorptivity Index tests were conducted. The DI testing of the PRM mixes was done at 28 days in accordance with the Durability Index Testing Procedure Manual 2010 (Ver. 2.0, May 2010). The detailed test procedure is described in Appendix B.10.

4.7.3 Methodology for sensitivity analysis

The simultaneous optimisation of multiple mix design parameters in cement-based mixes is a difficult process. It cannot be achieved using any intuitive design approach because there are many design criteria and variables involved. Furthermore, the need to amalgamate the wide range of requirements related to the mechanical properties, technological

conditions and economies within a broad array of boundary conditions needs robust multi-criteria optimisation techniques. The determination of the sensitivity of cracking to mix design parameters entailed the use of factorial experimental design techniques. Factorial experiments have been used in cement and concrete research to optimise mix designs and to investigate the effect of multiple mix design parameters on material properties and costs. Typical examples of the use of factorial experimental design approach in cement and concrete research comprise:

i. Kovler et al. (1999b) used factorial experiments to investigate the influence of w/b, SF content and curing on splitting tensile strength of high strength concrete under two curing conditions.

ii. Nehdi and Sumner (2002) used factorial experiments to investigate possible synergistic effects in ternary cementitious blends.

iii. Carrasco et al. (2005) used a central composite factorial experiment to optimise the strength of tailor-made cement using limestone filler and blast furnace slag.

iv. Filho and Sanjuán (1999) used a 2^3 factorial experimental design to investigate the effect of low modulus sisal and polypropylene fibre on the free and restrained shrinkage of mortars at early age.

v. Abouhussien and Hassan (2014) used factorial designs to optimise the mix proportions of high strength self-compacting concrete containing Metakaolin.

The age at cracking was the reference parameter in the determination of the sensitivity of cracking to the investigated mix design parameters and their corresponding interactions. Sensitivity was evaluated by determining the magnitude of the contrast of each factor in the factorial experiment, and their corresponding interactions, with respect to the age of cracking of each PRM mix. The magnitude of the contrast of each factorial effect, and their corresponding interactions, is equal to its sensitivity. The sensitivity of cracking to each mix design parameter/factor could also be assessed visually from a Pareto plot of the standardised effects of each factor with respect to the cracking performance of the trial mixes. Sensitivity could also be obtained by looking at the sum of squares of the analysed factorial experiments. Parameters that are significant have a higher sum of squares in comparison to those that are not significant. The p-value of the factorial design could also be used to identify significant factors. MINITAB 16 was used to design the factorial experiment and analyse the test results.

4.8 Closure

This chapter has presented a detailed description of the experimental design approach used in this study, the testing philosophy and other relevant information pertaining to the experimental work. The experimental work was organised into two phases: phase one and phase two. In phase one, the effect of water content, binder content, curing

method, SRA dosage and binder type - and their corresponding interactions - on cracking and crack-determining material properties in non-structural PRMs made in accordance with the EN 1504-3:2005 were investigated. The results from this phase were used to establish the sensitivity of cracking to the listed mix design parameters in the PRMs under investigation. The design of experiments in phase one entailed the use of a 2^5 factorial experiment with three replicates. The reasons that informed the selection of factorial experiments are provided within this chapter. 32 different trial mixes were cast in this phase. The sensitivity of the mentioned mix design parameters was evaluated vis-á-vis the age at cracking in ring specimens made in accordance with the ASTM-C1581. In phase two, the effects of water content, binder content, w/b, polymer type and polymer content on the age at cracking and other crack-determining material properties were investigated. The design of mixes in phase two was informed by the information and trends that were gleaned from the tests done in phase one and the results from the sensitivity analysis. Eight different mixes were designed and tested in phase two. The mixes in phase two were further tested for the following material properties: compressive strength, direct tensile strength, static modulus of elasticity in compression, drying shrinkage, age at cracking, initial crack width, tensile relaxation and durability indexes. The test standards that were used to prepare and test the various specimens for the listed properties and the test procedures have been discussed in this chapter. The compressive strength and durability indexes were used to characterise the specimens. The specimens in this study were exposed to a controlled laboratory environment. The laboratory environment was consistent with the requirements in test standards that a specific test ascribed to. Finally, to the knowledge of the author, there are no established standards for the testing of direct tensile strength and tensile relaxation in mortar specimens. Thus, there is a need to develop standards for these two tests so that results from different studies can be correlated.

Chapter 5

RESULTS AND DISCUSSIONS

This chapter presents the results from the experimental work. The analysed results from tests are presented in graphs, figures and tables. An in-depth analysis and discussion of the test results is presented in this chapter.

5.1 Effect of mix design parameters on age at cracking and crack widths (Phase one)

The sensitivity of cracking to five mix design parameters - binder type, binder content, water content, curing method and SRA dosage - was determined in this phase. The sensitivity of cracking was evaluated using the age at cracking test results from ring specimens cast in accordance with the ASTM-C1581. Prior to the analysis of results, outliers within a set of test results were detected using the Dixons test at a confidence interval of 95%. The detected outliers were discarded and the specific test repeated. Details regarding this statistical technique have been provided in Appendix D.2 (NB: the test results, throughout this study, were assumed to be normally distributed). Unless otherwise stated, the reported test results are a mean of three measurements. The magnitude of the error bars in each column graph is equivalent to an offset of 5% of its mean result. Throughout this subsection, the term control mix refers to mixes that were cast without admixtures - i.e., they did not have SAPs and/or SRAs. The statistical formulae used in the analysis of data in this study - e.g., correlation analysis and regression analysis - are in Appendix D.

5.1.1 Effect of binder type

The effect of binder type on the age at cracking and crack width across the trial control specimens is presented in this subsection. Unless otherwise stated, the reported comparisons are between PC and PC/GGBS mixes with identical w/b.

5.1.1.1 Age at cracking

The effect of w/b on the age at cracking in control mixes is presented in Figure 5.1.

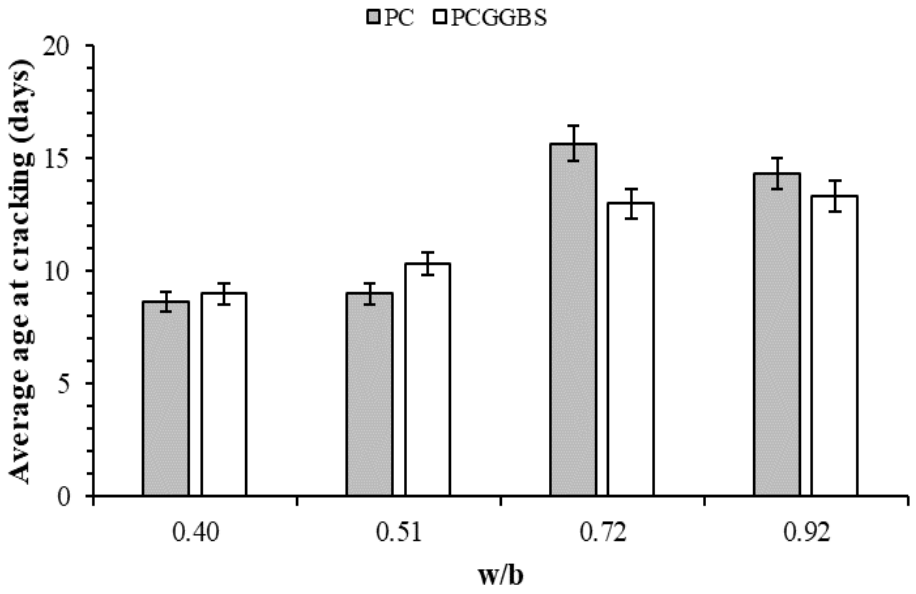

FIGURE 5.1: Effect of w/b on age at cracking in control mixes

An increase in w/b, within the ranges under investigation, delayed cracking in all test specimens regardless of the binder type as seen in Figure 5.1. A strong positive linear correlation - with a correlation coefficient of 0.86 - exists between the age at cracking and w/b. This correlation coefficient implies that an increase in w/b delays cracking. The observed delay in cracking with an increase in w/b are consistent with the findings of Banthia and Gupta (2009), Arito et al. (2016a) and Beushausen and Bester (2016). Banthia and Gupta (2009) attributed the delay in cracking to the reduction in the total amount of heat evolved during hydration. According to Atrushi (2003), a reduction in w/b results in an earlier build-up of internal tensile stresses - due to the high heat of hydration generated during hydration and an increased elastic modulus - which increase the susceptibility to early cracking. Byard et al. (2012) and Li et al. (2012) report that increasing the w/b provides more water for hydration - a phenomenon that reduces self-desiccation and shrinkage stresses caused by the consumption of water in the micropores. The reduction in self-desiccation and shrinkage stresses reduces susceptibility of mixes to undergo autogenous shrinkage consequently delaying cracking.

Hypothetically, the delay in cracking due to an increase in w/b can be attributed to the combined effects and interactions among four material properties: elastic modulus, shrinkage, tensile relaxation and capillary pore pressure. The interactions among these properties could explain which one among them plays a dominant role at any instance; consequently, dictating their contribution to the net state of stresses within the PRM.

The presence of freely available water - above the quantity needed for hydration - due to an increase in w/b increases shrinkage (He and Li, 2005; Uys, 1983). Increasing the w/b also reduces the elastic modulus; consequently reducing the stresses due to restrained deformations. An increase in w/b increases tensile relaxation (Taylor, 1997). An increase in tensile relaxation delays cracking due to an increase in the magnitude of stress relief. Low w/b mixes are characterised with reduced capillary pores (Byard et al., 2012). The movement of water within small capillary pores generates high pressures and capillary stresses within the mortar matrix which would increase the susceptibility to cracking. It is evident, therefore, that knowledge of the interplay between shrinkage, elastic modulus, tensile relaxation and capillary pore pressure is critical to the understanding of cracking.
The addition of GGBS resulted in varied effects. Changes in the age at cracking due to the addition of GGBS in specimens with w/b of 0.72 and 0.92 were not statistically significant. The addition of GGBS delayed cracking in specimens with w/b of 0.51 significantly and reduced the age at cracking in specimens with w/b of 0.72 significantly. These observations could not be explained considering the limited tests that were conducted in phase one. These observations, however, are consistent with the discussions in Section 3.4.1. It can be observed that there is no clear trend regarding the effect of GGBS on cracking - an observation that has also been reported by Li et al. (2012) and Luković (2016).
A delay in cracking due to the addition of GGBS in mixes with w/b of 0.51 (and 0.40 which experienced a negligible delay) could be inferred to result from the reduction in the total heat of hydration - and their corresponding thermal stresses and strains - and pore refinement as discussed in Section 3.4.1. A reduction in the heat of hydration and pore refinement - which translates to a high tensile strength and elastic modulus - and the reduction in the rate of drying shrinkage could have counterbalanced the high tensile stresses in the mix. The rate of development of tensile strength and elastic modulus in mixes cast using GGBS is slow. Thus, GGBS mixes can accommodate large strains at early ages due to their extensibility; consequently delaying cracking.
The addition of GGBS reduced the age at cracking in mixes with w/b of 0.72 and 0.92. It can be inferred that the reduction in the age at cracking resulted from an increase in capillary pore pressure due to pore refinement, the increased elastic modulus and drying shrinkage, the low matrix strength at early ages and reduced tensile relaxation at later ages (Bouzoubaâ and Fournier, 2003; Concrete-Society, 2003a; Darquennes et al., 2011b; Jaufeerally, 2001; Kanna et al., 1998; Langan et al., 2002; Luković, 2016; Mehta and Monteiro, 2006; Neto et al., 2008; Ortega et al., 2012; Taylor, 2014; Tazawa et al., 1989; Toutanji et al., 2004; Uys, 1983). High tensile stresses due to high capillary pore pressures and drying shrinkage on the relatively weak PC/GGBS matrix at early ages would increase the susceptibility to cracking. From the observations above, it can be posited that the influence of GGBS on shrinkage depends on the interactions that exist between the stresses emanating from the heat of hydration, drying shrinkage and capillary pressure and the mechanical properties that accompany the resulting mix - specifically tensile strength at early ages. The veracity of this proposition, however,

could not be ascertained because shrinkage, elastic modulus, and tests for capillary pore pressure were not undertaken in phase one.
The delay in cracking due to an increase in w/b can also be attributed to the increased aggregate content within the specimens. Increasing the volume of aggregates dilutes the paste. Dilution reduces the quantity of cement - the phase associated with shrinkage deformations - thereby delaying cracking. Mixes with w/b of 0.72 and 0.92 had the highest volume of aggregates (74% and 69% respectively) and were characterised by a delay in cracking. Increasing the aggregate volume - due to the reduction in binder content - also increases the internal restraining action of aggregates. An increase in restraint due to aggregates reduced shrinkage. Mallows (1985), Maruyama and Sasano (2013) report that aggregates restrain the movement of the cement paste because they are dimensionally stable. Dittmer and Beushausen (2014) also report that an increase in aggregate content delays cracking significantly; with this effect being more pronounced at high w/b than at low w/b.

5.1.1.2 Crack width

The effect of w/b on crack width in control mixes is presented in Figure 5.2. The crack widths varied widely across the entire range of specimens as seen from Figure 5.2. This variability is partly attributed to the fact that cracks were left to occur at random and on their own without undue influence on their location and width - e.g., by making notches of a specific width at predetermined locations - and variations in specimen manufacture such as compaction. A negative correlation - with a correlation coefficient of -0.67 - exists between w/b and crack widths. This correlation coefficient implies that an increase in w/b results in a reduction in crack widths. The reduction in crack width due to an increase in w/b is consistent with the findings of Beushausen and Bester (2016) and Arito et al. (2016a). Increasing w/b reduces elastic modulus and increases tensile relaxation; consequently reducing the magnitude of displacement of opposite crack faces. The addition of GGBS resulted in varied effects. The incorporation of GGBS increased the crack widths in mixes with w/b of 0.40 significantly and reduced the crack widths in mixes with w/b of 0.51 and 0.92 significantly. There was no significant difference in crack widths in mixes with w/b of 0.72 due to the incorporation of GGBS. Mixes with w/b of 0.72 exhibited the smallest crack widths. GGBS mixes, except for the mix with w/b of 0.40, were generally characterised by smaller crack widths in comparison to PC-only mixes.
The relationships and trends that exist between aggregate volume, aggregate:binder ratio (abbreviated as a/b hereafter) and the crack widths, based on the observed data, are not well-defined. A negative linear correlation - with a correlation coefficient of -0.78 - exists between crack widths and a/b. Thus, it can be posited that an increase a/b reduces crack widths. Similarly, a linear negative correlation - with a correlation coefficient of -0.61 - exists between crack width and aggregate volume. It can also be posited that an increase in aggregate volume reduces crack widths. It can be inferred

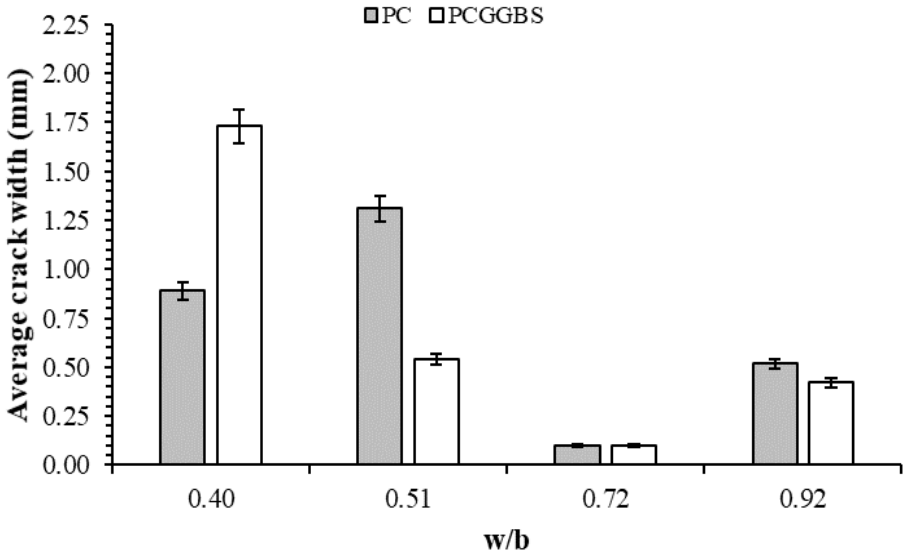

FIGURE 5.2: Effect of w/b on crack width in control mixes

that the observed reduction in crack widths - due to an increase in aggregate volume and a/b - resulted from a reduction in shrinkage within the cement paste due to the internal restraining action of aggregates. A reduction in shrinkage manifests as a reduction of the displacement within opposite crack faces. The observed reduction in crack widths corroborate the findings of Banthia and Gupta (2009) and Dittmer and Beushausen (2014).

5.1.1.3 Summary

The effect of w/b and binder type on the age at cracking and crack widths in control mixes is summarised in Table 5.1. Throughout the presented data, the number in front of any given specimen refers to its unique mix identity as presented in Table 4.2 and Table 4.3. The constituents of each mix are presented in Section 4.7.1. The number in brackets within any reported value refers to its standard deviation from the mean.

5.1.2 Effect of SRA

The effect of SRA on the age at cracking and crack width across the specimens in phase one is presented in this subsection. SRA was the only admixture used to prepare the mixes discussed in this subsection.

5.1.2.1 Age at cracking

The effect of SRA on the age at cracking in PC-only and PC/GGBS mixes is presented in Figure 5.3 and 5.4. The addition of SRA, except for PC/GGBS mixes with w/b of

TABLE 5.1: Effect of binder type and w/b on age at cracking and crack width in control mixes

Mix ID	Binder type	w/b	Age at cracking (days)	Crack width (mm)
30	PC-only	0.40	9 (0.58)	0.89 (0.27)
22	PC/GGBS		9 (0)	1.73 (0.46)
9	PC-only	0.51	9 (0)	1.31 (0.44)
3	PC/GGBS		10 (0.58)	0.54 (0.12)
15	PC-only	0.72	16 (1.15)	0.10 (0.02)
20	PC/GGBS		13 (1.00)	0.10 (0.02)
25	PC-only	0.92	14 (0.58)	0.52 (0.18)
24	PC/GGBS		13 (0.58)	0.42 (0.18)

0.72, delayed cracking significantly across the specimens under investigations as seen in Figure 5.3 and Figure 5.4. The delay in cracking in the PC/GGBS mixes with w/b of 0.72 was not statistically significant. The observed delay in cracking, due to the incorporation of SRA, was expected and is consistent with literature. It can be inferred that SRAs reduced the surface tension associated with the movement of water within the capillary pores in the mortar matrix. The reduction in surface tension reduced drying and autogenous shrinkage and eventually delayed cracking (Banthia and Gupta, 2009; Carlswärd, 2006; Gopinath, 2010).

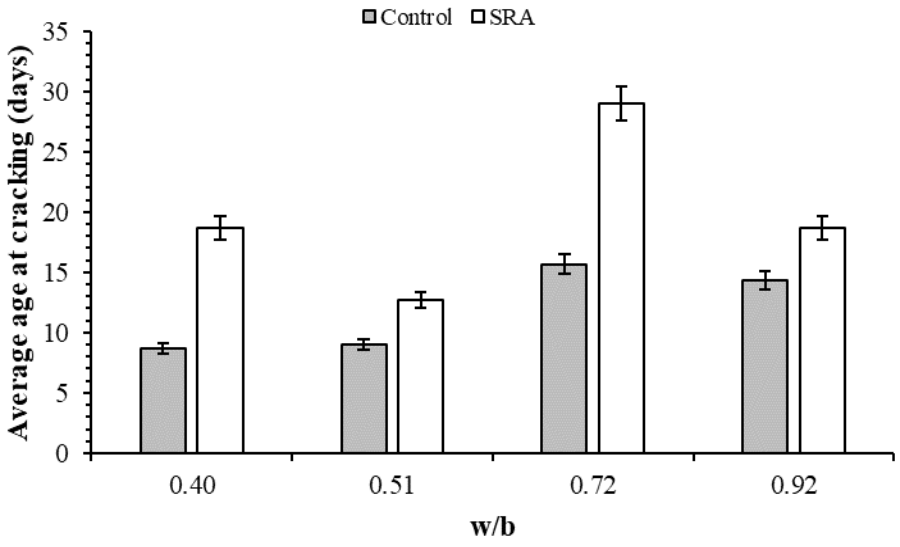

FIGURE 5.3: Effect of SRA on age at cracking in PC-only mixes

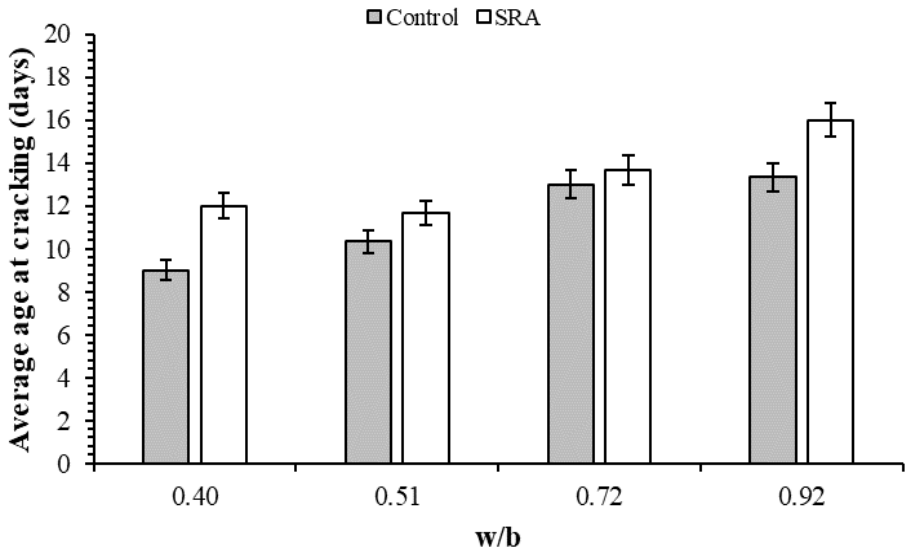

FIGURE 5.4: Effect of SRA on age at cracking in PC/GGBS mixes

According to Gopinath (2010), SRAs can retard the hydration of cement and the temperature development. The retardation in hydration and temperature development ensures that thermal stresses are generated in a material after it has developed sufficient strength to withstand them. This phenomenon reduces the susceptibility to crack. The percentage increase in the age at cracking due to the reduction in shrinkage was observed to be dependent on w/b. This phenomenon corroborates the observations of Rixom and Mailvaganam (1999). The highest percentage increase in age at cracking was observed in mixes with w/b of 0.40. A weak positive linear correlation - with a correlation coefficient of 0.34 - exists between the age at cracking and w/b in specimens with SRA. From the correlation coefficient, it can be posited that an increase in w/b delays cracking. A similar inference was also made in the control specimens. The effect of w/b on the age at cracking is discussed in Section 5.1.1.1.

5.1.2.2 Crack width

The effect of SRA on crack width in PC-only and PC/GGBS mixes is shown in Figure 5.5 and Figure 5.6. The variability in crack widths in the specimens - as seen in Figure 5.5 and Figure 5.6 - was large. There was no clearly defined trend between crack widths and w/b in PC-only specimens with SRAs. Crack widths in PC/GGBS specimens with SRAs except for the mix with w/b of 0.92 - decreased with an increase in w/b. A weak negative linear correlation - with a correlation coefficient of -0.47 - exists between crack widths and w/b. It can be inferred, from the correlation coefficients, that an increase in w/b resulted in a reduction in crack width in mixes with SRA. This trend was also observed in the control mixes. Also, the addition of SRA resulted in a significant

reduction in crack width, except for mixes with w/b of 0.72. The percentage reduction in crack width due to the addition of SRA was generally higher in PC-only mixes than in PC/GGBS mixes with w/b of 0.40 and 0.51; and higher in PC/GGBS mixes than in PC-only mixes with w/b of 0.72 and 0.92.

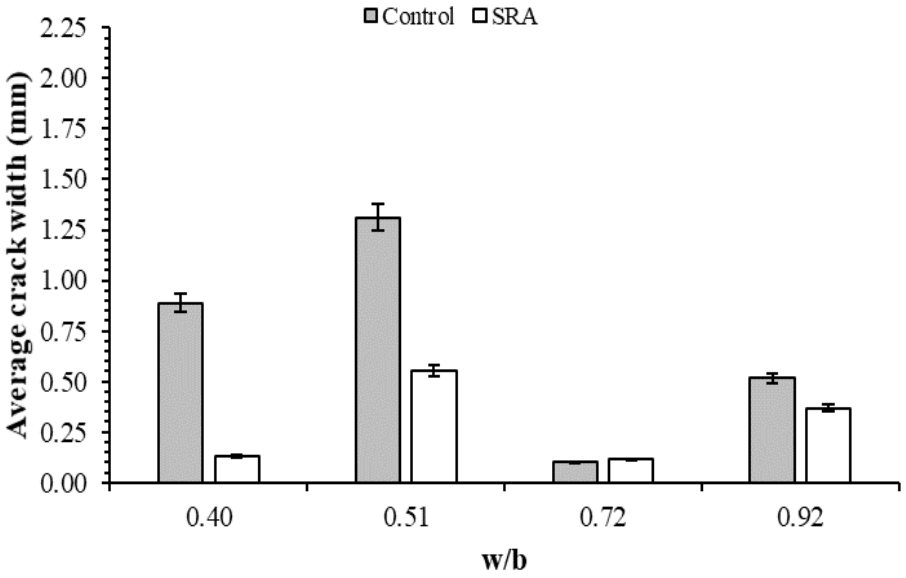

FIGURE 5.5: Effect of SRA on crack width in PC-only mixes

It can be inferred that the reduction in crack width due to the incorporation of SRA resulted from the reduction in the magnitude of autogenous and drying shrinkage among the mixes. A reduction in shrinkage reduces the magnitude of the displacement between two crack faces. Also, the significant reduction in crack widths in mixes with low w/b could be due to the ability of the SRA to reduce both autogenous and drying shrinkage, unlike in mixes with high w/b where SRAs reduce drying shrinkage only. Details on how SRAs reduce cracking and crack widths can be found in Section 2.6.1 and Section 3.4.5.2.

5.1.2.3 Summary

The effect of SRA, binder type and w/b on the age at cracking and crack width is summarised in Table 5.2. Throughout the presented data, the number in front of any given specimen refers to its unique mix identity as presented in Table 4.2 and Table 4.3. The constituents of each mix are presented in Section 4.7.1. The number in brackets within any reported value refers to its absolute standard deviation from the mean. From the discussions in the preceding subsections, it is evident that the most significant reductions in crack width were observed in mixes with w/b of 0.40. Also, the incorporation of SRAs

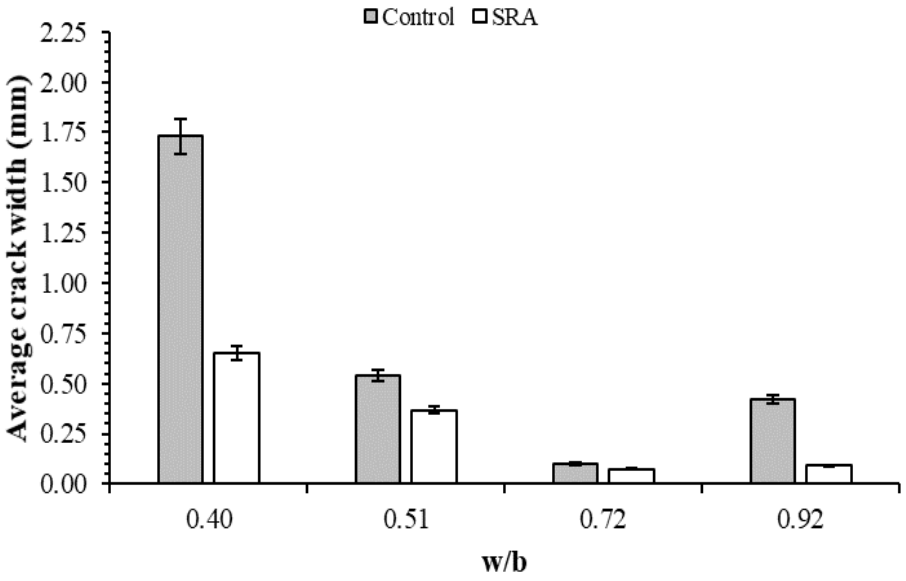

FIGURE 5.6: Effect of SRA on crack width in PC/GGBS mixes

- in most cases - generally improved the performance of the mixes under investigation significantly by delaying cracking and reducing crack widths.

TABLE 5.2: Effect of binder type, SRA and w/b on age at cracking and crack widths

Mix ID	**Binder type**	**Specimen type**	**w/b**	**Age at cracking (days)**	**Crack width (mm)**
30	PC-only	Control	0.40	9 (0.58)	0.89 (0.27)
21		SRA		19 (2.08)	0.13 (0.03)
22	PC/GGBS	Control		9 (0)	1.73 (0.46)
6		SRA		12 (1.00)	0.65 (0.05)
9	PC-only	Control	0.51	9 (0)	1.31 (0.44)
11		SRA		13 (0.58)	0.55 (0.31)
3	PC/GGBS	Control		10 (0.58)	0.54 (0.12)
23		SRA		12 (0.58)	0.37 (0.13)
15	PC-only	Control	0.72	16 (1.15)	0.10 (0.02)
28		SRA		29 (3.00)	0.11 (0.04)
20	PC/GGBS	Control		13 (1.00)	0.10 (0.02)
16		SRA		14 (1.15)	0.08 (0.01)
25	PC-only	Control	0.92	14 (0.58)	0.52 (0.18)
12		SRA		19 (1.53)	0.37 (0.13)
24	PC/GGBS	Control		13 (0.58)	0.42 (0.18)
29		SRA		16 (1.73)	0.09 (0.03)

5.1.3 Effect of SAP

The effect of SAP on the age at cracking and crack width across the test specimens in phase one is presented in this subsection. SAP was the only admixture used to prepare the mixes discussed in this subsection.

5.1.3.1 Age at cracking

The effect of SAP on age at cracking in PC-only and PC/GGBS mixes is presented in Figure 5.7 and Figure 5.8. SAPs delayed cracking significantly in mixes with w/b of 0.40 and 0.92 across the entire range of binders. The delay in cracking in mixes with w/b of 0.51 and 0.72, however, was not statistically significant. The observed delay in crack, due to addition of SAP, was expected and is consistent with the findings of Byard et al. (2012) and Beushausen and Gillmer (2014). The delay in cracking due to the addition of SAPs generally increased with an increase in w/b across all binder types. A strong positive linear correlation - with a correlation coefficient of 0.92 - exists between the age at cracking in mixes with SAP and w/b. It can be inferred, from the reported correlation coefficient, that an increase in w/b delays cracking. Similar observations were made in both the control and SRA specimens.

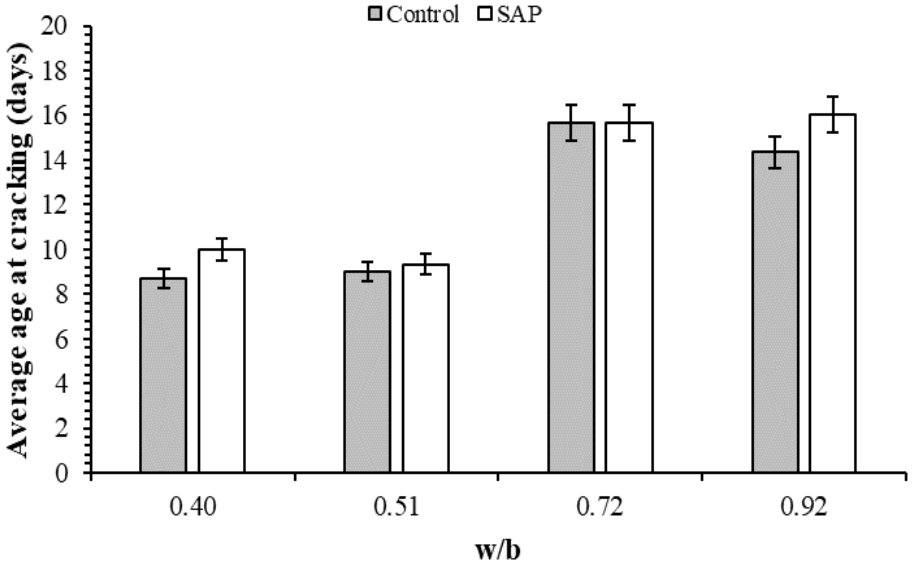

FIGURE 5.7: Effect of SAP on age at cracking in PC-only mixes

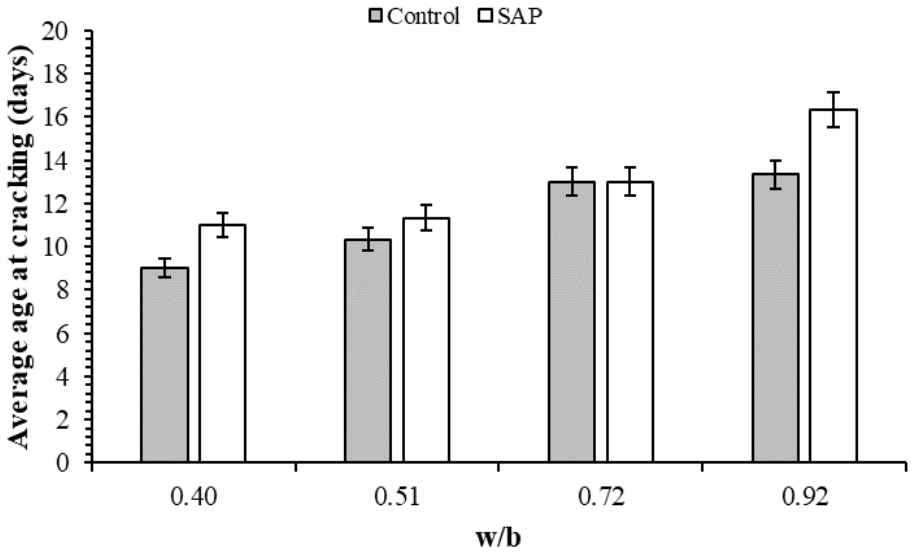

FIGURE 5.8: Effect of SAP on age at cracking in PC/GGBS mixes

The delay in cracking due to the addition of SAPs was greater in PC/GGBS mixes than in PC-only mixes. While further tests could not be done to establish the reason behind the PC/GGBS mixes performing best with respect to SAPs; it can be inferred that the behaviour of PC/GGBS mixes is usually dependent on curing - a proposition that has also been reported by Al-Gahtani and Khan (2003). SAPs improved curing. The improved curing increased tensile strength and reduced both autogenous and drying shrinkage (de Sensale and Goncalves, 2014). SAPs also increase the tensile relaxation, reduce elastic modulus due to the creation of empty pores within the matrix when they lose water during hydration - consequently delaying cracking as discussed in Section 3.4.6 (Beushausen and Gillmer, 2014; Byard et al., 2012; Craeye et al., 2011; Cusson et al., 2011; Mechtcherine, 2011; Mechtcherine and Dudziak, 2011; Mechtcherine et al., 2013; Ye et al., 2012). Mechtcherine and Dudziak (2011) also report that SAPs counteract the build-up of stresses in restrained ring specimens effectively.

5.1.3.2 Crack width

The effect of SAP on crack width in PC-only and PC/GGBS mixes is presented in Figure 5.9 and Figure 5.10.

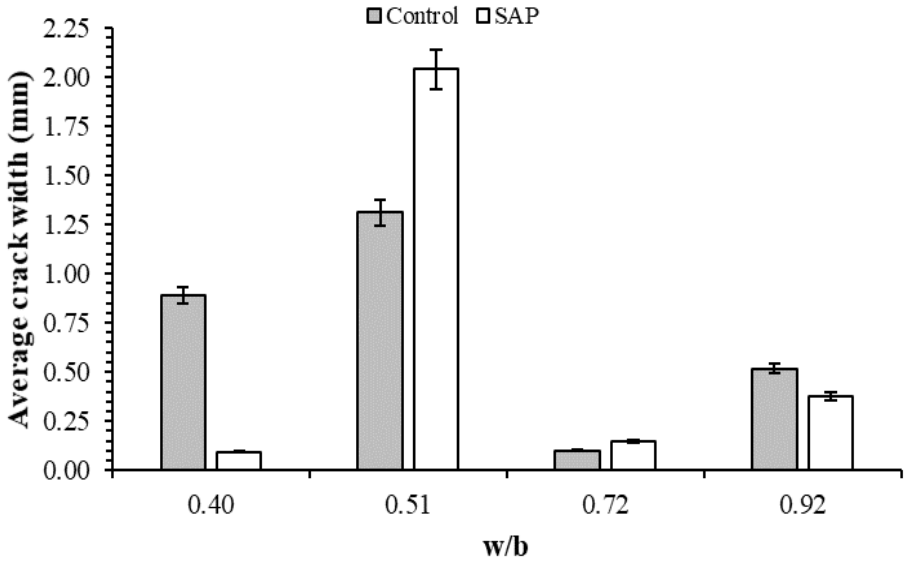

FIGURE 5.9: Effect of SAP on crack width in PC-only mixes

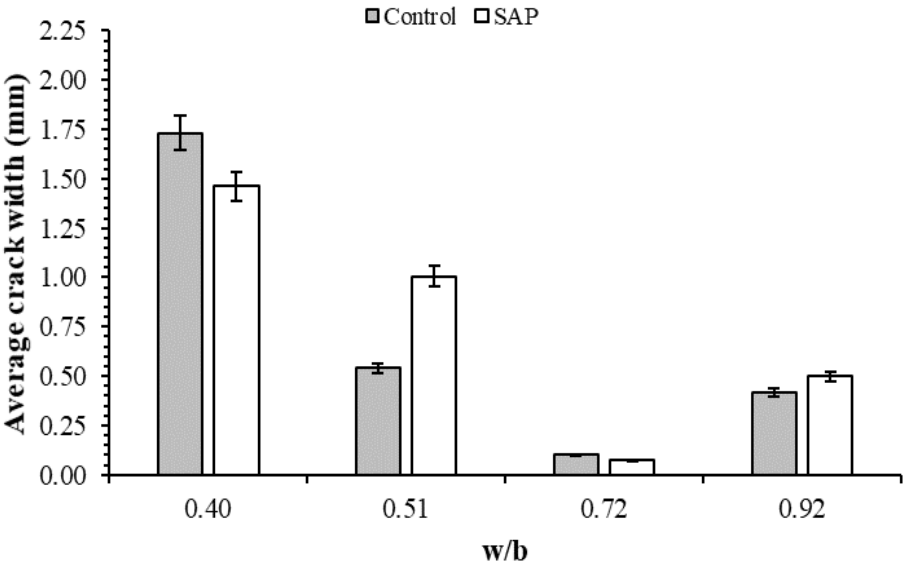

FIGURE 5.10: Effect of SAP on crack width in PC/GGBS mixes

There was a wide variability in crack widths in mixes with SAPs a phenomenon that was also observed in control mixes and mixes with SRA. A clear and well-defined trend between w/b and crack widths in mixes with SAPs could not be observed in PC-only

mixes. Except for the PC/GGBS mix with w/b of 0.92, an increase in w/b in mixes with SAP resulted in a reduction in crack width. A weak negative linear correlation - with a correlation coefficient of -0.45 - exists between crack widths in SAP mixes and w/b. From the reported correlation coefficient, it can be inferred that an increase in w/b reduces crack widths. This relationship was also observed in the control and SRA mixes.

5.1.3.3 Summary

The effect of SAP, binder type and w/b on the age at cracking and crack width is summarised in Table 5.3. Throughout the presented data, the number in front of any given specimen refers to its unique mix identity as presented in Table 4.2 and Table 4.3. The constituents of each mix are presented in Section 4.7.1. The number in brackets within any reported value refers to its absolute standard deviation from the mean. From the discussions above, it is evident that the effect of SAP on the age at cracking was more pronounced in mixes that have been cast using w/b of 0.40 and 0.92. Generally, the magnitude of the positive effect of SAP in delaying cracking was small.

Table 5.3: Effect of binder type, SAP and w/b on age at cracking and crack widths

Mix ID	Binder type	Specimen type	w/b	Age at cracking (days)	Crack width (mm)
30	PC-only	Control	0.40	9 (0.58)	0.89 (0.27)
27		SAP		10 (0)	0.09 (0.02)
22	PC/GGBS	Control		9 (0)	1.73 (0.46)
2		SAP		11 (1.00)	1.46 (0.14)
9	PC-only	Control	0.51	9 (0)	1.31 (0.44)
31		SAP		9 (0.58)	2.04 (0.51)
3	PC/GGBS	Control		10 (0.58)	0.54 (0.12)
4		SAP		11 (0.58)	1.01 (0.08)
15	PC-only	Control	0.72	16 (1.15)	0.10 (0.02)
13		SAP		16 (0.58)	0.14 (0.04)
20	PC/GGBS	Control		13 (1.00)	0.10 (0.02)
32		SAP		13 (1.00)	0.07 (0.02)
25	PC-only	Control	0.92	14 (0.58)	0.52 (0.18)
1		SAP		16 (1.00)	0.38 (0.17)
24	PC/GGBS	Control		13 (0.58)	0.42 (0.18)
14		SAP		16 (1.53)	0.50 (0.16)

5.1.4 Combined effect of SAP and SRA

The combined effect of SAP and SRA on the age at cracking and crack width across the test specimens in phase one is presented in this subsection. Both SAP and SRA were used to cast the mixes discussed in this subsection.

5.1.4.1 Age at cracking

The combined effect of SAP and SRA on the age at cracking in PC-only and PC/GGBS mixes is presented in Figure 5.11 and Figure 5.12. The simultaneous addition of SAP and SRA delayed cracking significantly across the entire range of w/b and binder types as seen in Figure 5.11 and Figure 5.12. A weak positive linear correlation - with a correlation coefficient of 0.6 - exists between the age at cracking and w/b in mixes with SAP and SRA. This correlation can be inferred to mean that increasing w/b delays cracking. The inferred relationship, however, is very weak when compared to previous mixes. Also, it can be inferred that the combination of SAP and SRA counteracts the negative effect of low w/b; considering that SRAs reduce shrinkage while SAPs improve microstructure - due to continuous hydration of the cement. Specifically, a reduction in shrinkage reduces the susceptibility to cracking. Also, an improvement in hydration increases tensile strength and consequently the susceptibility of the material to withstand tensile stresses. Further research into this inference ought to be undertaken in future.

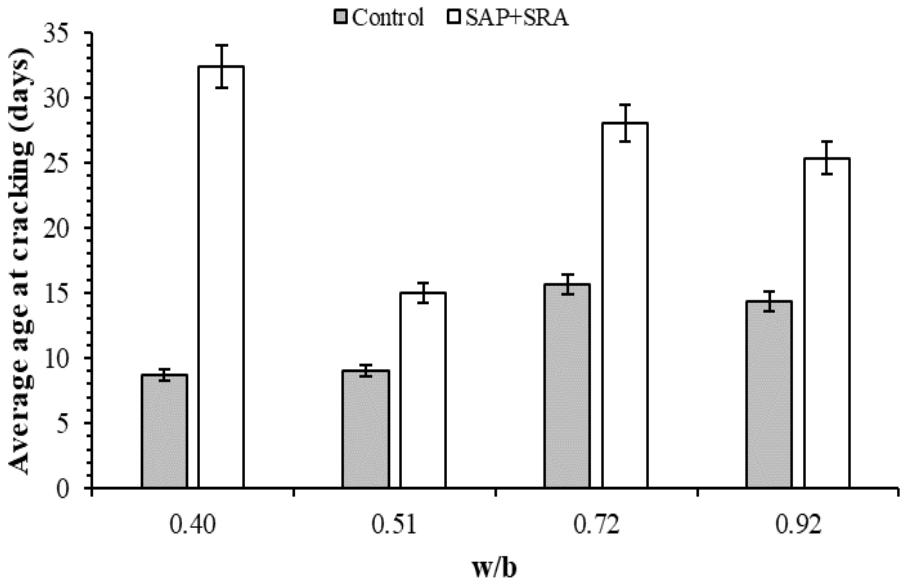

FIGURE 5.11: Effect of SAP and SRA on age at cracking in PC-only mixes

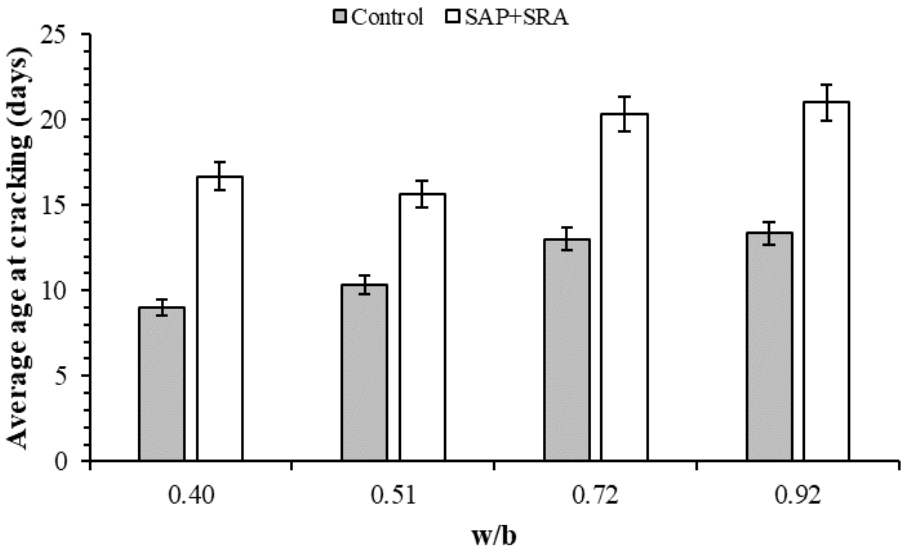

FIGURE 5.12: Effect of SAP and SRA on age at cracking in PC/GGBS mixes

The effect of the simultaneous addition of SAP and SRA on the age at cracking was more pronounced than the individual effects of SAP and SRA - see Table 5.4 in Section 5.1.4.3 for a summary of the test results. Thus, it can be inferred that a positive synergy exists between SAP and SRA. While it can be inferred that a positive synergy exists between SAP and SRA, it can also be posited that the contribution of SRA to the delay in cracking was more than the contribution of SAPs see Table 5.4 for a comparison of the individual and combined effects of SAP and SRA. The synergy between SAP and SRA ought to be critically investigated in future studies.

5.1.4.2 Crack width

The combined effect of SRA and SAP on crack width in PC-only and PC/GGBS mixes is presented in Figure 5.13 and Figure 5.14. There was a wide variability in crack widths a phenomenon that has been seen throughout the entire set of test results in phase one. The incorporation of SAP and SRAs - as seen in Figure 5.13 and Figure 5.14 - reduced crack widths across the entire set of specimens significantly except for PC-only specimens with w/b of 0.40. A significant reduction in crack width in PC/GGBS mixes due to the addition of SAP and SRA was only observed in the mix with w/b of 0.40. It can be inferred that the reduction in crack widths due to the incorporation of SAP and SRA resulted from the combined effects of reduced modulus of elasticity and autogenous and drying shrinkage in these mixes as discussed in the preceding subsections.

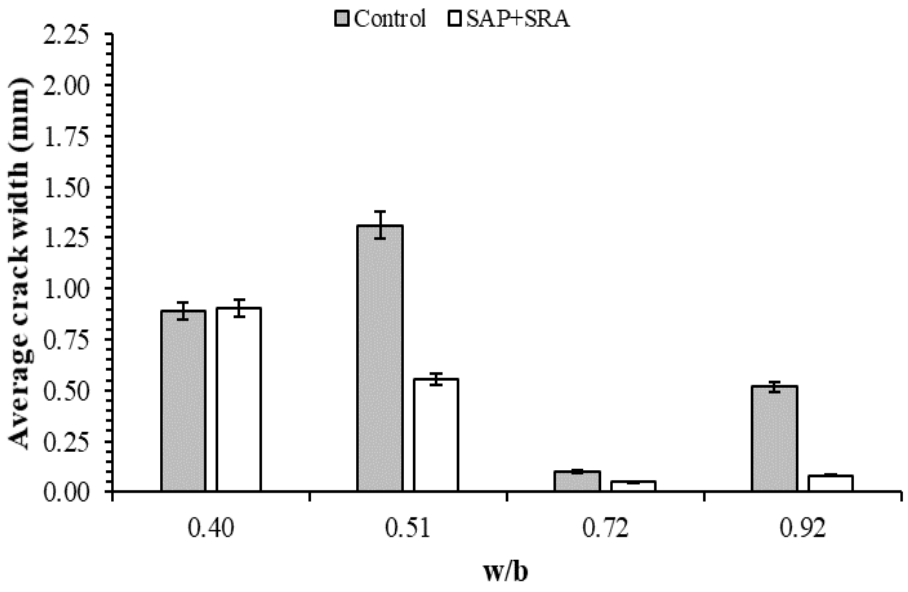

FIGURE 5.13: Effect of SAP and SRA on crack width in PC-only mixes

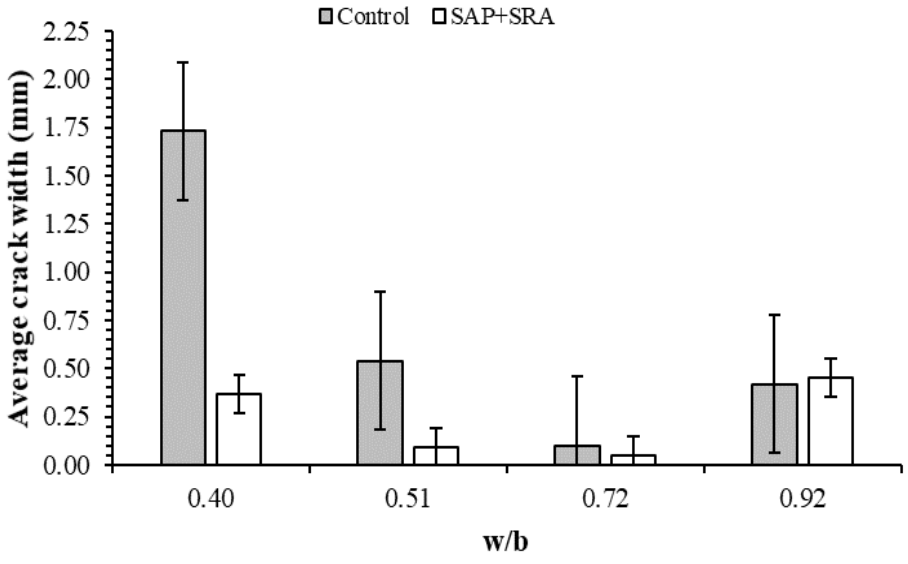

FIGURE 5.14: Effect of SAP and SRA on crack width in PC/GGBS mixes

5.1.4.3 Summary

The effect of SRA, SAP, binder type and w/b across the entire set of mixes on the age at cracking and crack width is summarised in Table 5.4. Throughout the presented data, the number in front of any given specimen refers to its unique mix identity as presented in Table 4.2 and Table 4.3. The constituents of each mix are presented in Section 4.7.1. The number in brackets within any reported value refers to its absolute standard deviation from the mean.

Table 5.4: Effect of binder type, SRA, SAP and w/b on the age at cracking and crack widths in specimens

Mix ID	Binder type	Specimen type	w/b	Age at cracking (days)	Crack width (mm)
30	PC-only	Control	0.40	9 (0.58)	0.89 (0.27)
21		SRA		19 (2.08)	0.13 (0.03)
27		SAP		10 (0)	0.09 (0.02)
17		SRA & SAP		32 (1.53)	0.90 (0.22)
22	PC/GGBS	Control		9 (0)	1.73 (0.46)
6		SRA		12 (1.00)	0.65 (0.05)
2		SAP		11 (1.00)	1.46 (0.14)
8		SRA & SAP		17 (1.15)	0.37 (0.21)
9	PC-only	Control	0.51	9 (0)	1.31 (0.44)
11		SRA		13 (0.58)	0.55 (0.31)
31		SAP		9 (0.58)	2.04 (0.51)
0		SRA & SAP		15 (0)	0.56 (0.23)
3	PC/GGBS	Control		10 (0.58)	0.54 (0.12)
23		SRA		12 (0.58)	0.37 (0.13)
4		SAP		11 (0.58)	1.01 (0.08)
5		SRA & SAP		16 (2.08)	0.09 (0.01)
15	PC-only	Control	0.72	16 (1.15)	0.10 (0.02)
28		SRA		29 (3.00)	0.11 (0.04)
13		SAP		16 (0.58)	0.14 (0.04)
19		SRA & SAP		28 (1.00)	0.05 (0.01)
20	PC/GGBS	Control		13 (1.00)	0.10 (0.02)
16		SRA		14 (1.15)	0.08 (0.01)
32		SAP		13 (1.00)	0.07 (0.02)
18		SRA & SAP		20 (0.58)	0.05 (0.01)
25	PC-only	Control	0.92	14 (0.58)	0.52 (0.18)
12		SRA		19 (1.53)	0.37 (0.13)
1		SAP		16 (1.00)	0.38 (0.17)
26		SRA & SAP		25 (1.53)	0.08 (0.01)
24	PC/GGBS	Control		13 (0.58)	0.42 (0.18)
29		SRA		16 (1.73)	0.09 (0.03)
14		SAP		16 (1.53)	0.50 (0.16)
7		SRA & SAP		21 (1.73)	0.45 (0.13)

5.2 Sensitivity analysis of mix design parameters

An analysis of the sensitivity of cracking to each of the five mix design parameters under investigation in phase one informed the selection of mix design parameters for the reference mix. The reference mix was scheduled to be modified further to improve its resistance to cracking. The sensitivity of cracking to the mix design parameters under investigation, and their corresponding interactions, was done by analysing the factorial experiment using a commercial statistical analysis software - MINITAB 16. The level of significance in the factorial analysis was set at $\alpha = 0.05$. A summary of the main effects from the factorial analysis is presented in Table 5.5. Details of the effects of the mix design parameters and their corresponding interaction are presented in Appendix D.1. The investigated mix design parameters played a significant role in cracking owing to their null p-values (which was less than the selected level of significance of $\alpha = 0.05$) as observed in Table 5.5. The sensitivity of cracking to each of the investigated mix design parameters was determined from the magnitude of the absolute value of its effect (i.e., the second column). The higher the magnitude of the absolute value of the effect, the more significant it was in comparison to other mix design parameters.

TABLE 5.5: Summary of significant main effects with respect to age at cracking

Mix design parameter	**Effect**	**p-Value**
SRA dosage	6.92	0.000
Binder content	-4.75	0.000
Binder type	-3.38	0.000
Curing method	3.21	0.000
Water content	-1.92	0.000

From Table 5.5, it can be observed that the contribution of the five mix design parameters to cracking - based on the tests that were conducted in this study - decreases in the following order of significance: SRA dosage, binder content, binder type, curing method and water content. An analysis of the main and interaction effect plots (see Appendix D.1 for the plots) from this investigation and the values presented in Table 5.5 further revealed the following:

i. The interaction effects among the investigated mix design factors are very significant to the age at cracking. An analysis of the interaction plots revealed that the interactions among the mix design parameters, except for the method of curing, are significant to cracking. It is, thus, imperative that the optimisation of mix design parameters for resistance to cracking in PRMs considers these interactions inter alia, instead of the commonly used O-F-A-T (a one-factor-at-a-time) approach that optimises an individual mix design parameter without taking cognisance of the mentioned interactions.

ii. SRA dosage: an increase in SRA dosage delays cracking.

iii. Binder content: a reduction in binder content delays cracking.

iv. Binder type: the use of 100% CEM II B-M (L) delays cracking in comparison to a 50/50 CEM II B-M (L)/GGBS blend.

v. Water content: reducing the water content delays cracking.

vi. Curing method: the simultaneous use of SAP and wet hessian delays cracking in comparison to curing using wet hessian only.

5.3 Effect of mix design modification on cracking parameters and crack-determining material properties (Phase two)

The choice of mix design parameters for the mixes in phase two was informed by the trends identified in phase one. The three mix design parameters with the most significant contribution to cracking - as determined from sensitivity analysis - were used to cast the reference mix. The developed reference mix was subsequently modified to improve its crack resistance as discussed in Section 4.1 and Section 4.7.2. The mix design parameters for the reference mix comprised the following:

i. Binder type: CEM II/B-M (L), 42.5 N.

ii. w/b: 0.72 (i.e., water content = 180 l/m^3; binder content = 250 kg/m^3).

iii. SRA dosage: 3%.

The author confined the use of SAP to trial mixes, albeit their positive contribution to cracking resistance, because of the following reasons: the quantity of SAP available for this research was insufficient to cater for the subsequent tests and the need to minimise the number of experimental variables by focussing on the first three parameters that played a more dominant role on cracking. SAPs were, therefore, not incorporated into the mixes in phase two. The mix design of the reference mix was further modified by changing the water- and binder- contents and the inclusion of polymers considering the trends identified from factorial analysis and as discussed in Section 4.1 and Section 4.7.1. The effect of mix design modification on cracking and crack-determining material properties on the mixes developed in phase two are presented in the subsequent subsections. Throughout the entire set of test results presented hereafter, Mix C250_P0 refers to the reference mix (also referred to as the control mix interchangeably). This mix has been used as the basis for comparison. A summary of the identity of each of the eight mixes that were investigated is presented below.

i. Mix C250_P0: cement content = 250 kg/m^3, water content = 180 l/m^3, polymer content = 0%, w/b = 0.72.

ii. Mix C230_P0: cement content = 230 kg/m^3, water content = 165 l/m^3, polymer content = 0%, w/b = 0.72.

iii. Mix C210_P0: cement content = 210 kg/m^3, water content = 150 l/m^3, polymer content = 0%, w/b = 0.72.

iv. Mix C225_P0: cement content = 225 kg/m^3, water content = 180 l/m^3, polymer content = 0%, w/b = 0.80.

v. Mix C250_P1-10: cement content = 250 kg/m^3, water content = 180 l/m^3, EVA content = 10%, w/b = 0.72.

vi. Mix C250_P2-10: cement content = 250 kg/m^3, water content = 180 l/m^3, SA content = 10%, w/b = 0.72.

vii. Mix C250_P1-15: cement content = 250 kg/m^3, water content = 180 l/m^3, EVA content = 15%, w/b = 0.72.

viii. Mix C250_P1-20: cement content = 250 kg/m^3, water content = 180 l/m^3, EVA content = 20%, w/b = 0.72.

Additional details regarding the above eight mixes are provided in Section 4.7.1.2 and Table 4.4. Throughout this subsection, the patterned graphs with a light-grey background represent the polymer-modified mixes. Similarly, plain graphs with a light grey background represent the reference mix. Throughout this section, comparisons among the mixes are done with respect to the reference mix unless otherwise stated.

5.3.1 Consistence

The flow test was used to characterise the mixes and to assess their consistence. The average flow test results are presented in Figure 5.15 and summarised in Appendix C.1.

5.3.1.1 Effect of water content, binder content and w/b

An increase in w/b from 0.72 to 0.80 resulted in an increase in flow. The observed increase was expected and is consistent with literature as presented in Section 3.4.3. The simultaneous reduction in water- and binder contents in unmodified mixes reduced flow negligibly in comparison to the reference mix. A logical explanation for this effect could not be provided because the superplasticiser dosage varied with each mix. The variation of superplasticiser dosage would, thus, have confounded the interpretation of flow test results. The reduction in water- and binder contents also resulted in an increase in superplasticiser dosage. The increased superplasticer dosage could be attributed to the need to overcome the internal friction forces that resulted from the increased aggregate interlock - due to the reduction in binder content and the slight increase in aggregate content.

5.3.1.2 Effect of polymer modification

The incorporation of redispersible polymers increased flow significantly in relation to the reference mix. This increase was expected and is consistent with the observations

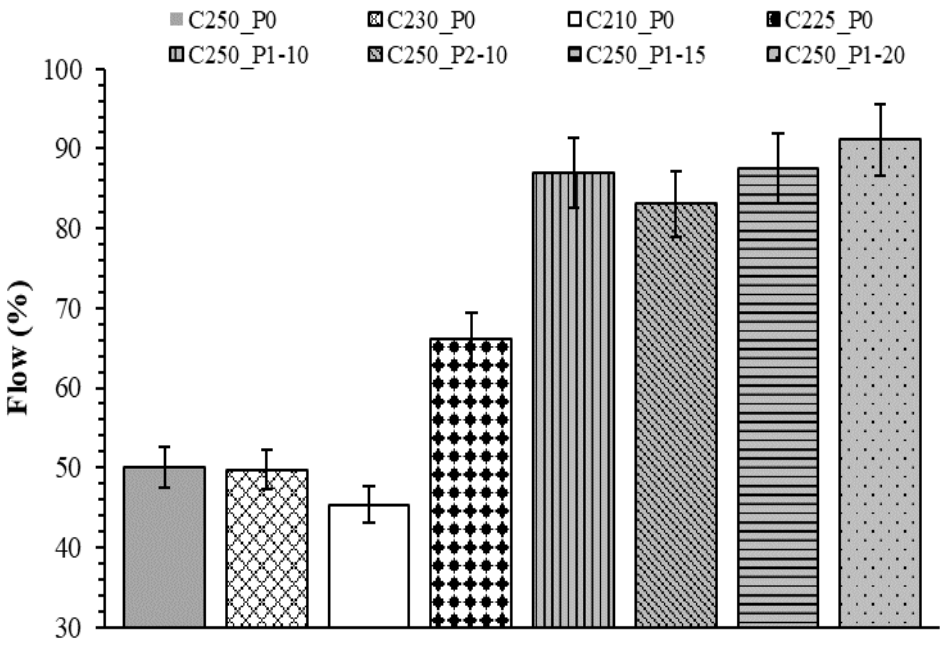

FIGURE 5.15: Flow test results

by Peier (1986), Ohama (1995), Ohama (1998), Miller (2005), Brandt (2009), Ramli and Tabassi (2012b), Ramli and Tabassi (2012a) and Raupach and Büttner (2014). The increase in consistence in polymer-modified mortars can be attributed to the improved consistency due to the ball-bearing action of polymers which eases the relative movement of cement and hydrating particles and the entrained air and surfactants in the polymers (Kardon, 1997; Miller, 2005; Ohama, 1998; Rixom and Mailvaganam, 1999). Whereas Miller (2005) attributes the increase in flow in polymer-modified mixes to the free emulsifier within the polymers; Ohama (1995) attributes this increase to the surface activity of the polymers that prevents the 'dry out' phenomena. Kardon (1997) also reports that surfactants in polymers reduce segregation, increase slump and reduce water demand.
The flow of EVA polymer-modified mixes (C250_P1-10) was higher than that of SA polymer-modified mixes (C250_P2-10) at a polymer content of 10% by mass of binder - an observation that is consistent with those of Ngassam et al. (2016). The difference in flow between these two polymer mixes, however, was not statistically significant in magnitude. There was a negligible increase in flow with an increase in polymer content from 10% to 20% among the EVA-polymer-modified mixes - i.e., mixes C250_P1-10, C250_P1-15 and C250_P1-20.

5.3.2 Compressive and direct tensile strength

The mortars under investigation are non-structural. Compressive strength, however, was used to characterise these mortars and to fulfil the requirements of the EN 1504-3:2005 which states that the compressive strength must be specified always. The average compressive and direct tensile strength test results are presented in Figure 5.16 and Figure 5.17 and summarised Appendix C.2 and Appendix C.3.

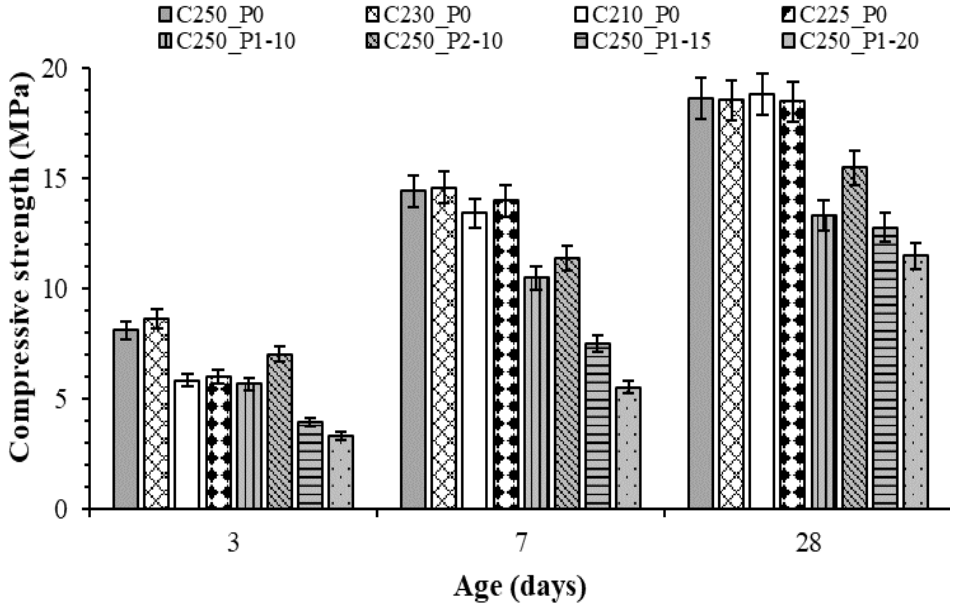

FIGURE 5.16: Compressive strength test results

5.3.2.1 Effect of water content, binder content and w/b

The reduction in water and binder contents - from 180 l/m^3 to 165 l/m^3 and from 250 kg/m^3 to 230 kg/m^3 respectively - did not result in a statistically significant change in compressive and direct tensile strengths at 7 and 28 days in comparison to the reference mix. The reported reduction in binder and water content, however, increased the 3-day compressive strength of Mix C230_P0 in comparison to the reference mix by 0.5 MPa and reduced the tensile strength of the same mix by 0.12 MPa. These changes, however, were practically insignificant. A reduction in water- and binder content from 180 l/m^3 to 150 l/m^3 and from 250 kg/m^3 to 210 kg/m^3 respectively reduced compressive strength at 3 and 7 days significantly in relation to the reference mix. The effect of this reduction on the 28-day compressive strength was not significant. The reported reduction in water- and binder content reduced tensile strength significantly at all ages.

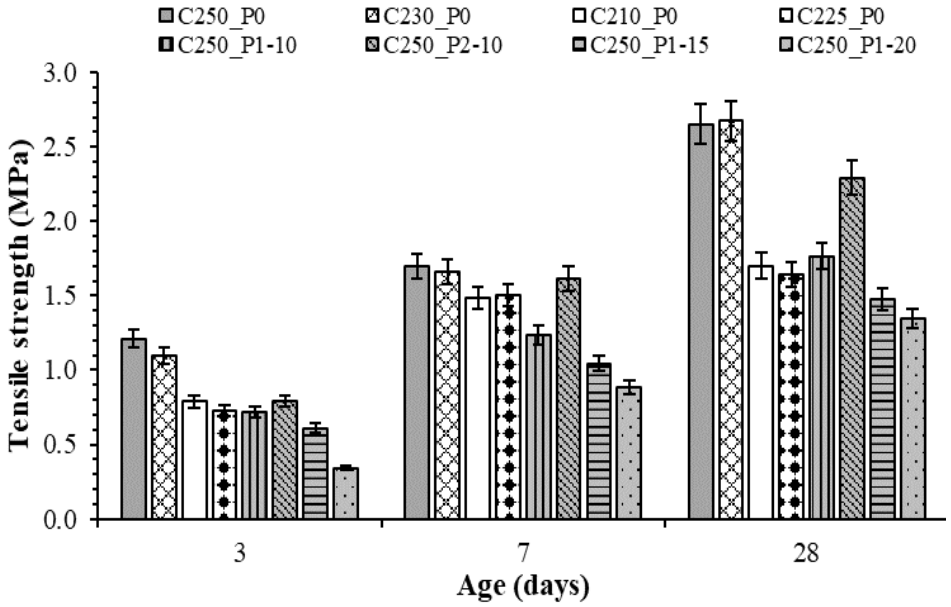

FIGURE 5.17: Direct tensile strength test results

Whereas Popovics and Ujhelyi (2008) report that a reduction in binder content in mixes with a constant w/b ought to result in an increase in compressive strength - owing to an increased aggregate interlock resulting from a corresponding increase in aggregate content in lean mixes - the results from this study do not corroborate their observations in totality. It can be inferred that the observed reduction in tensile strength resulted from the relatively weak bonding between the HCP and the aggregates in the lean mixes. A reduction in cement content reduces the quantity of CSH - a stress-bearing product of hydration. The formation of less CSH also implies that the bonding between the aggregate phase and the HCP was weak and consequently susceptible to microcracking. Increasing the susceptibility to microcracking translates to a reduction in tensile strength as discussed in the previous chapters. This inference was not proved experimentally owing to the challenge of proper sample preparation and the lack of a readily available microscopy equipment.

Except for the compressive strength at 7 and 28 days, an increase in w/b from 0.72 to 0.80 generally resulted in a significant reduction in compressive and tensile strength. These observations were expected and are consistent with Abrams formula as discussed in Section 3.4.3. The reduction in strength can be attributed to the increased porosity in the cement paste. An increase in porosity results in a reduction in strength (Popovics and Ujhelyi, 2008). The compressive and tensile strengths of mix C210_P0 and mix C225_P0 were not significantly different from each other at all ages despite differences in their w/b - i.e., 0.72 and 0.80 respectively. This observation was unexpected and could not be explained by the tests done.

5.3.2.2 Effect of polymer modification

The compressive and tensile strengths of EVA polymer-modified mixes was significantly lower than those of SA polymer-modified mixes at a constant polymer content at all ages. This observation could be attributed to the unique chemical properties of the polymers. Judge et al. (1986), Ohama (1995), Rixom and Mailvaganam (1999) and Miller (2005) report that the chemical properties of the polymers is critical to their behaviour. Polymer-modification reduced compressive and tensile strengths at all ages significantly in comparison with the reference mix. The magnitude of this reduction, in EVA polymer-modified mixes, increased with an increase in polymer content from 10% to 20%. The observed reduction in strength are inconsistent with the findings of Ohama (1995), Ohama (1998), Ohama (2011), Kardon (1997), Miller (2005), Brandt (2009), Bezerra et al. (2011) and Ramli and Tabassi (2012a) who report that polymers increase strength. The reported increase in strength, in the listed studies, has been attributed to an improvement in bonding at the ITZ (Ohama, 1998, 2011; Rixom and Mailvaganam, 1999). Ohama (1995), Ohama (1998) and Miller (2005) also acknowledge that polymer-modification, depending on the conditions of testing, could either result in a slight reduction or negligible change in compressive strength. Rixom and Mailvaganam (1999) report that the modification by polymers does not improve compressive strength. Kardon (1997) further reports that the compressive strength of polymer-modified cement-based materials is lower than that of unmodified ones when both materials are prepared with the same w/b. Considering the conditions of testing, the observations by Kardon (1997) corroborates the ones made in this study. The use of a different binder and polymer types and curing regime, in this study in comparison to the ones used in studies by Ohama (1995), might have contributed to the contradictory observations.

Ohama (1995), Rixom and Mailvaganam (1999) and Miller (2005) report that the curing environment influences the microstructural development of polymer-modified materials and consequently its material properties. Kovler et al. (1999b) and Ramli and Tabassi (2012a) acknowledge the importance of curing on strength. Kovler et al. (1999b) specifically reports that the effect of curing is more pronounced on tensile strength than on compressive strength. The increased strengths in polymer-modified mixes, from studies by Ohama (1995), were observed in polymer-modified mortars which were water-cured for 3 days and thereafter left to dry in the air to maximise their strength development due to the formation of polymer films. The specimens in this study, however, were water-cured continuously for 3, 7 and 28 days depending on the age at with the strength was determined. Rixom and Mailvaganam (1999), Ramli and Tabassi (2012a) and Soufi et al. (2016) specifically report that prolonged water curing of polymer-modified systems weakens the polymer films and interferes with their formation. Thus, it can be inferred that the prolonged curing of the mixes in this study could have either weakened the polymer films or hindered the formation of the polymer films; thereby reducing their tensile and compressive strength.

The excess air entrainment and the presence of polymer granules within the mortar matrix due to polymer-modification results in discontinuities within the cement paste matrix (Ohama, 1995; Rixom and Mailvaganam, 1999). These discontinuities weaken the bonding between HCP and the aggregate phases consequently resulting in a reduction in strength (Chorinsky, 1986; Miller, 2005; Ohama, 1995). Also, the reduction in the quantity of cement and the coating of hydrating cement grains by polymer films (Bezerra et al., 2011) lowers the amount of CSH produced during cement hydration in comparison to the reference mix. It can be inferred that the reduction in the quantity of CSH - which is responsible for strength - in the mix, the slow hydration due to the dispersing effects of the polymers (Kardon, 1997), and the coating of cement grains by polymer films reduced compressive and tensile strength. Also, the fact that water molecules are held within the polymer matrix, owing to the inability of water to react independently with polymers, implies polymer-modified mortars are characterised by high localised w/b. An increase in the localised w/b within these mixes reduces their overall strength. This concept has also been reported by Raupach and Büttner (2014). Furthermore, large-sized polymers form large voids within the cementitious microstructure. These voids could reduce strength. Polymer-modified mortars are also susceptible to increased autogenous shrinkage (Miller, 2005). An increase in autogenous shrinkage would translate into an increase in microcracking within the cement matrix of the mortar. An increase in microcracking affects the fracture mechanics as well as mechanisms through which stresses are transferred within the HCP and consequently a reduction in strength.

5.3.3 Elastic modulus

The stress-strain curves from tests on PRM specimens at 7 and 28 days are presented in Figure 5.18 and Figure 5.19. The average elastic modulus results are presented in Fig 5.20 and in Appendix C.4. Also, it is important to note that the PRM specimens were loaded to 30% of their ultimate load at failure.

5.3.3.1 Effect of water content, binder content and w/b

The simultaneous reduction in water- and binder content reduced the elastic modulus of unmodified mixes at all ages significantly in relation to the reference mix as seen in Figure 5.20. A logical explanation to this phenomenon could not be provided based the tests that were undertaken in phase two. Nevertheless, it can be inferred that the reduction in the amount of CSH, due to the reduction in cement content, resulted in weak pastes.

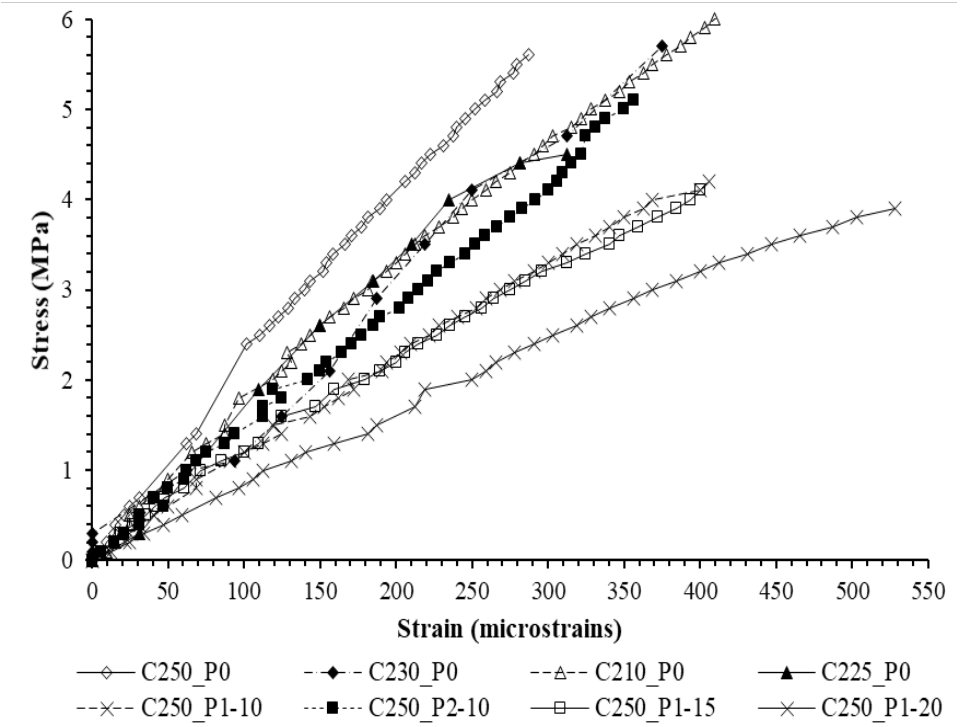

FIGURE 5.18: Stress-strain curves of PRM specimens at 7 days

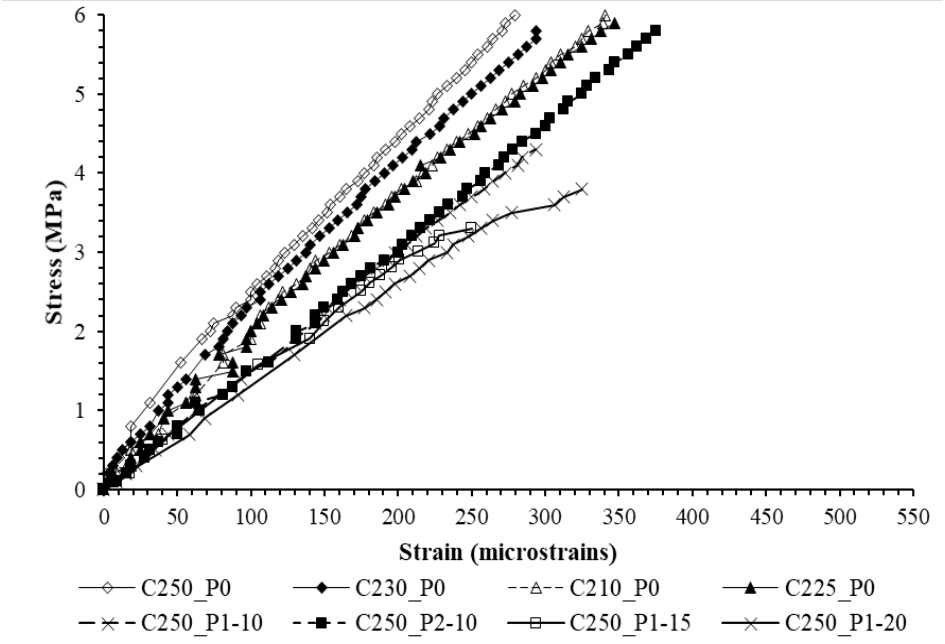

FIGURE 5.19: Stress-strain curves of PRM specimens at 28 days

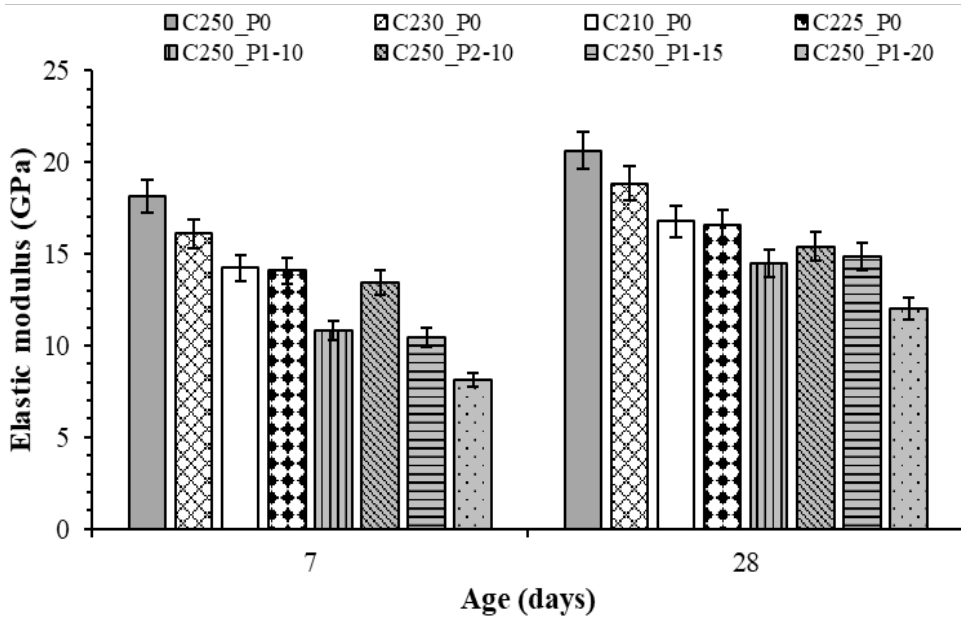

FIGURE 5.20: Static elastic modulus in compression test results

Weak pastes would result in a reduced elastic modulus. The difference between the elastic modulus of the lean mix with w/b of 0.72 (C210_P0) and the mix with w/b of 0.80 (C225_P0) was not statistically significant at all ages. This phenomenon was also observed with respect to compressive and tensile strength.

5.3.3.2 Effect of polymer modification

Polymer-modification reduced elastic modulus significantly in comparison to the reference mix. The reduction in elastic modulus could be attributed to the poor bonding at the ITZ and the presence of discontinuities within the matrix - due to polymer granules and air entrainment - which affect that mechanisms through which stresses and strains are transferred within the PRM matrix negatively. Amba et al. (2010) further reports that polymer-modification increases deformability. Thus, it can be hypothesised that an increase in deformability, at a constant stress, would result in a reduction in elastic modulus. Also, an increase in EVA polymer content resulted in a reduction in elastic modulus. This observation corroborates those of Kardon (1997), Ohama (1998), Miller (2005) and Raupach and Büttner (2014). The difference in elastic modulus between EVA polymer-modified mixes with 10% and 15% polymers were not significant. Ohama (1995) also reports that polymer-modification does not change the elastic modulus in compression significantly; and that an increase in polymer:cement ratio reduces tensile and compression elastic modulus. The elastic modulus of SA polymer-modified mixes at 10% was higher than that of the EVA polymer-modified mixes at the same content. This observation is consistent with those of compressive and strength (see Section 5.3.2)

and can be attributed to the differences in the chemistry of the various polymer types as discussed in Section 5.3.2.

5.3.4 Drying shrinkage

The test results for drying shrinkage are presented in Figure 5.21, Figure 5.22 and Appendix C.5. Note that shrinkage measurements began immediately after water-curing the specimens for 7 days as discussed in Section 4.7.2.3. The abscissa of Figure 5.21 corresponds to the day on which the first shrinkage result was taken.

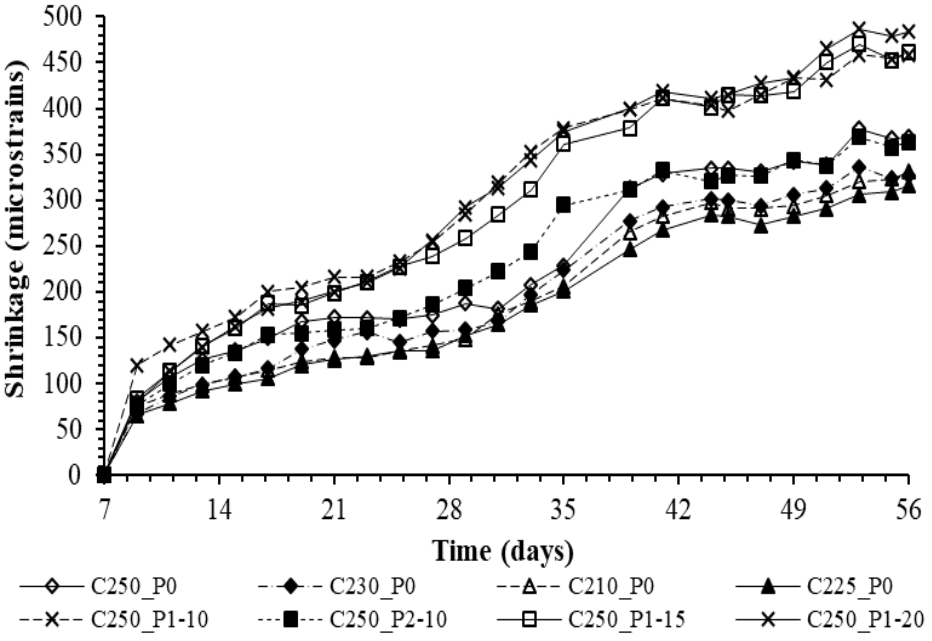

FIGURE 5.21: Scatter-line plot of drying shrinkage

A summary of the average drying shrinkage of the test specimens after 56 days from their date of casting is presented in Figure 5.22. The duration of monitoring of shrinkage results was made to correspond to the time taken by the best performing PRM mix to crack.

5.3.4.1 Effect of water content, binder content and w/b

The reduction in drying shrinkage due to the simultaneous reduction in water and binder contents in the unmodified mixes, except for mix C230_P0, was statistically significant in comparison to the reference mix as observed in Figure 5.22. This observation is consistent with the findings of Neville (1995) and Fowler and Treviño (2011). Whereas the reduction in drying shrinkage in mix C210_P0 in relation to the reference mix can be attributed to the increased restraint and dilution effects resulting from the slight increase in aggregate content - i.e., from 72% in the reference mix to 76% in mix C210_P0

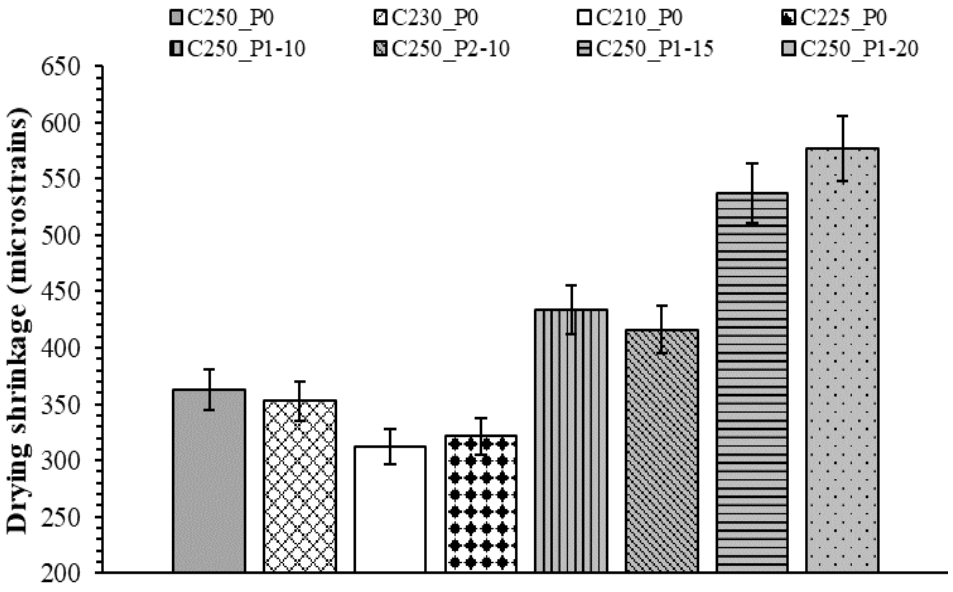

FIGURE 5.22: Drying shrinkage test results (at 56 days)

- the increase in shrinkage in mix C230_P0 could not be explained. The increase in aggregate content in mix C210_P0 increased the effects of dilution and restraint as reported by Dittmer and Beushausen (2014), Zhang et al. (2014) and Yurdakul et al. (2014). The increased aggregate content in mix C210_P0 in comparison to mix C250_P0 increased dimensional stability as well as prevented the propagation of microcracks (Bode and Dimmig-Osburg, 2011); consequently, reducing its susceptibility to shrink because microcracks create continuous pathways through which pore water is lost easily to the environment.

Also, an increase in aggregate content was accompanied by a proportional decrease in binder content. Thus, it can be inferred that the reduction in binder content - the phase that generates heat during hydration - resulted in a reduction in the heat of hydration, as reported by Fowler and Treviño (2011). A reduction in heat of hydration reduced the susceptibility to thermal shrinkage consequently contributing to the overall reduction in shrinkage. Increasing the w/b from 0.72 to 0.80 resulted in a significant reduction in drying shrinkage in comparison to the reference mix, even though the aggregate content in these mixes were almost equal. This observation was unexpected and could have been an anomaly resulting from the general variability in testing. The difference between drying shrinkage in mixes C210_P0 and C225_P0 was not statistical significant, even though these mixes had different w/b. This phenomenon was also observed in the results presented in the earlier subsections.

5.3.4.2 Effect of polymer modification

The modification of mixes with EVA and SA redispersible polymers increased drying shrinkage significantly in relation to the reference mix. Also, drying shrinkage in EVA polymer-modified mixes increased significantly with an increase in polymer content. The shrinkage in EVA polymer-modified mixes was higher than that of SA polymer-modified mixes at the same polymer content. The observed difference could be attributed to differences in polymer types as discussed by Rixom and Mailvaganam (1999), Ramli and Tabassi (2012a). Ohama (1998), Rixom and Mailvaganam (1999) and Miller (2005) further report that the magnitude of shrinkage in polymer-modified materials depends on the chemical nature of the polymer and the polymer:cement ratio. While Ohama (1995), Ohama (1998), Rixom and Mailvaganam (1999) and Miller (2005) report that the incorporation of polymers may either increase or decrease drying shrinkage in polymer-modified mortars in comparison with unmodified ones; the results from this study show that polymer-modification increased drying shrinkage. Bode and Dimmig-Osburg (2011) report that the incorporation of polymers increases shrinkage. However, Kardon (1997) and Miller (2005) report that properly cured polymer-modified materials exhibit a reduced shrinkage - an observation that contradicts what was observed in this study and the observation by Bode and Dimmig-Osburg (2011). Kardon (1997) attributes the reduction in shrinkage in polymer-modified mixes to their water-retention ability.
It can be inferred that the increase in drying shrinkage, due to an increase in polymer content, resulted from an increase in the voids within the pores of the specimens cast using polymer-modified mixes. An increase in pores - as described by Ohama (1995) - increases the susceptibility to shrink - especially in instances where the pores are interconnected. Interconnected pores act as pathways through which moisture is lost from the polymer-modified mixes to the environment. Miller (2005) specifically attributes the increased shrinkage in redispersible polymer-modified mixes to the formation of a three-dimensional network of films instead of the normal continuous films forms in latex-modified mortars when the polymer content is above 15%. Any shrinkage experienced by polymers within the three-dimensional network would be imposed on the bulk matrix; consequently, resulting in an increase in shrinkage. The increased shrinkage in polymer-modified mixes could also have resulted from the evaporation of a large volume of water held within its matrix - in the form of capillary pores - and the one held within the polymer films; unlike in the reference mix and other unmodified mixes where the water that was lost to the atmosphere is the one held within the capillary pores of the hydrated cement matrix.

5.3.5 Tensile relaxation

The role, and contribution, of tensile relaxation to cracking in PRMs has been discussed in the previous chapters. The average 48-hour tensile relaxation test results are presented in Figure 5.23 and in Appendix C.6. A load level corresponding to a tensile stress of 80% of the ultimate tensile strength was applied to the test specimens.

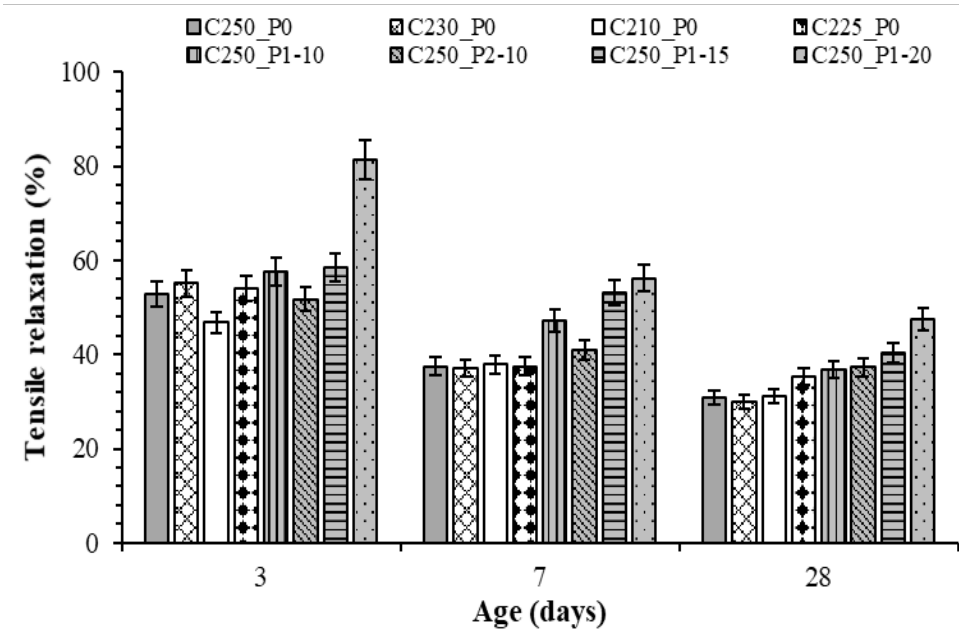

FIGURE 5.23: 48-hour tensile relaxation test results

5.3.5.1 Effect of water content, binder content and w/b

Except for mix C210_P0 at 3 days, the simultaneous reduction in water- and binder contents in the unmodified mixes did not result in a significant change in tensile relaxation at all ages as seen in Figure 5.23. The decrease in tensile relaxation in mix C210_P0 was treated as an anomaly. The aggregate content in unmodified mixes were almost equal. Thus, it can be inferred that the effects of dilution and restraint were not significantly different from each other. Increasing the w/b from 0.72 to 0.80 did not result in a significant increase in tensile relaxation at 3 and 7 days in comparison with the reference mix. The aggregate content of mixes C250_P0 and C225_P0 were also approximately equal. Thus, their effects of dilution and restraint on tensile relaxation were approximately equal. The 28-day tensile relaxation of mix C225_P0 at was higher than that of the reference mix. This observation would be attributed to the microcracking that results due to the weak microstructure in this mix due to the increased w/b. An increase in microcracking would release the tensile stresses. Unlike in the previous tests, a clear and well-defined trend could not be observed between the tensile relaxation in the unmodified mixes.

5.3.5.2 Effect of polymer modification

The addition of polymers, except for the SA polymer-modified mixes at 3 days, increased tensile relaxation at all ages in comparison to the reference mix. This observation was expected and is consistent with those reported by Brandt (2009). The 3- and 7-day tensile relaxation in mixes modified with 10% EVA polymers was significantly

higher than that of SA polymers at the same content. The 28-day tensile relaxation of EVA and SA polymer-modified mixes at a content of 10% did not differ significantly. The observed differences in tensile relaxation can be attributed to differences in the chemical composition of the polymers. Tensile relaxation in EVA polymer-modified mixes increased significantly with an increase in polymer content at all ages. The EVA polymers exhibited the highest tensile relaxation at all ages.

The increase in tensile relaxation in polymer-modified mixes was attributed to the reduction in the restraining action of aggregates resulting from a reduction in aggregate volume. Also, it can be inferred that the transfer of stresses from the relatively rigid hardened cement matrix to the relatively elastic polymer matrix when microcracks occurred translated to an increased tensile relaxation in the polymer-modified mixes. The coalescence of polymers into continuous films or membranes helped to bind cement hydrates together to form a monolithic network; consequently, bridging the microcracks in polymer-modified mortars that form from induced tensile stresses. Boyd and Smith (2007) report that polymers have an inherent high tensile relaxation. Thus, should microcracks develop in a stressed polymer-modified cement matrix, the induced stresses will be transferred to the polymer films bridging the microcracks. The stressed polymer films will undergo relaxation. The magnitude of the relaxation in polymer films would depend on its type, its chemical and physical properties. An increase in polymer content resulted in the transfer of more stresses from the matrix to the cement polymer, consequently resulting in higher relaxation.

It can be inferred, from the creep and relaxation theories discussed in Section 2.3.2, that the seepage of the water entrained within the continuous polymer films (Kardon, 1997) would occur when the polymer-modified mortars are stressed. This seepage results in a redistribution of stresses. An increase in polymer content results in an increase in the amount of water retained within the matrix; which would consequently increase the magnitude of tensile relaxation due to the seepage of a large volume of water. This effect - the redistribution of tensile stresses - would be more pronounced at earlier ages that at later ages owing to the large quantity of water available at the early ages of mortars before hydration, which consumes the internally bound water, takes place. Also, the excess voids that result from air entrainment in polymer-modified mixes would facilitate the ease of movement of entrapped water within the mortar matrix. This phenomenon would consequently influence the magnitude of tensile relaxation.

5.3.6 Restrained shrinkage cracking

The test for restrained shrinkage cracking entailed the monitoring of the age at cracking and surface crack widths using ring tests cast in accordance with ASTM-C1581. These parameters are subsequently discussed.

5.3.6.1 Age at cracking

The average age at cracking of the PRM specimens are presented in Figure 5.24 and Appendix C.7.

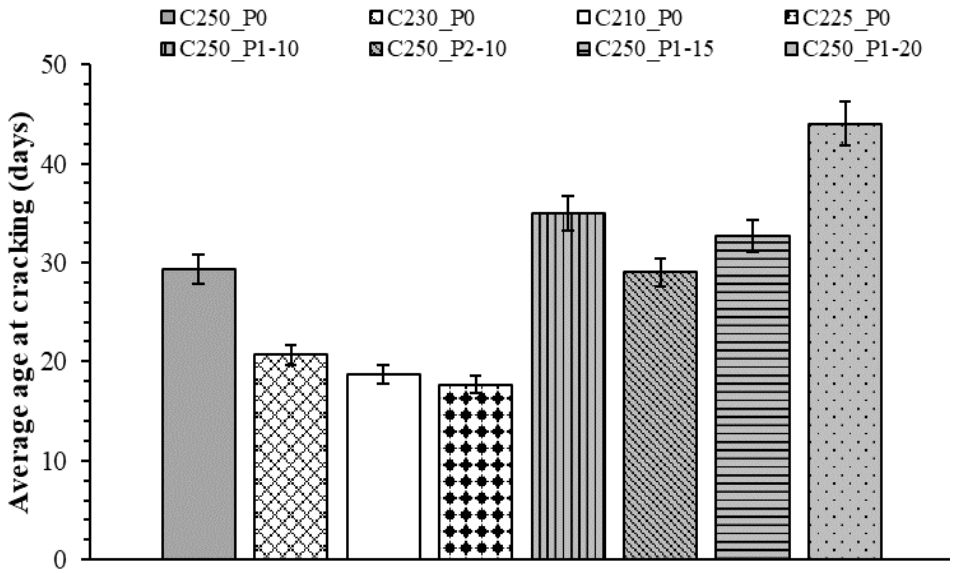

FIGURE 5.24: Age at cracking test results (ring test)

a) Effect of water content, binder content and w/b

The simultaneous reduction in water- and binder contents reduced the age at cracking significantly in the unmodified mixes, as shown in Figure 5.24, in comparison to the reference mix. It can be inferred that the weak microstructure of these pastes - as manifested by their low tensile strength in relation to the reference mix - could not resist the tensile stresses emanating from restrained deformations adequately; consequently, reducing their age at cracking. Also, the relaxation of these specimens was lower than that of the reference mix. Thus, the relief of tensile stresses due to restrained shrinkage was lower in these mixes than in the reference mixes; consequently increasing their susceptibility to cracking. An increase in w/b from 0.72 to 0.80 also reduced the age at cracking significantly in comparison to the reference mix. This observation was expected and is consistent with literature. It can be attributed to the inability of the weak microstructure of high w/b to withstand tensile stresses resulting from restrained shrinkage deformations. Also, the difference between the age at cracking in mixes C210_P0 and C225_P0 was not significant, even though these mixes had different w/b. This phenomenon was observed with respect to other materials properties that have been discussed earlier.

b) Effect of polymer modification

The incorporation of polymers, except for SA polymers at 10%, delayed cracking significantly in relation to the reference mix. Whereas the observed results could not be corroborated due to the lack of published information on restrained shrinkage cracking in ring specimens cast using polymer-modified mixes; the delay in cracking was expected - especially in consideration of the results from tensile strength, elastic modulus and tensile relaxation tests. Also, the delay in cracking is consistent with the observation by Amba et al. (2010) who reported that polymers reduce the susceptibility to cracking. The delay in cracking due to the addition of 10% EVA polymers was significantly higher than that of SA polymers at the same content. Also, there was no significant difference between the age at cracking in EVA polymer-modified mixes with polymer contents of 10% and 15%. The age at cracking in mixes with a polymer content of 20% were significantly higher than that of other polymer-modified mixes.

It can be inferred that the observed delay in cracking resulted from the effect of the polymers on the microstructure. According to Ohama (1995), polymer-modification increases discontinuities in cement-based systems due to the excess entrained air and the presence of polymer granules within the matrix. These discontinuities reduce elastic modulus and consequently the susceptibility of these mixes to crack from restrained deformations. Polymer-modified mixes were also characterised by high tensile relaxation, low elastic modulus and high drying shrinkage. Thus, it is evident that an amalgamation of high tensile relaxation and low elastic modulus reduces the magnitude of stresses due to restrained deformations significantly; consequently minimising the susceptibility of these mixes to crack despite their high drying shrinkage. The delay in cracking could also be attributed to the high deformability of polymer-modified mixes as reported by Amba et al. (2010). The high deformability of polymer-modified mixes results from their low elastic modulus. The veracity of this claim could have been ascertained had the tensile stress development in the ring specimens been monitored throughout the duration of these tests. The unavailability of strain gauges and their accompanying data acquisition system hindered the measurement and continuous monitoring of tensile stress development.

The bridging of microcracks by polymer chains in polymer-modified mortars - owing to an improved bonding at the ITZ and the continuous polymer films that have been described by Ohama (1995), Ohama (1998), Rixom and Mailvaganam (1999) and Knapen and Gemert (2011) - implies that the coalescence of microcracks into visible macrocracks would take a long time. An increase in the time taken by microcracks to transform into macrocracks manifests as a delay in the time to crack. This delay would increase with an increase in polymer content. The formation of polymer films within the matrix increases flexibility and deformability (Brandt, 2009; Miller, 2005). An increase in flexibility would increase the capability of these mixes to withstand restrained deformations associated with high drying shrinkage - a phenomenon that would reduce their susceptibility to cracking. Also, there is a high likelihood that the curing regime that was followed in

the ring specimens - in comparison to the regime used for the other tests - resulted in the delay in the time taken to first crack. Curing the ring specimens using wet hessian for seven days implies that the polymers coalesced to form stronger chains within the matrix as reported by Ohama (1998). These chains could have formed strong bonds which enhanced the bridging of microcracks within the cement paste. A better crack-bridging effect would consequently delay the transformation of invisible microcracks to visible macrocracks.

5.3.6.2 Crack width

The average surface crack widths of the ring specimens are presented in Figure 5.25. Crack widths were measured on the day they first occurred and at 1 day and 2 days after the initial crack.

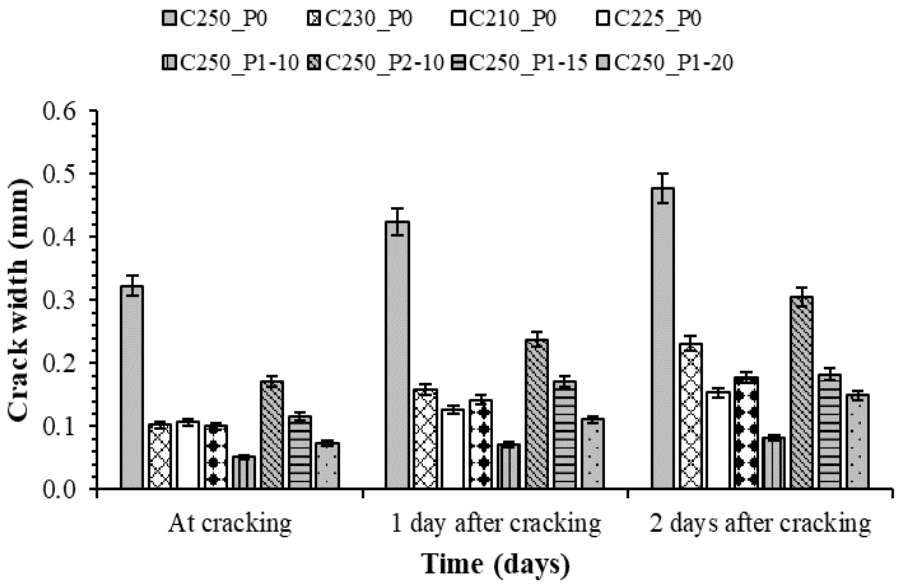

FIGURE 5.25: Crack width test results (ring specimens)

a) Effect of water content, binder content and w/b

The simultaneous reduction in water- and binder content resulted in a significant reduction in surface crack width throughout. This phenomenon could be attributed to the reduction in both elastic modulus and drying shrinkage in these mixes. A reduction in elastic modulus and drying shrinkage resulted in a corresponding reduction in the magnitude of displacement between opposite crack faces. The slight increase in aggregate content due to the reduction in water- and binder contents changed the fracture mechanics of these mortars. It can be inferred that the additional aggregates could have

bridged the microcracks consequently resulting in a reduction in surface crack widths. Also, an increase in w/b from 0.72 to 0.80 resulted in a reduction in surface crack width. This observation was expected and can be attributed to the increased tensile relaxation and reduced elastic modulus of these mixes. Also, there was no significant difference between the crack widths of mixes C230_P0, C210_P0 and C225_P0 despite the difference in w/b among these mixes. This observation was also observed in the other tests.

b) Effect of polymer modification

The addition of polymers resulted in a significant reduction in surface crack widths across the entire set of mixes. This observation could be attributed to the reduction in elastic modulus and the increase in tensile relaxation characterising these mixes which resulted in a reduction in the magnitude of the displacement of opposite crack faces despite the high drying shrinkage that characterised these mixes. Also, the EVA polymer-modified mixes exhibited smaller crack widths in comparison with the SA polymer-modified mixes at the same polymer content. This phenomenon could be attributed to the higher elastic modulus and lower tensile relaxation of SA polymer-modified mixes. The tensile stresses due to the higher elastic modulus and lower tensile relaxation in SA polymer-modified mixes resulted in an increase in magnitude of displacement of opposite crack faces due to tensile stresses resulting from restrained shrinkage. Throughout the entire set of PRM specimens, the crack widths increased with time. This phenomenon could be attributed to the continuous shrinkage strains within these mixes which manifest by the increase in the displacement between opposite crack faces.

5.3.7 Durability Indexes (DIs)

The penetrability of PRMs is important to their long-term performance. DI tests were used to assess the penetrability of the mortars under investigation as well as characterise their durability. The penetrability of the developed mortars was limited to the assessment of two DIs, namely: OPI and WSI at 28 days in accordance with the South African Durability Index testing approach.

5.3.7.1 Oxygen Permeability Index (OPI)

OPI represents the negative logarithm of the permeability coefficient of the specimens from the mixes under investigation. A high OPI value translates into low permeability. The results from OPI tests are presented in Figure 5.26 and in Appendix C.8.

a) Effect of water content, binder content and w/b

The simultaneous reduction in water- and binder contents, except for mix C230_P0, reduced OPI significantly in the unmodified mixes in comparison to the reference mix. An increase in w/b from 0.72 to 0.80 also reduced OPI significantly in relation to the

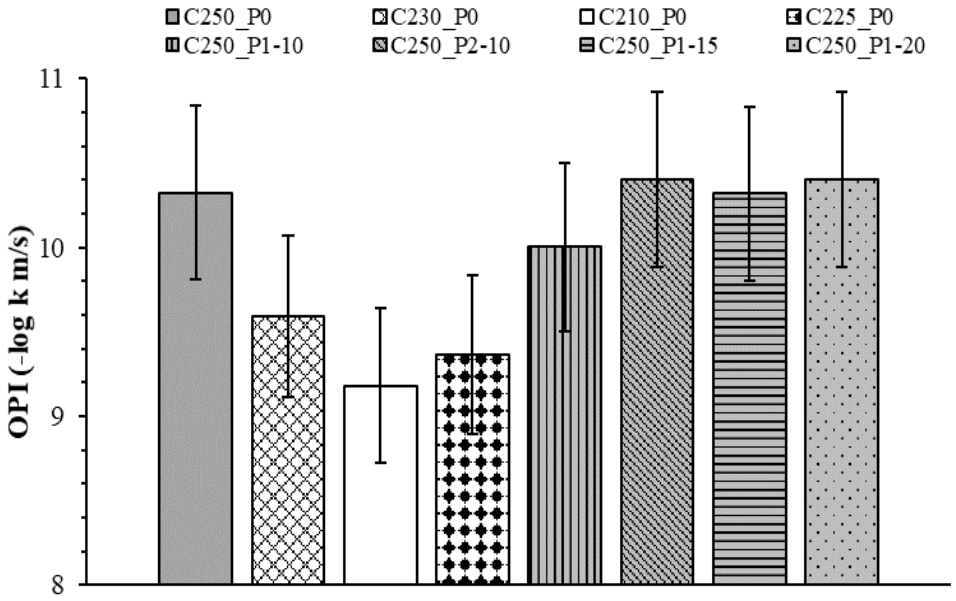

FIGURE 5.26: OPI test results

reference mix. The simultaneous reduction in water and binder content, and the corresponding increase in aggregate content, might have altered the transport properties of the mixes. Thus, it can be inferred that the reduction in paste content - due to the decrease in binder content - and the increase in aggregate content resulted in a porous microstructure with interconnected voids which enhanced the rate at which oxygen permeates through the specimen. The reduction in OPI due to an increase in w/b was expected and is consistent with literature. It can be attributed to the increased porosity of PRM specimens cast using this mix.

Considering the scatter in the test results, the effect of the simultaneous reduction in water and binder contents at w/b of 0.72 was not significantly different, statistically, from the effect of increasing the w/b from 0.72 to 0.80. This observation, though unexpected, might have resulted from the inherent variability in the testing. The relatively low flow of mix C210_P0 could have contributed to the wide variability in OPI. Mix C210_P0 was characterised by a high aggregate content and a low binder content. The challenge of compacting this mix necessitated the use of a high SP dosage to achieve sufficient flow. The high superplasticiser dosage resulted in bleeding and segregation in the freshly cast mixes - a phenomenon that might have resulted in the formation of interconnected voids and an increase in permeability. Also, the observed variability in the test results could have resulted from the general variability in testing and in specimen preparation - e.g. compaction of test specimens.

b) Effect of polymer modification

The incorporation of EVA and SA polymers did not result in a significant change in OPI in comparison with the reference mix. Also, it can be observed that there was no significant difference between the mean OPI results in specimens cast using EVA and SA redispersible polymers at a polymer content of 10%. An increase in the content of EVA polymers from 10% to 20% increased OPI slightly. This increase, however, was not statistically significant. The modification of cement-based materials with polymers creates a structure in which the large pores are either filled with polymers or are sealed with continuous polymer films during the cement hydration (Kardon, 1997; Miller, 2005; Ohama, 1998, 2011; Ramli and Tabassi, 2012b; Rixom and Mailvaganam, 1999; Soufi et al., 2016). This filling and/or sealing of pores by polymers can be inferred to reduce porosity, water absorption and permeability. Ohama (1995) further reports that the incorporation of polymers reduces porosity or pore volume in the large radii and increases the pore volume of smaller radii. An analysis of the microstructure of polymer-modified mixes by Miller (2005) also reveals that polymers enter and seal voids thereby resulting in a significant decrease in large pores. It can be inferred that the reported changes in porosity and the sealing effect of polymers would reduce permeability.

5.3.7.2 Water Sorptivity Index (WSI)

The test results for the WSI are presented in Figure 5.27 and in Appendix C.8.

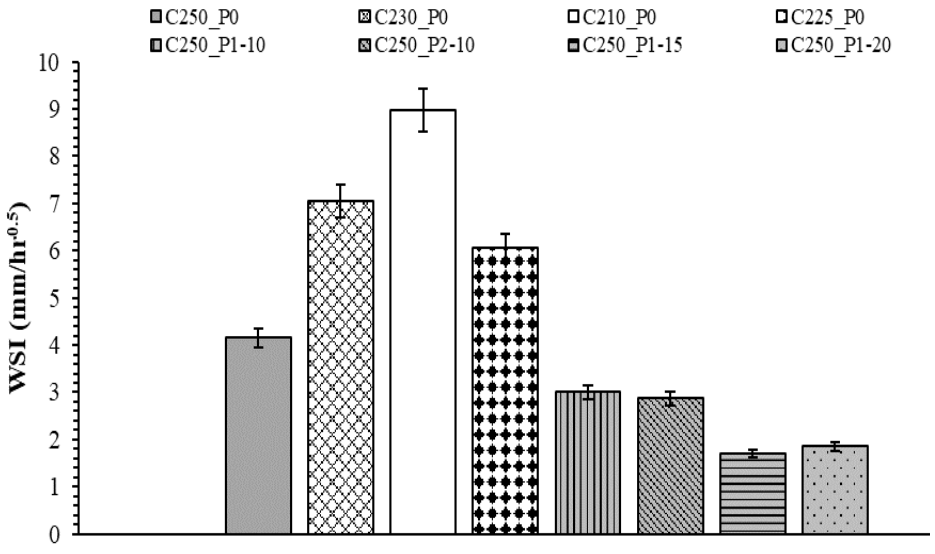

FIGURE 5.27: WSI test results

a) Effect of water content, binder content and w/b

The simultaneous reduction in water- and binder contents in unmodified mixes increased their sorptivity significantly in relation to the reference mix as seen in Figure 5.27. It can be inferred that the reduction in binder content might have increased the porosity of these mixes. The increased porosity in the lean mixes - C230_P0 and C210_P0 - was enhanced by their poor consistence, bleeding and segregation that could have resulted in interconnected voids as discussed in Section 5.3.7.1. An increase in voids enhanced the sorption of water through these specimens subsequently translating to high WSI. It can also be inferred that the reduction in cement paste altered the transport properties of the mortar. The reduction in paste content, and the corresponding increase in aggregate content, resulted in poor packing within the ITZ; thus, making it porous. A porous ITZ enhances the ease with which water moves through the specimen; thereby, resulting in an increase in WSI. An increase in the number of pathways through which water could seep through the mortar - i.e., an increased porosity of the cement paste and a permeable ITZ - would further increase WSI. Increasing the w/b from 0.72 to 0.80 resulted in a significant increase in WSI in relation to the reference mix (C250_P0). The increase in WSI due to an increase in w/b from 0.72 to 0.80 was expected and can also be attributed to an increased porosity - a phenomenon characteristic of high w/b mixes.

b)Effect of polymer modification

Polymer-modification resulted in a reduction in WSI. This observation was expected and is consistent with the observations of Soufi et al. (2016) who report that an increase in polymer dosage decreases capillary absorption significantly. WSI test results correlated well with those from OPI tests. It can be inferred that the sealing and pore blocking effect of polymers - as discussed in Section 5.3.7.1 - reduced WSI. There was no significant difference in WSI in mixes that were modified with EVA and SA polymers at 10%. This observation also correlated with those from OPI tests. Also, the incorporation of 10% EVA did not result in a significant reduction in WSI in relation to the reference mix, unlike the incorporation of 10% SA which resulted in a significant reduction in WSI. This observation could be attributed to the variability within the testing. An increase in the content of EVA polymers from 10% to 20% was accompanied by a corresponding reduction in WSI. This observation is consistent with literature and correlated with those from OPI tests. The reduction in WSI, due to an increase in polymer content, can be attributed to the reduction in penetrability and porosity as discussed in Section 5.3.7.1. Furthermore, Miller (2005) specifically reports that the ethylene monomer is hydrophobic in nature. It has a natural dislike for moisture. Increasing the content of EVA in a mix would consequently reduce WSI. The difference in the WSI of mixes modified with 15% and 20% EVA was not statistically significant. Also, it can be observed that the magnitude of the variability in mean WSI in mixes cast using EVA polymers at 15% and 20% was lower than in the other mixes. This reduction in variability resulted from an improvement in consistence as discussed in Section 5.3.7.1 and in Section 5.3.1.

To further understand the reasons behind the observed OPI and WSI, it was critical that the macroporosity of the specimens be investigated. The macroporosity of specimens from the investigated mixes was determined in accordance with the Durability Index Testing manual. Macroporosity was calculated from the average masses of four disk specimens per mix that had been vacuum-saturated in calcium hydroxide. The results of the macroporosity of the test specimens are presented in Figure 5.28.

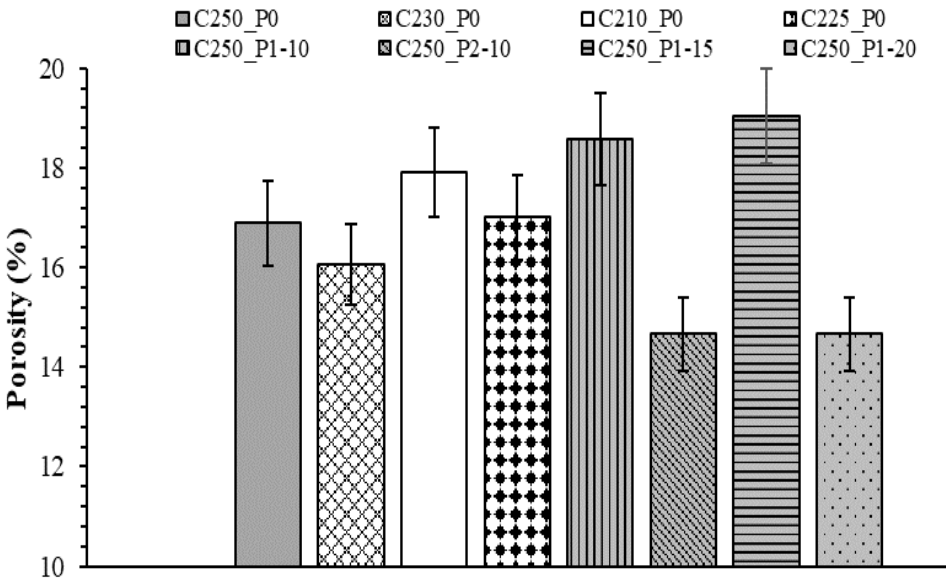

FIGURE 5.28: Macroporosity test results

From Figure 5.28, it can be observed that a clear trend between the macroporosity of the mixes and OPI could not be established. An explanation to this phenomenon could not be provided based on the tests that were undertaken.

5.4 Interrelationships among material properties and age at cracking

A comprehensive review of literature on the interrelationships among the selected mix design parameters and the age cracking - and their interactions - has been presented in the previous chapters. Luković (2016) and Arito et al. (2016a) report that the performance of repairs in service can be improved through an understanding of the influence of governing parameters and boundary conditions within a repair system. It was, therefore, necessary that an evaluation of the relationships between each of the investigated crack-determining material properties and the age at cracking be undertaken. Results from an analysis of the interrelationships between each of the investigated material properties and cracking were further used for the following purposes:

i. To investigate and clarify the contradictions identified in literature regarding the relationships between the investigated material properties and the age at cracking.

ii. To critique the existing empirical deterministic analytical model used to predict stresses and cracking and suggest improvements, if necessary.

iii. To critique the EN 1504-3:2005 performance specifications for non-structural PRMs as well as evaluate their contribution towards the realisation of cracking-resistance in PRMs in service.

Throughout this subsection, scatter plots have been used to represent the relationships under investigation. The preference of scatter plots is based on their lack of bias in representing experimental data.

5.4.1 Compressive and direct tensile strengths

It was necessary that the relationship between direct tensile strength and compressive strength and age at cracking be investigated vis-á-vis the information gleaned from literature even though these material properties do not serve as input parameters in the existing empirical deterministic analytical model - see Equation 1.1 in Section 1.6. Information gleaned from a critical review of literature suggests that PRMs ought to have a high tensile strength for them to withstand the tensile stresses emanating from restrained shrinkage deformations. It was, therefore, necessary to investigate the relationship between direct tensile strength and the age at cracking. The EN 1504-3:2005 recommends that compressive strength of PRMs must always be specified always regardless of its use - see Table 3.2. It is, therefore, important that the relationship between 28-day compressive strength and age at cracking be investigated.
Scatter plots of the 28-day compressive strength versus the age at cracking in unmodified and polymer-modified mixes are presented in Figure 5.29 and Figure 5.30. The data used to plot these figures were obtained from the tests conducted in phase one (compressive strength) and phase two (direct tensile strength). Scatter plots of the age at cracking versus the direct tensile strength at 28 days across the set of specimens cast in phase two are presented in Figure 5.31 and Figure 5.32. Three data points, in Figure 5.31, coincided consequently resulting in the apparent reduction in the number of data points.

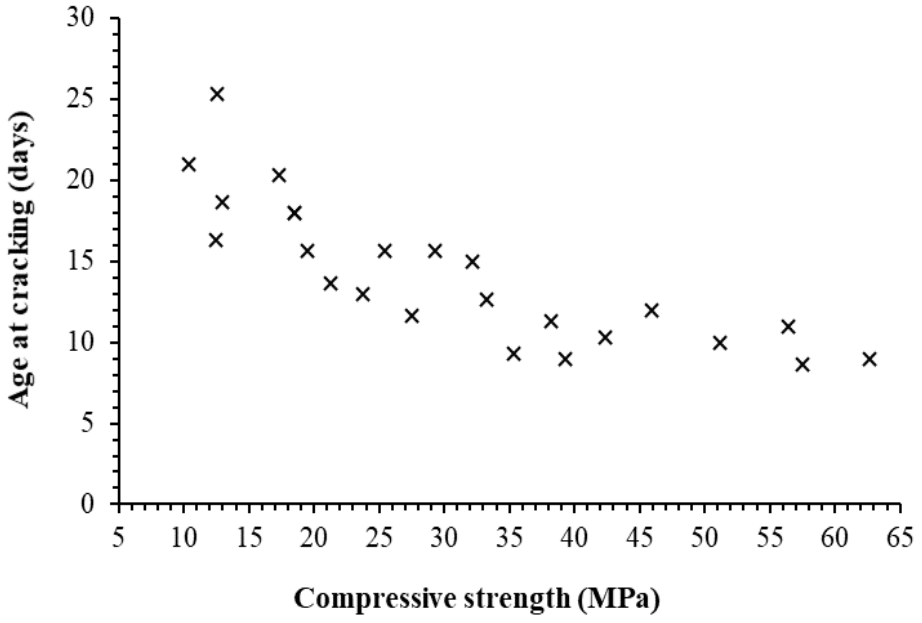

FIGURE 5.29: Age at cracking vs. compressive strength at 28 days (unmodified mixes)

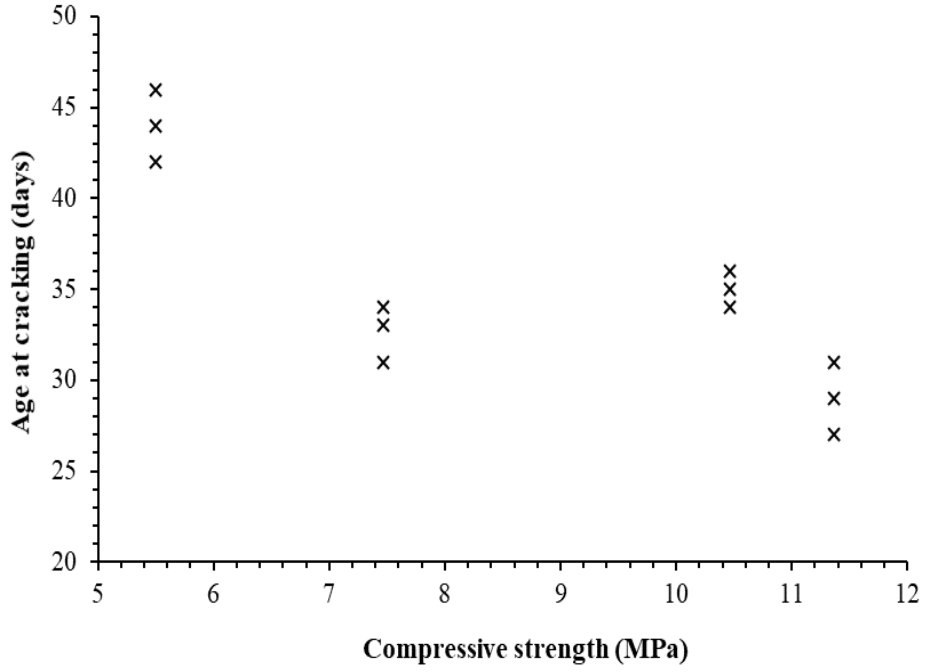

FIGURE 5.30: Age at cracking vs. compressive strength at 28 days (polymer-modified mixes)

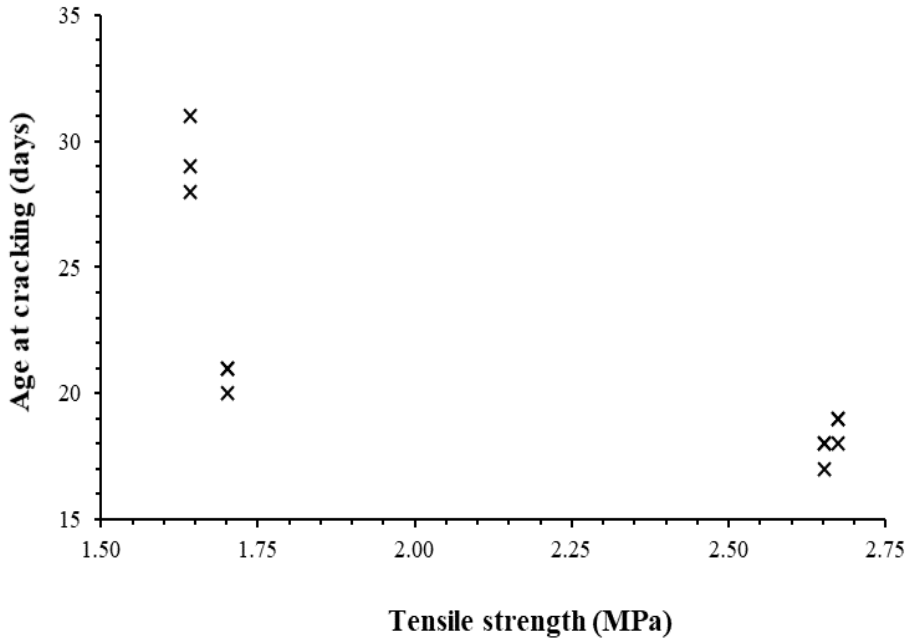

FIGURE 5.31: Age at cracking vs. tensile strength at 28 days (unmodified mixes)

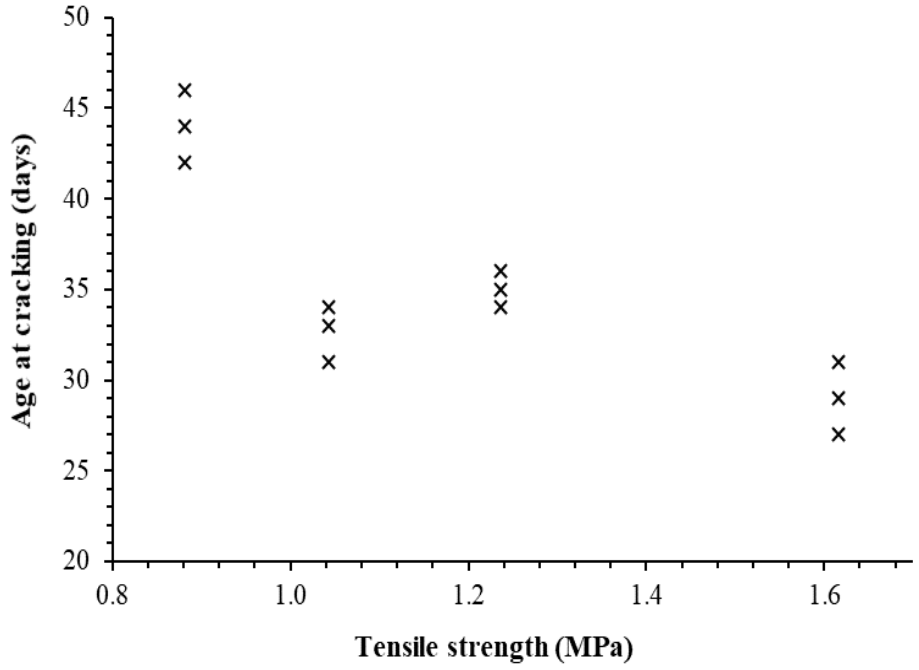

FIGURE 5.32: Age at cracking vs. tensile strength at 28 days (polymer-modified mixes)

An inverse relationship exists between the age at cracking and direct tensile and compressive strengths at 28 days despite the scatter in results. From the scatterplots, it is evident that the age at cracking decreases with an increase in 28-day strength (i.e., compressive and/or direct tensile strength). The reduction in the age at cracking due to an increase in strength was also observed by Dittmer and Beushausen (2014) and Arito et al. (2016b). Increasing compressive strength beyond approximately 35 MPa - as seen from the scatter plot in Figure 5.29 - did not change the age at cracking significantly. PRM mixes with a 28-day compressive strength greater than 35 MPa cracked before 12 days from their date of casting. Thus, it can be posited that the specification of high 28-day strength for non-structural PRMs with the expectation that they will not crack in service would be counterintuitive. An increase in compressive strength is commonly accompanied by a corresponding increase in elastic modulus and a decrease in tensile relaxation. With other factors held constant, this results in higher stresses when shrinkage deformations are restrained. Wittmann (2002) further reports that an increase in strength would generally result in low ductility and consequently an increased risk for crack formation. Strength, therefore, is not a good indicator for the cracking performance of PRMs in service.

Furthermore, the observed relationship between direct tensile strength at 28 days and the age at cracking disproves the misconception in literature that a high tensile strength is necessary for crack prevention. Ghezal and Assaf (2014) have also reported that an increase in tensile strength does not necessarily translate to an increase in resistance to cracking. The specification of high strengths (i.e., compressive and/or tensile) for non-structural PRMs, in contradistinction to the results from this study, increases their susceptibility to crack. The observed relationships between strength and the age at crack, therefore, ought to inform the specification of performance requirements for strength for non-structural PRMs in future.

5.4.2 Elastic modulus

Scatter plots of the age at cracking versus the static modulus of elasticity in compression at 28 days across the set of mortar specimens cast in phase two are presented in Figure 5.33 and Figure 5.34. Three data points, in Figure 5.33, coincided consequently resulting in the 'apparent' reduction in the number of data points. An increase in elastic modulus at 28 days resulted in a reduction in the age at cracking. The observed reduction in the age at cracking due to an increase in elastic modulus was expected and can be attributed to the increased tensile stresses due to restrained shrinkage deformations. This relationship has been discussed in Section 5.3.3 and Section 5.4.1.

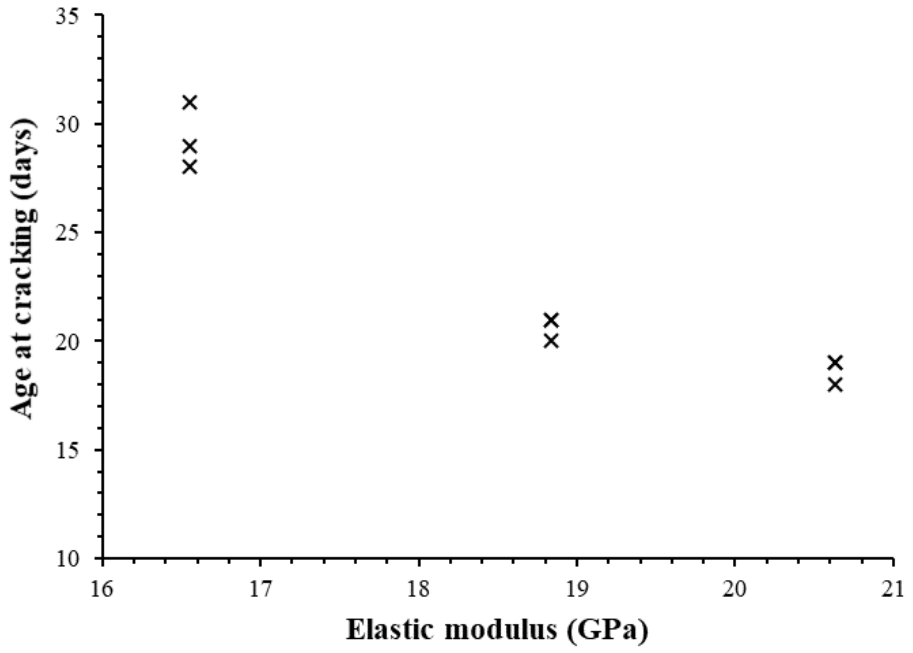

FIGURE 5.33: Age at cracking versus elastic modulus in compression at 28 days (unmodified mixes)

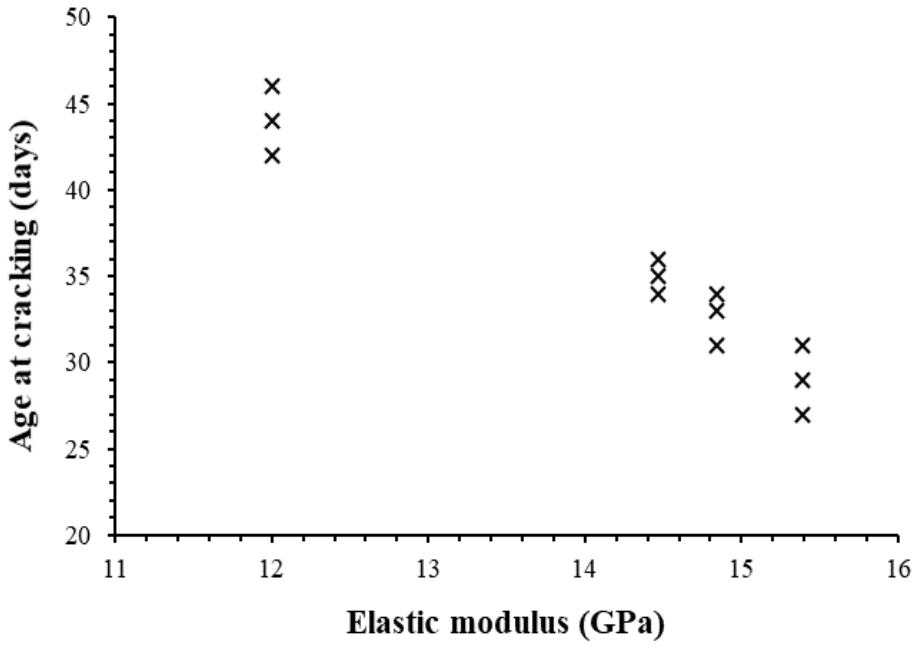

FIGURE 5.34: Age at cracking versus elastic modulus in compression at 28 days (polymer-modified mixes)

The observed relationship between the age at cracking and elastic modulus disproves the misconception in literature that a high elastic modulus reduces the susceptibility to cracking.

5.4.3 Drying shrinkage

Scatter plots of drying shrinkage versus age at cracking across the mortar mixes cast in phase two are presented in Figure 5.35 and Figure 5.36. Three data points, in Figure 5.35, coincided consequently resulting in the 'apparent' reduction in the number of data points.

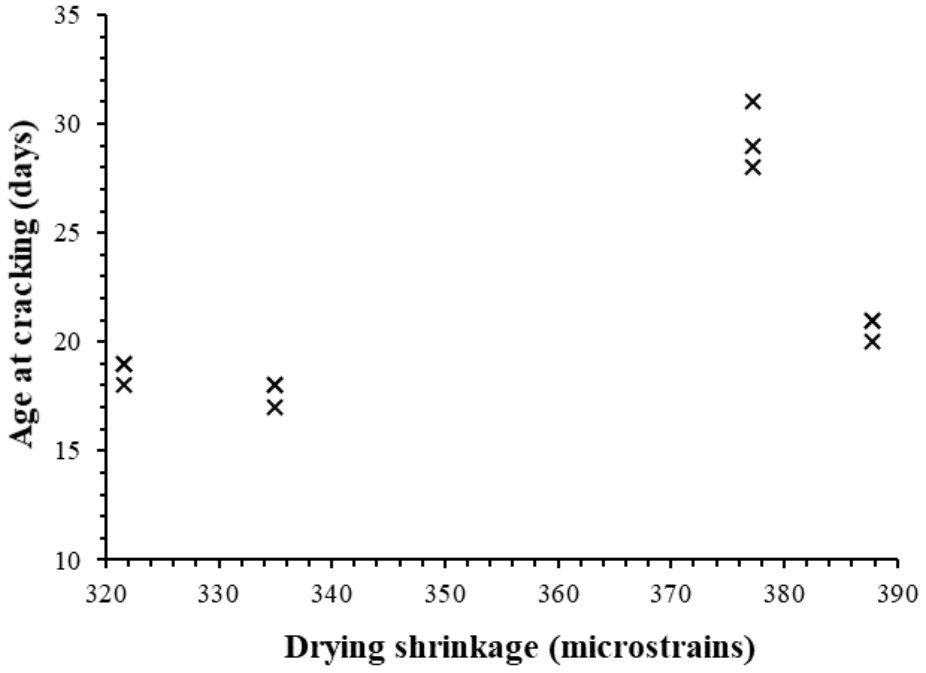

FIGURE 5.35: Age at cracking versus drying shrinkage (unmodified mixes)

An increase in drying shrinkage delayed cracking.This observation disproves the predominating misconception in most literature that an increase in shrinkage increases the susceptibility to cracking. From the test results, it can be inferred that the susceptibility of a mix to crack is not necessarily increased by an increase in drying shrinkage; but rather, by the interactions among multiple crack-determining material properties. PRM mixes that exhibited high shrinkage - especially the polymer-modified mixes - were also characterised by high tensile relaxation and low elastic modulus. Thus, the tensile stresses resulting from the high restrained shrinkage deformations was counteracted by the combined effects of low elastic modulus and high relaxation; consequently, delaying cracking. It is, therefore, necessary that the susceptibility of a material to crack ought to be informed by an evaluation of all crack-determining material properties inter alia.

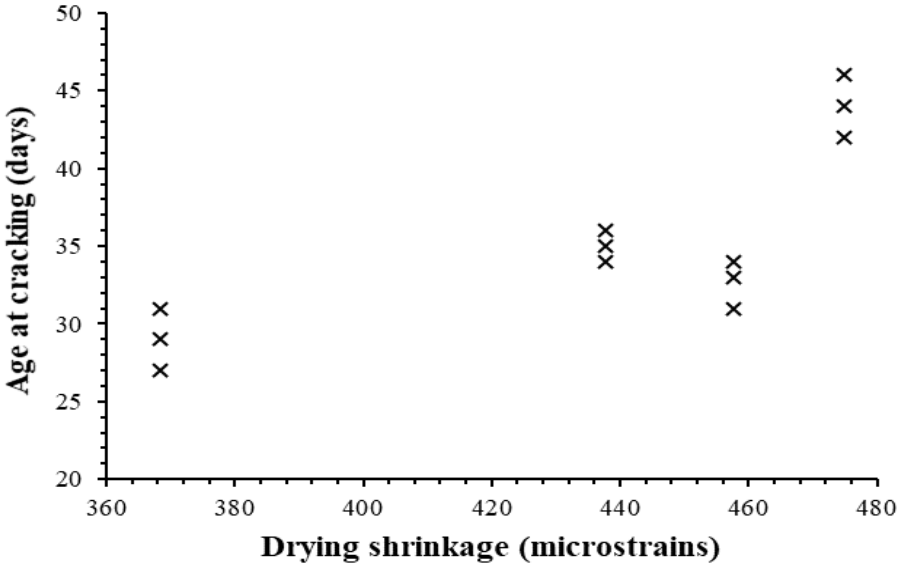

FIGURE 5.36: Age at cracking versus drying shrinkage (polymer-modified mixes)

5.4.4 Tensile relaxation

Scatter plots of the age at cracking versus tensile relaxation at 3, 7 and 28 days across the entire set of specimens tested in the phase two are hereby presented. Three data points, in Figure 5.37, Figure 5.39 and Figure 5.41, coincided consequently resulting in the 'apparent' reduction in the number of data points. Though the cracking of a PRM is mostly affected by the stress relaxation at early ages, i.e., at 3 days and 7 days; tensile relaxation at 28 days has also been presented to maintain consistency - especially with respect to the use of the material properties at 28 days - in the presented data. The tensile relaxation at later ages - i.e., after 7 days - also helped in the modelling of tensile stresses in the PRM specimens under investigation.

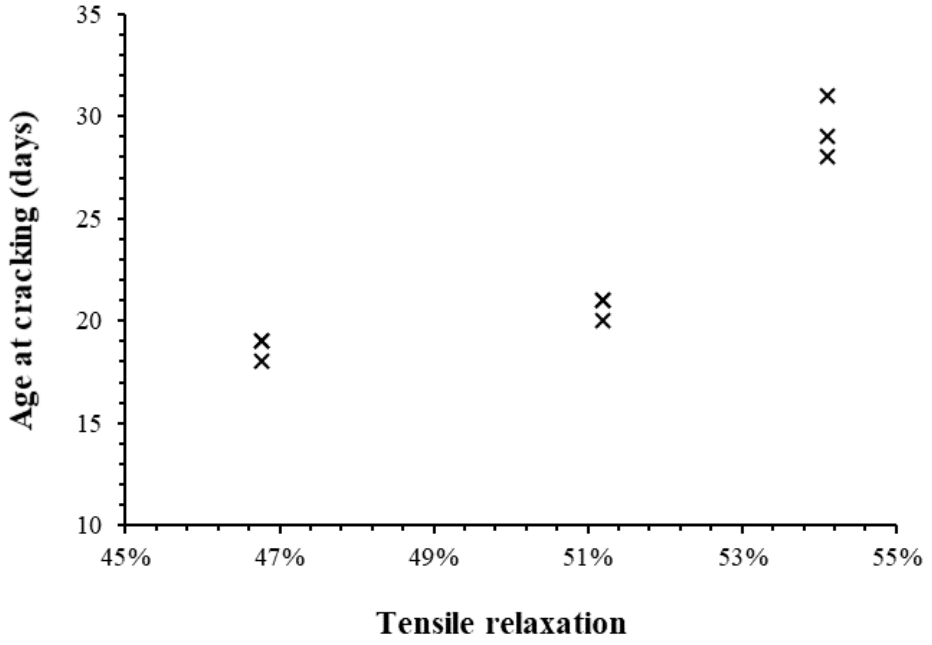

FIGURE 5.37: Age at cracking versus tensile relaxation at 3 days (unmodified mixes)

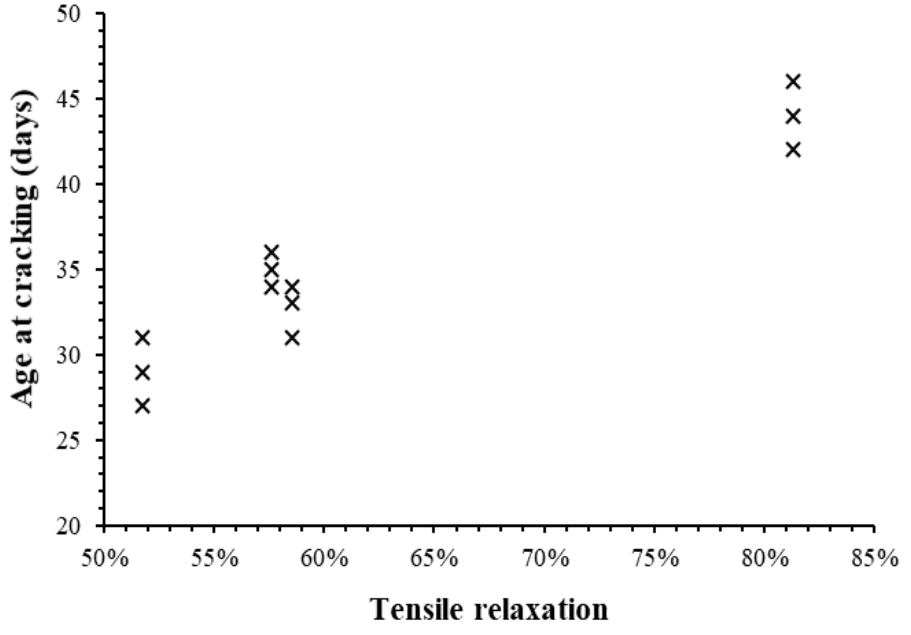

FIGURE 5.38: Age at cracking versus tensile relaxation at 3 days (polymer-modified mixes)

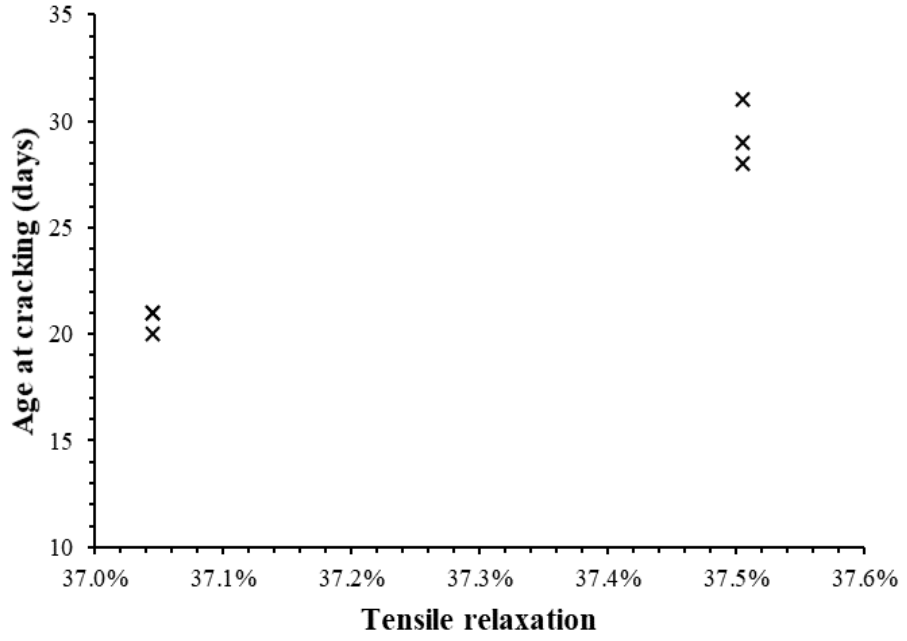

FIGURE 5.39: Age at cracking versus tensile relaxation at 7 days (unmodified mixes)

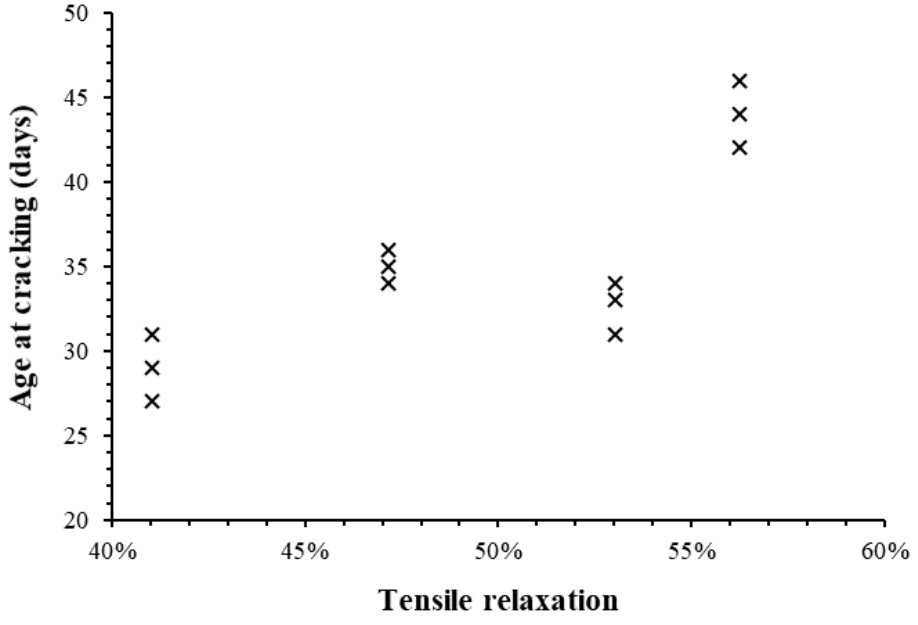

FIGURE 5.40: Age at cracking versus tensile relaxation at 7 days (polymer-modified mixes)

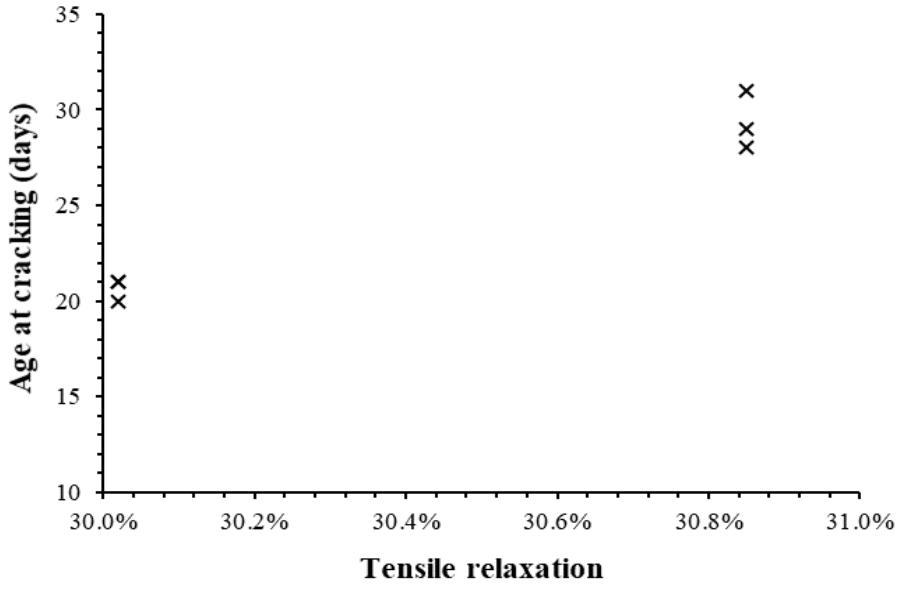

FIGURE 5.41: Age at cracking versus tensile relaxation at 28 days (unmodified mixes)

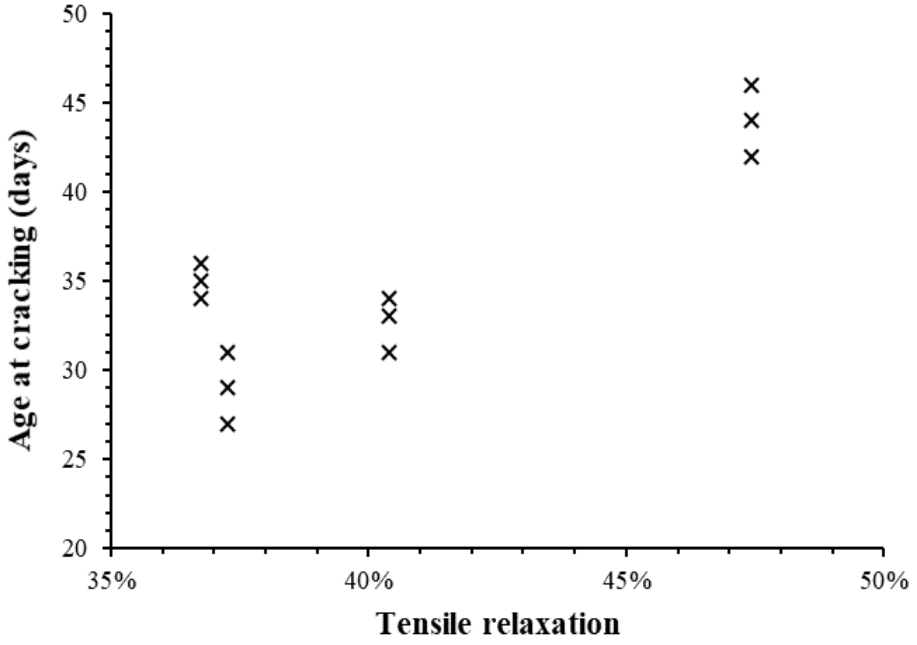

FIGURE 5.42: Age at cracking versus tensile relaxation at 28 days (polymer-modified mixes)

It is evident, from the scatter plots presented, that increasing tensile relaxation delayed cracking. This observation was expected and is also consistent with literature - especially with the observations by Ghezal and Assaf (2014). Tensile relaxation ought to be considered during the design, development and specification of performance requirements for non-structural PRMs. A high tensile relaxation enhances cracking resistance. Additional details on the relationship between tensile relaxation and cracking have been presented in Section 2.3.2.2 and throughout Chapter 3.

5.4.5 Summary

From an analysis of the relationship between the age at cracking and the investigated crack-determining material properties, the predominating misconceptions in literature regarding the relationship between tensile strength, elastic modulus, drying shrinkage and the age at cracking have been highlighted and challenged. An increase in tensile and compressive strength increases the susceptibility to crack while an increase in tensile relaxation delays cracking. An increase in drying shrinkage does not necessarily translate to a reduction in the age at cracking. Nevertheless, it was inferred that the susceptibility of non-structural PRMs to crack depends on the interactions among multiple crack-determining material properties.

The relationships between the investigated material properties and the age at cracking were inferred to take the general form of a power relationship. Thus, it can be inferred that the crack-determining material properties that serve as input parameters to the empirical deterministic analytical model for the prediction of stresses and age at cracking - see Equation 1.1 in Section 1.6 - are not orthogonal as suggested by form of the existing linear empirical analytical model. More specifically, the lack of a perfectly linear relationship between the investigated crack-determining material properties and the age at cracking implies that interactions exist among crack-determining material properties and cracking. There is a need, therefore, to revise the general form of the existing deterministic empirical analytical model for predicting tensile stresses and the time to crack. The revised empirical analytical model ought to take the general form of a power model instead of the existing linear model.

5.5 Analytical modelling of tensile stresses and prediction of time to crack

Extensive studies on the prediction of tensile stresses in cement-based materials using the empirical deterministic analytical model - $\sigma = \mu \times E(t) \times (1 - \frac{\varphi(t)}{100}) \times \varepsilon(t)$ - has been done by Beushausen and Chilwesa (2013), Dittmer and Beushausen (2014) and Beushausen and Bester (2016). The concept used in the analytical modelling of tensile stresses in the mortars under investigation was based on the time development of selected material properties to estimate the time to crack in ring specimens. The duration of the test was

divided into several separate time intervals and changes in shrinkage strains and selected material properties used to determine the resulting additional stress increments. This approach was founded on the principle of superposition where the increments in strains applied at any time are not affected by the strains applied before or after the given time.

5.5.1 Non-linear regression analysis of input parameters

To assess the adequacy and accuracy of this model - and its corresponding improvement, if any - in predicting stresses and the time to crack in the PRMs under investigation, it was necessary that the input parameters for the model be determined for each mix under investigation. Since the material properties of the mixes were tested at specific ages - 3, 7 and 28 days in most instances - there was a need to interpolate the values of these properties at ages when these properties were not tested. Non-linear regression analysis was used to interpolate these material properties. A level of significance of 5% (i.e., $\alpha = 0.05$) was used throughout this analysis. Details on the formulae used to calculate the non-linear regression coefficients are provided in Appendix E.1. The input parameters for the analytical model were represented with non-linear regression models of the following general forms:
Elastic modulus at time t, E(t),

$$E\ (t) = A\ ln\ (t) + B \tag{5.1}$$

Tensile relaxation at time t, $\varphi\ (t)$

$$\varphi\ (t) = C\ ln\ (t) + D \tag{5.2}$$

Tensile strength at time t, $F_{tensile}\ (t)$

$$F_{tensile}\ (t) = F\ ln\ (t) + G \tag{5.3}$$

Shrinkage at time t, $\varepsilon\ (t)$

$$\varepsilon\ (t) = H\ ln\ (t) + J \tag{5.4}$$

The terms A, B, C, D, F, G, H and J in the equations above refer to the non-linear regression coefficients. The selection of natural logarithm regression functions was informed by the research of Beushausen and Chilwesa (2013), Beushausen and Gillmer (2014) and Beushausen and Bester (2016). Also, the natural logarithm regression functions were the best fit for the experimental data. Drying shrinkage was monitored daily over a duration of 56 days from casting. Thus, the measured drying shrinkage test results were input into the existing empirical analytical model directly in mixes that cracked before 56 days. Equation 5.4, however, was used to predict shrinkage in mixes whose predicted age at cracking exceeded 56 days.
To predict tensile stresses in the mixes under investigation, it was necessary that the degree of restraint, μ, of the steel rings be estimated. The degree of restraint was

randomly varied between 0.40 and 0.75 - in increments of 0.05. The degree of restraint that was subsequently used in modelling was selected after an analysis of the plot of the actual versus the predicted age at cracking - see Section 5.5.2 for details on this analysis. The complex interactions among factors that influence cracking in PRMs necessitated the need to make assumptions on shrinkage strains and tensile relaxation. Considering the w/b used in this study - w/b = 0.72 - the contribution of autogenous shrinkage to cracking was not considered. Thus, the prediction of stresses used the results from drying shrinkage tests only.

Most researchers agree that stress relief from tensile relaxation occurs early after loading (Atrushi, 2003; Dittmer and Beushausen, 2014). Thus, the ultimate tensile relaxation was limited to the 48-hour relaxation value. The general unavailability of testing equipment necessitated the use of the 48-hour relaxation as discussed in Section 4.2. To predict the tensile stresses and the age at cracking in the PRM specimens cast using the mixes under investigation, it was necessary that the regression coefficients of the listed non-linear regression models be calculated. These coefficients were calculated using a statistical analysis software - MINITAB 16 - and are summarised in Table 5.6 and Table 5.7. The calculated regression coefficients were used to estimate the material properties for the existing empirical analytical model. Graphs of the non-linear regression prediction models for the input parameters are presented in Appendix E.1. The role of the reported regression coefficients was to produce a curve that resulted in the 'best-fit' to the experimental results.

Table 5.6: Non-linear regression coefficients for unmodified mixes

Regression	**Mix ID**			
coefficient	C250_P0	C230_P0	C210_P0	C225_P0
A	1.79	1.99	1.83	1.77
B	14.66	12.22	10.66	10.64
C	-0.09	-0.11	-0.07	-0.08
D	0.60	0.64	0.53	0.59
F	0.65	0.71	0.38	0.38
G	0.47	0.30	0.51	0.48

5.5.2 Prediction of age at cracking (existing empirical analytical model)

The estimated material properties were consequently input into the existing empirical deterministic analytical model (Equation 1.1) and used to predict tensile stresses and the age at cracking in the PRM mixes under investigation. The stresses were predicted using the range of degree of restraints that have been mentioned above. Scatter plots of the predicted versus the actual age at cracking were plotted for each degree of restraint. These scatter plots are presented in Appendix E.2.

TABLE 5.7: Non-linear regression coefficients for polymer-modified mixes

Regression coefficient	**Mix ID**			
	C250_P1-10	C250_P2-10	C250_P1-15	C250_P1-20
A	2.65	1.44	3.16	2.80
B	5.64	10.61	4.32	2.68
C	-0.09	-0.06	-0.08	-0.14
D	0.67	0.56	0.68	0.92
F	0.46	0.65	0.38	0.44
G	0.26	0.18	0.24	-0.08
H	132.13	115.01	138.26	152.39
J	-85.84	-89.62	-100.74	-132.93

The plot that exhibited the least departure from a linear relationship was selected and used in the prediction of tensile stresses and the age at cracking. A comparison of the actual versus the predicted age at cracking in the mixes under investigation, at different degrees of restraint, are presented in Table 5.8 and Table 5.9. Within the selected range of values for the degree of restraint under investigation, it can be inferred, that a degree of restraint of 0.55 resulted in better predictions of the age at cracking in comparison to the others, especially in polymer-modified mixes. Restraint values lower than 0.45 did not yield sensible results - i.e., the predicted age at cracking deviated significantly from the actual age at accuracy within the limits of practicality. The differences between the actual and the predicted age at a cracking in the mortars under investigation - at a degree of restraint of 0.55 - are shown in Figure 5.43 and Figure 5.44. Graphs of the predicted tensile stresses and age at cracking are presented in Appendix E.3.

The predicted age at cracking in the unmodified mixes were significantly higher than the actual age at cracking as observed in Figure 5.43. These observations are consistent with the test results from a study by Bester (2015). The ratio of the predicted age at cracking versus the actual age at cracking ranged between 1.33 and 2.15. These ratios fall within the range of ratios of 1.33 and 2.0 as gleaned from studies by Beushausen and Chilwesa (2013) and Beushausen and Bester (2016), despite the significant differences in the mixes under investigation in these studies. Comparing the trends in predicted ages at cracking due to changes in water- and binder contents and in w/b vis--vis the ones from the actual age at cracking in unmodified mixes, it can be inferred that the existing empirical analytical model did not detect the effects of these changes in mix design parameters.

TABLE 5.8: Actual vs. predicted age at cracking in unmodified mixes

Degree of restraint, μ	**Age at cracking (days)**	**Mix ID**			
		C250_P0	C230_P0	C210_P0	C225_P0
0.40	Actual	29	21	19	18
	Predicted	151	138	126	102
	Actual/Predicted	0.19	0.15	0.15	0.18
0.45	Actual	29	21	19	18
	Predicted	90	86	83	68
	Actual/Predicted	0.32	0.24	0.23	0.26
0.50	Actual	29	21	19	18
	Predicted	51	53	51	49
	Actual/Predicted	0.58	0.39	0.37	0.36
0.55	Actual	29	21	19	18
	Predicted	39	40	40	38
	Actual/Predicted	0.75	0.52	0.47	0.46
0.60	Actual	29	21	19	18
	Predicted	38	37	37	37
	Actual/Predicted	0.77	0.56	0.50	0.48
0.65	Actual	29	21	19	18
	Predicted	36	35	36	36
	Actual/Predicted	0.81	0.59	0.52	0.49
0.70	Actual	29	21	19	18
	Predicted	35	33	35	34
	Actual/Predicted	0.84	0.63	0.53	0.52
0.75	Actual	29	21	19	18
	Predicted	34	32	34	32
	Actual/Predicted	0.86	0.65	0.55	0.55

TABLE 5.9: Actual vs. predicted age at cracking in polymer-modified mixes

Degree of restraint,	**Age at cracking (days)**	**Mix ID**			
		C250_P1-10	C250_P2-10	C250_P1-15	C250_P2-20
0.40	Actual	35	29	33	44
	Predicted	61	709	40	50
	Actual/Predicted	0.57	0.04	0.82	0.88
0.45	Actual	35	29	33	44
	Predicted	47	366	36	40
	Actual/Predicted	0.74	0.08	0.91	1.10
0.50	Actual	35	29	33	44
	Predicted	36	211	33	37
	Actual/Predicted	0.97	0.14	0.99	1.19
0.55	Actual	35	29	33	44
	Predicted	32	133	32	33
	Actual/Predicted	1.09	0.22	1.02	1.33
0.60	Actual	35	29	33	44
	Predicted	31	89	31	32
	Actual/Predicted	1.13	0.33	1.05	1.38
0.65	Actual	35	29	33	44
	Predicted	29	65	28	30
	Actual/Predicted	1.21	0.45	1.17	1.47
0.70	Actual	35	29	33	44
	Predicted	28	48	26	28
	Actual/Predicted	1.25	0.60	1.26	1.57
0.75	Actual	35	29	33	44
	Predicted	27	36	24	27
	Actual/Predicted	1.30	0.81	1.36	1.63

The predicted age at cracking in the polymer-modified mixes, except for mix C250_P2-10, were lower than the actual age at cracking. The observed trend in mix C250_P2-10 was treated as an anomaly and was not used in subsequent analyses. The ratio of the predicted age at cracking versus the actual age at cracking in the polymer-modified mixes ranged between 0.75 and 0.98. The variability in the predicted age at cracking in polymer-modified mixes was lower than in unmodified mixes.

Comparing the trends from the predicted age at cracking due to the increase in polymer content vis-á-vis the ones from the actual age at cracking, it can be inferred that the existing empirical analytical model did not detect the effect of the change in polymer content from 10% to 20% by mass of binder. The sensitivity of the existing analytical model to the change in polymer type could not be determined due to the observed anomaly in mix C250_P2-10.

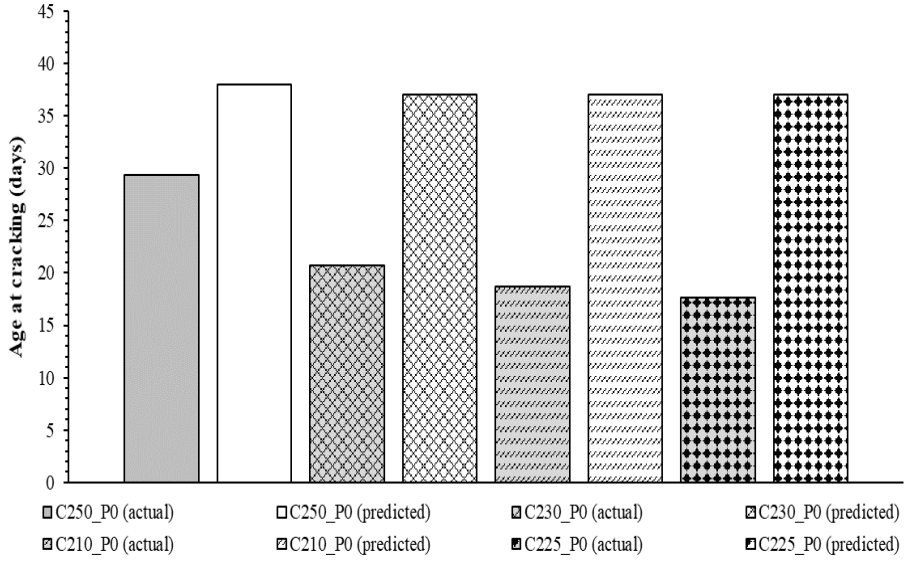

FIGURE 5.43: Actual vs. predicted age at cracking (unmodified mixes, $\mu = 0.55$)

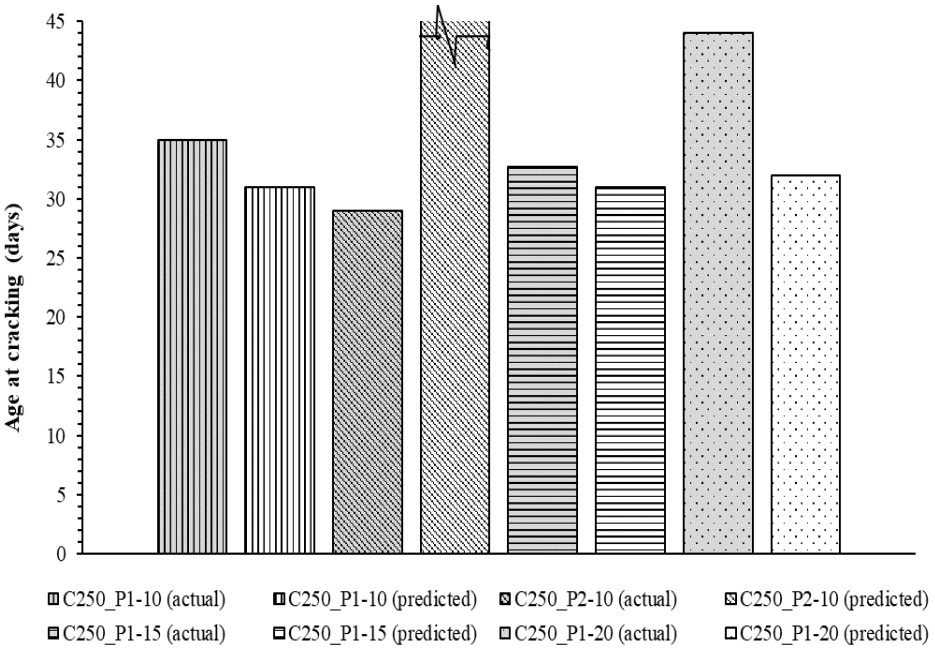

FIGURE 5.44: Actual vs. predicted age at cracking (polymer-modified mixes, $\mu = 0.55$)

5.5.3 Proposed prediction model

From the observations highlighted, it is evident that the existing empirical analytical model is not sensitive enough to detect the effects of the simultaneous reduction in water- and binder contents and changes in w/b and polymer content in the PRMs under investigation. Changes due to w/b, polymer content and the simultaneous reduction in water- and binder content, affect the microstructure of the paste and its fracture mechanics. Whereas polymers affect the permeability of the mix and the bonding between the HCP and the aggregates, the simultaneous reduction in water- and binder content increased the restraining action of the aggregates due to the increased aggregate content. An increase in aggregate content influences the fracture mechanics of the PRM mixes - especially the bonding between the aggregates and the HCP. Thus, it can be inferred that the existing empirical analytical model ought to be modified to improve its adequacy and accuracy in predicting tensile stresses in the mixes under investigation by modifying it to include the effects of fracture mechanics and the microstructural changes in the PRM matrix.

Furthermore, it can be inferred that the existing empirical analytical model is underpinned by the premise that the each of its constituting variables are orthogonal - i.e., all input parameters are independent - and that they all have an equal contribution to the development of tensile stresses that result in cracking due to restrained shrinkage deformations. However, it is evident, from the discussions in Section 5.4, that the model input parameters are dependent and interrelated - an observation that has also been reported by Arito et al. (2016a). A 50% increase in drying shrinkage, for example, does not result in a proportionate reduction in the age at cracking. Thus, the general form of the existing empirical analytical model ought to be modified so that it is sensitive to the relative contribution of each input material parameter to cracking and their corresponding interactions. An assessment of the relationships between the investigated input model parameters and the age at cracking in Section 5.4 reinforces the need to revise the general form of the existing analytical model to a power relationship instead of a linear relationship. The proposed empirical deterministic prediction model (referred to as the proposed model hereafter) ought to be a power relationship with the following general form:

$$\sigma = \mu \times E\ (t)^a \times (1 - \frac{\varphi\ (t)}{100})^b \times \varepsilon\ (t)^c \tag{5.5}$$

where the symbols $\sigma\ (t)$, μ, E(t), $\varphi\ (t)$, $\varepsilon\ (t)$ in Equation 5.5 carry the same meanings as defined in Section 1.6. The exponents a, b and c are experimentally-determined empirical constants that cater for the relative contribution of each of these individual crack-determining material properties, and their corresponding interactions, to cracking. This model is based on a simple stress versus strain relationship.

The lack of equipment - especially strain gauges - that could accurately monitor the development of tensile stresses in the PRM ring specimens due to restrained shrinkage deformations in real-time hindered the accurate determination of the constants a, b and

c and the further development, refinement and calibration of the proposed model. The inability to measure the tensile stresses in real-time implied that there was no logical reference point from which a comparison of the actual and predicted tensile stresses could be undertaken. To overcome this challenge, the estimated tensile strength at the actual age at cracking - as determined through non-linear regression - was used. Thereafter, the exponents a, b and c in Equation 5.5 were estimated by solving the linear logarithmic form of this equation simultaneously. The matrix method of solving simultaneous equations was used. The simultaneous equations that were solved were of the following general form:

$$\log_{10}\ \sigma = \log_{10}\ \mu + a\ \log_{10}\ E(t) + b\ \log_{10}\ (1 - \frac{\varphi\ (t)}{100}) + c\ \log_{10}\ \varepsilon\ (t) \tag{5.6}$$

where the symbols $\sigma_i(t)$, μ, $E_i(t)$, $\varphi_i(t)$ and $\varepsilon_i(t)$ refer to the tensile stress, degree of restraint, elastic modulus, tensile relaxation and shrinkage strains of specimen, i, at time, t, respectively. The degree of restrained was fixed at 0.55. A summary of the calculated exponents a, b, and c is presented in Table 5.10.

TABLE 5.10: Coefficients of the proposed model

Mix type	**a**	**b**	**c**
Unmodified	2.47	0.33	2.69
Polymer-modified	2.33	7.45	1.25

The tensile stresses in the unmodified mixes were predicted using Equation 5.7.

$$\sigma\ (t) = 0.55 \times E(t)^{2.47} \times (1 - \frac{\varphi\ (t)}{100})^{0.33} \times \varepsilon\ (t)^{2.69} \tag{5.7}$$

The tensile stresses in the polymer-modified mixes were predicted using Equation 5.8.

$$\sigma\ (t) = 0.55 \times E(t)^{2.33} \times (1 - \frac{\varphi\ (t)}{100})^{7.45} \times \varepsilon\ (t)^{1.25} \tag{5.8}$$

It is important to note that the poposed models were only meant to provide an assessment on which among the investigated crack-determining material properties are dominant to cracking. The purpose of the proposed model was not to develop "valid" numerical coefficients but to present an assessment of the quantitative influence of each material parameter to cracking. Further studies ought to be done to refine the proposed models and improve their accuracy in predicting tensile stresses. From Equation 5.7 and Equation 5.8, it can be observed that the proposed model factors the relative contributions of tensile relaxation and shrinkage strains. Specifically, it can be observed that the contribution of tensile relaxation and shrinkage strain to cracking are not equal, but vary depending on the type of mix. The drying shrinkage had the most significant contribution to cracking in unmodified mixes while the tensile relaxation had the most significant contribution to cracking in polymer-modified mixes. The contribution of the elastic modulus to cracking did not vary significantly depending on the type of

mix. While the influence of the tensile strength could not be assessed directly using the proposed model, it is important to note that the interactions among elastic modulus, tensile relaxation and shrinkage strains vis-á-vis the tensile strength will dictate the susceptibility to cracking.

The proposed analytical models were subsequently used to predict tensile stresses and the age at cracking. Graphs of the predicted tensile stresses and the age at cracking using the proposed prediction model are presented in Appendix E.3.3. A comparison of the predicted ages at cracking is presented in Table 5.11 and Figure 5.45. Except for mix C210_P0, it can be observed that the predicted ages at cracking using the proposed model was significantly lower than the actual age at cracking in the unmodified mixes. More specifically, the predicted ages at cracking using the proposed model were lower by a factor that ranged between 0.34 and 1.23.

TABLE 5.11: Comparison of the predicted age at cracking using the existing and the proposed analytical models

Mix	**Age at cracking (days)**		
ID	Actual	Predicted (existing model)	Predicted (proposed model)
C250_P0	29	39	10
C230_P0	21	40	12
C210_P0	19	40	23
C225_P0	18	38	16
C250_P1-10	35	32	28
C250_P2-10	29	133	33
C250_P1-15	33	32	32
C250_P1-20	44	33	39

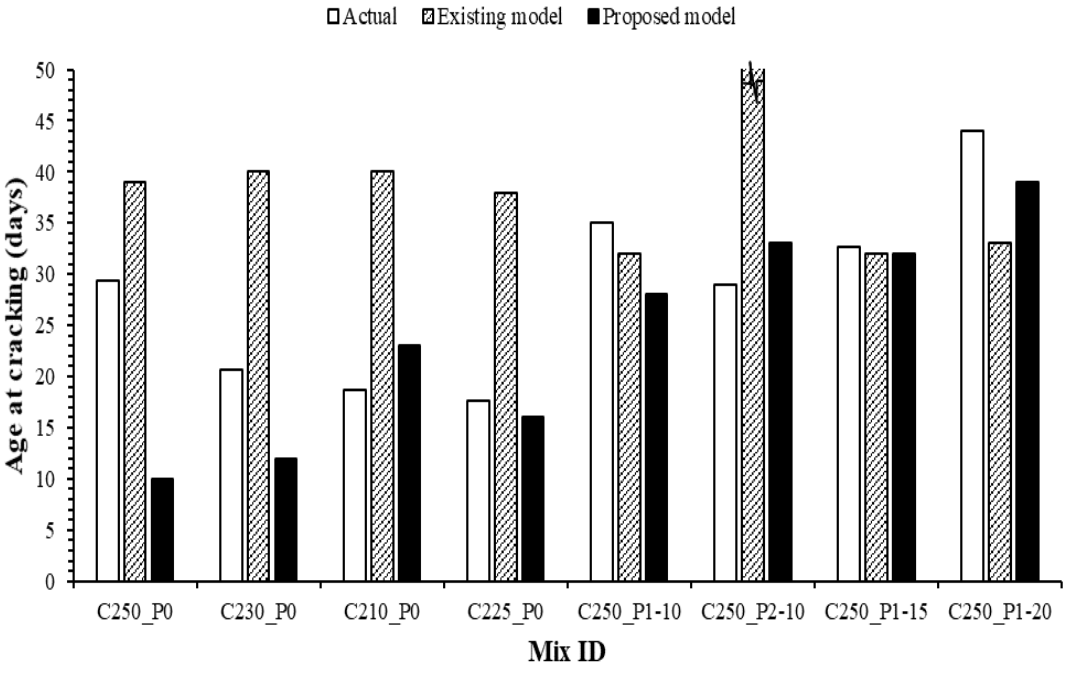

FIGURE 5.45: Actual vs. predicted age at cracking

The predicted age at cracking using the proposed model were significantly lower than those predicted using the existing analytical model in unmodified mixes. The proposed model did not capture the effects of water- and binder content reduction as well as the change in w/b. Furthermore, it can be observed that the predicted age at cracking in the polymer modified mixes using the proposed model were lower than the actual age at cracking - except for mix C250_P2-10 which was treated as an anomaly. The actual ages at cracking were higher than the predicted ages at cracking using the proposed model by a factor that ranged between 1.02 and 1.25. While the proposed model was sensitive to changes in polymer content, it can be observed that the proposed model did not capture the effect of polymer content on cracking accurately. The proposed model needs to be refined further in future research.

5.6 Closure

Results from the experimental work have been analysed, discussed and presented within this chapter. The influence of selected mix design parameters - water content, binder content, binder type, curing type, SA dosage - and their corresponding interactions on cracking was investigated in the first phase of this study. The relative levels of sensitivity of the selected mix design parameters to cracking were also determined. The effect of

polymer modification on restrained shrinkage cracking and selected crack-determining material properties was also investigated in the second phase of this study.

Owing to the large number of experimental variables and the need to investigate the levels of sensitivity of the selected mix design parameters, a full 2^5 factorial experimental design approach with three replicates was used. Factorial analysis was observed to be a robust experimental design and analytical tool. It helped determine the levels of sensitivity of qualitative parameters such as binder type and curing type, and the quantification of the relative levels of sensitivity of the mix design parameters under investigation. Factorial analysis was also observed to be an efficient research tool. Minimal resources - with respect to time and materials - were used to arrive at meaningful conclusions. The sensitivity of the selected mix design parameters to cracking decreased in the following order of significance: SRA dosage, binder content, binder type, curing method and water content. The age at cracking in ring specimens cast in accordance with the ASTM C 1581 was the reference parameter for sensitivity analysis.

The partial replacement of cement with GGBS yielded mixed results with respect to the age at cracking. These effects depended on w/b. The incorporation of GGBS, for example, delayed cracking in mixes with w/b of 0.40 and 0.51 and reduced the age at cracking in mixes with w/b of 0.72 and 0.92. Except for the mix with w/b of 0.40, crack widths in PC/GGBS specimens were smaller than those of PC-only specimens. An increase in w/b increased flow, reduced strength, reduced OPI and increased the WSI of the investigated mortars mixes. The general increase in w/b from 0.40 to 0.92 delayed cracking and reduced crack widths. This phenomenon was attributed to the effect of w/b on elastic modulus, drying shrinkage and capillary pore pressure as discussed in this chapter.

The effect of the simultaneous reductions in water- and binder content at a constant w/b on direct tensile strength and compressive strength varied with the age of the specimens. These reductions also resulted in the following effects: reduction in elastic modulus, reduction in age at cracking, reduction in crack widths, reduction in OPI and an increase in WSI. The effects of this reduction on tensile relaxation were not significant. The effect of the simultaneous reductions in water and binder content on drying shrinkage was not clear. It resulted in mixed effects. Details regarding these variations on specific material properties have been presented within this chapter. The effect of the simultaneous reduction in water content from 180 l/m^3 to 150 l/m^3 and binder content from 250 kg/m^3 to 210 kg/m^3 - at a fixed w/b of 0.72 - was not significantly different from the effect of an increase in w/b from 0.72 to 0.80 with respect to the following material properties: direct tensile strength and compressive strength, elastic modulus, drying shrinkage, crack widths, tensile relaxation at early ages and age at cracking. There was a large variability in the observed crack widths in phase one. Thus, an accurate assessment of mix design parameters on crack widths could not be conducted using the mixes developed in this phase. Nevertheless, regarding the specimens cast in phase two, the simultaneous reduction in water- and binder content reduced crack widths significantly. Also, there was no significant difference in the crack widths resulting

from an increase in w/b from 0.72 and the simultaneous reduction in water-and binder contents. The modification of the mixes with polymers resulted in a reduction in crack widths. Furthermore, an increase in aggregate volume and the aggregate:binder ratio reduced crack widths. This observation was attributed to the reduction in shrinkage, due to the increase in these two parameters, which reduces the magnitude of displacement of crack faces. The crack widths in the specimens in phase two widened with time.

SRAs delayed cracking significantly. They also reduced crack widths. These effects have been described in detail within this chapter; and can be attributed to the contribution of SRA to the reduction in autogenous and drying shrinkage. The incorporation of SAPs delayed cracking significantly in mixes with either high w/b (0.92) or low w/b (0.40). The delay in cracking, due to the incorporation of SAPs, in mixes with intermediate w/b (i.e., 0.51 and 0.72) was not significant. This phenomenon ought to be investigated further in future studies. The delay in cracking due to SAPs was more pronounced in PC/GGBS mixes than in PC-only mixes. This observation was attributed to the effect of improved curing on crack-determining material properties as discussed within this chapter. The combined use of SAP and SRA reduced crack widths and delayed cracking significantly. The effect of the combined use of these admixtures, however, was more pronounced in PC-only mixes than in PC/GGBS mixes. The general observations on the effects of the individual contributions of SRA, GGBS and SAP on cracking corroborated most literature.

Polymer-modification also resulted in the following effects: increase in flow, reduction in direct tensile and compressive strength at all ages, reduction in elastic modulus, increase in drying shrinkage, increase in tensile relaxation, delay in cracking and a reduction in WSI. The magnitude of the reported effects of polymer-modification on the listed material properties increased with an increase in polymer content. The mechanisms responsible for these effects have been presented in this chapter. Also, there was no significant difference between the OPIs of polymer-modified and unmodified mixes. The observed lack of difference could have resulted from the variability in testing. Also, the variability in OPI results in polymer-modified mixes was lower than in unmodified mixes. This observation was attributed to the improved compaction resulting from polymer-modification. SA polymer-modified mixes were characterised by lower flow, higher direct tensile and compressive strength at all ages, higher elastic modulus, reduced drying shrinkage, reduced tensile relaxation at 28 days and a reduced age at cracking when compared to EVA polymer-modified mixes. Contradictions in literature regarding the effects of polymers on tensile and compressive strength and shrinkage were observed. Details of the effects of polymer on the listed properties as well as the highlighted contradictions in literature have been presented within this chapter.

The relationships between the age at cracking and selected material properties (compressive strength, tensile strength, static modulus of elasticity, drying shrinkage and tensile relaxation) of the PRMs under study were investigated. The following critical insights were gleaned from this analysis:

i. An increase in compressive strength, tensile strength and elastic modulus reduced the age at cracking. Specifying high compressive and tensile strengths, therefore, increases the susceptibility to cracking.

ii. An increase in the 28-day compressive strength beyond approximately 35 MPa did not change the age at cracking significantly.

iii. An increase in drying shrinkage does not necessarily translate into an increase in the susceptibility to cracking.

iv. An increase in tensile relaxation delays cracking significantly.

The observed relationships challenged the common misconceptions in literature on the effect of strength (i.e., compressive and direct tensile), elastic modulus and drying shrinkage on cracking. It can be inferred that the cracking resistance of PRMs can be improved by increasing tensile relaxation and by reducing the compressive strength, direct tensile strength and elastic modulus. Considering the information gleaned from an analysis of the relationships between crack-determining material properties and cracking, it is evident that there is a need to rethink the philosophy and approach used in the development of performance requirements for non-structural PRMs. An improvement in the cracking resistance of non-structural PRMs in service, can be achieved through the revision of several existing requirements and the introduction of new performance requirements that are more relevant to cracking.

Non-linear regression analysis was used to predict the input parameters for the analytical modelling of stresses and the age at cracking in the PRM mixes under investigation. The predicted input parameters were subsequently used to assess the adequacy and the accuracy of an existing empirical analytical model in predicting stresses and the age at cracking in the mixes under investigation. A degree of restraint of 0.55 was used as it was found to best relate to the cracking behaviour of test specimens. The prediction of stresses and the age at cracking using the existing empirical analytical model revealed the following:

i. The predicted age at cracking in the unmodified mixes were higher than the actual age at cracking. The ratio of the predicted age at cracking/actual age at cracking ranged between 1.33 and 2.15.

ii. The predicted age at cracking in polymer-modified mixes were lower than the actual age at cracking. The ratio between the predicted age at cracking/actual age at cracking ranged between 0.75 and 0.98.

iii. The existing analytical model was not sensitive to the effects of changes in water- and binder contents at a constant w/b and the change in w/b from 0.72 and 0.80.

iv. The general form of the existing analytical model ought to be modified. It ought to be changed from a linear model to a power model so that it can be sensitive enough to account for the interrelationships among its input parameters and the

relative contribution of crack-dependent material properties to restrained shrinkage cracking.

Owing to the weaknesses highlighted in the existing analytical empirical model in predicting tensile stresses and the age at cracking in non-structural PRMs, two deterministic empirical analytical power models have been proposed for the prediction of tensile stresses in the unmodified and polymer-modified mixes. The general form of these models is $\sigma = \mu \times E(t)^a \times (1 - \frac{\varphi\ (t)}{100})^b \times \varepsilon\ (t)^c$.The coefficients of the exponents were determined and have been presented in Section 5.5.3. The proposed model was further used to predict the stresses and the age at cracking in the PRM mixes under investigation. The prediction of stresses and the age at cracking using the proposed empirical analytical model revealed the following:

i. The predicted age at cracking in the unmodified mixes, except for mix C210_P0, were lower than the actual age at cracking. The ratio of the predicted age at cracking/actual age at cracking ranged between 0.34 and 1.23.

ii. The predicted age at cracking in polymer-modified mixes, except for mix C250_P2-10 which was treated as an anomaly - were lower than the actual age at cracking. The ratio between the predicted age at cracking/actual age at cracking ranged between 1.05 and 1.25.

iii. The proposed model was sensitive to the effects of changes in water- and binder contents at a constant w/b, change in polymer content and the change in w/b from 0.72 and 0.80.

iv. The proposed model can factor the relative contribution of elastic modulus, tensile relaxation and shrinkage strains. From the proposed model, it was observed that the contribution of shrinkage strain and tensile relaxation to cracking depend on the type of mix. The contribution of elastic modulus to cracking did not vary significant with respect to the type of mix.

Chapter 6

CONCLUSIONS AND RECOMMENDATIONS

The conclusions that have been arrived at during this study and the recommendations for further research are presented within this chapter.

6.1 Introduction

The principal objective of this study was to generate new knowledge that would inform the design and development of non-structural PRMs and the future development of performance requirements for these PRMs through an investigation into the influence of multiple mix design parameters on restrained shrinkage cracking. This study also sought to achieve the following sub-objectives:

i. To investigate the influence of mix design parameters on crack-determining material properties and cracking in non-structural PRMs.

ii. To establish the relative sensitivity of cracking in non-structural PRMs to mix design parameters.

iii. To evaluate the contribution of the EN 1504-3:2005 performance specifications towards the realisation of non-structural PRMs with an improved resistance to cracking in service.

iv. To improve the accuracy of an existing empirical analytical model to predict the age at cracking in ethylene vinyl acetate and styrene acrylate polymer-modified mortars.

These objectives were met through a critical review of literature and laboratory experiments. The conclusions from this study pertain to three distinct aspects:

i. The role and contribution of multiple mix design parameters and crack-determining material properties to cracking in non-structural PRMs.

ii. The role of the existing performance requirements for non-structural PRM and their contribution to cracking.

iii. The improvement of an existing empirical analytical model to predict cracking in polymer-modified mixes.

The above conclusions are discussed in the following subsections.

6.2 Effects of multiple mix design parameters and material properties on cracking

The role and contribution of multiple mix design parameters and crack determining material properties to cracking are hereby discussed.

6.2.1 Trend and sensitivity analysis

The sensitivity of cracking to five mix design parameters - water content, binder content, curing method, SRA dosage and the type of binder - was investigated. An analysis of the sensitivity of cracking to the investigated mix design parameters revealed that cracking in non-structural PRMs is sensitive to the investigated mix design parameters in the following order of decreasing sensitivity: SRA dosage, binder content, binder type, curing method and water content. An analysis of the trends between the investigated mix design parameters - within the selected domain of the experimental variables - and the age at cracking in PRM specimens corroborated the information in literature; consequently, leading to the following conclusions:

i. The interaction effects among the investigated mix design parameters affect cracking significantly. Thus, the optimisation of multiple mix design parameters for resistance to cracking ought to consider these interactions inter alia.

ii. SRA dosage: an increase in SRA dosage delays cracking significantly.

iii. Binder content: a reduction in binder content delays cracking. A reduction in the age at cracking occurred when the binder content was reduced below 250 kg/m^3 in mixes cast with w/b of 0.72. It is important to note that the minimum binder content of 250 kg/m^3 is unique to this study and cannot be generalised.

iv. Binder type: the use of 100% CEM II B-M (L) delayed cracking in comparison to a blend of 50/50 CEM II B-M(L)/GGBS. Replacing CEM II B-M (L) with 50% slag reduced the age at cracking significantly.

v. Water content: a reduction in water content delayed cracking. A reduction in the age at cracking occurred when the water content was reduced below 150 l/m^3 in mixes cast with w/b of 0.72. The reported minimum water content is unique to this study and cannot be generalised.

vi. The curing of mortars through the combined use of SAP and wet hessian delayed cracking in comparison to curing using wet hessian only.

6.2.2 Effect of water content, binder content and w/b

The blanket use of the term 'water:binder ratio' without recognising its individual components - i.e., water content and binder content - ought to be reconsidered. The effect of the simultaneous reduction in water content from 180 l/m^3 to 150 l/m^3 and binder content from 250 kg/m^3 to 210 kg/m^3 - at a fixed w/b of 0.72 - was not significantly different from the effect of an increase in w/b from 0.72 to 0.80 with respect to the following material properties: direct tensile strength and compressive strength, elastic modulus, drying shrinkage, tensile relaxation at early ages and age at cracking. Furthermore, it was observed that a reduction in water and binder contents - at a constant w/b of 0.72 - reduced direct tensile and compressive strength, elastic modulus, crack widths and the age at cracking. The effects of this reduction on tensile relaxation were not significant. The simultaneous reductions in water and binder content on drying shrinkage resulted in mixed results. The w/b ought to be considered in tandem with its constituting water and binder contents instead of a digit. Mortar mixes with relatively high w/b (w/b = 0.72 and 0.92) had the highest volume of aggregates (74% and 69% respectively) and consequently took longer to crack. Mixes with relatively low w/b (w/b = 0.40 and 0.51) had the lowest volume of aggregates (67% and 62% respectively) and cracked early. An increase in w/b also increased flow, reduced strength, reduced OPI and increased the WSI of the investigated PRM mixes.

6.2.3 Effect of SAP and SRA

The addition of SRAs to the mortar mixes delayed cracking significantly. In addition, crack widths were reduced. These observations were attributed to the reduction in autogenous and drying shrinkage due to SRA usage. The effectiveness of the contribution of SRAs was observed to be dependent on the type of binder. The incorporation of SAPs delayed cracking significantly in mixes with either high w/b (0.92) or low w/b (0.40). The delay in cracking, due to the incorporation of SAPs, in mixes with intermediate w/b (i.e., 0.51 and 0.72) was not significant. The influence of SAPs on the age at cracking was more pronounced in PC/GBS mixes than in PC-only mixes. This observation further corroborated the view that the extent to which GGBS influences cracking in cement-based materials depends on curing. The interaction between SAP and SRA resulted in positive synergy. The effect of the simultaneous use of SAP and SRA on the age at cracking was more pronounced than their individual effects. This synergistic effect was independent of the type of binder. The use of SAP and SRA simultaneously reduced crack widths and delayed cracking significantly.

6.2.4 Effect of polymer modification

The modification of the mixes by ethylene vinyl acetate (EVA) and styrene acrylate (SA) polymers resulted in an increase in flow, a reduction in compressive and direct tensile strengths at all ages, a reduction in elastic modulus, an increase in drying shrinkage, a delay in cracking, a reduction in crack widths, an increase in tensile relaxation and a decrease in WSI. The magnitude of the reported effects of polymer-modification on the listed material properties increased with an increase in polymer content. The material properties of SA polymer-modified mixes were significantly different from those of EVA polymer-modified mixes at the same polymer content. SA polymer-modified mixes were characterised by lower flow, higher direct tensile and compressive strength at all ages, higher elastic modulus, reduced drying shrinkage, reduced tensile relaxation at 28 days and a reduced age at cracking in comparison to EVA polymer-modified mixes. Considering the tests that were conducted in this study, it can be concluded the recent developments in admixtures - specifically redispersible polymers, SRA and SAPs - can potentially improve the performance of non-structural PRMs in service with respect to resistance to cracking. Polymer modification reduced crack widths significantly.

6.2.5 Effect of material properties

An investigation into the relationships between the investigated material properties and cracking resulted in the following conclusions:

i. An increase in compressive strength, tensile strength and elastic modulus reduced the age at cracking.

ii. An increase in drying shrinkage does not necessarily translate into an increase in the susceptibility to cracking.

iii. An increase in tensile relaxation delayed cracking significantly.

The observed relationships challenged the common misconceptions in literature on the effect of strength (i.e., compressive and direct tensile), elastic modulus and drying shrinkage on cracking. The cracking resistance of non-structural PRMs can be improved by increasing their tensile relaxation and by reducing their strength (tensile and compressive) and elastic modulus.

6.2.6 Miscellaneous

The test results for initial crack widths were characterised with a wide scatter - especially in phase one. The wide variability in initial crack widths hindered the derivation of meaningful conclusions between the investigated mix design parameters and crack-determining material properties on the initial crack widths. Nevertheless, an increase in w/b resulted in a reduction in initial crack widths. The aggregate content and a/b played a significant role in the cracking of the PRMs under investigation. An increase

in a/b and aggregate content reduced initial crack widths across the entire set of mixes. An increase in w/b and aggregate volume delayed cracking. The partial replacement of cement with GGBS resulted in mixed results with respect to the age at cracking. The effects of GGBS on cracking were dependent on w/b. The observed relationship between GGBS and cracking corroborated the findings in literature that report that the addition of GGBS produces mixed results. The partial replacement of cement with GGBS reduced the initial crack widths.

6.3 Role of performance requirements on cracking

There is no single non-structural PRM that is universally good - a proposition has also been reported by Morgan (1996), Vaysburd et al. (2008) and Luković (2016). The extent to which a PRM is good ought to be based on its performance within its unique exposure environment in relation to its performance requirements. Thus, it is important that repair manufacturers and design engineers who specify repair materials use the term 'good' cautiously. The evaluation of the 'goodness' or 'badness' of a non-structural PRM ought to be based on its performance requirements and the suitability of the performance requirements to the unique environment in which the PRM will be applied. There is a possibility that a repair material that has been termed good in one scenario would end up being bad in another.

Non-structural PRMs are primarily used to restore the alkalinity around corroding reinforcing steel, encapsulate the anodes in cathodic protection systems, or to restore the surface profile by filling cavities within concrete that has spalled. For these PRMs to be deemed effective for service, they ought to possess the following general characteristics:

i. They ought to be electrochemically similar to the existing concrete substrate to avoid the initiation and propagation of reinforcement corrosion. This property could be achieved by specifying electrochemical parameters such as electrical resistivity.

ii. The differential deformations between the concrete substrate and the PRM ought to be at a minimum to reduce the magnitude of tensile stresses that develop due to restrained deformations. To achieve this, material properties such as the coefficient of thermal expansion, elastic modulus and drying shrinkage ought to be specified.

iii. They ought to be impermeable to moisture, oxygen and other deleterious aggressive chemical species. The ease with which these chemical species penetrate the repair dictates the ease with which concrete and the embedded reinforcement deteriorates. It is important that penetrability properties of the material are specified.

iv. They ought to adhere to the concrete substrate. Adhesion between the PRM and its substrate can be achieved through the specification of its bond strength.

Enormous resources in terms of research and finances have been expended into the development of performance requirements of non-structural PRMs in the form of a code of practice - the EN 1504-3:2005. It is, therefore, important that the role and contribution of the performance requirements specified in the EN 1504-3:2005 be evaluated vis-á-vis the roles that non-structural PRMs ought to play to be deemed effective while in service. A critical analysis of the performance requirements for non-structural PRMs - as specified in the EN 1504-3:2005 - vis-á-vis the reviewed literature and the results this study reveal many glaring shortcomings. These shortcomings comprise:

i. The EN 1504-3:2005 has failed to recognise and specify important crack-determining material parameters such as elastic modulus, tensile relaxation and shrinkage strains despite the evidence in literature that explain the contribution of these material properties to cracking. The fact that these material properties are the main input parameters in the empirical analytical models that have been discussed extensively in this study - Equation 1.1 in Section 1.6 - implies that they are critical to cracking and thus, ought to be specified.

ii. The EN 1504-3:2005 has failed to deviate from the predominating paradigm of using compressive strength as a proxy for assessing the effectiveness in performance of non-structural PRMs in service. This code uses compressive strength at 28 days as a criterion for distinguishing the two classes of non-structural PRMs i.e., class R1 and class R2 mortars even though these PRMs do not serve any structural role.

iii. The recommended standard test procedures for assessing the performance requirement for shrinkage in the EN 1504-3:2005 seem to be restrictive. The code states that the test for restrained shrinkage ought to be done on a concrete substrate cast using w/b of 0.40. Details regarding the mix design parameters of the substrate and the degree of restraint to be achieved are not provided. Restricting the w/b of the concrete substrate without providing additional details on the mix designs and the degree of restraint, for example, makes the comparison of the susceptibility of various mortar mixes to cracking challenging. Variations in the degree of restraint between the substrate and the mortar mix, for example, would result in a wide variability in results, even in the case of two specimens cast using identical mixes. A less restrictive and more robust approach could entail the use of ring tests, especially when it is necessary to compare the susceptibility of various mortar mixes to crack. The ring test overcomes the problem of restraint; consequently, minimising the variability in test results that could lead to erroneous conclusions.

iv. Non-structural PRMs are meant to maintain the passivity of reinforcing steel so that corrosion does not take place. It is thus important that the transport

properties of the PRM that would provide information regarding its penetrability be specified. The EN 1504-3:2005 only specifies the chloride ion content for class R1 and R2 mortars. It does not specify the carbonation resistance or any other property that could be used to assess the penetrability of the PRM.

v. The EN 1504-3:2005 specifies a requirement for skid resistance even though non-structural PRMs are rarely subjected to such forces. The fact that the code specifies this property implies that it has failed to acknowledge the role of these PRMs in practice.

vi. The fact that the EN 1504-3:2005 relies on the use of visual inspection to assess the thermal compatibility of class one mortars is a matter of concern. The use of visual inspection as a tool for assessment is prone to errors because it tends to suffer from subjectivity among the inspectors. The extent to which an assessment will be made depends on the individual and there is a likelihood that two individuals might arrive at two contrasting conclusions while assessing a single repair.

vii. Corrosion of steel contributes to the cracking failure of PRMs in service. Corrosion of steel in and around patch repairs results from the incipient anode effect that results from differences in electrochemical properties between the PRM and the existing concrete substrate. The specification of material properties such as electrical resistivity could help ensure that the incipient anode effect is minimised. The EN 1504-3:2005 has not specified any performance requirements that would help in assessing differences in electrochemical properties.

Considering the highlighted shortcomings in the EN 1504-3:2005, it is presumed that the widespread failure of non-structural PRMs in service could be partly attributed to the inadequate, and sometime irrelevant, performance requirements that have been specified therein. This code, in its current state, does not fully recognise the primary role of non-structural PRMs in service. It is thus crucial that the performance requirements specified in the existing code of practice be revised and/or modified appropriately with respect to the specification of material properties that directly relate to cracking and the use of reliable tests that are not prone to misinterpretation. Also, there is a need to specify new performance requirements. It can be posited that strict compliance to the performance requirements in the EN 1504-3:2005, in its current state, might not ensure the realisation of effectiveness in performance of PRMs in service - especially with respect to cracking. The results from this study and the reviewed literature have also led to the conclusion that a cement-based non-structural PRM that is efficient in service with respect to resistance to cracking does not exist.

Furthermore, there is a need to transform compatibility from a theoretical concept to a practical concept. Most of the existing compatibility requirements for non-structural PRMs in service, as reported in literature, cannot be achieved in practice. The reviewed compatibility requirements contradict each other and have the potential to restrict innovation and creativity while designing PRMs. Most compatibility requirements ignore the

fact that material properties change with time. Thus, specifying compatibility requirements for a material based on immediate material properties without considering future changes in material properties could jeopardise the realisation of cracking effectiveness. A holistic understanding of compatibility is thus needed.

6.4 The accuracy of the existing deterministic empirical analytical model

The predicted age at cracking in unmodified mortar mixes using the existing deterministic empirical analytical model were higher than the actual age at cracking by a factor that ranged between 1.33 and 2.15. The predicted age at cracking in polymer-modified mixes, using the existing analytical model, were lower than the actual age at cracking by a factor that ranged between 0.75 and 0.98. The degree of restraint that resulted in the best prediction of stresses using the rings in this study was found to be 0.55. The existing empirical analytical model, in its current state, is neither adequate nor accurate in predicting the age at cracking in the PRMs under investigation. It is not sensitive to the effects of the simultaneous reductions in water content and binder content at a constant w/b, the slight change in w/b from 0.72 to 0.80 and an increase in polymer content. From the predicted results, it is evident that the accuracy of the existing model in predicting cracking, especially in the unmodified mixes, was poor.

Two deterministic empirical models have been proposed to predict tensile stresses in unmodified and polymer modified mixes. The general form of the proposed power model is - $\sigma = \mu \times E(t)^a \times (1 - \frac{\varphi\ (t)}{100})^b \times \varepsilon\ (t)^c$. The specific models for predicting the tensile stresses were $\sigma = 0.55 \times E(t)^{2.47} \times (1 - \frac{\varphi\ (t)}{100})^{0.33} \times \varepsilon\ (t)^{2.69}$ for unmodified mixes and $\sigma = 0.55 \times E(t)^{2.33} \times (1 - \frac{\varphi\ (t)}{100})^{7.45} \times \varepsilon\ (t)^{1.25}$ for polymer modified mixes. The proposed model is sensitive enough to account for the relative contribution of crack-determining material properties to restrained shrinkage cracking. However, these models were derived for the specific mixes used in this study and are not universally applicable. They are considered to present an indication on which material parameters are most relevant in relation to cracking performance, rather than to present accurate numerical values. From the proposed empirical analytical model, it was observed that tensile relaxation and shrinkage have a significant contribution to cracking in comparison to the elastic modulus. The extent to which tensile relaxation and shrinkage affect cracking, however, depends on the type of mix - i.e., whether it was modified with polymers or not. Strains due to shrinkage had the greatest contribution to the cracking performance in specimens cast without polymers. However, in polymer-modified mixes, the tensile relaxation had the greatest contribution to its cracking behaviour. The predicted age at cracking in unmodified mixes using the proposed model were lower than the actual age at cracking by a factor that ranged between 0.34 and 1.23. The actual age at cracking in the polymer-modified mixes were higher than the predicted age using the proposed model by a factor that ranged between 1.02 and 1.25.

6.5 Recommendations for further research

Based on the results and limitations of the present study, several recommendations for further research are hereby given:

i. The development of tensile stresses within the polymers ought to be continuously monitored so that a better understanding of the exact cause of cracking can be ascertained. The continuous monitoring of stress development, using instrumented rings, would further help in providing input parameters that could be used to refine the proposed empirical analytical model.

ii. To make the results more relevant in practice, nomographs could be developed to assist in the design of mixes and the prediction of the susceptibility of mixes to cracking. The parameters used to develop these nomographs ought to be kept at a minimum to make it an 'easy-to-use' tool for the material manufacturer, repair engineers and contractors.

iii. There is a need to develop a method that could be used to investigate the microstructure of low volume polymer-modified mortars. The volume of polymers in this study were very low in relation to the total volume of mortar (with the lowest being 2.3% and the highest being 4.5%). The preparation of slides for microscopy without the washing away of the polymers and the ability to detect and accurately investigate the polymers at such a low volume would pose a big challenge.

iv. The performance of the mortars developed in this study ought to be evaluated through field trials.

v. There is a need to develop a stochastic model for predicting tensile stresses and the age at cracking in PRMs. A stochastic model would help predict these two parameters within a reasonable degree of accuracy in comparison to the deterministic model that has been proposed.

References

Abbasnia, R., Godossi, P., and Ahmadi, J. (2005). Prediction of restrained shrinkage based on restraint factors in patching repair mortar. *Cement and Concrete Research*, 35(10):1909–1913.

Abdelkader, S. M., Pozo, E. R., and Terrades, A. M. (2010). Evolution of microstructure and mechanical behavior of concretes utilized in marine environments. *Materials & Design*, 31(7):3412–3418.

Abouhussien, A. A. and Hassan, A. A. A. (2014). Application of Statistical Analysis for Mixture Design of High-Strength Self-Consolidating Concrete Containing Metakaolin. *Journal of Materials in Civil Engineering*, 26(6):04014016.

Achtemichuk, S., Hubbard, J., Sluce, R., and Shehata, M. H. (2009). The utilization of recycled concrete aggregate to produce controlled low-strength materials without using Portland cement. *Cement and Concrete Composites*, 31(8):564–569.

ACI (2003). Chemical admixtures for concrete. Technical report, American Concrete Institute.

ACI209 (2005). Report on factors affecting shrinkage and creep of hardened concrete: Reported by ACI Committee 209. Technical report, American Concrete Institute.

ACI224 (2003). Causes, Evaluation and Repair of Cracks in Concrete Structures. In *Concrete Repair Manual*, volume 1, pages 485–506. American Concrete Institute and Building Research Establishment and The Concrete Society and The International Concrete Repair Institute, Second edition.

ACI503 (1993). Use of epoxy compounds with concrete: Reported by committee 503. Technical report, American Concrete Institute.

ACI546 (2003). Concrete Repair Guide. Technical report, American Concrete Institute.

Acker, P. (1993). Creep tests of concrete: why and how? In Bažant, Z. P. and Carol, I., editors, *Creep and shrinkage of concrete. Proceedings of the fifth international RILEM symposium*, pages 3–14. E&FN SPON, London.

Acker, P. (2004). Swelling, shrinkage and creep: a mechanical approach to cement hydration. *Materials and Structures*, 37(4):237–243.

Acker, P. and Ulm, F.-J. (2001). Creep and shrinkage of concrete: physical origins and practical measurements. *Nuclear Engineering and Design*, 203(2-3):143–158.

Akhavan, A., Shafaatian, S.-M.-H., and Rajabipour, F. (2012). Quantifying the effects of crack width, tortuosity, and roughness on water permeability of cracked mortars. *Cement and Concrete Research*, 42(2):313–320.

Al-Gahtani, A. S. and Khan, M. M. (2003). Drying shrinkage characteristics of plain and blended cements. In *Proceedings of the sixth CANMET/ACI International conference on recent advances in concrete technology*, pages 133–143.

Al-Ostaz, A., Irshidat, M., Tenkhoff, B., and Ponnapalli, P. S. (2010). Deterioration of Bond Integrity between Repair Material and Concrete due to Thermal and Mechanical Incompatibilities. *Journal of Materials in Civil Engineering*, 22(2):136–144.

Alahmad, S., Toumi, A., Verdier, J., and François, R. (2009). Effect of crack opening on carbon dioxide penetration in cracked mortar samples. *Materials and Structures*, 42(5):559–566.

Alexander, M., Ballim, Y., and Mackechnie, J. (2010). *Concrete durability index testing procedure manual Ver 2.0*. University of Cape Town and University of the Witwatersrand.

Alexander, M. and Beushausen, H. (2009). Deformation and volume change of hardened concrete. In Owens, G., editor, *Fulton's Concrete Technology*, chapter 8, pages 111–154. Cement & Concrete Institute, Ninth edition.

Alexander, M. and Mindess, S. (2005). *Aggregates in Concrete*. Taylor & Francis.

Amba, J. C., Balayssac, J. P., and Détriché, C. H. (2010). Characterisation of differential shrinkage of bonded mortar overlays subjected to drying. *Materials and Structures*, 43(1-2):297–308.

Arito, P. A., Beushausen, H., and Alexander, M. G. (2016a). An experimental investigation into the effects of water and binder-related parameters on restrained shrinkage cracking in concrete patch repair mortars. In Grantham, M. G., Papayianni, I., and Sideris, K., editors, *Concrete Solutions: Proceedings of Concrete Solutions, 6th International Conference on Concrete Repair, Thessaloniki, Greece, 20-23 June, 2016*, pages 247–252. Taylor & Francis.

Arito, P. A., Beushausen, H., and Alexander, M. G. (2016b). Barriers to the realisation of effectiveness in the performance of concrete patch repair mortars in service. In Beushausen, H., editor, *Proceedings of the fib SYMPOSIUM*

2016: Performance-Based Approaches for Concrete Structures, Cape Town, South Africa, 21-23 November 2016. fib, Fédération Internationale du béton (fib).

Arito, P. A., Beushausen, H., and Alexander, M. G. (2016c). Towards improved cracking resistance in concrete patch repair mortars. In Dehn, F., Beushausen, H.-D., Alexander, M. G., and Moyo, P., editors, *Concrete Repair, Rehabilitation and Retrofitting IV: Proceedings of the 4th International Conference on Concrete Repair, Rehabilitation and Retrofitting, ICCRRR 2015, Leipzig, Germany, 5-7 October, 2015*, pages 657–662. CRC Press.

ASTM-C136 (2006). Standard test method for Sieve Analysis of Fine and Coarse Aggregates.

ASTM-C143 (2005). Standard test method for Slump of Hydraulic Cement Concrete.

ASTM-C1437 (2015). Standard test method for Flow of Hydraulic Cement Mortar.

ASTM-C1581 (2004). Standard test method for Determining the Age at Cracking and Induced Tensile Stress Characteristics of Mortar and Concrete under Restrained Shrinkage.

ASTM-C192 (2013). Standard Practice for Making and Curing Concrete Test Specimens in the Laboratory.

ASTM-C29 (1997). Standard test method for bulk density ("Unit Weight") and voids in aggregate.

Atrushi, D. S. (2003). *Tensile and Compressive Creep of Early Age Concrete: Testing and Modelling*. PhD thesis, The Norwegian University of Science and Technology.

Ayyar, R. S. and Joshi, S. N. (1986). Effect of Temperature on the Creep Behaviour of Polymer Mortars. In *Adhesion between polymers and concrete / Adhésion entre polymères et béton - bonding, protection, repair. Proceedings of an International symposium organised by RILEM Technical Committee 52 - Resin Adherence to Concrete and Laboratoire Central des Ponts et Chaussées, P*, pages 75–84. Springer.

Bagheri, A. and Hashemi, S. (2006). Investigation of performance and compatibility of cement-based and polymer-modified cement-based repair concrete. In Grantham, M. G., Jaubertie, R. M., and Lanos, C., editors, *Concrete Solutions: Proceedings of the Second International Conference, June 2006, St Malo, France*, pages 610–618. IHS BRE Press.

Baldwin, N. J. R. and King, E. S. (2003). Field studies on the effectiveness of concrete repairs. Phase 1 report: Desk study and literature review. Technical Report 175, Mott MacDonald Ltd.

Baluch, M. H., Rahman, M. K., and Al-Gadhib, A. H. (2002). Risks of Cracking

and Delamination in Patch Repair. *Journal of Materials in Civil Engineering*, 14(4):294–302.

Banthia, N. and Gupta, R. (2009). Plastic shrinkage cracking in cementitious repairs and overlays. *Materials and Structures*, 42(5):567–579.

Banthia, N., Yan, C., and Mindess, S. (1996). Restrained shrinkage cracking in fiber reinforced concrete: A novel test technique. *Cement and Concrete Research*, 26(1):9–14.

Beddoe, R. E. and Lippok, R. (1999). Hygral stress in hardened cement paste. *Materials and Structures*, 32(9):627–634.

Beltzung, F. (2001). Early chemical shrinkage due to dissolution and hydration of cement. *Materials and Structures*, 34(239):279–283.

Bentur, A., ichi Igarashi, S., and Kovler, K. (2001). Prevention of autogenous shrinkage in high-strength concrete by internal curing using wet lightweight aggregates. *Cement and Concrete Research*, 31(11):1587–1591.

Bentur, A. and Kovler, K. (2003). Evaluation of early age cracking characteristics in cementitious systems. *Materials and Structures*, 36(3):183–190.

Bentz, D. (2008). A review of early-age properties of cement-based materials. *Cement and Concrete Research*, 38(2):196–204.

Bentz, D. P. (2009). Influence of internal curing using lightweight aggregates on interfacial transition zone percolation and chloride ingress in mortars. *Cement and Concrete Composites*, 31:285–289.

Bentz, D. P., Peltz, M. A., and Winpigler, J. (2009). Early-Age Properties of Cement-Based Materials. II: Influence of Water-to-Cement Ratio. *Journal of Materials in Civil Engineering*, 21(9):512–517.

Bentz, D. P., Sant, G., and Weiss, J. (2008). Early-Age Properties of Cement-Based Materials. I: Influence of Cement Fineness. *Journal of Materials in Civil Engineering*, 20(7):502–508.

Bernard, O. and Brühwiler, E. (2002). Influence of autogenous shrinkage on early age behaviour of structural elements consisting of concretes of different ages. *Materials and Structures*, 35(9):550–556.

Bester, N. (2015). The influence of curing on restrained shrinkage cracking of bonded overlays. Master's thesis, University of Cape Town.

Beushausen, H. and Alexander, M. (2006). Failure mechanisms and tensile relaxation of bonded concrete overlays subjected to differential shrinkage. *Cement and Concrete Research*, 36(10):1908–1914.

Beushausen, H. and Alexander, M. (2009). Concrete repair. In Owens, G., editor, *Fulton's Concrete Technology*, chapter 27, pages 393–412. Cement & Concrete Institute, Ninth edition.

Beushausen, H. and Alexander, M. G. (2007). Localised strain and stress in bonded

concrete overlays subjected to differential shrinkage. *Materials and Structures*, 40(2):189–199.

Beushausen, H. and Bester, N. (2016). The influence of curing on restrained shrinkage cracking of bonded concrete overlays. *Cement and Concrete Research*, 87:87–96.

Beushausen, H. and Chilwesa, M. (2013). Assessment and prediction of drying shrinkage cracking in bonded mortar overlays. *Cement and Concrete Research*, 53:256–266.

Beushausen, H. and Gillmer, M. (2014). The use of superabsorbent polymers to reduce cracking of bonded mortar overlays. *Cement and Concrete Composites*, 52:1–8.

Beushausen, H., Höhlig, B., and Talotti, M. (2017). The influence of substrate moisture preparation on bond strength of concrete overlays and the microstructure of the OTZ. *Cement and Concrete Research*, 92:84–91.

Beushausen, H., Masuku, C., and Moyo, P. (2012). Relaxation characteristics of cement mortar subjected to tensile strain. *Materials and Structures*, 45(8):1181–1188.

Beushausen, H.-D. (2005). *Long-term performance of bonded concrete overlays subjected to differential shrinkage*. PhD thesis, University of Cape Town.

Bezerra, U. T., Ferreira, R. M., and Castro-Gomes, J. P. (2011). The Effect of Latex and Chitosan Biopolymer on Concrete Properties and Performance. In Aguiar, J. and Czarnecki, L., editors, *Polymers in Concrete*, volume 466, pages 37–46. Trans Tech Publ, Trans Tech Publications.

Bhanja, S. and Sengupta, B. (2005). Influence of silica fume on the tensile strength of concrete. *Cement and Concrete Research*, 35(4):743–747.

Bhutta, M., Imamoto, K., and Ohama, Y. (2008). Air permeability of hardener-free epoxy-modified mortars as repair materials. In Alexander, M. G., Beushausen, H.-D., Dehn, F., and Moyo, P., editors, *Concrete Repair, Rehabilitation and Retrofitting II: 2nd International Conference on Concrete Repair, Rehabilitation and Retrofitting, ICCRRR-2, 24-26 November 2008, Cape Town, South Africa*, pages 329–330. CRC Press.

Bisschop, J. and van Mier, J. G. M. (2002). Effect of aggregates on drying shrinkage microcracking in cement-based composites. *Materials and Structures*, 35(8):453–461.

Bissonnette, B., Marchand, J., Morency, M., Nuta, A., and Vaysburd, A. (2008). Concrete repair and interfacial bond: Influence of surface preparation. In Alexander, M. G., Beushausen, H.-D., Dehn, F., and Moyo, P., editors, *Concrete Repair, Rehabilitation and Retrofitting II: 2nd International Conference on Concrete Repair, Rehabilitation and Retrofitting, ICCRRR-2, 24-26*

November 2008, Cape Town, South Africa, pages 345–346. CRC Press.

Bissonnette, B., Pierre, P., and Pigeon, M. (1999). Influence of key parameters on drying shrinkage of cementitious materials. *Cement and Concrete Research*, 29(10):1655–1662.

Bissonnette, B. and Pigeon, M. (1995). Tensile creep at early ages of ordinary, silica fume and fiber reinforced concretes. *Cement and Concrete Research*, 25(5):1075–1085.

Bode, K. A. and Dimmig-Osburg, A. (2011). Shrinkage Properties of Polymer-Modified Cement Mortars (PCM). In Aguiar, J. and Czarnecki, L., editors, *Polymers in Concrete*, volume 466, pages 29–36. Trans Tech Publ, Trans Tech Publications.

Boshoff, W. P. and van Zijl, G. P. (2007). Time-dependent response of ECC: Characterisation of creep and rate dependence. *Cement and Concrete Research*, 37(5):725–734.

Bouasker, M., Mounanga, P., Turcry, P., Loukili, A., and Khelidj, A. (2008). Chemical shrinkage of cement pastes and mortars at very early age: Effect of limestone filler and granular inclusions. *Cement and Concrete Composites*, 30(1):13–22.

Bouzoubaâ, N. and Fournier, B. (2003). Optimization of fly ash content in concrete. Part I: Non-air-entrained concrete made without superplasticizer. *Cement and Concrete Research*, 33(7):1029–1037.

Boyd, R. H. and Smith, G. D. (2007). *Polymer Dynamics and Relaxation*. Cambridge University Press.

Braga, M., de Brito, J., and Veiga, R. (2014). Reduction of the cement content in mortars made with fine concrete aggregates. *Materials and Structures*, 47(1-2):171–182.

Brandt, A. M. (2009). *Cement-based composites: materials, mechanical properties and performance*. Taylor and Francis, Second edition.

BRE-DME-D53 (2003). Guide to maintenance, repair and monitoring of reinforced concrete structures. In *Concrete Repair Manual*, volume 1, pages 691–804. American Concrete Institute and Building Research Establishment and The Concrete Society and The International Concrete Repair Institute, Second edition.

BRE-DME-D62 (2003). European standards affecting the maintenance and repair or reinforced concrete structures. In *Concrete Repair Manual*, volume 1, pages 807–868. American Concrete Institute and Building Research Establishment and The Concrete Society and The International Concrete Repair Institute, Second edition.

BSI (1983). BS 1881-121:1983: Method for determination of static modulus of elasticity in compression.

BSI (2005). BS EN 1504-3:2005: Products and systems for the protection and repair of concrete structures - definitions, requirements, quality control and evaluation of conformity - Part 3: Structural and non-structural repair.

Byard, B. E., Schindler, A. K., and Barnes, R. W. (2012). Early-Age Cracking Tendency and Ultimate Degree of Hydration of Internally Cured Concrete. *Journal of Materials in Civil Engineering*, 24(8):1025–1033.

Capener, J.-M. (2008). Properties of modern rendering systems based on mineral binders modified by organic admixtures. In Alexander, M. G., Beushausen, H.-D., Dehn, F., and Moyo, P., editors, *Concrete Repair, Rehabilitation and Retrofitting II: 2nd International Conference on Concrete Repair, Rehabilitation and Retrofitting, ICCRRR-2, 24-26 November 2008, Cape Town, South Africa*, pages 319–320. CRC Press.

Cardon, A. and Hiel, C. (1986). Durability analysis of adhesive joints. In *Adhesion between polymers and concrete / Adhésion entre polymères et béton - bonding, protection, repair. Proceedings of an International symposium organised by RILEM Technical Committee 52 - Resin Adherence to Concrete and Laboratoire Central des Ponts et Chaussées, P*, pages 3–7. Springer.

Carlswärd, J. (2006). *Shrinkage cracking of steel fibre reinforced self compacting concrete overlays: test methods and theoretical modelling: test methods and theoretical modelling*. PhD thesis, Luleå tekniska universitet.

Carrasco, M., Menéndez, G., Bonavetti, V., and Irassar, E. (2005). Strength optimization of "tailor-made cement" with limestone filler and blast furnace slag. *Cement and Concrete Research*, 35(7):1324–1331.

Castro, J., Spragg, R., and Weiss, J. (2012). Water Absorption and Electrical Conductivity for Internally Cured Mortars with a W/C between 0.30 and 0.45. *Journal of Materials in Civil Engineering*, 24(2):223–231.

Chen, D.-H., Lin, H.-H., and Sun, R. (2011). Field performance evaluations of partial-depth repairs. *Construction and Building Materials*, 25(3):1369–1378.

Choi, S. J., Lee, S. S., and Monteiro, P. J. M. (2012). Effect of Fly Ash Fineness on Temperature Rise, Setting, and Strength Development of Mortar. *Journal of Materials in Civil Engineering*, 24(5):499–505.

Chorinsky, E. G. (1986). Repair of concrete floors with polymer modified cement mortars. In *Adhesion between polymers and concrete / Adhésion entre polymères et béton - bonding, protection, repair. Proceedings of an International symposium organised by RILEM Technical Committee 52 - Resin Adherence to Concrete and Laboratoire Central des Ponts et Chaussées, P*,

pages 230–234. Springer.

Cleland, D., Naderi, M., and Long, A. (1986). Bond strength of patch repair mortars for concrete. In *Adhesion between polymers and concrete / Adhésion entre polymères et béton - bonding, protection, repair. Proceedings of an International symposium organised by RILEM Technical Committee 52 - Resin Adherence to Concrete and Laboratoire Central des Ponts et Chaussées, P*, pages 235–244. Springer.

Concrete-Society (2003a). Concrete Society Technical Report No. 22 - Non-structural cracks in concrete. In *Concrete Repair Manual*, volume 1, pages 507–551. American Concrete Institute and Building Research Establishment and The Concrete Society and The International Concrete Repair Institute, Second edition.

Concrete-Society (2003b). Concrete Society Technical Report No. 54 - Diagnosis of deterioration in concrete structures - Identifications of defects, evaluation and development of remedial action. In *Concrete Repair Manual*, volume 1, pages 115–182. American Concrete Institute and Building Research Establishment and The Concrete Society and The International Concrete Repair Institute, Second edition.

Corinaldesi, V., Giuggiolini, M., and Moriconi, G. (2002). Use of rubble from building demolition in mortars. *Waste Management*, 22(8):893–899.

Corinaldesi, V., Gnappi, G., Moriconi, G., and Montenero, A. (2005). Reuse of ground waste glass as aggregate for mortars. *Waste Management*, 25(2):197–201.

Corinaldesi, V., Mazzoli, A., and Moriconi, G. (2011). Mechanical behaviour and thermal conductivity of mortars containing waste rubber particles. *Materials & Design*, 32(3):1646–1650.

Corinaldesi, V. and Moriconi, G. (2009). Behaviour of cementitious mortars containing different kinds of recycled aggregate. *Construction and Building Materials*, 23(1):289–294.

Courard, L. (2000). Parametric study for the creation of the interface between concrete and repair products. *Materials and Structures*, 33(1):65–72.

Coussy, O., Dangla, P., Lassabatère, T., and Baroghel-Bouny, V. (2004). The equivalent pore pressure and the swelling and shrinkage of cement-based materials. *Materials and Structures*, 37(1):15–20.

Craeye, B., Geirnaert, M., and Schutter, G. D. (2011). Super absorbing polymers as an internal curing agent for mitigation of early-age cracking of high-performance concrete bridge decks. *Construction and Building Materials*, 25(1):1–13.

Crosswell, S. (2009). Sand-cement - mortars, plasters and screeds. In Owens, G.,

editor, *Fulton's Concrete Technology*, chapter 26, pages 381–392. Cement & Concrete Institute, Ninth edition.

Cusson, D., Mechtcherine, V., and Lura, P. (2011). Practical Applications of Superabsorbent Polymers in Concrete and Other Building Materials. In Mechtcherine, V. and Reinhardt, H.-W., editors, *Application of Super Absorbent Polymers (SAP) in Concrete Construction*, volume 2, chapter 10, pages 137–148. Springer Netherlands.

Czarnecki, L. (2008). Adhesion – A challenge for concrete repair. In Alexander, M. G., Beushausen, H.-D., Dehn, F., and Moyo, P., editors, *Concrete Repair, Rehabilitation and Retrofitting II: 2nd International Conference on Concrete Repair, Rehabilitation and Retrofitting, ICCRRR-2, 24-26 November 2008, Cape Town, South Africa*, pages 343–344. CRC Press.

DANSK-Standard (2004). *Repair of Concrete Structures to EN 1504*. Elsevier.

Darquennes, A., Khokhar, M., Rozière, E., Loukili, A., Grondin, F., and Staquet, S. (2011a). Early age deformations of concrete with high content of mineral additions. *Construction and Building Materials*, 25(4):1836–1847.

Darquennes, A., Staquet, S., and Espion, B. (2011b). Behaviour of slag cement concrete under restraint conditions. *European Journal of Environmental and Civil Engineering*, 15(5):787–798.

Davies, H. (2003). British standards for repair and protection of concrete. In *Concrete Repair Manual*, volume 1, pages 63–72. American Concrete Institute and Building Research Establishment and The Concrete Society and The International Concrete Repair Institute, Second edition.

Davies, H. and Robery, P. (2006). European standards for repair and protection of concrete. In Grantham, M. G., Jaubertie, R. M., and Lanos, C., editors, *Concrete Solutions: Proceedings of the Second International Conference, June 2006, St Malo, France*, pages 40–51. IHS BRE Press.

Dawood, E. T. and Ramli, M. (2011). High strength characteristics of cement mortar reinforced with hybrid fibres. *Construction and Building Materials*, 25(5):2240–2247.

de Sensale, G. R. and Goncalves, A. F. (2014). Effects of fine LWA and SAP as internal water curing agents. *International Journal of Concrete Structures and Materials*, 8(3):229–238.

Denarié, E., Silfwerbrand, J., and Beushausen, H. (2011). Structural Behaviour. In Bissonnette, B., Courard, L., Fowler, D. W., and Granju, J.-L., editors, *Bonded Cement-Based Material Overlays for the Repair, the Lining or the Strengthening of Slabs or Pavements*, volume 3, chapter 5, pages 81–106. Springer Netherlands.

Diamond, S. (2004). The microstructure of cement paste and concrete—a visual primer. *Cement and Concrete Composites*, 26(8):919–933.

Dittmer, T. and Beushausen, H. (2014). The effect of coarse aggregate content and size on the age at cracking of bonded concrete overlays subjected to restrained deformation. *Construction and Building Materials*, 69:73–82.

Dittmer, T. J. (2013). The effect of aggregate on the age at cracking of bonded concrete overlays subjected to restrained deformation. Master's thesis, University of Cape Town.

Elsharief, A., Cohen, M. D., and Olek, J. (2003). Influence of aggregate size, water cement ratio and age on the microstructure of the interfacial transition zone. *Cement and Concrete Research*, 33(11):1837–1849.

Elsharief, A., Cohen, M. D., and Olek, J. (2005). Influence of lightweight aggregate on the microstructure and durability of mortar. *Cement and Concrete Research*, 35(7):1368–1376.

Etxeberria, M., Vázquez, E., Marí, A., and Barra, M. (2007). Influence of amount of recycled coarse aggregates and production process on properties of recycled aggregate concrete. *Cement and Concrete Research*, 37(5):735–742.

Filho, R. and Sanjuán, M. (1999). Effect of low modulus sisal and polypropylene fibre on the free and restrained shrinkage of mortars at early age. *Cement and Concrete Research*, 29(10):1597–1604.

Filho, R. D. T., Ghavami, K., Sanjuán, M. A., and England, G. L. (2005). Free, restrained and drying shrinkage of cement mortar composites reinforced with vegetable fibres. *Cement and Concrete Composites*, 27(5):537–546.

Filho, R. D. T., Silva, E. F., Lopes, A. N. M., Mechtcherine, V., and Dudziak, L. (2011). Effect of Superabsorbent Polymers on the Workability of Concrete and Mortar. In Mechtcherine, V. and Reinhardt, H.-W., editors, *Application of Super Absorbent Polymers (SAP) in Concrete Construction*, pages 39–50. Springer Netherlands.

Fowler, D. W. (2011). Maintenance and Repair of Overlays. In Bissonnette, B., Courard, L., Fowler, D. W., and Granju, J.-L., editors, *Bonded Cement-Based Material Overlays for the Repair, the Lining or the Strengthening of Slabs or Pavements*, volume 3, chapter 9, pages 171–174. Springer Netherlands.

Fowler, D. W. and Treviño, M. (2011). Overlay Design Process. In Bissonnette, B., Courard, L., Fowler, D. W., and Granju, J.-L., editors, *Bonded Cement-Based Material Overlays for the Repair, the Lining or the Strengthening of Slabs or Pavements*, volume 3, chapter 2, pages 5–16. Springer Netherlands.

Friedrich, S. (2011). Superabsorbent Polymers (SAP). In Mechtcherine, V. and Reinhardt, H.-W., editors, *Application of Super Absorbent Polymers (SAP)*

in Concrete Construction, pages 13–19. Springer Netherlands.

Gagné, R., Aouad, I., Shen, J., and Poulin, C. (1999). Development of a new experimental technique for the study of the autogenous shrinkage of cement paste. *Materials and Structures*, 32(9):635–642.

Gallias, J., Kara-Ali, R., and Bigas, J. (2000). The effect of fine mineral admixtures on water requirement of cement pastes. *Cement and concrete research*, 30(10):1543–1549.

Gao, J., Qian, C., Wang, B., and Morino, K. (2002). Experimental study on properties of polymer-modified cement mortars with silica fume. *Cement and Concrete Research*, 32(1):41–45.

Gérard, B. and Marchand, J. (2000). Influence of cracking on the diffusion properties of cement-based materials: Part I: Influence of continuous cracks on the steady-state regime. *Cement and Concrete research*, 30(1):37–43.

Ghezal, A. F. and Assaf, G. J. (2014). Restrained Shrinkage Cracking of Self-Consolidating Concrete. *Journal of Materials in Civil Engineering*, 27(10):04014266.

Gilbert, R. (1988). *Time Effects in Concrete Structures (Developments in Civil Engineering)*, volume 23. Elsevier Science Ltd.

Gillmer, M. (2012). Investigating repair mortars containing superabsorbent polymers as a method of internal curing to improve concrete patch repair performance. Master's thesis, University of Cape Town.

Gopinath, R. (2010). Effect of shrinkage reducing admixtures on the properties of cement mortar. Master's thesis, Indian Institute of Technology Madras.

Granju, J.-L. (2001). Debonding of Thin Cement-Based Overlays. *Journal of Materials in Civil Engineering*, 13(2):114–120.

Grieve, G. (2009). Aggregates for concrete. In Owens, G., editor, *Fulton's Concrete Technology*, chapter 3, pages 25–61. Cement & Concrete Institute, Ninth edition.

Grondin, F., Mounanga, P., Rozičre, E., Loukili, A., Farah, M., Regoin, J.-P., and Pertué, A. (2012). Improving the characterization of early age cracking of concrete: Engineering issues and scientific answers. In *CONCRACK 3 - RILEM-JCI International workshop on crack control of mass concrete and related issues concerning early-age concrete structures.*, pages 89–98.

Gutsch, A. W. (2002). Properties of early age concrete-Experiments and modelling. *Materials and Structures*, 35(2):76–79.

Hammer, T. A. (2001). Effect of silica fume on the plastic shrinkage and pore water pressure of high-strength concretes. *Materials and Structures*, 34(5):273–278.

Hannawi, K., Prince, W., and Bernard, S. K. (2013). Strain Capacity and Cracking Resistance Improvement in Mortars by Adding Plastic Particles. *Journal of*

Materials in Civil Engineering, 25(11):1602–1610.

Hayakawa, K. and Soshiroda, T. (1986). Effects of cellulose ether on bond between matrix and aggregate in concrete. In *Adhesion between polymers and concrete / Adhésion entre polymères et béton - bonding, protection, repair. Proceedings of an International symposium organised by RILEM Technical Committee 52 - Resin Adherence to Concrete and Laboratoire Central des Ponts et Chaussées, P*, pages 22–31. Springer.

He, Z. and Li, Z. (2005). Influence of alkali on restrained shrinkage behavior of cement-based materials. *Cement and Concrete Research*, 35(3):457–463.

Henkensiefken, R., Castro, J., Bentz, D., Nantung, T., and Weiss, J. (2009). Water absorption in internally cured mortar made with water-filled lightweight aggregate. *Cement and Concrete Research*, 39(10):883–892.

Ho, A., Turatsinze, A., and Vu, D. (2008). On the potential of rubber aggregates obtained by grinding end-of-life tyres to improve the strain capacity of concrete. In Alexander, M. G., Beushausen, H.-D., Dehn, F., and Moyo, P., editors, *Concrete Repair, Rehabilitation and Retrofitting II: 2nd International Conference on Concrete Repair, Rehabilitation and Retrofitting, ICCRRR-2, 24-26 November 2008, Cape Town, South Africa*, pages 95–96. CRC Press.

Hossain, A. B. and Weiss, J. (2006). The role of specimen geometry and boundary conditions on stress development and cracking in the restrained ring test. *Cement and Concrete Research*, 36(1):189–199.

Hotta, H. and Takiguchi, K. (1995). Influence of drying and water supplying after drying on tensile strength of cement mortar. *Nuclear Engineering and Design*, 156(1-2):219–228.

Hua, C., Acker, P., and Ehrlacher, A. (1995). Analyses and models of the autogenous shrinkage of hardening cement paste: I. Modelling at macroscopic scale. *Cement and Concrete Research*, 25(7):1457–1468.

Huang, W.-H. (2001). Improving the properties of cement–fly ash grout using fiber and superplasticizer. *Cement and Concrete Research*, 31(7):1033–1041.

Hubert, F. X., Burlion, N., and Shao, J. F. (2003). Drying of concrete: modelling of a hydric damage. *Materials and Structures*, 36(1):12–21.

ICRI (2003). Technical guidelines: Guide for selecting and specifying materials for repair of concrete surfaces. Guideline No. 03733. In *Concrete Repair Manual*, volume 1, pages 835–868. American Concrete Institute and Building Research Establishment and The Concrete Society and The International Concrete Repair Institute, Second edition.

Igarashi, S.-I., Bentur, A., and Kovler, K. (2000a). Autogenous shrinkage and induced restraining stresses in high-strength concretes. *Cement and Concrete Research*, 30(11):1701–1707.

Igarashi, S.-I. and Kawamura, M. (2002). Effects of microstructure on restrained autogenous shrinkage behavior in high strength concretes at early ages. *Materials and Structures*, 35(2):80–84.

Igarashi, S.-I., Kubo, H. R., and Kawamura, M. (2000b). Long-term volume changes and microcracks formation in high strength mortars. *Cement and Concrete Research*, 30(6):943–951.

Jacobs, J. (2006). Current industry practice, research and repair. In Grantham, M. G., Jaubertie, R. M., and Lanos, C., editors, *Concrete Solutions: Proceedings of the Second International Conference, June 2006, St Malo, France*, pages 16–24. IHS BRE Press.

Jaufeerally, H. (2001). Performance and properties of structural concrete made with corex slag. Master's thesis, University of Cape Town.

Jennings, H. M. (2004). Colloid model of C-S-H and implications to the problem of creep and shrinkage. *Materials and Structures*, 37(1):59–70.

Jensen, O. M. and Hansen, P. F. (2001a). Autogenous deformation and RH-change in perspective. *Cement and Concrete Research*, 31(12):1859–1865.

Jensen, O. M. and Hansen, P. F. (2001b). Water-entrained cement-based materials: I. Principles and theoretical background. *Cement and Concrete Research*, 31(4):647–654.

Jensen, O. M. and Hansen, P. F. (2002). Water-entrained cement-based materials: II. Experimental observations. *Cement and Concrete Research*, 32(6):973–978.

Jingang, W., Shuxiang, Z., Haiqin, Y., Xiangzheng, K., Xikui, W., and Zhongmao, G. (2005). Study of cement mortars modified by emulsifier-free latexes. *Cement and Concrete Composites*, 27(9-10):920–925.

Judge, A., Cheriton, L., and Lambe, R. (1986). Bonding Systems for Concrete Repair - An Assessment of Commonly Used Materials. In *Adhesion between polymers and concrete / Adhésion entre polymères et béton - bonding, protection, repair. Proceedings of an International symposium organised by RILEM Technical Committee 52 - Resin Adherence to Concrete and Laboratoire Central des Ponts et Chaussées, P*, pages 661–681. Springer.

Juenger, M. C. G. and Jennings, H. M. (2002). Examining the relationship between the microstructure of calcium silicate hydrate and drying shrinkage of cement pastes. *Cement and Concrete Research*, 32(2):289–296.

Kanna, V., Olson, R., and Jennings, H. (1998). Effect of shrinkage and moisture content on the physical characteristics of blended cement mortars. *Cement and Concrete Research*, 28(10):1467–1477.

Kardon, J. B. (1997). Polymer-Modified Concrete: Review. *Journal of Materials in Civil Engineering*, 9(2):85–92.

Kellerman, J. and Crosswell, S. (2009). Properties of fresh concrete. In Owens, G., editor, *Fulton's Concrete Technology*, chapter 6, pages 83–95. Cement & Concrete Institute, Ninth edition.

Khan, M., Lynsdale, C., and Waldron, P. (2000). Porosity and strength of PFA/S-F/OPC ternary blended paste. *Cement and Concrete Research*, 30(8):1225–1229.

Kim, B. and Weiss, W. (2003). Using acoustic emission to quantify damage in restrained fiber-reinforced cement mortars. *Cement and Concrete Research*, 33(2):207–214.

Knapen, E. and Gemert, D. V. (2011). Microstructural Analysis of Paste and Interfacial Transition Zone in Cement Mortars Modified with Water-Soluble Polymers. In Aguiar, J. and Czarnecki, L., editors, *Polymers in Concrete*, volume 466, pages 21–28. Trans Tech Publ, Trans Tech Publications.

Kovler, K. (2011). Effect of Superabsorbent Polymers on the Mechanical Properties of Concrete. In Mechtcherine, V. and Reinhardt, H.-W., editors, *Application of Super Absorbent Polymers (SAP) in Concrete Construction*, pages 99–114. Springer Netherlands.

Kovler, K., Igarashi, S., and Bentur, A. (1999a). Tensile creep behavior of high strength concretes at early ages. *Matérials and structures*, 32(5):383–387.

Kovler, K. and Jensen, O. M. (2005). Novel techniques for concrete curing: new methods for low w/cm mixtures. *Concrete International*, pages 39–42.

Kovler, K., Schamban, I., Igarashi, S., and Bentur, A. (1999b). Influence of mix proportions and curing conditions on tensile splitting strength of high strength concretes. *Materials and Structures*, 32(7):500–505.

Kronlöf, A., Leivo, M., and Sipari, P. (1995). Experimental study on the basic phenomena of shrinkage and cracking of fresh mortar. *Cement and Concrete Research*, 25(8):1747–1754.

Lam, L., Wong, Y., and Poon, C. (1998). Effect of Fly Ash and Silica Fume on Compressive and Fracture Behaviors of Concrete. *Cement and Concrete Research*, 28(2):271–283.

Lambe, R. (1988). Repair materials for damaged reinforced concrete - Development and application. In *Symposium on Concrete Failure - Cause and Cure*, number 13, page 20. Concrete Society of Southern Africa.

Langan, B., Weng, K., and Ward, M. (2002). Effect of silica fume and fly ash on heat of hydration of Portland cement. *Cement and Concrete Research*, 32(7):1045–1051.

Lawrence, P., Cyr, M., and Ringot, E. (2003). Mineral admixtures in mortars: Effect of inert materials on short-term hydration. *Cement and Concrete Research*, 33(12):1939–1947.

Li, G., Stubblefield, M. A., Garrick, G., Eggers, J., Abadie, C., and Huang, B. (2004). Development of waste tire modified concrete. *Cement and Concrete Research*, 34(12):2283–2289.

Li, Y., qian Yan, Q., and Du, X. (2012). Relationship between Autogenous Shrinkage and Tensile Strength of Cement Paste with SCM. *Journal of Materials in Civil Engineering*, 24(10):1268–1273.

Lin, Y.-H., Tyan, Y.-Y., Chang, T.-P., and Chang, C.-Y. (2004). An assessment of optimal mixture for concrete made with recycled concrete aggregates. *Cement and Concrete Research*, 34(8):1373–1380.

Loukili, A., Chopin, D., Khelidj, A., and Touzo, J.-Y. L. (2000). A new approach to determine autogenous shrinkage of mortar at an early age considering temperature history. *Cement and Concrete Research*, 30(6):915–922.

Luković, M. (2016). *Influence of interface and strain hardening cementitious composite (SHCC) properties on the performance of concrete repairs*. PhD thesis, Delft University of Technology.

Luo, R., Cai, Y., Wang, C., and Huang, X. (2003). Study of chloride binding and diffusion in GGBS concrete. *Cement and Concrete Research*, 33(1):1–7.

Lura, P., Friedemann, K., Stallmach, F., Mönnig, S., Wyrzykowski, M., and Esteves, L. P. (2011). Kinetics of Water Migration in Cement-Based Systems Containing Superabsobent Polymers. In Mechtcherine, V. and Reinhardt, H.-W., editors, *Application of Super Absorbent Polymers (SAP) in Concrete Construction*, pages 21–37. Springer Netherlands.

Ma, Y., Tan, M., and Wu, K. (2002). Effect of different geometric polypropylene fibers on plastic shrinkage cracking of cement mortars. *Materials and Structures*, 35(247):165–169.

Ma, Y., Zhu, B., Tan, M., and Wu, K. (2004). Effect of Y type polypropylene fiber on plastic shrinkage cracking of cement mortar. *Materials and Structures*, 37(2):92–95.

Maage, M. (2003). European standards for protection and repair of concrete structures. In *Proceedings of the sixth CANMET/ACI International conference on recent advances in concrete technology*, pages 43–62.

Mallat, A. and Alliche, A. (2006). Mechanical behaviour and bond characterization of fibre-reinforced repair mortars. In Grantham, M. G., Jaubertie, R. M., and Lanos, C., editors, *Concrete Solutions: Proceedings of the Second International Conference, June 2006, St Malo, France*, pages 568–580. IHS BRE Press.

Mallows, F. A. (1985). The influence of various South African aggregates on the creep of concrete. Master's thesis, University of Cape Town.

Mangat, P. and Limbachiya, M. (1997). Repair material properties for effective structural application. *Cement and Concrete Research*, 27(4):601–617.

Mangat, P. and O'Flaherty, F. (2000). Influence of elastic modulus on stress redistribution and cracking in repair patches. *Cement and Concrete Research*, 30(1):125–136.

Marais, A. (2009). Chemical admixtures. In Owens, G., editor, *Fulton's Concrete Technology*, chapter 5, pages 71–81. Cement & Concrete Institute, Ninth edition.

Marchand, J., Hornain, H., Diamond, S., Pigeon, M., and Guiraud, H. (1996). The microstructure of dry concrete products. *Cement and Concrete Research*, 26(3):427–438.

Maruyama, I. and Sasano, H. (2013). Strain and crack distribution in concrete during drying. *Materials and Structures*, 47(3):517–532.

Masuku, C. (2009). Tensile relaxation of bonded concrete overlays. Master's thesis, University of Cape Town.

Masuku, C., Beushausen, H.-D., and Moyo, P. (2008). Proposal of an experimental programme for determining tensile relaxation in bonded concrete overlays. In Alexander, M. G., Beushausen, H.-D., Dehn, F., and Moyo, P., editors, *Concrete Repair, Rehabilitation and Retrofitting II: 2nd International Conference on Concrete Repair, Rehabilitation and Retrofitting, ICCRRR-2, 24-26 November 2008, Cape Town, South Africa*, pages 369–370. CRC Press, CRC Press.

Matthews, S. (2007). CONREPNET: Performance-based approach to the remediation of reinforced concrete structures: Achieving durable repaired concrete structures. *Journal of Building Appraisal*, 3(1):6–20.

Matthews, S. and Morlidge, J. (2006a). Vision for the use of performance concepts to achieve durable remediation of concrete structures. In Grantham, M. G., Jaubertie, R. M., and Lanos, C., editors, *Concrete Solutions: Proceedings of the Second International Conference, June 2006, St Malo, France*, pages 52–60. IHS BRE Press.

Matthews, S. and Morlidge, J. (2006b). Whats wrong: concrete repair – solution or problem? In Grantham, M. G., Jaubertie, R. M., and Lanos, C., editors, *Concrete Solutions: Proceedings of the Second International Conference, June 2006, St Malo, France*, pages 3–10. IHS BRE Press.

Matthews, S. and Morlidge, J. (2008). Performance based rehabilitation of reinforced concrete structures. In Alexander, M. G., Beushausen, H.-D., Dehn, F., and Moyo, P., editors, *Concrete Repair, Rehabilitation and Retrofitting II: 2nd International Conference on Concrete Repair, Rehabilitation and Retrofitting, ICCRRR-2, 24-26 November 2008, Cape Town, South Africa*,

pages 277–278. CRC Press, CRC Press.

Mauroux, T., Benboudjema, F., Turcry, P., Aït-Mokhtar, A., and Deves, O. (2012). Study of cracking due to drying in coating mortars by digital image correlation. *Cement and Concrete Research*, 42(7):1014–1023.

MDoT (1996). Evaluating pavement patching materials: polymers and elastomeric concretes. *Materials and Technology Research Record*, (81):4.

Mechtcherine, V. (2011). Introduction. In Mechtcherine, V. and Reinhardt, H.-W., editors, *Application of Super Absorbent Polymers (SAP) in Concrete Construction*, pages 1–6. Springer Netherlands.

Mechtcherine, V. and Dudziak, L. (2011). Effects of Superabsorbent Polymers on Shrinkage of Concrete: Plastic, Autogenous, Drying. In Mechtcherine, V. and Reinhardt, H.-W., editors, *Application of Super Absorbent Polymers (SAP) in Concrete Construction*, pages 63–98. Springer Netherlands.

Mechtcherine, V., Gorges, M., Schroefl, C., Assmann, A., Brameshuber, W., Ribeiro, A. B., Cusson, D., Custódio, J., da Silva, E. F., Ichimiya, K., ichi Igarashi, S., Klemm, A., Kovler, K., de Mendonça Lopes, A. N., Lura, P., Nguyen, V. T., Reinhardt, H.-W., Filho, R. D. T., Weiss, J., Wyrzykowski, M., Ye, G., and Zhutovsky, S. (2013). Effect of internal curing by using superabsorbent polymers (SAP) on autogenous shrinkage and other properties of a high-performance fine-grained concrete: results of a RILEM round-robin test. *Materials and Structures*, 47(3):541–562.

Mehta, P. K. and Monteiro, P. J. (2006). *Concrete: Microstructure, Properties, and Materials*. McGraw-Hill, Third edition.

Merchant, I., Macphee, D., Chandler, H., and Henderson, R. (2001). Toughening cement-based materials through the control of interfacial bonding. *Cement and Concrete Research*, 31(12):1873–1880.

Miller, M. (2005). *Polymers in Cementitious Materials*. Rapra Technology Limited.

Montgomery, D. C. (2001). *Design and Analysis of Experiments*. John Wiley & Sons Inc, Fifth edition.

Montgomery, D. C. and Runger, G. C. (2003). *Applied Statistics and Probability for Engineers*. John Wiley & Sons Inc, Third edition.

Morgan, D. (1996). Compatibility of concrete repair materials and systems. *Construction and Building Materials*, 10(1):57–67.

Naderi, M., Cleland, D., and Long, A. E. (1986). Insitu Test Methods for Repaired Concrete Structures. In Sasse, H., editor, *Adhesion between polymers and concrete / Adhésion entre polymères et béton - bonding, protection, repair. Proceedings of an International symposium organised by RILEM Technical Committee 52 - Resin Adherence to Concrete and Laboratoire Central des*

Ponts et Chaussées, P, pages 707–718. Springer US.

Nagaraj, T., Shashiprakash, S., and Kameswara, R. B. (1990). Generalized Abram's law. In Wierig, H.-J., editor, *Properties of Fresh Concrete: Proceedings of the RILEM Colloquium*. Chapman and Hall.

Nehdi, M. and Sumner, J. (2002). Optimization of ternary cementitious mortar blends using factorial experimental plans. *Materials and Structures*, 35:495–503.

Nepomuceno, M., Oliveira, L., and Lopes, S. (2012). Methodology for mix design of the mortar phase of self-compacting concrete using different mineral additions in binary blends of powders. *Construction and Building Materials*, 26(1):317–326.

Neto, A. A. M., Cincotto, M. A., and Repette, W. (2008). Drying and autogenous shrinkage of pastes and mortars with activated slag cement. *Cement and Concrete Research*, 38(4):565–574.

Neubauer, C., Jennings, H., and Garboczi, E. (1996). A three-phase model of the elastic and shrinkage properties of mortar. *Advanced Cement Based Materials*, 4(1):6–20.

Neville, A. (1995). *Properties of Concrete*. Pearson Prentice Hall, Fourth edition.

Ngassam, I. L. T., Arito, P., and Beushausen, H. (2016). Rethinking the formulation of (patch) repair mortars. In Schmidt, W. and Msinjili, N. S., editors, *Proceedings of the International Conference on Advances in Cement and Concrete Technology in Africa*, pages 517–524. BAM Federal Institute for Materials Research and Testing.

Nguyen, T.-H., Toumi, A., and Turatsinze, A. (2010). Mechanical properties of steel fibre reinforced and rubberised cement-based mortars. *Materials & Design*, 31(1):641–647.

Nguyen, T.-H., Toumi, A., Turatsinze, A., and Tazi, F. (2012). Restrained shrinkage cracking in steel fibre reinforced and rubberised cement-based mortars. *Materials and Structures*, 45(6):899–904.

Nilsen, A. U., Monteiro, P. J., and Gjørv, O. E. (1995). Estimation of the elastic moduli of lightweight aggregate. *Cement and Concrete Research*, 25(2):276–280.

Nossoni, G. and Harichandran, R. S. (2010). Improved Repair of Concrete Structures Using Polymer Concrete Patch and FRP Overlay. *Journal of Materials in Civil Engineering*, 22(4):314–322.

Ohama, Y. (1995). *Handbook of Polymer-Modified Concrete and Mortars: Properties and Process Technology*. Noyes Publications.

Ohama, Y. (1996). Polymer-based materials for repair and improved durability: Japanese experience. *Construction and Building Materials*, 10(1):77–82.

Ohama, Y. (1997). Recent progress in concrete-polymer composites. *Advanced Cement Based Materials*, 5(2):31–40.

Ohama, Y. (1998). Polymer-based admixtures. *Cement and Concrete Composites*, 20(2-3):189–212.

Ohama, Y. (2011). Concrete-Polymer Composites – The Past, Present and Future. In Aguiar, J. and Czarnecki, L., editors, *Polymers in Concrete*, volume 466, pages 1–14. Trans Tech Publ, Trans Tech Publications.

Ohama, Y., Demura, K., Nagao, H., and Ogi, T. (1986). Adhesion of polymer-modified mortars to ordinary cement mortar by different test methods. In *Adhesion between polymers and concrete / Adhésion entre polymères et béton - bonding, protection, repair. Proceedings of an International symposium organised by RILEM Technical Committee 52 - Resin Adherence to Concrete and Laboratoire Central des Ponts et Chaussées, P*, pages 719–729. Springer.

Ortega, J., Sánchez, I., and Climent, M. (2012). Service properties and microstructure of mortars with different contents of slag and fly ash exposed to different hardening environments. In *Second International Conference on Microstructural-related Durability of Cementitious Composites, 11-13 April 2012, Amsterdam.*

Østergaard, L., Lange, D. A., Altoubat, S. A., and Stang, H. (2001). Tensile basic creep of early-age concrete under constant load. *Cement and Concrete Research*, 31(12):1895–1899.

Otsuki, N. and Ryu, J.-S. (2001). Use of Electrodeposition for Repair of Concrete with Shrinkage Cracks. *Journal of Materials in Civil Engineering*, 13(2):136–142.

Pane, I. and Hansen, W. (2002). Early age creep and stress relaxation of concrete containing blended cements. *Materials and Structures*, 35(246):92–96.

Pane, I. and Hansen, W. (2008a). Investigation on key properties controlling early-age stress development of blended cement concrete. *Cement and Concrete Research*, 38(11):1325–1335.

Pane, I. and Hansen, W. (2008b). Predictions and verifications of early-age stress development in hydrating blended cement concrete. *Cement and Concrete Research*, 38(11):1315–1324.

Park, D., Ahn, J., Oh, S., Song, H., and Noguchi, T. (2009). Drying effect of polymer-modified cement for patch-repaired mortar on constraint stress. *Construction and Building Materials*, 23(1):434–447.

Peier, W. (1986). Adhesion testing of polymer modified cement mortars. In *Adhesion between polymers and concrete / Adhésion entre polymères et béton - bonding, protection, repair. Proceedings of an International symposium organised by RILEM Technical Committee 52 - Resin Adherence to Concrete*

and Laboratoire Central des Ponts et Chaussées, P, pages 730–740. Springer.

Perez, F., Bissonnette, B., Courard, L., and Morency, M. (2008). Correlation between the roughness of the substrate surface and the debonding risk. In Alexander, M. G., Beushausen, H.-D., Dehn, F., and Moyo, P., editors, *Concrete Repair, Rehabilitation and Retrofitting II: 2nd International Conference on Concrete Repair, Rehabilitation and Retrofitting, ICCRRR-2, 24-26 November 2008, Cape Town, South Africa*, pages 347–348. CRC Press, CRC Press.

Perrie, B. (1994). The testing of curing compounds for concrete. Master's thesis, University of the Witwatersrand.

Perrie, B. (2009). Strength of hardened concrete. In Owens, G., editor, *Fulton's Concrete Technology*, chapter 7, pages 97–110. Cement & Concrete Institute, Ninth edition.

Pistolesi, C., Maltese, C., and Bovassi, M. (2008). Low shrinking self-compacting concretes for concrete repair. In Alexander, M. G., Beushausen, H.-D., Dehn, F., and Moyo, P., editors, *Concrete Repair, Rehabilitation and Retrofitting II: 2nd International Conference on Concrete Repair, Rehabilitation and Retrofitting, ICCRRR-2, 24-26 November 2008, Cape Town, South Africa*, pages 321–322. CRC Press, CRC Press.

Popovics, S. and Ujhelyi, J. (2008). Contribution to the Concrete Strength versus Water-Cement Ratio Relationship. *Journal of Materials in Civil Engineering*, 20(7):459–463.

Poppe, A.-M. and Schutter, G. D. (2005). Cement hydration in the presence of high filler contents. *Cement and Concrete Research*, 35(12):2290–2299.

Radlińska, A. and Weiss, J. (2012). Toward the Development of a Performance-Related Specification for Concrete Shrinkage. *Journal of Materials in Civil Engineering*, 24(1):64–71.

Ramesh, G., Sotelino, E., and Chen, W. (1998). Effect of transition zone on elastic stresses in concrete materials. *Journal of Materials in Civil Engineering*, 10(4):275–282.

Ramli, M. and Tabassi, A. A. (2012a). Effects of Different Curing Regimes on Engineering Properties of Polymer-Modified Mortar. *Journal of Materials in Civil Engineering*, 24(4):468–478.

Ramli, M. and Tabassi, A. A. (2012b). Influences of Polymer Modification and Exposure Conditions on Chloride Permeability of Cement Mortars and Composites. *Journal of Materials in Civil Engineering*, 24(2):216–222.

Ranaivomanana, N., Multon, S., and Turatsinze, A. (2013). Basic creep of concrete under compression, tension and bending. *Construction and Building Materials*, 38:173–180.

Rao, G. A. (2001a). Long-term drying shrinkage of mortar - influence of silica fume and size of fine aggregate. *Cement and Concrete Research*, 31(2):171–175.

Rao, G. A. (2001b). Role of water-binder ratio on the strength development in mortars incorporated with silica fume. *Cement and Concrete Research*, 31(3):443–447.

Rao, G. A. (2003). Investigations on the performance of silica fume-incorporated cement pastes and mortars. *Cement and Concrete Research*, 33(11):1765–1770.

Rao, G. A. and Prasad, B. K. R. (2004). Influence of type of aggregate and surface roughness on the interface fracture properties. *Materials and Structures*, 37(5):328–334.

Rao, G. A. and Prasad, B. R. (2002). Influence of the roughness of aggregate surface on the interface bond strength. *Cement and Concrete Research*, 32:253–257.

Raupach, M. (2008). Research in the field of repair - Actual approaches and future needs. In Alexander, M. G., Beushausen, H.-D., Dehn, F., and Moyo, P., editors, *Concrete Repair, Rehabilitation and Retrofitting II: 2nd International Conference on Concrete Repair, Rehabilitation and Retrofitting, ICCRRR-2, 24-26 November 2008, Cape Town, South Africa*, pages 61–62. CRC Press, CRC Press.

Raupach, M. and Büttner, T. (2014). *Concrete Repair to EN 1504*. CRC Press.

Reinhardt, H.-W. and Assmann, A. (2011). Effect of Superabsorbent Polymers on Durability of Concrete. In Mechtcherine, V. and Reinhardt, H.-W., editors, *Application of Super Absorbent Polymers (SAP) in Concrete Construction*, pages 115–135. Springer Netherlands.

Reinhardt, H.-W., Cusson, D., and Mechtcherine, V. (2011). Terminology. In Mechtcherine, V. and Reinhardt, H.-W., editors, *Application of Super Absorbent Polymers (SAP) in Concrete Construction*, pages 7–12. Springer Netherlands.

Reis, J. M. L. and Jurumenha, M. A. G. (2013). Investigation on the effects of polymer impregnated aggregate on polymer mortars properties. *Materials and Structures*, 46(8):1383–1388.

Ribeiro, A. B., Medina, V., Gomes, A., and Gonçalves, A. (2011). Chemical Shrinkage of Pastes Made with Shrinkage Reducing Admixtures. In Aguiar, J. and Czarnecki, L., editors, *Polymers in Concrete*, volume 466, pages 105–113. Trans Tech Publ, Trans Tech Publications.

Rixom, R. and Mailvaganam, N. (1999). *Chemical Admixtures for Concrete*. E & FN Spon Ltd, Third edition.

Rossi, P., Tailhan, J.-L., and Maou, F. L. (2013). Comparison of concrete creep in

tension and in compression: Influence of concrete age at loading and drying conditions. *Cement and Concrete Research*, 51:78–84.

Rüsch, H., Jungwirth, D., and Hilsdorf, H. K. (1983). *Creep and Shrinkage: Their Effect on the Behavior of Concrete Structures*. Springer-Verlag Berlin and Heidelberg GmbH & Co. K.

Ryan, T. P. (2007). *Modern Experimental Design*. John Wiley & Sons INC.

SABS (2006a). SANS 5863: Concrete Tests - compressive strength of hardened concrete. SABS Standards Division.

SABS (2006b). SANS 6085: Concrete tests - Initial drying shrinkage and wetting expansion of concrete. SABS Standards Division.

Sahamitmongkol, R. and Kishi, T. (2011). Tensile behavior of restrained expansive mortar and concrete. *Cement and Concrete Composites*, 33(1):131–141.

Sahmaran, M., Yücel, H. E., Yildirim, G., Al-Emam, M., and Lachemi, M. (2014). Investigation of the Bond between Concrete Substrate and ECC Overlays. *Journal of Materials in Civil Engineering*, 26(1):167–174.

Sakai, E., Miyahara, S., Ohsawa, S., Lee, S.-H., and Daimon, M. (2005). Hydration of fly ash cement. *Cement and Concrete Research*, 35(6):1135–1140.

Sakulich, A. R. and Bentz, D. P. (2013). Mitigation of autogenous shrinkage in alkali activated slag mortars by internal curing. *Materials and Structures*, 46(8):1355–1367.

Saliba, J., Rozière, E., Grondin, F., and Loukili, A. (2011). Influence of shrinkage-reducing admixtures on plastic and long-term shrinkage. *Cement and Concrete Composites*, 33(2):209–217.

Sanjuán, M. and Filho, R. T. (1998). Effectiveness of Crack Control at Early Age on the Corrosion of Steel Bars in Low Modulus Sisal and Coconut Fibre-Reinforced Mortars. *Cement and Concrete Research*, 28(4):555–565.

Schulze, J. (1999). Influence of water-cement ratio and cement content on the properties of polymer-modified mortars. *Cement and Concrete Research*, 29(6):909–915.

Schulze, J. and Killermann, O. (2001). Long-term performance of redispersible powders in mortars. *Cement and Concrete Research*, 31(3):357–362.

Schutter, G. D. (2002). Influence of hydration reaction on engineering properties of hardening concrete. *Materials and Structures*, 35(8):447–452.

Schutter, G. D. and Poppe, A.-M. (2004). Quantification of the water demand of sand in mortar. *Construction and Building Materials*, 18(7):517–521.

Segre, N. and Joekes, I. (2000). Use of tire rubber particles as addition to cement paste. *Cement and Concrete Research*, 30(9):1421–1425.

Sikora, K. S. and Klemm, A. J. (2014). Effect of Superabsorbent Polymers on Workability and Hydration Process in Fly Ash Cementitious Composites.

Journal of Materials in Civil Engineering, 27(5):04014170.

Silfwerbrand, J. (1986). Bonding between new and old concrete in structures loaded by static and time-dependent load. In *Adhesion between polymers and concrete / Adhésion entre polymères et béton - bonding, protection, repair. Proceedings of an International symposium organised by RILEM Technical Committee 52 - Resin Adherence to Concrete and Laboratoire Central des Ponts et Chaussées, P*, pages 309–319. Springer.

Silfwerbrand, J., Beushausen, H., and Courard, L. (2011). Bond. In Bissonnette, B., Courard, L., Fowler, D. W., and Granju, J.-L., editors, *Bonded Cement-Based Material Overlays for the Repair, the Lining or the Strengthening of Slabs or Pavements*, volume 3, chapter 4, pages 51–79. Springer Netherlands.

Siriwatwechakul, W., Siramanont, J., and Vichit-Vadakan, W. (2012). Behavior of Superabsorbent Polymers in Calcium- and Sodium-Rich Solutions. *Journal of Materials in Civil Engineering*, 24(8):976–980.

Smaoui, N., Bérubé, M., Fournier, B., Bissonnette, B., and Durand, B. (2005). Effects of alkali addition on the mechanical properties and durability of concrete. *Cement and Concrete Research*, 35(2):203–212.

Soliman, A. M. and Nehdi, M. L. (2013). Self-Restraining Shrinkage Ultra-High-Performance Concrete: Mechanisms and Evidence. *ACI Materials Journal*, 110(4):355–364.

Soshiroda, T., Hayakawa, K., Yoda, K., and Tanaka, M. (1986). Effects of Cellulose Ether on Homogeneity of Concrete in Structures - Relating Quality Variations and Construction Joints. In *Adhesion between polymers and concrete / Adhésion entre polymères et béton - bonding, protection, repair. Proceedings of an International symposium organised by RILEM Technical Committee 52 - Resin Adherence to Concrete and Laboratoire Central des Ponts et Chaussées, P*, pages 125–133. Springer.

Soufi, A., Mahieux, P.-Y., Aït-Mokhtar, A., and Omiri, O. (2016). Influence of polymer proportion on transfer properties of repair mortars having equivalent water porosity. *Materials and Structures*, 49.

Sugiyama, M. (2003). Improving concrete durability using an admixture to reduce drying shrinkage. In *Proceedings of the sixth CANMET/ACI International conference on recent advances in concrete technology*, pages 105–115.

Swaddiwudhipong, S., Lu, H.-R., and Wee, T.-H. (2003). Direct tension test and tensile strain capacity of concrete at early age. *Cement and Concrete Research*, 33(12):2077–2084.

Tan, K. H. and Du, H. (2013). Use of waste glass as sand in mortar: Part I – Fresh, mechanical and durability properties. *Cement and Concrete Composites*, 35(1):109–117.

Tanyildizi, H., Yazicioğlu, S., and Coskun, A. (2006). Influence on bond strength of concrete repair materials (mineral admixtures). In Grantham, M. G., Jaubertie, R. M., and Lanos, C., editors, *Concrete Solutions: Proceedings of the Second International Conference, June 2006, St Malo, France*, pages 514–521. IHS BRE Press.

Taylor, H. (1997). *Cement chemistry*. Thomas Telford, Second edition.

Taylor, P. C. (2014). *Curing Concrete*. CRC Press.

Tazawa, E.-I. and Miyazawa, S. (1995). Influence of cement and admixture on autogenous shrinkage of cement paste. *Cement and Concrete Research*, 25(2):281–287.

Tazawa, E.-I., Miyazawa, S., and Kasai, T. (1995). Chemical shrinkage and autogenous shrinkage of hydrating cement paste. *Cement and Concrete Research*, 25(2):288–292.

Tazawa, E.-I., Yonekura, A., and Tanaka, S. (1989). Drying shrinkage and creep of concrete containing granulated blast furnace slag. In Malhotra, V., editor, *Proceedings of the Third international conference: Fly Ash, Silica Fume, Slag, and Natural Pozzolans in Concrete, Trondheim, Norway*, volume 2, pages 1325–1344. American Concrete Institute.

Theodorakopoulos, D. (1995). Creep characteristics of glass reinforced cement under flexural loading. *Cement and Concrete Composites*, 17(4):267–279.

Thomas, J. J. and Jennings, H. M. (2003). Changes in the size of pores during shrinkage (or expansion) of cement paste and concrete. *Cement and Concrete Research*, 33(11):1897–1900.

Tilly, G. (2006). Past performance of concrete repairs. In Grantham, M. G., Jaubertie, R. M., and Lanos, C., editors, *Concrete Solutions: Proceedings of the Second International Conference, June 2006, St Malo, France*, pages 11–15. IHS BRE Press.

Tilly, G. and Jacobs, J. (2007). *Concrete Repairs: Performance in Service and Current Practice*. IHS BRE Press.

Topçu, İ. B. (1995). The properties of rubberized concretes. *Cement and Concrete Research*, 25(2):304–310.

Topçu, İ. B. (1997). Assessment of the brittleness index of rubberized concretes. *Cement and Concrete Research*, 27(2):177–183.

Topçu, İ. B. and Avcular, N. (1997a). Analysis of rubberized concrete as a composite material. *Cement and Concrete Research*, 27(8):1135–1139.

Topçu, İ. B. and Avcular, N. (1997b). Collision behaviours of rubberized concrete. *Cement and Concrete Research*, 27(12):1893–1898.

Topçu, İ. B. and Bilir, T. (2010). Experimental investigation of drying shrinkage cracking of composite mortars incorporating crushed tile fine aggregate.

Materials & Design, 31(9):4088–4097.

Toutanji, H. (1996). The use of rubber tire particles in concrete to replace mineral aggregates. *Cement and Concrete Composites*, 18(2):135–139.

Toutanji, H., Delatte, N., Aggoun, S., Duval, R., and Danson, A. (2004). Effect of supplementary cementitious materials on the compressive strength and durability of short-term cured concrete. *Cement and Concrete Research*, 34(2):311–319.

Toutanji, H., Liu, L., and El-Korchi, T. (1999). The role of silica fume in the direct tensile strength of cement-based materials. *Materials and Structures*, 32(3):203–209.

Toutanji, H. A. and El-Korchi, T. (1995). The influence of silica fume on the compressive strength of cement paste and mortar. *Cement and Concrete Research*, 25(7):1591–1602.

Turatsinze, A., Beushausen, H., Gagné, R., Granju, J.-L., Silfwerbrand, J., and Walter, R. (2011). Debonding. In Bissonnette, B., Courard, L., Fowler, D. W., and Granju, J.-L., editors, *Bonded Cement-Based Material Overlays for the Repair, the Lining or the Strengthening of Slabs or Pavements*, volume 3, chapter 6, pages 107–139. Springer Netherlands.

Turatsinze, A., Bonnet, S., and Granju, J.-L. (2005). Mechanical characterisation of cement-based mortar incorporating rubber aggregates from recycled worn tyres. *Building and Environment*, 40(2):221–226.

Turatsinze, A., Bonnet, S., and Granju, J.-L. (2007). Potential of rubber aggregates to modify properties of cement based-mortars: Improvement in cracking shrinkage resistance. *Construction and Building Materials*, 21(1):176–181.

Turatsinze, A., Granju, J.-L., and Bonnet, S. (2006). Positive synergy between steel-fibres and rubber aggregates: Effect on the resistance of cement-based mortars to shrinkage cracking. *Cement and Concrete Research*, 36(9):1692–1697.

Turki, M., Zarrad, I., Bretagne, E., and Quéneudec, M. (2012). Influence of Filler Addition on Mechanical Behavior of Cementitious Mortar-Rubber Aggregates: Experimental Study and Modeling. *Journal of Materials in Civil Engineering*, 24(11):1350–1358.

Uys, A. J. (1983). The influence of fly ash on the strength, elastic modulus, shrinkage and creep of concrete made with Cape Town aggregates, with particuar reference to alkali-aggregate reaction. Master's thesis, University of Cape Town.

van Breugel, K. (1980). Relaxation of young concrete. Technical Report Report-5-80-D8, Delft University of Technology.

van Breugel, K. (2001). Numerical modelling of volume changes at early ages - Potential, pitfalls and challenges. *Materials and Structures*, 34(239):293–301.

Vassie, P. (1989). The influence of steel condition on the effectiveness of repairs to reinforced concrete. *Construction and Building Materials*, 3(4):201–207.

Vaysburd, A. and Emmons, P. (2000). How to make todays repairs durable for tomorrow – corrosion protection in concrete repair. *Construction and Building Materials*, 14(4):189–197.

Vaysburd, A., Emmons, P., and Bissonnette, B. (2008). Concrete repair: Research and practice - The critical dimension. In Alexander, M. G., Beushausen, H.-D., Dehn, F., and Moyo, P., editors, *Concrete Repair, Rehabilitation and Retrofitting II: 2nd International Conference on Concrete Repair, Rehabilitation and Retrofitting, ICCRRR-2, 24-26 November 2008, Cape Town, South Africa*, pages 275–276. CRC Press, CRC Press.

Vaysburd, M., Bissonnette, B., and Morin, R. (2011). Practice and Quality Assurance. In Bissonnette, B., Courard, L., Fowler, D. W., and Granju, J.-L., editors, *Bonded Cement-Based Material Overlays for the Repair, the Lining or the Strengthening of Slabs or Pavements*, volume 3, chapter 8, pages 157–170. Springer Netherlands.

Wall, J., Shrive, N., and Gamble, B. (1986). Testing of bond between fresh and hardened concrete. In Sasse, H., editor, *Adhesion between polymers and concrete / Adhésion entre polymères et béton - bonding, protection, repair. Proceedings of an International symposium organised by RILEM Technical Committee 52 - Resin Adherence to Concrete and Laboratoire Central des Ponts et Chaussées, P*, pages 335–344. Springer US.

Wasserman, R. and Bentur, A. (2013). Efficiency of curing technologies: strength and durability. *Materials and Structures*, 46(11):1833–1842.

Westerholm, M., Lagerblad, B., Silfwerbrand, J., and Forssberg, E. (2008). Influence of fine aggregate characteristics on the rheological properties of mortars. *Cement and Concrete Composites*, 30(4):274–282.

Wittmann, F. (2002). Crack formation and fracture energy of normal and high strength concrete. *Sadhana*, 27(4):413–423.

Wittmann, F. (2008). Heresies on shrinkage and creep mechanisms. In aki Tanabe, T., Sakata, K., Mihashi, H., Sato, R., Maekawa, K., and Nakamura, H., editors, *Proceedings of the 8th International Conference on Creep, Shrinkage and Durability Mechanics of Concrete and Concrete Structures (CONCREEP 8), Sept*, volume 1, pages 3–9. CRC Press.

Wong, Y., Lam, L., Poon, C., and Zhou, F. (1999). Properties of fly ash-modified cement mortar-aggregate interfaces. *Cement and Concrete Research*, 29(12):1905–1913.

Wyrzykowski, M. and Lura, P. (2013). Controlling the coefficient of thermal expansion of cementitious materials - A new application for superabsorbent polymers. *Cement and Concrete Composites*, 35(1):49–58.

Xu, B., Toutanji, H. A., Lavin, T., and Gilbert, J. A. (2011). Characterization of Poly(vinyl Alcohol) Fiber Reinforced Organic Aggregate Cementitious Materials. In Aguiar, J. and Czarnecki, L., editors, *Polymers in Concrete*, volume 466, pages 73–83. Trans Tech Publ, Trans Tech Publications.

Xu, G., Beaudoin, J., Jolicoeur, C., and Pagé, M. (2000). The effect of a polynaphthalene sulfonate superplasticizer on the contribution of the interfacial transition zone to the electrical resistivity of mortars containing silica and limestone fine aggregate. *Cement and Concrete Research*, 30(5):683–691.

Yao, X. and Wei, Y. (2014). Design and verification of a testing system for strength, modulus, and creep of concrete subject to tension under controlled temperature and humidity conditions. *Construction and Building Materials*, 53:448–454.

Ye, G., van Breugel, K., Lura, P., and Mechtcherine, V. (2012). Hardening Process of Binder Paste and Microstructure Development. In Mechtcherine, V. and Reinhardt, H.-W., editors, *Application of Super Absorbent Polymers (SAP) in Concrete Construction*, pages 51–62. Springer Netherlands.

Yuan, Y., Li, G., and Cai, Y. (2003). Modeling for prediction of restrained shrinkage effect in concrete repair. *Cement and Concrete Research*, 33(3):347–352.

Yurdakul, E., Taylor, P. C., Ceylan, H., and Bektas, F. (2014). Effect of Water-to-Binder Ratio, Air Content, and Type of Cementitious Materials on Fresh and Hardened Properties of Binary and Ternary Blended Concrete. *Journal of Materials in Civil Engineering*, 26(6):04014002.

Yurtdas, I., Burlion, N., and Skoczylas, F. (2004). Experimental characterisation of the drying effect on uniaxial mechanical behaviour of mortar. *Materials and Structures*, 37(3):170–176.

Yurtdas, I., Peng, H., Burlion, N., and Skoczylas, F. (2006). Influences of water by cement ratio on mechanical properties of mortars submitted to drying. *Cement and Concrete Research*, 36:1286–1293.

Zelić, J., Rušić, D., Vea, D., and Krstulović, R. (2000). The role of silica fume in the kinetics and mechanisms during the early stage of cement hydration. *Cement and Concrete Research*, 30(10):1655–1662.

Zhang, J., Han, Y. D., and Gao, Y. (2014). Effects of Water-Binder Ratio and Coarse Aggregate Content on Interior Humidity, Autogenous Shrinkage, and Drying Shrinkage of Concrete. *Journal of Materials in Civil Engineering*, 26(1):184–189.

Zhang, J., Liu, Q., and Wang, L. (2005). Effect of coarse aggregate size on relationships between stress and crack opening in normal and high strength concretes. *Journal of Material Science and Technology*, 21(5):691–700.

Zhou, J., Li, M., Ye, G., Schlangen, E., van Breugel, K., and Li, V. C. (2008). Modelling the performance of ECC repair systems under differential volume changes. In Alexander, M. G., Beushausen, H.-D., Dehn, F., and Moyo, P., editors, *Concrete Repair, Rehabilitation and Retrofitting II: 2nd International Conference on Concrete Repair, Rehabilitation and Retrofitting, ICCRRR-2, 24-26 November 2008, Cape Town, South Africa*, pages 363–364. CRC Press, CRC Press.

Zhou, X., Dong, W., and Oladiran, O. (2014). Experimental and Numerical Assessment of Restrained Shrinkage Cracking of Concrete Using Elliptical Ring Specimens. *Journal of Materials in Civil Engineering*, 26(11):04014087.

Appendix A

MATERIAL PROPERTIES

The properties of the materials used in this study are hereby presented.

A.1 Cement

The physical and chemical characteristics of the CEM II/B-M (L) 42.5 N are summarised in Table A.1 and Table A.2 respectively. Limestone is the only additive in this cement. The content of limestone is 20%.

TABLE A.1: Physical characteristics of CEM II/B-M (L) 42.5 N (Source: AfriSam)

Physical characteristic	**Value**
Relative density (g/ml)	2.79
Loose bulk density after consolidation (kg/l)	1.19

TABLE A.2: Typical chemical composition of CEM II/B-M (L) 42.5 N (Source: AfriSam)

Chemical compound (% by mass, ignited basis)	**Value**
Loss on ignition	9.43
SiO_2	19.55
P_2O_5	0
Al_2O_3	3.91
Fe_2O_3	2.53
CaO	65.5
MgO	3.13
K_2O	0.57
TiO_2	0.22
Na_2O	0.07
SO_3	2.64
Mn_2O_3	2.12

The typical performance criteria for CEM II/B-M (L) 42.5 N are provided in Table A.3.

TABLE A.3: Typical performance criteria in relation to SANS 50197-1 criteria (Source: Afrisam)

Criterion	**SANS 50197-1 Class 42.5N**	**Typical performance**
Physical		
Early (2-day)strength, MPa	≥ 10	17.45
28-day strength, MPa	$\geq 32.5 \leq 52.5$	40.9
Initial setting time, minutes	≥ 60	175
Soundness: LeChatelier expansion, mm		0
Chemical		
Sulphate content, %	≤ 10	2.38
Chloride content, %	≤ 0.1	0.04

A.2 Ground Granulated Blastfurnace Slag

The physical and chemical characteristics of the GGBS are presented in Table A.4 and Table A.5 respectively.

TABLE A.4: Physical characteristics of GGBS (Source: AfriSam)

Test		**SANS 55167 1 requirements**	**SANS 1491 1 requirements**	**Value**
Relative density (g/ml)		x	x	2.89
Loose bulk density after consolidation (kg/m^3)		x	x	1000
Compact bulk density (kg/m^3)		x	x	1200
Absorption		x	x	Not hygroscopic
Activity index	7 days	≥ 45 (%)	x	59.8
% of test cement strength	28 days	≥ 70 (%)	x	80.4
Reactivity	7 days	x	≥ 12	21.0
Compressive strength (MPa)	28 days	x	≥ 32.5	37.1
Blaine (cm^2/g)		≥ 2750	≥ 3500	3750
Glass content (%)		≥ 67	≥ 95	96

Note: Slag activity index results are based on the average of 2 samples per week (% ratio of 50% GGBFS/50% CEM I 42.5 N to 100% CEM I 42.5 N test cement)

A.3 Sieve analysis

The procedure for sieve analysis is described in Appendix B.1. Results from the sieve analysis of the sands in this study are hereby presented.

A.3.1 Dune sand

The sieve analysis test results for dune sand are summarised in Table A.6.

TABLE A.5: Chemical characteristics of GGBS (Source: AfriSam)

Test	**SANS 55167-1 and SANS 1491-1 requirements**	**Test value**
LOI (%)	≤ 3.0	0.31
SiO_2 (%)	x	39.45
Al_2O_3 (%)	x	12.84
Fe (%)	x	0.36
CaO (%)	x	38.89
MgO (%)	≤ 18	7.34
K_2O (%)	x	0.92
TiO_2 (%)	x	0.58
MnO (%)	x	0.47
SO_3 (%)	≤ 2.5	0.48
Free H_2O	≤ 1.0	0.28
Sulphide (%)	≤ 2.0	1.08

TABLE A.6: Sieve analysis results for dune sand

Aperture size (mm)	**Mass retained (%)**			**Cumulative mass retained (%)**			**Cumulative mass passing (%)**		
	Test 1	Test 2	Test 3	Test 1	Test 2	Test 3	Test 1	Test 2	Test 3
4.750	0	0	0	0	0	0	100	100	100
2.360	0	0	0	0	0	0	100	100	100
1.180	0	0	0	0	0	0	100	100	100
0.600	13	13	13	13	13	13	88	88	87
0.300	60	69	69	73	82	82	28	19	19
0.150	24	16	16	97	97	98	4	3	3
0.075	3	3	2	100	100	100	1	1	1
Pan	1	1	1	100	100	100	0	0	0

Fineness modulus: 1.88.

The grading curve of dune sand is presented in Figure A.1.

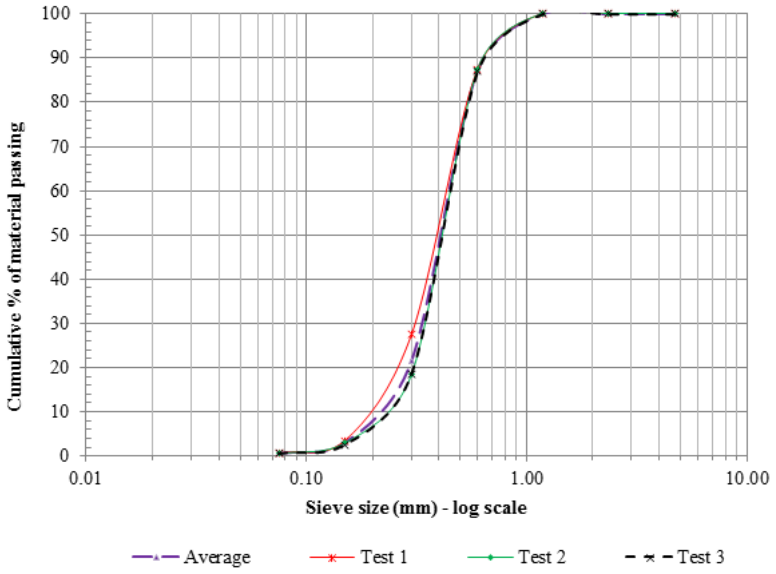

FIGURE A.1: Grading curve for dune sand

A.3.2 Crusher sand

The sieve analysis test results for crusher sand are summarised in Table A.7.

TABLE A.7: Sieve analysis results for crusher sand

Aperture size (mm)	**Mass retained (%)**			**Cumulative mass retained (%)**			**Cumulative mass passing (%)**		
	Test 1	Test 2	Test 3	Test 1	Test 2	Test 3	Test 1	Test 2	Test 3
4.750	1	2	1	1	2	1	99	99	99
2.360	20	18	17	21	20	18	79	81	82
1.180	24	24	23	45	43	41	55	57	60
0.600	24	26	25	69	69	66	31	31	35
0.300	15	15	17	84	84	82	17	16	18
0.150	11	11	12	95	95	94	6	5	6
0.075	5	5	5	99	100	99	1	1	1
Pan	1	1	1	100	100	100	0	0	0

Fineness modulus: 3.09.

The grading curve for crusher sand is shown in Figure A.2.

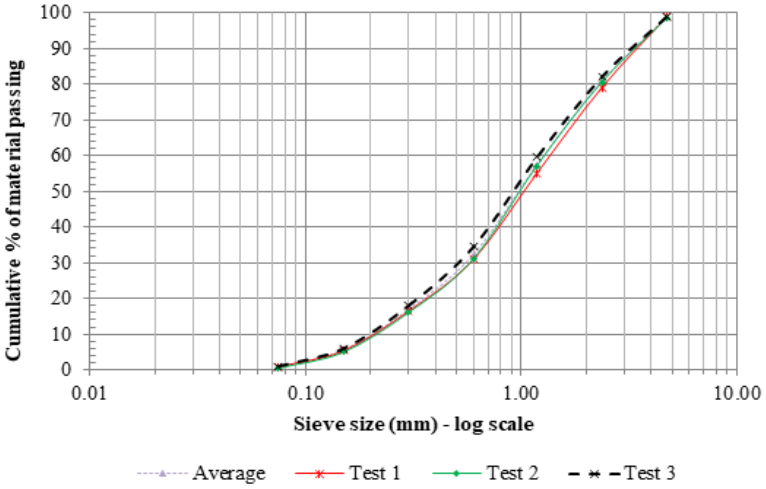

FIGURE A.2: Grading curve for crusher sand

A.3.3 50/50 dune/crusher sand

The sieve analysis test results for 50/50 dune/crusher sand is summarised in Table A.8.

TABLE A.8: Sieve analysis results for dune/crusher sand

Aperture size (mm)	**Mass retained (%)**			**Cumulative mass retained (%)**			**Cumulative mass passing (%)**		
	Test 1	Test 2	Test 3	Test 1	Test 2	Test 3	Test 1	Test 2	Test 3
4.750	1	2	2	1	2	2	99	99	99
2.360	13	13	13	14	14	14	87	86	86
1.180	12	12	12	26	26	26	75	74	74
0.600	22	24	21	48	50	47	53	50	54
0.300	35	33	34	83	83	81	18	18	20
0.150	15	16	17	98	98	97	3	2	3
0.075	2	2	3	100	100	100	1	0	1
Pan	1	0	1	100	100	100	0	0	0

Fineness modulus: 2.68.

The grading curve for the 50/50 dune/crusher sand is presented in Figure A.3.

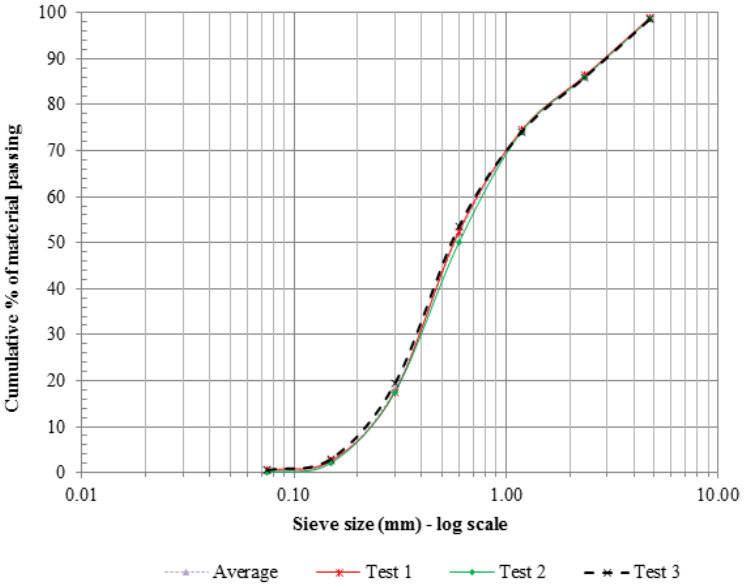

FIGURE A.3: Grading curve for 50/50 dune/crusher sand

A.4 Density of aggregates

A summary of the average density of the various sands is provided in Table A.9.

TABLE A.9: Summary of the average densities of various sands

Parameter	**Sand type**		
	Dune	**Crusher**	**50/50 dune/crusher**
Loose bulk density (kg/m^3)	1557	1655	1704
Compacted bulk density (kg/m^3)	1674	1889	1860

A.5 Plasticisers

The important properties of the plasticising admixture used in this research are summarised in Table A.10.

A.6 Superabsorbent polymers

Floset 27 CS is a cross linked copolymer of acrylamide and acrylate used to absorb/retain large quantities of water; thus acting as water retention systems. Important material properties of Floset 27 CS are presented in Table A.11.

TABLE A.10: Important properties of Chryso Plast Omega 122 (Source: ChrysoSA)

Characteristics	Nature: liquid Colour: brown Density (20^{o}C): 1.20 ± 0.02 pH: 7.5 ± 2.0 Cl- content: nil Na2O equivalent ≤ 2% Dry extract (halogen): 42% ± 1 Dry extract (EN 480-8): 42% ± 1
Domains of application	All types of cement, except white cement Very plastic concrete to fluid concrete Ready mix concrete Precast
Method of use	Dosage: 0.3 to 1.5 kg for 100 kg of cement. It is best to add Chryso ®Plast Omega 122 to the mixing water
Precautions	Store away from frost Should product freeze, it will recover its properties after thawing and agitating Shelf life: 12 months
Safety	Chryso Plast Omega 122 is a product classified as harmless. It is recommended to wear the normal protective equipment.

TABLE A.11: Important properties of Floset 27 CS (Source: SNF Floerger)

Product characteristics	Appearance: very fine white powder Particle size: <300 microns Ionic character: Anionic Approx. bulk density: 0.8 0.9 g/cm^3 Solubility: Insoluble in water
Typical characteristics	Gram of water per gram of dry powder find this In deionised water: 400 g/g In,water with 1000 ppm of NaCl: 110 g/g In water with 1000 pp of $CaCl_2$: 50 g/g
Storage and packaging	Storage temperature: 0 - 35^{o}C Shelf life: 2 years

A.7 Shrinkage reducing admixtures

The important properties of the SRA used in this research are summarised in Table A.12.

TABLE A.12: Important properties of Chryso Serenis (Source: ChrysoSA)

Characteristics	Nature: liquid Colour: light brown Density (20^oC): 0.930 ± 0.020 Cl- ions content: $\leq 10\%$ Na_2O equivalent *leq* 1.0% Active matter: >98%
Domains of application	All types of cement Ready mix concrete Prefabrication Flooring, industrial slabs
Method of use	Dosage: 0.5 to 3.0 kg for 100 kg of cement or binder. A 2.0% dosage of the product of the weight of cement is commonly used. Chryso ®Serenis can be added to the mixing water. The optimum dosage of Chryso ®Serenis can only be established after trial tests taking into account local conditions.
Precautions	Store away from frost and at a temperature between 5 - 30^oC. Should product freeze, it will recover its properties after thawing and agitating. Small splashed of Chryso ®Serenis may be cleaned with water. Should the product spill on coloured surfaces these may be altered. Shelf life: 12 months
Safety	The product is classified as irritating. Handling may cause irritation by contact. Wearing the appropriate protection equipment (safety glasses gloves, mask and/or covering clothes) according to the exposure is essential.

A.8 Polymers

Important properties of the two polymers - EVA and SA - used in this study are summarised in Table A.13 and Table A.14.

TABLE A.13: Important properties of ELOTEX FX2320 (EVA)

Product information	Trade name: ELOTEXFX2320
Composition/information on ingredients	Chemical nature: copolymer based on vinyl acetate and ethylene, with additives.
Physical and chemical properties	Appearance Form: powder Colour: white Odour: mild Odour threshold: no data available
Safety data	pH: 6.0 9.0 at 10% solution melting point/range: not applicable boiling point/range: not applicable flash point: not applicable ignition temperature: >200^{o}C method auto ignition of dust cloud according to EN 50281-2-1 evaporation rate: not applicable flammability (solid, gas): the product is not flammable lower explosion limit: 15000 mg/m^3 upper explosion limit: not applicable vapour pressure: not applicable relative vapour density: not applicable relative density: not applicable bulk density: 450 - 650 kg/m^3 water solubility: dispersible solubility in other solvents: not applicable partition coefficient: n-octanol water: no data available auto-ignition temperature: no data available decomposition temperature: no data available viscosity dynamic: not applicable viscosity kinematic: not applicable dust explosion class: St1 explosive properties: dust may form explosive mixture in air Oxidizing properties: not classified as oxidising
Stability and reactivity	Conditions to avoid: none known Materials to avoid: none known Hazardous decomposition products: no hazardous decomposition products are known Thermal decomposition: no data available Reactivity: stable under normal conditions Chemical stability: stable under recommended storage conditions Hazardous reactions: dust may form explosive mixture in air

TABLE A.14: Important properties of ELOTEX FX7000 (SA)

Product information	Trade name: ELOTEX FX7000
Composition/information on ingredients	Chemical nature: copolymer based on styrene and acrylic monomer with additive.
Physical and chemical properties	Appearance Form: powder Colour: white Odour: mild Odour threshold: no data available
Safety data	pH: 7.5 - 9.5 at 10% solution melting point/range: not applicable boiling point/boiling range: not applicable flash point: not applicable ignition temperature: >200^{o}C method auto ignition of dust cloud according to EN 50281-2-1 evaporation rate: not applicable flammability (solid gas): the product is not flammable lower explosion limit: 15000 mg/m^3 upper explosion limit: not applicable vapour pressure: not applicable relative vapour density: not applicable relative density: not applicable bulk density: 350 - 550 kg/m^3 water solubility: dispersible solubility in other solvents: not applicable partition coefficient: n-octanol water: no data available auto-ignition temperature: no data available decomposition temperature: no data available viscosity, dynamic: not applicable viscosity, kinematic: not applicable dust explosion class: St1 explosive properties: dust may form explosive mixture in air Oxidizing properties: not classified as oxidising
Stability and reactivity	Conditions to avoid: none known Materials to avoid: none known Hazardous decomposition products: no hazardous decomposition products are known Thermal decomposition: no data available Reactivity: stable under normal conditions Chemical stability: stable under recommended storage conditions Hazardous reactions: dust may form explosive mixture in air

Additional information regarding these product can be found in the product data sheets provided by the manufacturer.

Appendix B

TEST PROCEDURES

The standard procedures that were followed during testing for various material properties are summarised in the subsequent subsections.

B.1 Sieve analysis

The sieve analysis was done according to ASTM-C136. The procedure for sieve analysis is hereby summarised.

i. The wet sand samples were dried to a constant mass in an oven maintained at a temperature of 100 ± 5^{o}C for a period of 24 hours;

ii. Sieves with the following openings - 4.75 mm, 2.36 mm, 1.18 mm; 0.60 mm, 0.30 mm; 0.15 mm and 0.075 mm - were used. The sieves were nested in order of decreasing size of opening from top to bottom and 1 kg of the sample placed on top of the sieve. The sample in the sieve was agitated using a mechanical sieve shaker for a period of five minutes;

iii. The mechanical sieve shaker was stopped. Thereafter, the sieves were removed from the shaker;

iv. Both the mass of material retained in a specific sieve as well as the mass of the sieve were measured using a balance and recorded;

v. Thereafter, appropriate calculations were done to evaluate the grading of the various sand samples.

B.2 Bulk density

The density of the sand samples was determined according to ASTM-C29. Owing to the size of the sample, the rodding procedure was used. This procedure is hereby summarised.

i. One-third of the measure was filled with sand and the surface of the sand levelled using the fingers;

ii. The layer of sand was rodded with 25 strokes of the tamping rod evenly distributed over the surface. Care was taken to ensure that the tamping rod did not strike the bottom of the measure forcibly;

iii. The measure was filled to two-thirds full, its surface levelled and thereafter rodded as described before. Thereafter, the measure was filled to overflowing and rodded in the prescribed manner. The second and third layers were rodded using vigorous effort, but with care being taken to ensure that the rod did not penetrate to the previous layer;

iv. The surface of the aggregate was levelled with a straight edge in such a manner that any slight projections of the larger pieces of the aggregates approximately balanced the larger voids in the surface below the top of the measure;

v. The mass of the measure with its contents as well as the mass of the measure alone were determined using a balance and recorded;

vi. The recorded masses were used to calculate the density of the sand samples.

B.3 Consistence

Tests for consistence comprised the slump test and the flow test. These tests are hereby described.

B.3.1 Slump test

The test for slump was done according to ASTM-C143. A summary of the test procedure is hereby provided.

i. The mould was dampened and placed on a flat, moist and non-absorbent steel plate. The mould was held firmly during filling and its perimeter cleaned while standing on the foot pieces;

ii. The mix was filled in three layers immediately after casting. Each layer was approximately one-third the volume of the mould;

iii. Each layer was rodded with 25 strokes of the tamping rod. The strokes were uniformly distributed over the cross section of each layer. For the bottom layer, this necessitated inclining the rod slightly and making approximately half of the strokes near the perimeter and then progressing with vertical strokes spirally towards the centre. The bottom layer was rodded throughout its depth. The second layer and top layer were each rodded throughout their depth such that the strokes penetrated the underlying layer;

iv. After rodding the top layer, the surface of the mortar was struck off by means of a screeding and rolling motion of the tamping rod;

v. The mould was firmly held down and the mortar was removed from the area surrounding the base of the mould;

vi. The mould was removed immediately from the mortar by raising it carefully in a vertical direction. The mould was raised at 300 mm in 5 ± 2 seconds by a steady upward lift without lateral or torsional motion;

vii. The slump was measured immediately by determining the vertical difference between the top of the mould and the displaced original centre of the top surface of the mortar specimen. If a decided falling away or shearing off of the mortar from one side or portion of the mass occurred, the test was disregarded and a new test made using another portion of the sample;

viii. The slump was reported to the nearest 5 mm of subsidence of the specimen.

B.3.2 Flow test

The flow test was done in accordance with the ASTM-C1437. A summary of the test procedure is hereby presented.

i. The flow table was wiped clean and dry.

ii. The flow mould was placed at the centre of the flow table and a 25 mm thick layer of mortar was placed in the mould and tamped 20 times with the tamping rod/tamper. Care was taken to ensure that the tamping pressure was sufficient to ensure that the mould was filled uniformly. The tamping was uniformly distributed over the entire section of each layer of mortar.

iii. The mould was thereafter filled with mortar and tamped as in (ii) above.

iv. The compacted mortar in the mould was cut off to a plane surface flush with the top of the mould using a trowel with a sawing motion across the top of the mould.

v. The table top was wiped clean and dry with care being taken to ensure that water is removed from around the edge of the mould.

vi. The mould was lifted away from the mortar a minute after completing the mixing operation.

vii. The table was immediately dropped 25 times over a duration of 15 seconds.

viii. The diameter of the mortar along the four lines that have been scribed in the table top was measured using a calliper and recorded to the nearest millimetre.

B.4 Compaction

Compaction was done according to the ASTM-C192. Each freshly cast mortar in the pan mixer was placed in its respective specimen mould using a scoop. Care was taken to ensure that the mortar from the mixer was a perfect representation of the mixed batch as possible and that the number of layers used to fill each specimen mould corresponds to Table B.1. The dog-bone specimens, however, were filled in one layer.
Prior to the start of the consolidation, a tamping rod was used to further distribute the mortar within the mould. Owing to the requirements for slump that the mix was supposed to achieve (80 ± 20 mm) and the dimension of the various test specimens, external vibration using a vibrating table was used in most specimens. A combination of rodding and a vibrating table were used in the case of ring specimens.

TABLE B.1: Number of layers required for specimens

Specimen type	**Specimen size**	**Mode of consolidation**	**Number of layers of approximate equal depth**
	Diameter, in. (mm)		
Cylinders	3 or 4 (75 to 100)	Rodding	2
	6 (150)	Rodding	3
	9 (225)	Rodding	4
	Up to 9 (225)	Vibration	2
	Depth, in. (mm)		
Prisms and horizontal creep cylinders	Up to 8 (200)	Rodding	2
	Over 8 (200)	Rodding	3 or more
	Up to 8 (200)	Vibration	1
	Over 8 (200)	Vibration	2 or more

The compaction by rodding was done as follows:

i. The mortar was placed into the mould, in the required number of layers of approximately equal volume;

ii. Each layer of mortar was rodded using the required number of strokes with the rounded end of the standard tamping rod. Table B.2 presents the number of strokes per layer of material;

iii. The bottom layer was rodded throughout its depth. Care was taken to ensure that the strokes are distributed uniformly over the cross-section of the mould. Also, each upper layer was rodded in a manner than ensured that the rod penetrated through the layer being rodded and into the layer below by a depth of approximately 25 mm;

iv. After each layer was rodded, the outside of the mould was tapped lightly 10 to 15 times with a mallet to close any holes left by rodding and to release any large air bubbles that may have been trapped. After tapping, the mortar along the sides and ends of the moulds were spaded with a trowel.

The compaction by vibration was executed as follows:

Table B.2: Diameter of rod and number of roddings to be used in moulding test specimens

Cylinders		
Diameter of cylinder, in. (mm)	Diameter of rod in. (mm	Number of strokes/layer
2 (50) to <6 (150)	3/8 (10)	25
6 (150)	5/8 (16)	25
8 (200)	5/8 (16)	50
10 (250)	5/8 (16)	75
Beams and Prisms		
Top surface area of specimen in.^{2} (cm^2)	Diameter of rod in. (mm)	Number of roddings/layer
25 (160) or less	3/8 (10)	25
26 to 49 (165 to 310)	3/8 (10)	One for each 1 in.^{2} (7 cm^2) of surface
50 (320) or more	5/8 (16)	One for each 2 in.^{2} (14 cm^2) of surface
Horizontal creep cylinders		
Diameter of cylinder in. (mm)	Diameter of rod in. (mm)	Number of roddings/layer
6 (150)	5/8 (16)	50 total, 25 along both sides of axis

i. The moulds were filled in the required number of approximately equal layers. All the mortar for each layer was placed in the mould before the vibration for that specific layer began. When placing the final layer, care was taken to avoid overfilling by more than 6 mm;

ii. Vibration was done at a frequency of 60 Hz for one minute;

iii. Once the vibration was complete, enough mortar was added with a trowel to overfill the mould - to about 3 mm;

iii. Vibration was done at a frequency of 60 Hz for one minute;

iv. Care was taken to ensure that the duration of vibration of the specimens was uniform throughout a given range of specimens. Vibration was deemed sufficient when the surface of the mortar was relatively smooth and large air bubbles ceased to breathe through the top surface of the mortar in the mould;

v. The surface of each finished specimen was struck off with a trowel. All finishing was performed with the minimum manipulation that was necessary to produce a flat even surface that is level with the rim or edge of the mould and which has no depressions or projections larger than 3 mm.

B.5 Curing

The curing of the test specimens - other than the ring specimens - was done in accordance with ASTM-C192. To prevent the loss of moisture from the freshly cast test specimens in their moulds to the environment, a black plastic sheet was used to cover the specimens

for 24 ± 8 hours from the time of casting. Thereafter, the freshly cast mortar specimens were demoulded and then put into a curing tank maintained at a temperature of 23 ± 2^{o}C. The period in which the specimens remained in curing the tank was dependent on the age at which the specimens would be tested. The ring specimens, however, were not cured in a curing tank. They were covered with a wet hessian for seven days in a controlled laboratory environment (Temperature 23 ± 2^{o}C; Relative humidity $50 \pm 5\%$). Care was taken to ensure that the environment in which curing was done was free of vibrations.

B.6 Compressive strength

Compressive strength tests were done to characterise the mortar mixes. These tests were done in accordance to SANS 5863:2006a. Care was taken to ensure that each specimen was tested immediately after its removal from the curing tank. A summary of the test procedure is hereby presented.

i. The surface water, grit and projecting fins on the cured $100 \times 100 \times 100$ mm cube specimens was removed;

ii. The mass of each cube was measured (to an accuracy of 1%) using an electronic balance;

iii. The loading surfaces on the loading platens of the compression testing were wiped clean;

iv. The test cube was positioned in the machine in such a manner that the load was applied on any of the smooth surfaces that is perpendicular to the direction of casting;

v. The compression load was applied without shock continuously at a uniform rate that ranged between 0.3 MPa/s $\pm$ 0.1 MPa/s until the specimen failed.

vi. The maximum load that was applied was recorded. Also, the appearance of the specimen at failure, any unusual features in the specimen during failure - if any - and the type of failure was recorded.

B.7 Modulus of elasticity

The static modulus of elasticity in compression was determined according to BS 1881: Part 121:1983. This procedure is hereby described.

i. 3 No. $100 \times 100 \times 100$ mm cubes were cast in conjunction with the elastic modulus specimens that were subsequently tested for compressive strength. The average compressive strength of these cubes was recorded.

ii. The ends of each cylindrical test specimen were made plane and perpendicular to the plane of the axis using a grinder. Utmost care was taken to ensure that specimens were tested within 1 hour after their removal from a curing tank.

iii. The diameter of each test specimen was measured using callipers to the nearest 0.25 mm by averaging two diameters measured at right angles to each other near the centre of the length of the specimen. The length of each specimen was also measured and recorded to the nearest 2.54 mm.

iv. LVDTs were attached to each specimen. Care was taken to ensure that the effective length of each gauge line is not less than three times the maximum size of the aggregate in the concrete or more than two thirds the height of the specimen.

v. The specimens, with the strain measuring equipment attached, was placed on the lower platen of the testing machine. The axis of the specimen was carefully aligned with the centre of thrust of the spherically-seated upper bearing block.

vi. The data acquisition system of the stress and strains (via the LVDT readings) was switched on.

vii. A compressive stress of 0.5 MPa was applied to the machine and the load gradually increased at a rate of 0.6 $\pm$ 0.4 MPa/s until a stress equal to one-third of the average compressive strength of the cubes in (i).

viii. The load in the machine was released.

ix. Steps (iv) and (v) were repeated twice and the corresponding stress and strains recorded.

x. Specimens were thereafter loaded until failure and their compressive strength at failure recorded.

xi. The recorded stresses and their corresponding strains were used to calculate the secant modulus of elasticity of the specimens.

B.8 Drying shrinkage

The drying shrinkage tests were done in accordance with SANS 6085:2006b. A summary of the procedure is hereby described.

i. The freshly-cast $100 \times 100 \times 300$ mm prism specimens in the mould were covered with an impervious plastic sheet and stored for 20 - 24 hours in a place that was free from vibration and in an atmosphere whose temperature varied between 22^{o}C and 25^{o}C and a relative humidity of at least 90%;

ii. The specimens were demoulded after 24 hours.

iii. Strain targets at a gauge length of 100 mm were affixed to two opposite faces in the longitudinal direction.

iv. The specimens were water cured for six days, after demoulding, in potable water maintained at a temperature that varied between 22^{o}C to 25^{o}C.

v. The specimens were removed from the water bath after 7 days ± 2 hours after demoulding. Excess water was wiped off.

vi. The distance between the strain targets was measured immediately to the nearest 2 μm. The specimens were also marked such that one end was always oriented in the same direction in relation to the strain gun.

vii. The specimens were transferred to an environmental room whose temperature and relative humidity were maintained at 23 ± 2^{o}C and 50 ± 4% respectively. These environmental conditions corresponded to the one for ring tests.

viii. The distance between the strain targets within any one face of a specimen was measured using the strain gun every two days. The measurement for shrinkage was monitored daily over a duration of 56 days.

B.9 Restrained shrinkage

The restrained shrinkage cracking was done according to ASTM-C1581, but with modifications owing to lack of equipment such as strain gauges. The test procedure is summarised as follows:

i. The freshly cast mortar was placed into a mould in two approximately equal layers. Each layer was rodded 75 times using a 10 mm diameter rod and thereafter vibrated on a vibrating table to consolidate it. Three specimens were made from each mix under investigation.

ii. The top of each specimen was levelled after consolidation using a trowel. Finishing was done with minimum manipulation necessary to achieve a flat surface. Any fresh mortar that had spilled inside the steel ring or outside was removed so that the base remained clean. The test specimens were thereafter transferred to the testing environment within 10 minutes after the completion of casting;

iii. The specimens were moist cured in the moulds for 24 hours using wet hessian covered with polyethylene film. The environmental parameters under which these specimens were cured, and tested, are: temperature 23 ± 2^{o}C; relative humidity 50±4%. An electronic data logger Rotronic®Hydrolog data logger with a software HW4 was used to record the temperature and relative humidity at 10-minute intervals;

iv. The wet hessian, polyethylene sheet and outer ring of the freshly cast specimens were removed after 24 hours from the time of casting;

v. Any loose materials from the top surface of the specimen, if present, was removed gently;

vi. The top surface of the specimen was sealed using paraffin wax using a 38 mm wide brush. Care was taken to ensure that the outer circumference of the specimen is not coated with paraffin wax.

vii. The specimens were cured using wet hessian for six days. The hessian was dipped in clean potable water three times and day and then wrapped around the specimens.

viii. The mortar specimens were monitored three times a day - at six-hour intervals for cracking (i.e., at 09h00, 15h00 and 21h00) - for cracking. The duration of monitoring a specimen began immediately after casting and ended upon its cracking. Also, the daily ambient temperature and relative humidity of the test environment were recorded.

ix. The crack width of the cracked specimens was measured using a microscope. The crack measurements from a single specimen were taken 10 mm from its top, at its mid-height and 10 mm from the bottom of each crack.

B.10 Durability indexes

Two Durability Indexes were measured: Oxygen Permeability Index and Water Sorptivity Index. Specific details pertaining to each of these tests are described in the sub-sections below. Four specimens were used for each durability index test.

B.10.1 Specimen preparation for DI tests

The specimens for Durability Index (DI) tests were prepared as stated in the Durability Index Testing Procedure Manual (Ver 2.0, May 2010). A summary of the steps that were involved in the sample preparation are presented below.

i. A water-cooled diamond tipped core barrel attached to a coring drill was used to core circular discs from $100 \times 100 \times 100$ mm mortar cube specimens that had been and cured. The internal diameter of the coring barrel was 70 ± 2 mm. The direction of coring was perpendicular to that of casting;

ii. The cored cubes were further sliced into discs whose thickness was 30 ± 2 mm;

iii. The discs were marked with the correct reference number on the original interior face for identification purposes. Specimens that were damaged during the coring and cutting process were not used for testing;

iv. The cut and marked discs were transferred to an oven maintained at a temperature of 50 ± 2^{o}C for a period of 7 days $\pm$ 4 hours.

v. The specimen from the oven were cooled in a desiccator maintained at 23 ± 2^{o}C. The duration of cooling raged from a minimum of 2 hours to a maximum of 4 hours.

vi. The specimens were removed from the desiccator and tested for the various durability indexes.

B.10.2 Oxygen Permeability Index (OPI)

The tests on the OPI of the mortar mixes were conducted as follows:

i. The test specimens were prepared as specified in the Durability Index Testing Procedure Manual (Ver. 2.0, 2010) and as described in Appendix B.10.1;

ii. Test specimens were removed from the oven and put in a desiccator for a minimum of 2 hours and a maximum of 4 hours;

iii. The diameter and thickness of each specimen, after removal from the desiccator, was measured and recorded (to the nearest 0.02 mm) using a vernier calliper at four points that are equally spaced around the perimeter of the specimen. The average of the four readings was determined and recorded to the nearest 0.02 mm;

iv. Each test specimen was placed in the compressible collar within the rigid sleeve of the permeameter with the test face (outer face) at the bottom. Care was taken to ensure that gaps are not visible between the sides of the specimen and the collar. The specimens were placed so that the outer face rests against the lip of the collar;

v. The specimen, collar and rigid sleeve was placed on top of the test chamber so that it covers the hole. The solid ring was then placed on top of the collar with care being taken to ensure that there are no visible gaps between the collar and the sleeve. The cover plate was then placed on top of the solid ring;

vi. The top screw was partially tightened on the cover plate to ensure that it is centred;

vii. The oxygen inlet and outlet valves of the permeability cells were opened. Thereafter, the valve of the oxygen supply tank was opened to between 100 kPa and 120 kPa and the oxygen allowed to flow through the permeameter for 5 seconds;

viii. Thereafter the oxygen outlet valve of the permeability cells was closed;

ix. The inlet valve was closed when the pressure indicated on the gauge of the permeability cell was above 100 kPa;

x. The gauge was tapped to ensure that the reading is correct. Thereafter, the pressure in the cell was adjusted to 100 kPa ± 5 kPa by a slight opening of the outlet valve;

xi. Readings were taken automatically using a data logger. The test was terminated when the pressure had dropped to 50 ± 2.5 kPA or after 6 hours ± 15 minutes, whichever occurred first;

xii. The recorded readings were thereafter downloaded from the data logger and analysed.

B.10.3 Water Sorptivity Index (WSI)

The test for the water sorptivity index was done in accordance with the Durability Index Testing Procedure Manual (Ver 2.0, 2010). Four specimens were used for each mix under investigation. The testing procedure is described below.

i. The vertical curved sides of the specimens from the desiccator were sealed using a packaging tape. Care was taken to ensure that any part of the test face was blocked;

ii. The diameter and thickness of each specimen was measured to the nearest 0.02 mm using a vernier calliper at 4 points that are equally spaced around the perimeter of the specimen and recorded. The average of the four readings was determined and recorded to the nearest 0.02 mm;

iii. Ten layers of paper towel were placed on the plastic tray;

iv. A solution of water saturated with calcium hydroxide (referred to as calcium hydroxide hereafter) was poured into the tray. Care was taken to ensure that the paper towel is saturated and water is visible on the top surface. All air bubbles were removed by smoothing the paper pad towards the edges of the tray. The final level of the solution was slightly above the bottom edge and a maximum 2 mm up the side of the specimen. An additional piece of paper that was used to remove excess water from the specimen was dampened and kept next to the tray to be used during the test;

v. Within 30 minutes from their removal from the desiccator, the specimens were placed with their test face (outer face originally exposed face) on the wet paper pad and a stop watch started. The time of starting the stopwatch was recorded as time t_o;

vi. Each specimen was weighed at 3, 5, 7, 9, 12, 16, 20, and 25 minutes, after patting it once on the damp piece of absorbent paper. Care was taken to ensure that the specimen appeared as saturated surface dry (SSD) on the exposed face at the time the mass was determined. Care was also taken to prevent the dripping of the

solution from one specimen onto the top of another during removal from the tray for weighing;

vii. The mass of the specimen was recorded to the nearest 0.01 g within 10 seconds of removal of the specimen from the tray and wiping excess water. The specimens were replaced each time with the test face on the wet paper. The stopwatch was not stopped during the entire weighing procedure;

viii. At the end of the weighing of the specimen, each specimen was placed in a vacuum saturation tank with the tape in place. The specimens were arranged in the tank by standing them upon their curved edges rather than on their flat side. The lid of the tank was sealed with petroleum jelly and closed;

ix. The tank was evacuated to between -75 and -80 kPa and the specimens maintained under a vacuum of between -75 and -80 kPa for 3 hoursb± 15 minutes. The pressure was not allowed to rise above -75 kPa during this period;

x. After 3 hours ± 15 minutes, the tank was isolated and calcium hydroxide saturated water allowed to flow into the chamber until the water level was approximately 40 mm above the top of the specimens. Care was taken to ensure that air does not enter the vacuum chamber during this procedure;

xi. The vacuum was re-established between -75 and -80 kPa. This pressure was maintained for 1 hour ± 15 minutes. Care was taken to ensure that the vacuum does not rise above -75 kPa during this time;

xii. After 1 hour ± 15 minutes, the vacuum was released and air allowed to enter. Thereafter, the specimens were soaked for further 18 ± 1 hours;

xiii. The specimens were removed from the solution after 18 ± 1 hour of soaking. The surface of each specimen was dried to a saturated surface dry (SSD) condition with a paper towel and immediately weighed to an accuracy of 0.01 g. This mass was recorded as the vacuum saturated mass M_{sv}.

Appendix C

TEST RESULTS

The results from the experiments are presented within this section. Throughout the tables within this subsection, the following terminology has been used: Comp = compressive strength; Avg. = average; Std. Dev = standard deviation.

C.1 Consistence

The consistence of the mixes under investigation was assessed using the slump test (in phase one) and flow test (in phase two). The results from these tests are hereby presented.

TABLE C.1: Flow of mortar mixes (phase two)

Mix ID	**Flow (%)**
C250_P0	50
C230_P0	50
C210_P0	45
C225_P0	66
C250_P1-10	87
C250_P2-10	83
C250_P1-15	87
C250_P1-20	91

TABLE C.2: Slump test results (phase one)

Mix ID	**SP dosage (ml) per 35 l batch**	**Slump (mm)**
1	0	70
2	500	190
3	0	170
4	70	70
5	50	100
6	50	135
7	0	150
8	330	190
9	0	140
10	40	60
11	0	Collapse
12	0	Collapse
13	400	70
14	0	70
15	60	65
16	80	145
17	290	145
18	200	75
19	390	120
20	70	100
21	100	220
22	100	150
23	0	160
24	0	Collapse
25	0	Collapse
26	0	Collapse
27	620	210
28	70	90
29	0	Collapse
30	120	155
31	85	120
32	300	80

C.2 Compressive strength

TABLE C.3: 3-day compressive strength test results (phase one)

Mix ID		Saturated mass (g)	Density (kg/m^3)	Failure load (kN)	Comp. strength (MPa)	Avg. comp. strength (MPa)
	1	2095	2095	72	7.2	
1	2	2110	2110	73	7.3	7.3
	3	2135	2135	75	7.5	
	1	2320	2320	186	18.6	
2	2	2280	2280	184	18.4	18.5
	3	2305	2305	185	18.5	
	1	2245	2245	101	10.1	
3	2	2240	2240	98	9.8	10.0
	3	2230	2230	100	10.0	
	1	2150	2150	91	9.1	
4	2	2170	2170	92	9.2	9.2
	3	2180	2180	92	9.2	
	1	2170	2170	56	5.6	
5	2	2180	2180	56	5.6	5.6
	3	2150	2150	55	5.5	
	1	2295	2295	119	11.9	
6	2	2200	2200	116	11.6	11.8
	3	2280	2280	118	11.8	
	1	2115	2115	16	1.6	
7	2	2160	2160	18	1.8	1.6
	3	2150	2150	15	1.5	
	1	2250	2250	110	11.0	
8	2	2205	2205	114	11.4	11.2
	3	2220	2220	112	11.2	
	1	2250	2250	287	28.7	
9	2	2270	2270	289	28.9	28.7
	3	2280	2280	285	28.5	
	1	2160	2160	171	17.1	
10	2	2145	2145	173	17.3	17.2
	3	2135	2135	172	17.2	
	1	2270	2270	183	18.3	
11	2	2230	2230	185	18.5	18.4
	3	2250	2250	184	18.4	
	1	2155	2155	58	5.8	
12	2	2175	2175	60	6.0	5.9
	3	2160	2160	59	5.9	
	1	2155	2155	115	11.5	
13	2	2160	2160	109	10.9	11.2
	3	2140	2140	112	11.2	
	1	2105	2105	22	2.2	
14	2	2130	2130	25	2.5	2.4
	3	2100	2100	24	2.4	
	1	2200	2200	175	17.5	
15	2	2255	2255	176	17.6	17.6
	3	2230	2230	177	17.7	

TABLE C.4: 3-day compressive strength test results (phase one) - cont'd

Mix ID		Saturated mass (g)	Density (kg/m^3)	Failure load (kN)	Comp. strength (MPa)	Avg. comp. strength (MPa)
	1	2240	2240	32	3.2	
16	2	2220	2220	33	3.3	3.3
	3	2260	2260	33	3.3	
	1	2260	2260	294	29.4	
17	2	2305	2305	299	29.9	29.6
	3	2290	2290	295	29.5	
	1	2230	2230	37	3.7	
18	2	2135	2135	35	3.5	3.6
	3	2200	2200	36	3.6	
	1	2250	2250	82	8.2	
19	2	2215	2215	86	8.6	8.4
	3	2230	2230	84	8.4	
	1	2165	2165	46	4.6	
20	2	2160	2160	42	4.2	4.4
	3	2150	2150	44	4.4	
	1	2360	2360	279	27.9	
21	2	2310	2310	275	27.5	27.9
	3	2340	2340	282	28.2	
	1	2275	2275	209	20.9	
22	2	2250	2250	209	20.9	20.9
	3	2260	2260	209	20.9	
	1	2175	2175	46	4.6	
23	2	2185	2185	45	4.5	4.6
	3	2160	2160	46	4.6	
	1	2225	2225	21	2.1	
24	2	2145	2145	22	2.2	2.2
	3	2190	2190	22	2.2	
	1	2245	2245	76	7.6	
25	2	2165	2165	72	7.2	7.4
	3	2200	2200	74	7.4	
	1	2110	2110	54	5.4	
26	2	2180	2180	58	5.8	5.6
	3	2150	2150	56	5.6	
	1	2280	2280	354	35.4	
27	2	2275	2275	346	34.6	35.0
	3	2260	2260	350	35.0	
	1	2185	2185	116	11.6	
28	2	2175	2175	124	12.4	12.0
	3	2170	2170	120	12.0	
	1	2120	2120	15	1.5	
29	2	2115	2115	15	1.5	1.5
	3	2100	2100	15	1.5	
	1	2190	2190	420	42.0	
30	2	2345	2345	426	42.6	42.3
	3	2250	2250	423	42.3	
	1	2145	2145	250	25.0	
31	2	2190	2190	252	25.2	25.2
	3	2155	2155	254	25.4	
	1	2140	2140	39	3.9	
32	2	2205	2205	41	4.1	4.0
	3	2180	2180	40	4.0	

TABLE C.5: 7-day compressive strength test results (phase one)

Mix ID		Saturated mass (g)	Density (kg/m^3)	Failure load (kN)	Comp. strength (MPa)	Avg. comp. strength (MPa)
1	1	2145	2145	104	10.4	10.5
	2	2110	2110	106	10.6	
	3	2130	2130	105	10.5	
2	1	2290	2290	360	36.0	35.8
	2	2310	2310	358	35.8	
	3	2235	2235	356	35.6	
3	1	2255	2255	195	19.5	19.6
	2	2245	2245	194	19.4	
	3	2230	2230	200	20.0	
4	1	2200	2200	190	19.0	19.2
	2	2155	2155	194	19.4	
	3	2180	2165	193	19.3	
5	1	2165	2165	126	12.6	12.6
	2	2135	2135	125	12.5	
	3	2165	2165	128	12.8	
6	1	2300	2300	238	23.8	23.9
	2	2285	2285	243	24.3	
	3	2340	2340	236	23.6	
7	1	2095	2095	39	3.9	3.9
	2	2115	2115	38	3.8	
	3	2110	2110	39	3.9	
8	1	2240	2240	238	23.8	23.6
	2	2250	2250	234	23.4	
	3	2220	2220	236	23.6	
9	1	2160	2160	347	34.7	34.7
	2	2230	2230	343	34.3	
	3	2220	2220	351	35.1	
10	1	2225	2225	248	24.8	24.9
	2	2230	2230	250	25.0	
	3	2210	2210	250	25.0	
11	1	2240	2240	249	24.9	25.0
	2	2235	2235	248	24.8	
	3	2205	2205	253	25.3	
12	1	2160	2160	97	9.7	9.9
	2	2155	2155	100	10.0	
	3	2170	2170	99	9.9	
13	1	2185	2185	160	16.0	16.1
	2	2195	2195	158	15.8	
	3	2210	2210	164	16.4	
14	1	2150	2150	51	5.1	5.3
	2	2180	2180	55	5.5	
	3	2170	2170	53	5.3	
15	1	2245	2245	208	20.8	21.2
	2	2280	2280	215	21.5	
	3	2260	2260	212	21.2	
16	1	2165	2165	86	8.6	8.6
	2	2210	2210	85	8.5	
	3	2180	2180	86	8.6	

TABLE C.6: 7-day compressive strength test results (phase one) contd

Mix ID		Saturated mass (g)	Density (kg/m^3)	Failure load (kN)	Comp. strength (MPa)	Avg. comp. strength (MPa)
	1	2225	2225	362	36.2	
17	2	2285	2285	357	35.7	36.8
	3	2240	2240	360	36.0	
	1	2170	2170	80	8.0	
18	2	2145	2145	80	8.0	8.0
	3	2150	2150	80	8.0	
	1	2240	2240	127	12.7	
19	2	2225	2225	129	12.9	12.8
	3	2230	2230	128	12.8	
	1	2205	2205	104	10.4	
20	2	2155	2155	100	10.0	10.1
	3	2180	2180	100	10.0	
	1	2335	2335	369	36.9	
21	2	2285	2285	375	37.5	37.0
	3	2305	2305	367	36.7	
	1	2230	2230	396	39.6	
22	2	2245	2245	388	38.8	39.2
	3	2255	2255	392	39.2	
	1	2180	2180	107	10.7	
23	2	2150	2150	109	10.9	11.0
	3	2165	2165	115	11.5	
	1	2175	2175	50	5.0	
24	2	2105	2105	50	5.0	5.0
	3	2150	2150	50	5.0	
	1	2230	2230	118	11.8	
25	2	2235	2235	115	11.5	11.7
	3	2220	2220	117	11.7	
	1	2135	2135	93	9.3	
26	2	2165	2165	93	9.3	9.3
	3	2170	2170	93	9.3	
	1	2290	2290	445	44.5	
27	2	2270	2270	439	43.9	44.1
	3	2265	2265	438	43.8	
	1	2235	2235	156	15.6	
28	2	2130	2130	155	15.5	15.8
	3	2190	2190	156	15.6	
	1	2210	2210	43	4.3	
29	2	2190	2190	43	4.3	4.3
	3	2195	2195	43	4.3	
	1	2315	2315	510	51.0	
30	2	2280	2280	515	51.5	51.1
	3	2300	2300	507	50.7	
	1	2205	2205	319	31.9	
31	2	2115	2115	314	31.4	31.9
	3	2185	2185	323	32.3	
	1	2165	2165	98	9.8	
32	2	2225	2225	96	9.6	10.2
	3	2180	2180	105	10.5	

TABLE C.7: 28-day compressive strength test results (phase one)

Mix ID		Saturated mass (g)	Density (kg/m^o)	Failure load (kN)	Comp. strength (MPa)	Avg. comp. strength (MPa)
	1	2145	2145	138	13.8	
1	2	2140	2140	132	13.2	13.5
	3	2135	2135	135	13.5	
	1	2320	2320	566	56.6	
2	2	2295	2295	568	56.8	56.5
	3	2290	2290	560	56.0	
	1	2280	2280	427	42.7	
3	2	2255	2255	420	42.0	42.4
	3	2265	2265	424	42.4	
	1	2165	2165	384	38.4	
4	2	2185	2185	384	38.4	38.2
	3	2155	2155	378	37.8	
	1	2205	2205	294	29.4	
5	2	2145	2145	296	29.6	29.3
	3	2195	2195	290	29.0	
	1	2330	2330	464	46.4	
6	2	2320	2320	454	45.4	45.9
	3	2325	2325	459	45.9	
	1	2095	2095	102	10.2	
7	2	2130	2130	105	10.5	10.4
	3	2110	2110	104	10.4	
	1	2270	2270	458	45.8	
8	2	2260	2260	452	45.2	45.7
	3	2265	2265	460	46.0	
	1	2245	2245	397	39.7	
9	2	2205	2205	392	39.2	39.3
	3	2160	2160	389	38.9	
	1	2275	2275	318	31.8	
10	2	2215	2215	322	32.2	32.2
	3	2220	2220	326	32.6	
	1	2230	2230	332	33.2	
11	2	2230	2230	329	32.9	33.3
	3	2230	2230	337	33.7	
	1	2195	2195	134	13.4	
12	2	2155	2155	130	13.0	12.9
	3	2130	2130	122	12.2	
	1	2200	2200	190	19.0	
13	2	2145	2145	198	19.8	19.5
	3	2205	2205	196	19.6	
	1	2075	2075	122	12.2	
14	2	2100	2100	130	13.0	12.5
	3	2080	2080	122	12.2	
	1	2250	2250	250	25.0	
15	2	2255	2255	260	26.0	25.5
	3	2235	2235	254	25.4	
	1	2165	2165	209	20.9	
16	2	2185	2185	212	21.2	21.2
	3	2215	2215	216	21.6	

TABLE C.8: 28-day compressive strength test results (phase one) contd

Mix ID		Saturated mass (g)	Density (kg/m^3)	Failure load (kN)	Comp. strength (MPa)	Avg. comp. strength (MPa)
	1	2265	2265	460	46.0	
17	2	2265	2265	458	45.8	45.7
	3	2335	2335	452	45.2	
	1	2170	2170	174	17.4	
18	2	2195	2195	172	17.2	17.3
	3	2170	2170	172	17.2	
	1	2210	2210	176	17.6	
19	2	2195	2195	170	17.0	17.2
	3	2250	2250	170	17.0	
	1	2135	2135	240	24.0	
20	2	2130	2130	238	23.8	23.7
	3	2075	2075	234	23.4	
	1	2260	2260	442	44.2	
21	2	2280	2280	436	43.6	44.1
	3	2350	2350	446	44.6	
	1	2320	2320	631	63.1	
22	2	2355	2355	626	62.6	62.7
	3	2250	2250	624	62.4	
	1	2185	2185	274	27.4	
23	2	2190	2190	280	28.0	27.5
	3	2195	2195	270	27.0	
	1	2115	2115	139	13.9	
24	2	2195	2195	142	14.2	13.9
	3	2175	2175	135	13.5	
	1	2185	2185	150	15.0	
25	2	2195	2195	152	15.2	15.0
	3	2215	2215	147	14.7	
	1	2150	2150	127	12.7	
26	2	2135	2135	128	12.8	12.6
	3	2180	2180	123	12.3	
	1	2145	2145	509	50.9	
27	2	2220	2220	512	51.2	51.2
	3	2135	2135	515	51.5	
	1	2255	2255	194	19.4	
28	2	2200	2200	190	19.0	19.4
	3	2205	2205	198	19.8	
	1	2160	2160	119	11.9	
29	2	2205	2205	110	11.0	11.5
	3	2175	2175	115	11.5	
	1	2330	2330	570	57.0	
30	2	2315	2315	575	57.5	57.5
	3	2335	2335	580	58.0	
	1	1990	1990	358	35.8	
31	2	2035	2035	352	35.2	35.3
	3	1980	1980	349	34.9	
	1	2090	2090	192	19.2	
32	2	2125	2125	188	18.8	19.1
	3	2070	2070	194	19.4	

TABLE C.9: 3-day compressive strength test results (phase two)

Mix ID		**Saturated mass (g)**	**Density (kg/m^3)**	**Failure load (kN)**	**Comp. strength (MPa)**	**Avg. comp. strength (MPa)**
C250_P0	1	2180	2180	80	8.0	8.1
	2	2210	2210	83	8.3	
	3	2175	2175	80	8.0	
C230_P0	1	2205	2205	86	8.6	8.6
	2	2260	2260	87	8.7	
	3	2220	2220	85	8.5	
C210_P0	1	2265	2265	58	5.8	5.8
	2	2300	2300	61	6.1	
	3	2225	2225	56	5.6	
C225_P0	1	2205	2205	62	6.2	6.0
	2	2210	2210	59	5.9	
	3	2165	2165	59	5.9	
C250_P1-10	1	2155	2155	57	5.7	5.7
	2	2135	2135	60	6.0	
	3	2010	2010	53	5.3	
C250_P2-10	1	2245	2245	73	7.3	7.0
	2	2265	2265	68	6.8	
	3	2280	2280	69	6.9	
C250_P1-15	1	2195	2195	40	4.0	3.9
	2	2170	2170	40	4.0	
	3	2100	2100	38	3.8	
C250_P1-20	1	2175	2175	33	3.3	3.3
	2	2010	2010	31	3.1	
	3	2020	2020	35	3.5	

TABLE C.10: 7-day compressive strength test results (phase two)

Mix ID		**Saturated mass (g)**	**Density (kg/m^3)**	**Failure load (kN)**	**Comp. strength (MPa)**	**Avg. comp. strength (MPa)**
C250_P0	1	2260	2260	140	14.0	14.4
	2	2250	2250	146	14.6	
	3	2265	2265	146	14.6	
C230_P0	1	2310	2130	142	14.2	14.6
	2	2275	2275	146	14.6	
	3	2285	2285	149	14.9	
C210_P0	1	2290	2290	132	13.2	13.4
	2	2300	2300	136	13.6	
	3	2275	2275	134	13.4	
C225_P0	1	2230	2230	141	14.1	14.0
	2	2220	2220	137	13.7	
	3	2270	2270	141	14.1	
C250_P1-10	1	2125	2125	105	10.5	10.5
	2	2125	2125	108	10.8	
	3	2085	2085	101	10.1	
C250_P2-10	1	2150	2150	111	11.1	11.4
	2	2190	2190	115	11.5	
	3	2200	2200	115	11.5	
C250_P1-15	1	2090	2090	78	7.8	7.5
	2	2025	2025	71	7.1	
	3	2080	2080	75	7.5	
C250_P1-20	1	2015	2015	53	5.3	5.5
	2	2035	2035	57	5.7	
	3	2080	2080	55	5.5	

TABLE C.11: 28-day compressive strength test results (phase two)

Mix ID		Saturated mass (g)	Density (kg/m^3)	Failure load (kN)	Comp. strength (MPa)	Avg. comp. strength (MPa)
C250_P0	1	2320	2320	187	18.7	18.6
	2	2265	2265	189	18.9	
	3	2295	2295	183	18.3	
C230_P0	1	2270	2270	181	18.1	18.5
	2	2295	2295	188	18.8	
	3	2260	2260	187	18.7	
C210_P0	1	2285	2285	189	18.9	18.8
	2	2250	2250	188	18.8	
	3	2265	2265	187	18.7	
C225_P0	1	2240	2240	183	18.3	18.5
	2	2255	2255	184	18.4	
	3	2295	2295	187	18.7	
C250_P1-10	1	2170	2170	133	13.3	13.3
	2	2210	2210	130	13.0	
	3	2165	2165	136	13.6	
C250_P2-10	1	2180	2180	156	15.6	15.5
	2	2160	2160	157	15.7	
	3	2215	2215	151	15.1	
C250_P1-15	1	2210	2210	128	12.8	12.8
	2	2110	2110	125	12.5	
	3	2185	2185	130	13.0	
C250_P1-20	1	2135	2135	113	11.3	11.5
	2	2205	2205	117	11.7	
	3	2115	2115	114	11.4	

C.3 Direct tensile strength

The direct tensile strength tests were conducted on dog-bone specimens at 3, 7 and 28 days. The test results are hereby presented.

TABLE C.12: 3-day direct tensile strength test results (phase two)

Mix ID		**Tensile strength (MPa)**	**Avg. tensile strength MPa)**	**Std. Dev**
C250_P0	1	1.200	1.211	0.03
	2	1.189		
	3	1.243		
C230_P0	1	1.083	1.096	0.03
	2	1.126		
	3	1.080		
C210_P0	1	0.752	0.788	0.04
	2	0.790		
	3	0.823		
C225_P0	1	0.736	0.727	0.01
	2	0.733		
	3	0.713		
C250_P1-10	1	0.724	0.715	0.01
	2	0.703		
	3	0.718		
C250_P2-10	1	0.790	0.790	0
	2	0.795		
	3	0.786		
C250_P1-15	1	0.622	0.609	0.01
	2	0.600		
	3	0.605		
C250_P1-20	1	0.319	0.342	0.02
	2	0.348		
	3	0.358		

TABLE C.13: 7-day direct tensile strength test results (phase two)

Mix ID		**Tensile strength (MPa)**	**Avg. tensile strength (MPa)**	**Std. Dev**
C250_P0	1	1.672	1.695	0.02
	2	1.699		
	3	1.715		
C230_P0	1	1.622	1.650	0.04
	2	1.650		
	3	1.701		
C210_P0	1	1.476	1.483	0.03
	2	1.513		
	3	1.459		
C225_P0	1	1.478	1.500	0.02
	2	1.508		
	3	1.514		
C250_P1-10	1	1.229	1.236	0.02
	2	1.223		
	3	1.255		
C250_P2-10	1	1.624	1.616	0.01
	2	1.599		
	3	1.625		
C250_P1-15	1	1.070	1.042	0.03
	2	1.039		
	3	1.018		
C250_P1-20	1	0.885	0.881	0.01
	2	0.892		
	3	0.867		

TABLE C.14: 28-day direct tensile strength test results (phase two)

Mix ID		Tensile strength (MPa)	Avg. tensile strength (MPa)	Std. Dev
C250_P0	1	2.675	2.653	0.08
	2	2.717		
	3	2.567		
C230_P0	1	2.680	2.675	0.06
	2	2.615		
	3	2.729		
C210_P0	1	1.686	1.701	0.02
	2	1.719		
	3	1.698		
C225_P0	1	1.713	1.642	0.08
	2	1.557		
	3	1.656		
C250_P1-10	1	1.767	1.764	0.02
	2	1.785		
	3	1.740		
C250_P2-10	1	2.277	2.291	0.02
	2	2.285		
	3	2.312		
C250_P1-15	1	1.471	1.471	0.01
	2	1.479		
	3	1.464		
C250_P1-20	1	1.356	1.348	0.02
	2	1.326		
	3	1.361		

C.4 Static modulus of elasticity

The static modulus of elasticity in compression test results at 7 and 28 days are hereby presented.

TABLE C.15: 7-day elastic modulus test results (phase two)

Mix ID		**Elastic modulus (GPa)**	**Avg. elastic modulus (GPa)**	**Std. Dev**
C250_P0	1	18.5	18.14	0.35
	2	18.0		
	3	17.9		
C230_P0	1	16.4	16.09	0.30
	2	15.8		
	3	16.1		
C210_P0	1	14.4	14.22	0.19
	2	14.0		
	3	14.2		
C225_P0	1	13.8	14.09	0.29
	2	14.4		
	3	14.1		
C250_P1-10	1	10.8	10.80	0.39
	2	11.2		
	3	10.4		
C250_P2-10	1	13.0	13.40	0.39
	2	13.8		
	3	13.4		
C250_P1-15	1	10.8	10.47	0.32
	2	10.3		
	3	10.3		
C250_P1-20	1	8.1	8.13	0.40
	2	7.7		
	3	8.5		

TABLE C.16: 28-day elastic modulus test results (phase two)

Mix ID		Elastic modulus (GPa)	Avg. elastic modulus (GPa)	Std. Dev
C250_P0	1	20.5	20.63	0.48
	2	21.2		
	3	20.2		
C230_P0	1	18.9	18.84	0.03
	2	18.8		
	3	18.8		
C210_P0	1	16.8	16.76	0.25
	2	16.5		
	3	17.0		
C225_P0	1	17.0	16.55	0.37
	2	16.5		
	3	16.2		
C250_P1-10	1	14.3	14.47	0.40
	2	14.9		
	3	14.2		
C250_P2-10	1	15.7	15.39	0.33
	2	15.1		
	3	15.4		
C250_P1-15	1	14.8	14.84	0.35
	2	14.5		
	3	15.2		
C250_P1-20	1	11.8	12.00	0.16
	2	12.2		
	3	12.0		

C.5 Drying shrinkage

The drying shrinkage of each test mix was monitored over a period of 56 days from the date of casting. The shrinkage measurements began after 7 days from the date of casting. The test results are hereby presented.

TABLE C.17: Drying shrinkage test results (phase two)

Age (days)	**Drying shrinkage (microstrains)**							
	C250_ P0	C230_ P0	C210_ P0	C225_ P0	C250_ P1-10	C250_ P2-10	C250_ P1-15	C250_ P1-20
7	0	0	0	0	0	0	0	0
8	55	46	40	33	57	35	50	40
9	110	093	80	67	113	70	100	80
10	127	108	82	83	125	85	113	98
11	143	123	83	90	137	100	127	117
12	150	133	85	100	142	110	140	132
13	157	143	87	110	147	120	153	147
14	165	148	92	117	152	130	162	158
15	173	153	97	123	157	140	170	170
16	172	165	100	125	168	152	187	178
17	170	177	103	127	180	163	203	187
18	178	190	108	140	187	165	202	187
19	187	203	113	153	193	167	200	187
20	188	207	117	157	198	167	201	193
21	190	210	120	160	203	167	203	200
22	190	222	120	160	202	169	208	207
23	190	233	120	160	200	170	213	213
24	190	225	125	165	215	175	222	223
25	190	217	130	170	230	180	230	233
26	190	220	133	172	242	190	238	248
27	190	223	137	173	253	198	247	263
28	200	227	142	180	268	207	255	282
29	210	230	147	187	283	218	263	300
30	207	232	158	192	300	230	272	308
31	203	233	170	197	317	242	280	317
32	213	253	178	207	335	253	293	335
33	223	273	187	217	353	288	307	353
34	233	282	197	222	365	323	338	367
35	243	290	207	227	377	325	370	380
36	263	304	223	242	381	327	376	388
37	282	318	240	257	385	328	382	395
38	301	333	257	272	389	330	388	403
39	320	347	273	287	393	343	393	410
40	335	353	278	292	400	357	408	423
41	350	360	283	297	407	350	423	437
42	351	361	289	302	408	343	417	433
43	352	362	294	308	410	337	410	430
44	353	363	300	313	397	350	403	427
45	357	367	297	313	402	347	423	423
46	352	362	293	307	407	343	417	430
47	347	357	290	300	418	353	410	437

TABLE C.18: Drying shrinkage test results (phase two) contd

Age (days)	**Drying shrinkage (microstrains)**							
	C250_ P0	C230_ P0	C210_ P0	C225_ P0	C250_ P1-10	C250_ P2-10	C250_ P1-15	C250_ P1-20
48	353	362	292	303	418	363	423	442
49	360	367	293	307	430	362	426	447
50	357	370	300	315	430	360	430	463
51	353	373	307	323	430	372	445	480
52	373	385	312	325	445	383	460	488
53	393	397	317	327	460	382	470	497
54	390	393	317	335	453	380	480	495
55	387	390	317	343	447	380	471	493
56	385	395	317	347	450	380	476	495

C.6 Tensile relaxation

The 48-hour tensile relaxation test results at 3, 7 and 28 days are hereby presented.

TABLE C.19: 48-hour tensile relaxation test results at 3 days (phase two)

Mix ID		**Tensile relaxation (%)**	**Avg. tensile relaxation (%)**	**Std. Dev**
C250_P0	1	53.78	52.88	1.28
	2	51.97		
C230_P0	1	54.09	55.32	1.73
	2	56.54		
C210_P0	1	45.33	46.76	2.02
	2	48.19		
C225_P0	1	55.87	54.11	2.49
	2	52.35		
C250_P1-10	1	58.84	57.59	1.77
	2	56.34		
C250_P2-10	1	53.26	51.77	2.11
	2	50.27		
C250_P1-15	1	59.64	58.57	1.52
	2	57.49		
C250_P1-20	1	80.72	81.31	0.83
	2	81.89		

TABLE C.20: 48-hour tensile relaxation test results at 7 days (phase two)

Mix ID		Tensile relaxation (%)	Avg. tensile relaxation (%)	Std. Dev
C250_P0	1	38.76	37.51	1.77
	2	36.25		
C230_P0	1	38.63	37.05	2.24
	2	35.46		
C210_P0	1	38.60	37.92	0.96
	2	37.24		
C225_P0	1	38.59	37.53	1.50
	2	36.47		
C250_P1-10	1	46.30	47.15	1.20
	2	48.00		
C250_P2-10	1	39.61	41.06	2.05
	2	42.51		
C250_P1-15	1	54.85	53.01	2.60
	2	51.17		
C250_P1-20	1	56.75	56.25	0.71
	2	55.75		

TABLE C.21: 48-hour tensile relaxation test results at 28 days (phase two)

Mix ID		Tensile relaxation (%)	Avg. tensile relaxation (%)	Std. Dev
C250_P0	1	30.38	30.85	0.66
	2	31.32		
C230_P0	1	28.00	30.02	2.88
	2	32.04		
C210_P0	1	32.01	31.14	1.24
	2	30.26		
C225_P0	1	36.80	35.27	2.16
	2	33.74		
C250_P1-10	1	36.26	36.75	0.69
	2	37.23		
C250_P2-10	1	38.84	37.26	2.23
	2	35.68		
C250_P1-15	1	39.50	40.40	1.27
	2	41.30		
C250_P1-20	1	49.37	47.42	2.76
	2	45.47		

C.7 Restrained shrinkage

The results from restrained shrinkage cracking are hereby presented.

TABLE C.22: Restrained shrinkage test results (phase one)

Mix ID		**Crack width (mm)**		**Age at cracking (days)**		
		Measured	Mean	Measured	Mean	Std. Dev
1	1	0.56	0.38	15	16.00	1.00
	2	0.35		17		
	3	0.22		16		
2	1	1.35	1.46	12	11.00	1.00
	2	1.63		11		
	3	1.41		10		
3	1	0.40	0.54	11	10.33	0.58
	2	0.62		10		
	3	0.60		10		
4	1	0.95	1.01	12	11.33	0.58
	2	1.10		11		
	3	0.97		11		
5	1	0.08	0.09	18	15.67	2.08
	2	0.11		14		
	3	0.09		15		
6	1	0.71	0.65	12	12.00	1.00
	2	0.60		13		
	3	0.65		11		
7	1	0.35	0.45	20	21.00	1.73
	2	0.60		20		
	3	0.40		23		
8	1	0.52	0.37	16	16.67	1.15
	2	0.80		18		
	3	0.35		16		
9	1	1.58	1.31	9	9.00	0
	2	0.81		9		
	3	1.55		9		
10	1	0.52	0.56	15	15.00	0
	2	0.80		15		
	3	0.35		15		
11	1	0.23	0.55	13	12.67	0.58
	2	0.85		13		
	3	0.58		12		
12	1	0.35	0.37	17	18.67	1.53
	2	0.50		19		
	3	0.25		20		
13	1	0.19	0.14	16	15.67	1.15
	2	0.11		15		
	3	0.14		16		
14	1	0.33	0.50	18	16.33	1.15
	2	0.65		15		
	3	0.52		16		
15	1	0.10	0.10	15	15.67	1.53
	2	0.12		17		
	3	0.08		15		
16	1	0.07	0.08	13	13.67	0.58
	2	0.07		15		
	3	0.09		13		

TABLE C.23: Restrained shrinkage test results (phase one) contd

Mix ID		**Crack width (mm)**		**Age at cracking (days)**		
		Measured	Mean	Measured	Mean	Std. Dev
	1	0.65		32		
17	2	1.06	0.90	34	32.33	1.53
	3	1.00		31		
	1	0.05		20		
18	2	0.05	0.05	21	20.33	0.58
	3	0.04		20		
	1	0.05		27		
19	2	0.06	0.05	28	28.00	1.00
	3	0.05		29		
	1	0.12		12		
20	2	0.10	0.10	14	13.00	1.00
	3	0.08		13		
	1	0.14		21		
21	2	0.15	0.13	18	18.67	2.08
	3	0.10		17		
	1	1.97		9		
22	2	1.20	1.73	9	9.00	0
	3	2.03		9		
	1	0.30		11		
23	2	0.28	0.37	12	11.67	0.58
	3	0.52		12		
	1	0.24		14		
24	2	0.42	0.42	12	13.33	0.58
	3	0.60		13		
	1	0.50		14		
25	2	0.35	0.52	15	14.33	0.58
	3	0.70		14		
	1	0.09		24		
26	2	0.08	0.08	27	25.33	1.53
	3	0.07		25		
	1	0.08		10		
27	2	0.08	0.09	10	10.00	0
	3	0.12		10		
	1	0.08		26		
28	2	0.10	0.11	29	29.00	3.00
	3	0.16		32		
	1	0.06		15		
29	2	0.09	0.09	15	16.00	1.73
	3	0.12		18		
	1	0.72		9		
30	2	0.75	0.89	9	8.67	0.58
	3	1.20		8		
	1	2.53		10		
31	2	2.07	2.04	9	9.33	0.58
	3	1.51		9		
	1	0.09		14		
32	2	0.06	0.07	13	13.00	1.00
	3	0.07		12		

TABLE C.24: Restrained shrinkage test results (phase two)

Mix ID		Crack width (mm)		Age at cracking (days)		
		Measured	Mean	Measured	Mean	Std. Dev
C250_P0	1	0.17	0.32	31	29.33	1.53
	2	0.13		28		
	3	0.67		29		
C230_P0	1	0.07	0.10	21	20.67	0.58
	2	0.17		21		
	3	0.07		20		
C210_P0	1	0.06	0.11	19	18.67	0.58
	2	0.15		18		
	3	0.11		19		
C225_P0	1	0.14	0.10	17	17.67	0.58
	2	0.07		18		
	3	0.09		18		
C250_P1-10	1	0.07	0.05	34	35.00	1.00
	2	0.06		36		
	3	0.02		35		
C250_P2-10	1	0.17	0.17	27	29.00	2.00
	2	0.10		29		
	3	0.24		31		
C250_P1-15	1	0.11	0.12	31	32.67	1.53
	2	0.07		33		
	3	0.17		34		
C250_P1-20	1	0.11	0.07	42	44.00	2.00
	2	0.05		46		
	3	0.06		44		

C.8 Durability indexes

The results from durability index (DI) tests are summarised in Table C.25.

TABLE C.25: Durability Index test results (phase two)

Mix ID	Durability Index		Porosity (%)
	OPI*	WSI (mm/hr$^{0.5}$)*	
C250_P0	10.3	4.2	16.89
C230_P0	9.6	7.1	16.06
C210_P0	9.2	9.0	17.92
C225_P0	9.4	6.1	17.01
C250_P1-10	10.0	3.0	18.57
C250_P2-10	10.4	2.9	14.66
C250_P1-15	10.3	1.7	19.04
C250_P1-20	10.4	1.9	14.66

* Mean durability index value from four test specimens

Appendix D

DATA ANALYSIS TECHNIQUES

The results from this study were analysed using several statistical techniques. These techniques, and the corresponding results are hereby presented.

D.1 Factorial analysis

The factorial analysis of the mix design parameters in phase one are presented in Table D.1. The normal plots, main effects plots and interaction effects plots at a level of significance of $\alpha = 0.05$ are hereby presented in Figure D.1, Figure D.2 and Figure D.3.

TABLE D.1: Estimated effects and coefficients for age at cracking ($\alpha = 0.05$)

Term	**Effect**	**Coefficient**	**SE Coeff**	**T**	**p-Value**
Constant	-	15.708	0.1228	127.91	0.000
A	-3.375	-1.688	0.1228	-13.74	0.000
B	-1.917	-0.958	0.1228	-7.80	0.000
C	-4.750	-2.375	0.1228	-19.34	0.000
D	3.208	1.604	0.1228	13.06	0.000
E	6.917	3.458	0.1228	28.16	0.000
AB	2.792	1.396	0.1228	11.37	0.000
AC	1.125	0.563	0.1228	4.58	0.000
AD	0.083	0.042	0.1228	0.34	0.736
AE	-3.208	-1.604	0.1228	-13.06	0.000
BC	-1.000	-0.500	0.1228	-4.07	0.000
BD	-0.208	-0.104	0.1228	-0.85	0.399
BE	-2.417	-1.208	0.1228	-9.84	0.000
CD	0.458	0.229	0.1228	1.87	0.067
CE	0.083	0.042	0.1228	0.34	0.736
DE	2.042	1.021	0.1228	8.31	0.000
ABC	0.208	0.104	0.1228	0.85	0.399
ABD	0.167	0.083	0.1228	0.68	0.500
ABE	1.958	0.979	0.1228	7.97	0.000
ACD	-0.833	-0.417	0.1228	-3.39	0.001
ACE	-0.208	-0.104	0.1228	-0.85	0.399
ADE	-0.250	-0.125	0.1228	-1.02	0.313
BCD	-1.542	-0.771	0.1228	-6.28	0.000
BCE	-0.833	-0.417	0.1228	-3.39	0.001
BDE	-0.542	-0.271	0.1228	-2.21	0.031
CDE	0.458	0.229	0.1228	1.87	0.067
ABCD	1.167	0.583	0.1228	4.75	0.000
ABCE	0.542	0.271	0.1228	2.21	0.031
ABDE	0.000	0.000	0.1228	0.00	1.000
ACDE	-0.833	-0.417	0.1228	-3.39	0.001
BCDE	-0.708	-0.354	0.1228	-2.88	0.005
ABCDE	1.333	0.667	0.1228	5.43	0.000

NOTE: A = binder type; B = water content; C = binder content; D =curing method; E = SRA dosage. SE Coef = Standard error in the coefficient; T = value from t-distribution and p = p-Value.

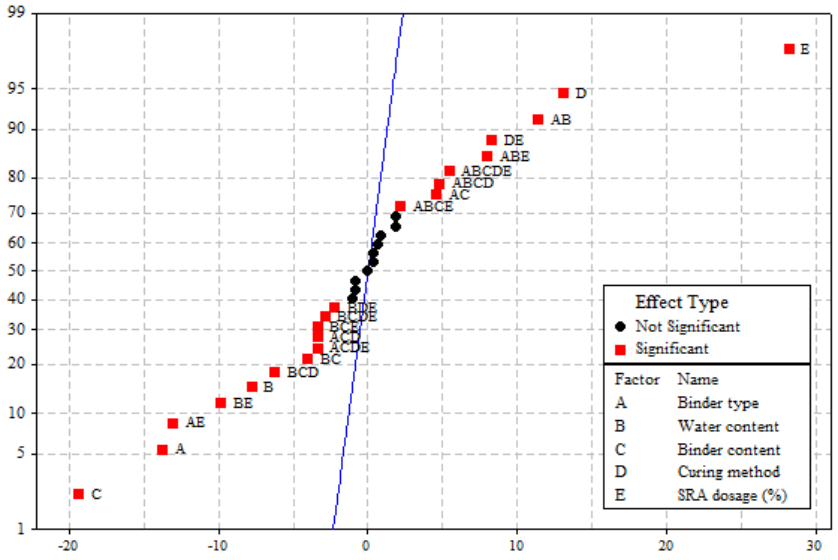

FIGURE D.1: Normal plot of the standardised effects

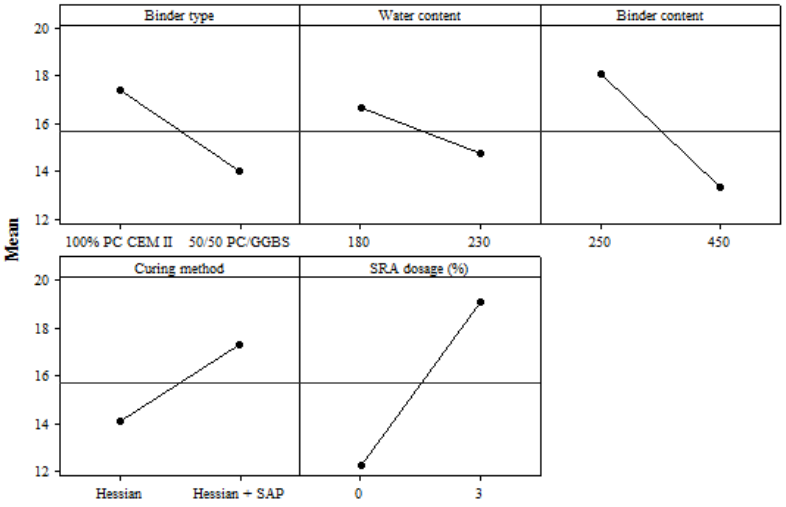

FIGURE D.2: Main effects plot for age at cracking

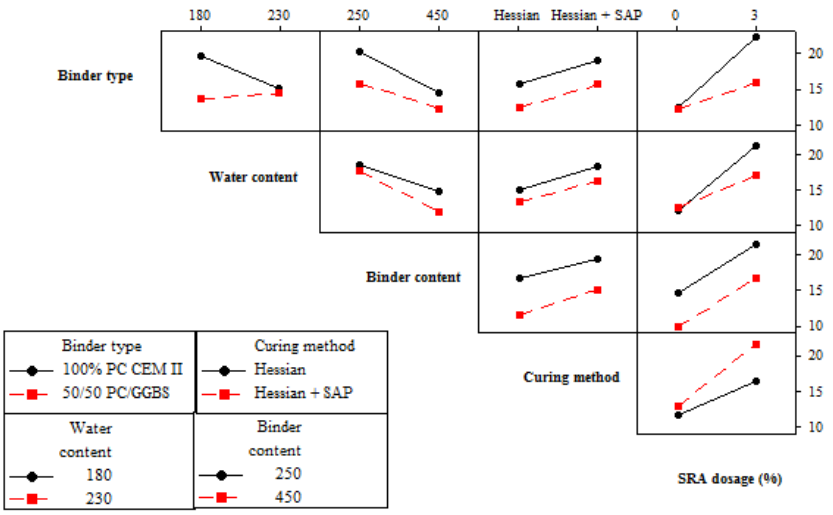

FIGURE D.3: Interaction plots for age at cracking

D.2 Dixon outlier test

This test is also known as the Q test. This test was used to test for outliers within a set of ranked data. The suspected outlier was recorded as the first observation. The formula for the test statistic is:

$$Q = \frac{X_n - X_{n-1}}{X_n - X_1} \tag{D.1}$$

Where the terms in the equation refer to the following:
X_n is the suspected outlier; X_{n-1} is the next ranked observation; and X_1 is the largest ranked observation.

D.3 Correlation coefficient

The correlation coefficient between two variables X and Y measures the linear association between them. It is mathematically defined as:

$$R = \frac{\sum_{i=1}^{n} Y_i(X_i - \bar{X})}{\sqrt{\sum_{i=1}^{n}(X_i - \bar{X})^2 \sum_{i=1}^{n}(Y_i - \bar{Y})^2}} \tag{D.2}$$

Appendix E

ANALYTICAL MODELLING

The analytical modelling comprised the determination of the non-linear regression curves for the input parameters for the model and the prediction of the stresses in the PRMs. The non-linear prediction curves and the stresses in the PRMs are subsequently presented.

E.1 Non-linear regression curves

Non-linear regression analysis was used to plot the regression curves for the input parameters for the analytical model using the test data. These curves are hereby presented.

E.1.1 Elastic modulus

Non-linear regression analysis was used to plot the regression curves for the input parameters for the analytical model using the test data. These curves are hereby presented.

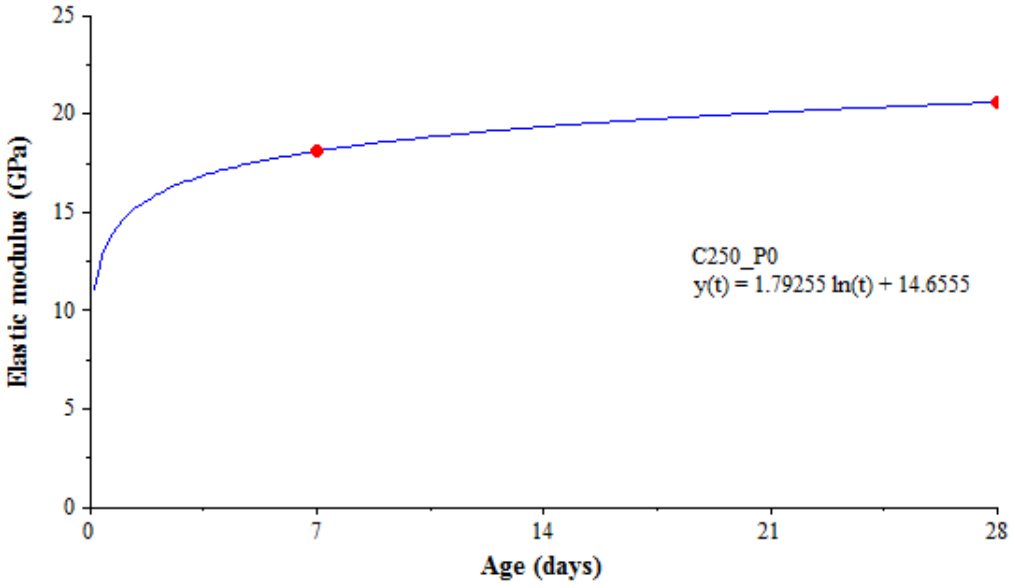

FIGURE E.1: Elastic modulus regression curve for mix C250_P0

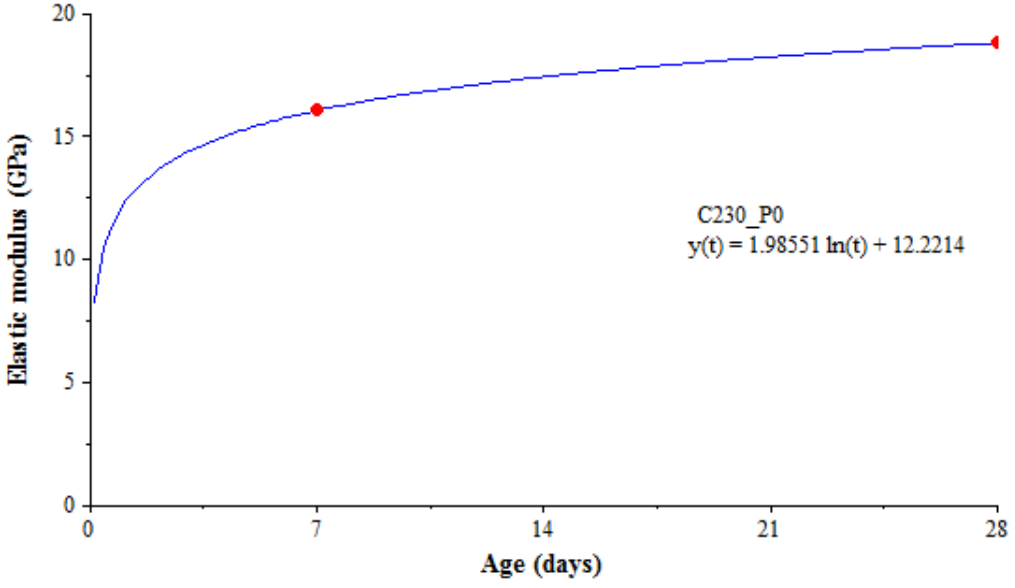

FIGURE E.2: Elastic modulus regression curve for mix C230_P0

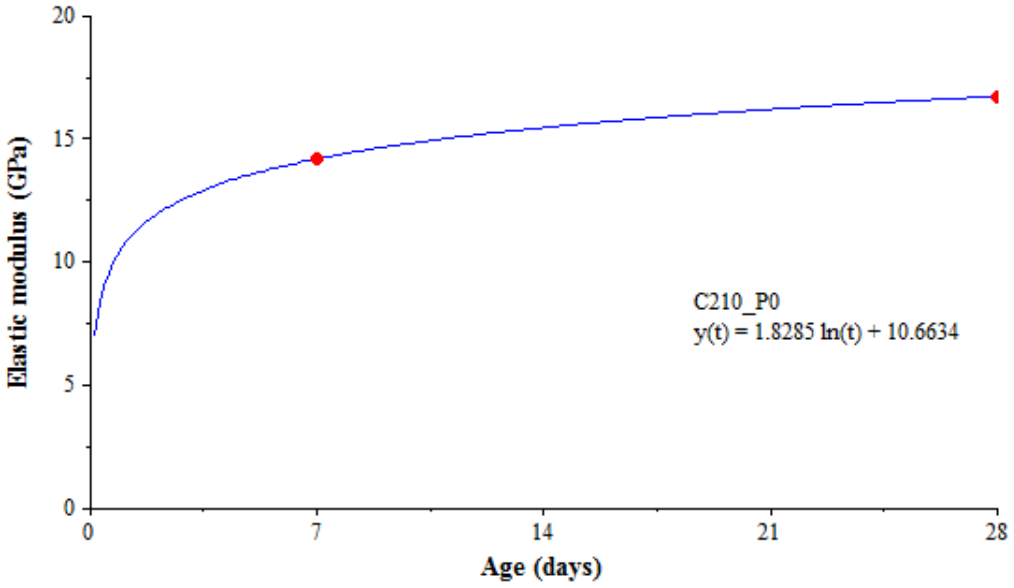

FIGURE E.3: Elastic modulus regression curve for mix C210_P0

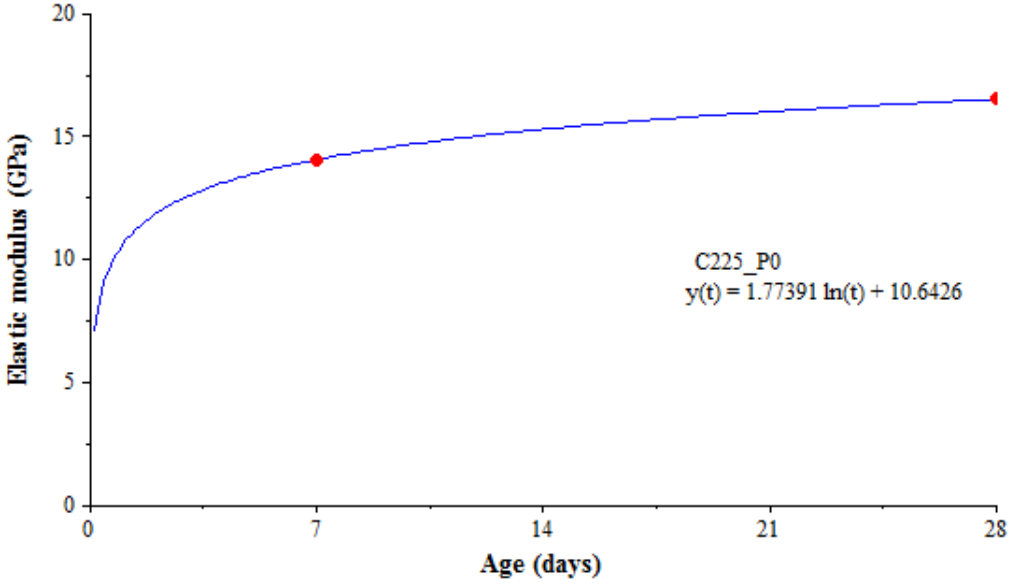

FIGURE E.4: Elastic modulus regression curve for mix C225_P0

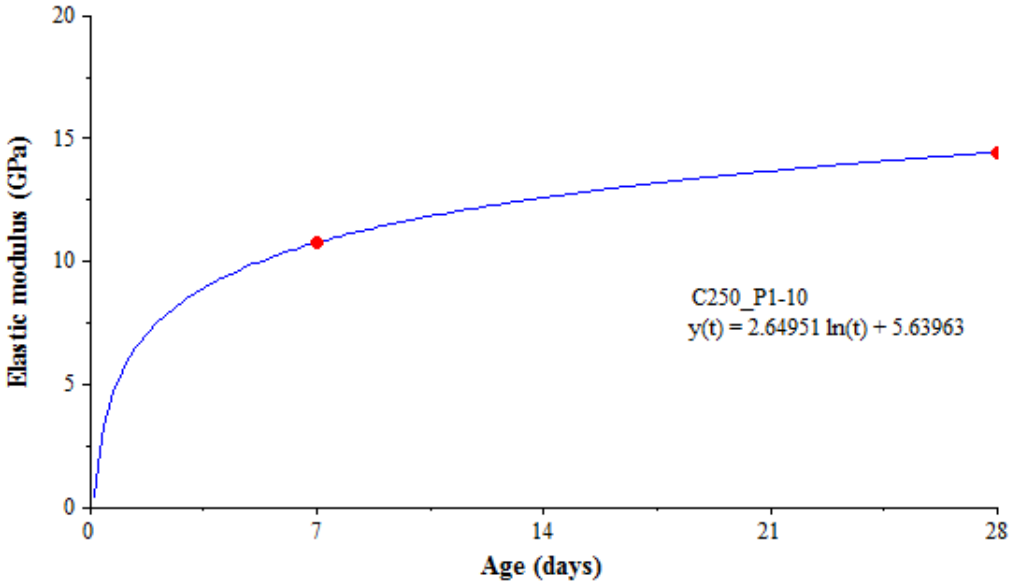

FIGURE E.5: Elastic modulus regression curve for mix C250_P1-10

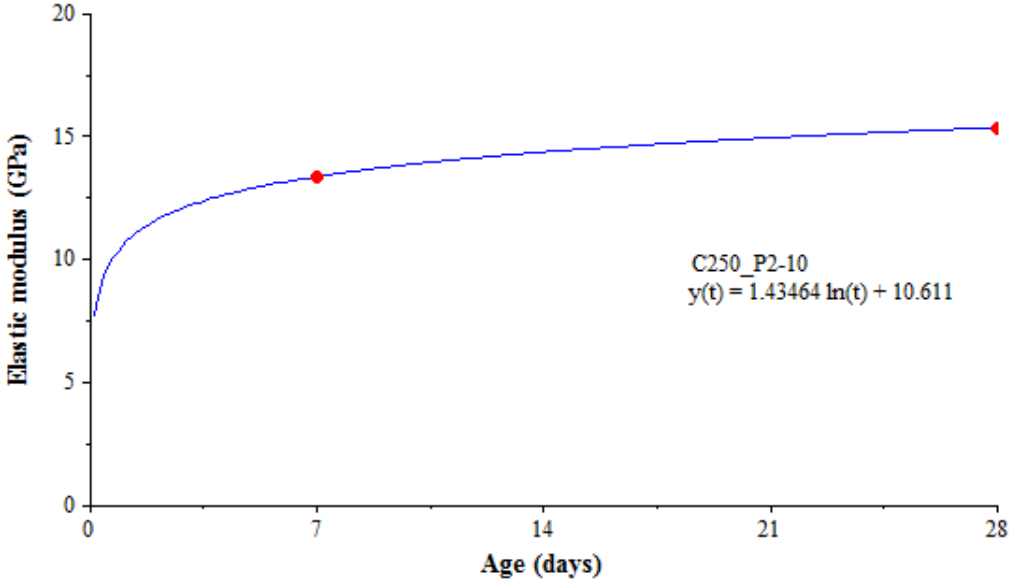

FIGURE E.6: Elastic modulus regression curve for mix C250_P2-10

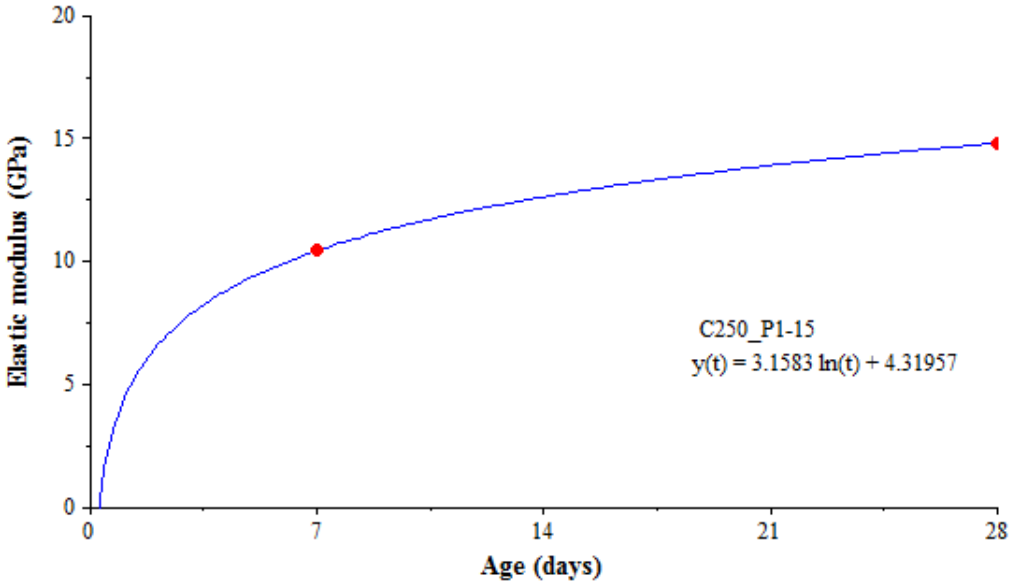

FIGURE E.7: Elastic modulus regression curve for mix C250_P1-15

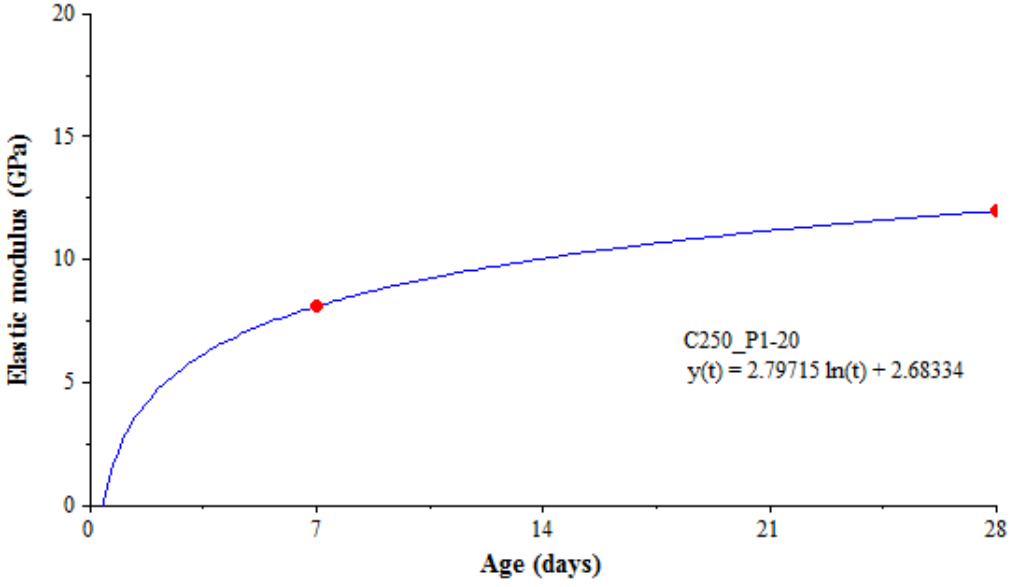

FIGURE E.8: Elastic modulus regression curve for mix C250_P1-20

E.1.2 Direct tensile strength

The non-linear regression curves for direct tensile strength for the various PRM mixes are hereby presented.

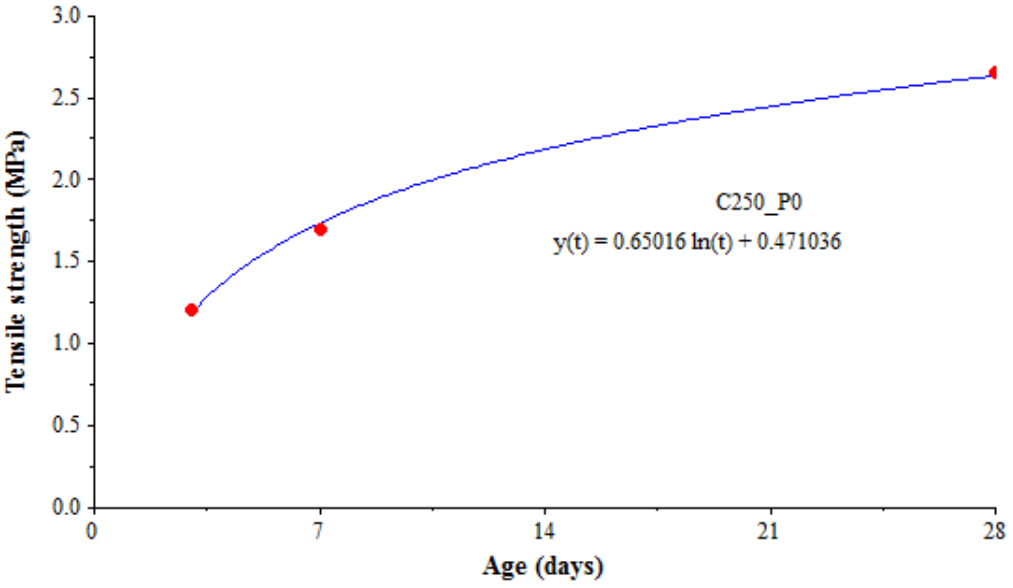

FIGURE E.9: Direct tensile strength regression curve for mix C250_P0

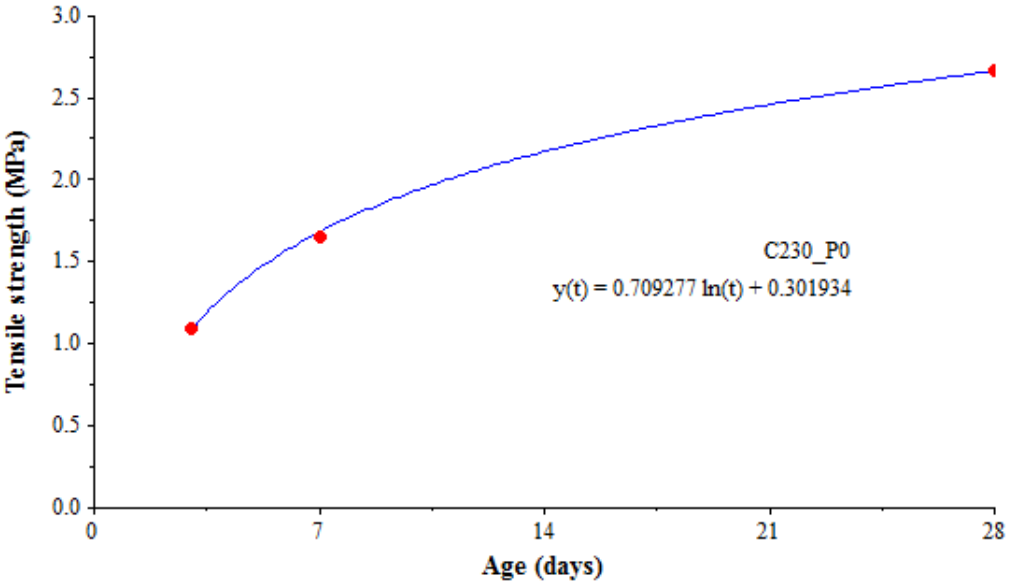

FIGURE E.10: Direct tensile strength regression curve for mix C230_P0

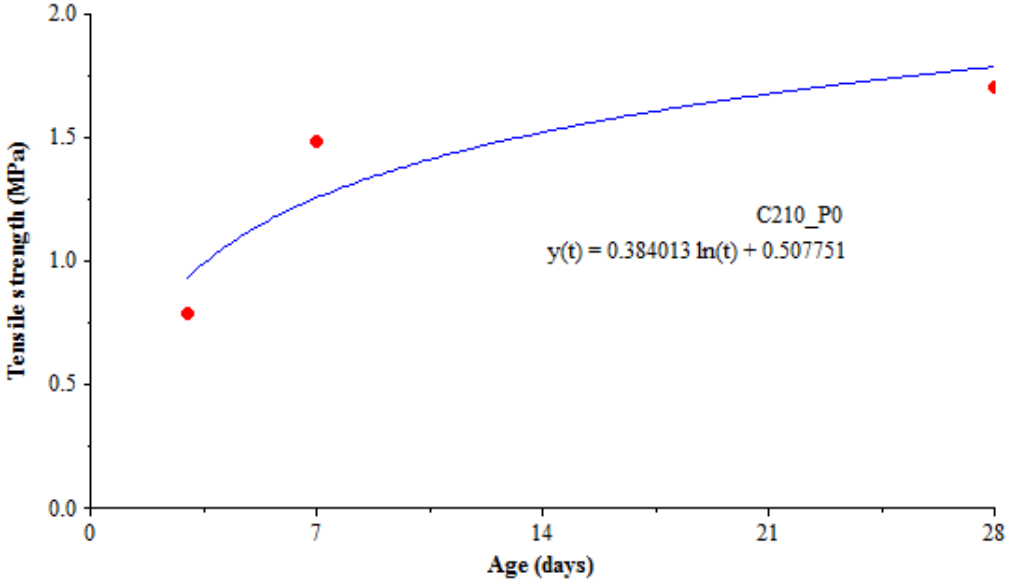

FIGURE E.11: Direct tensile strength regression curve for mix C210_P0

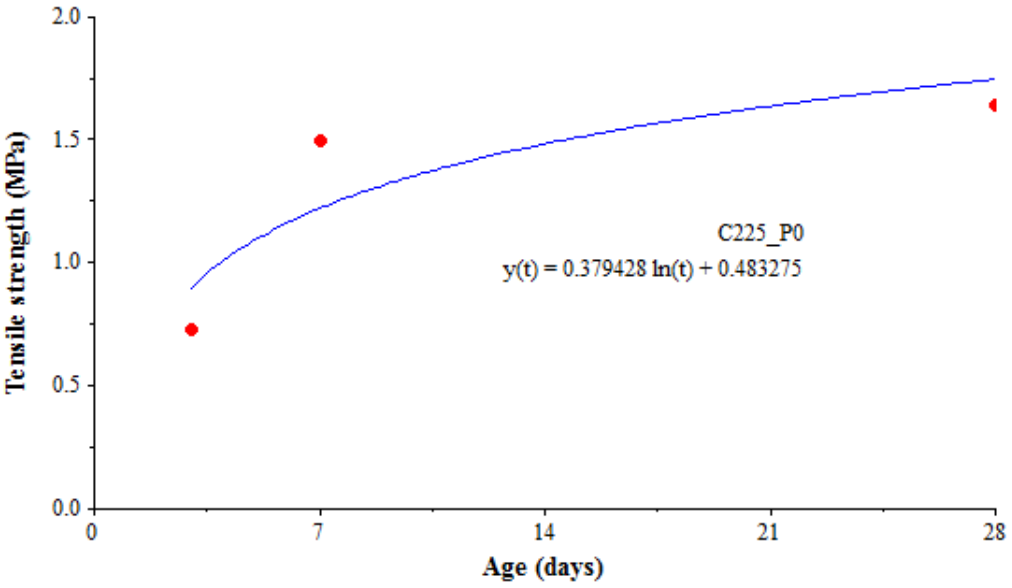

FIGURE E.12: Direct tensile strength regression curve for mix C225_P0

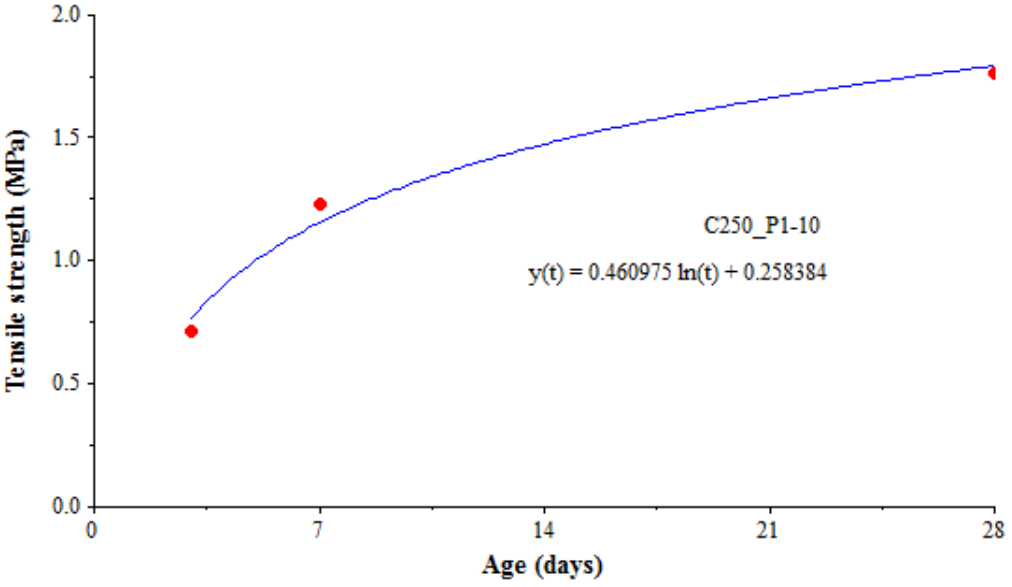

FIGURE E.13: Direct tensile strength regression curve for mix C250_P1-10

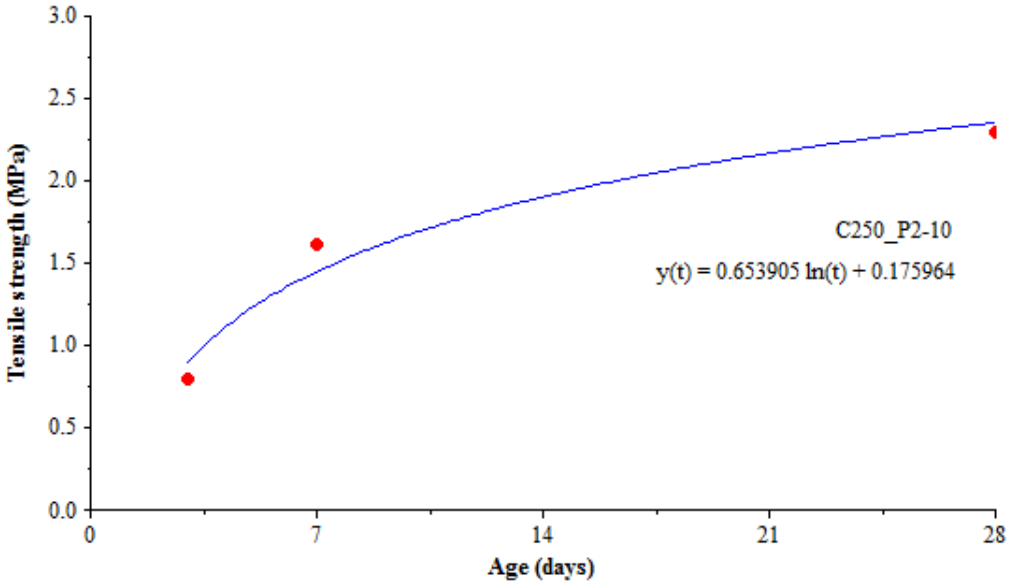

FIGURE E.14: Direct tensile strength regression curve for mix C250_P2-10

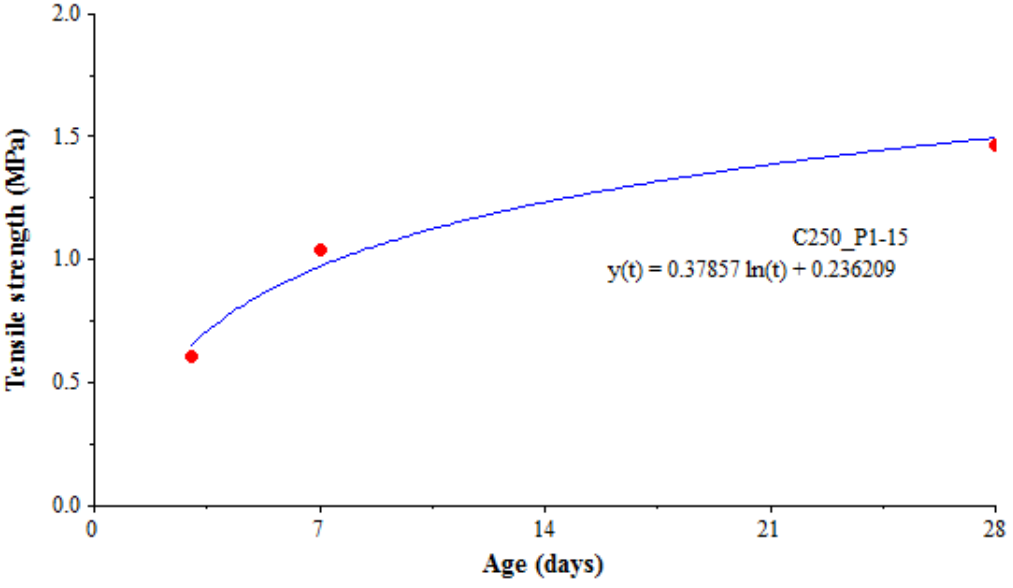

FIGURE E.15: Direct tensile strength regression curve for mix C250_P1-15

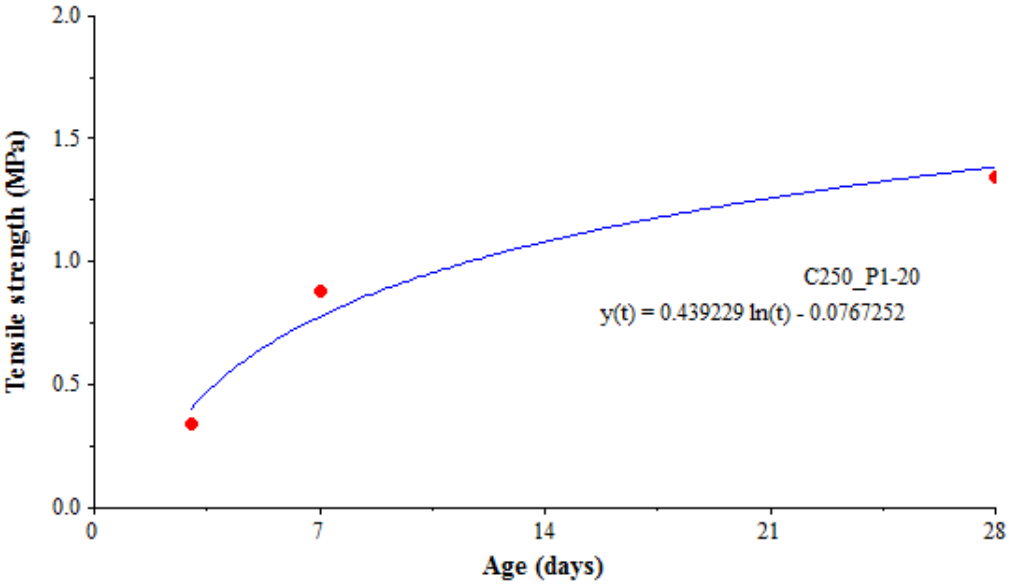

FIGURE E.16: Direct tensile strength regression curve for mix C250_P1-20

E.1.3 Tensile relaxation

The non-linear regression curves for tensile relaxation for the various PRM mixes are hereby presented.

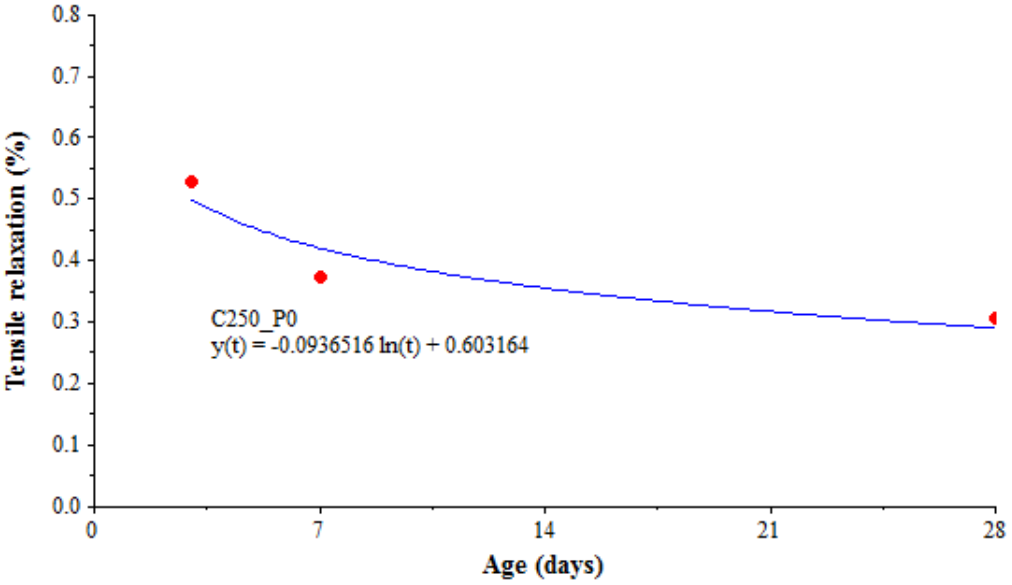

FIGURE E.17: Tensile relaxation regression curve for mix C250_P0

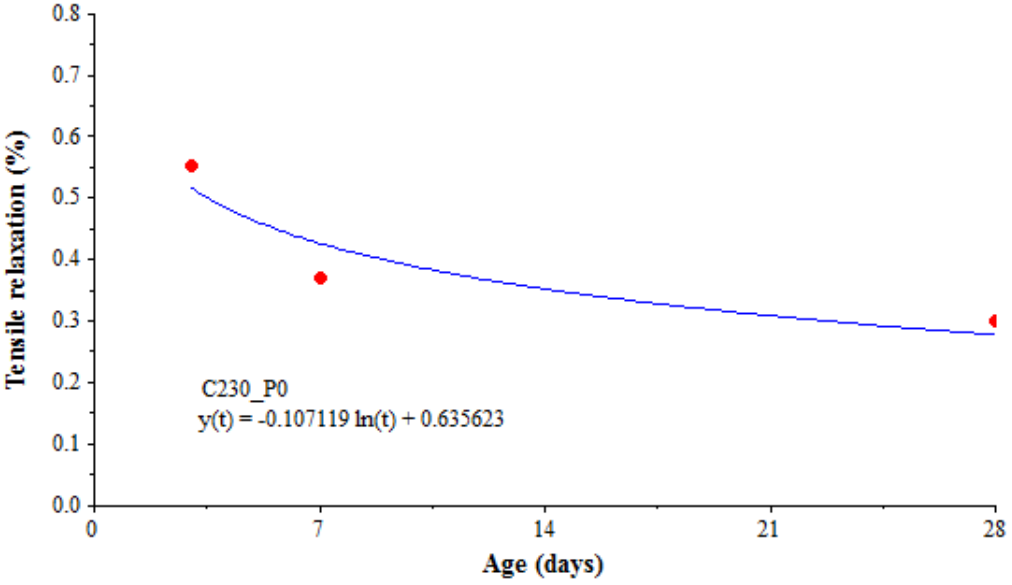

FIGURE E.18: Tensile relaxation regression curve for mix C230_P0

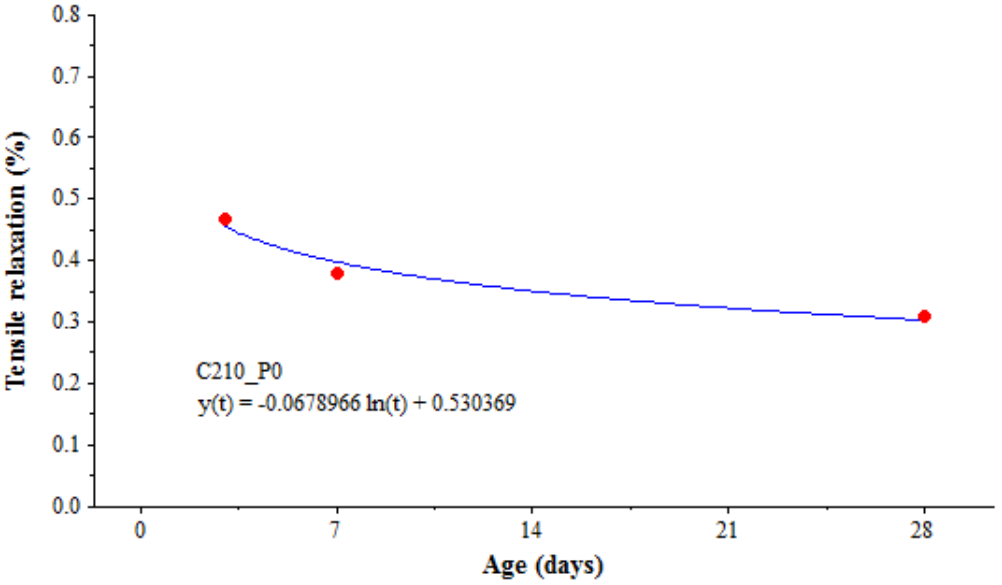

FIGURE E.19: Tensile relaxation regression curve for mix C210_P0

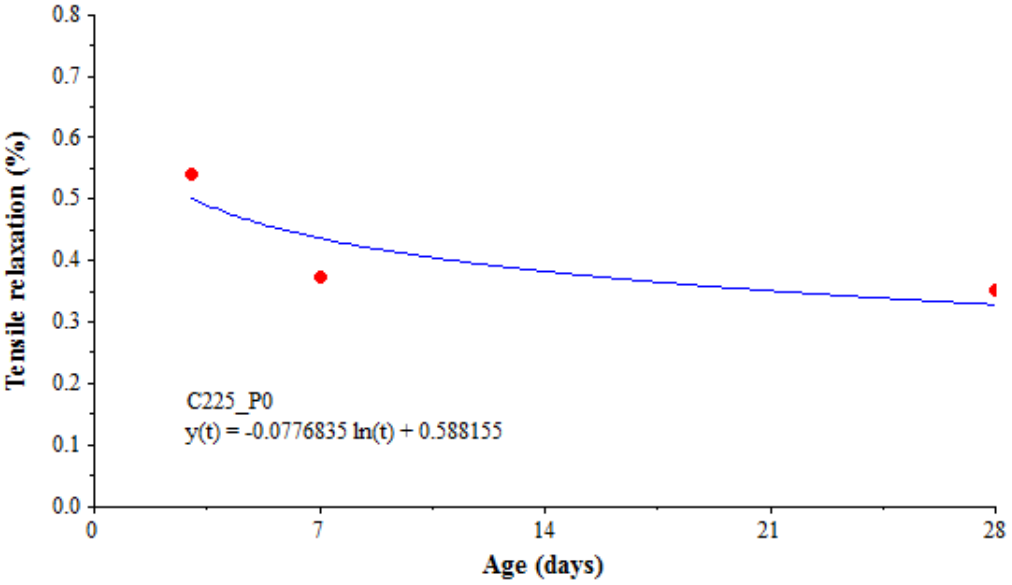

FIGURE E.20: Tensile relaxation regression curve for mix C225_P0

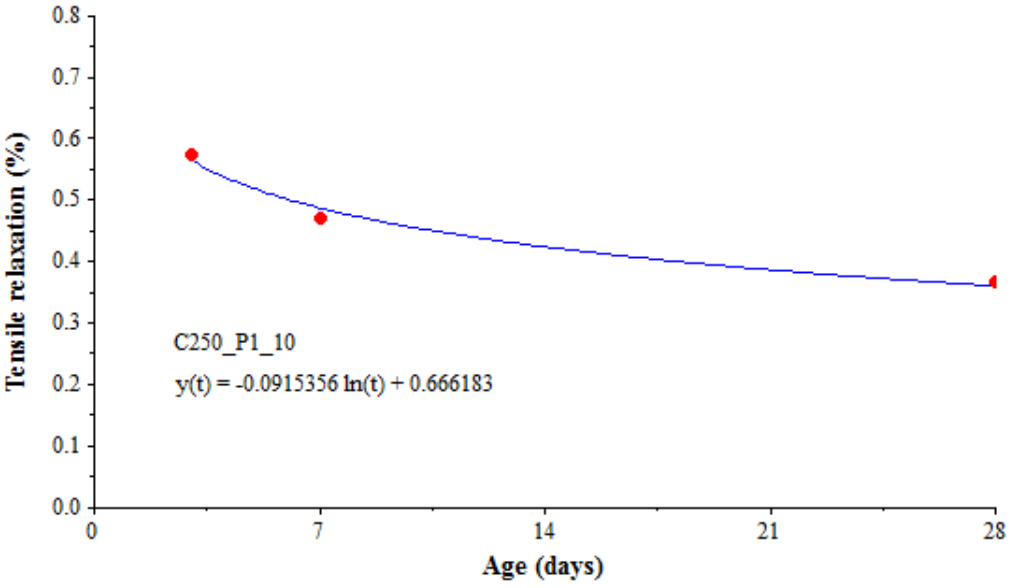

FIGURE E.21: Tensile relaxation regression curve for mix C250_P1-10

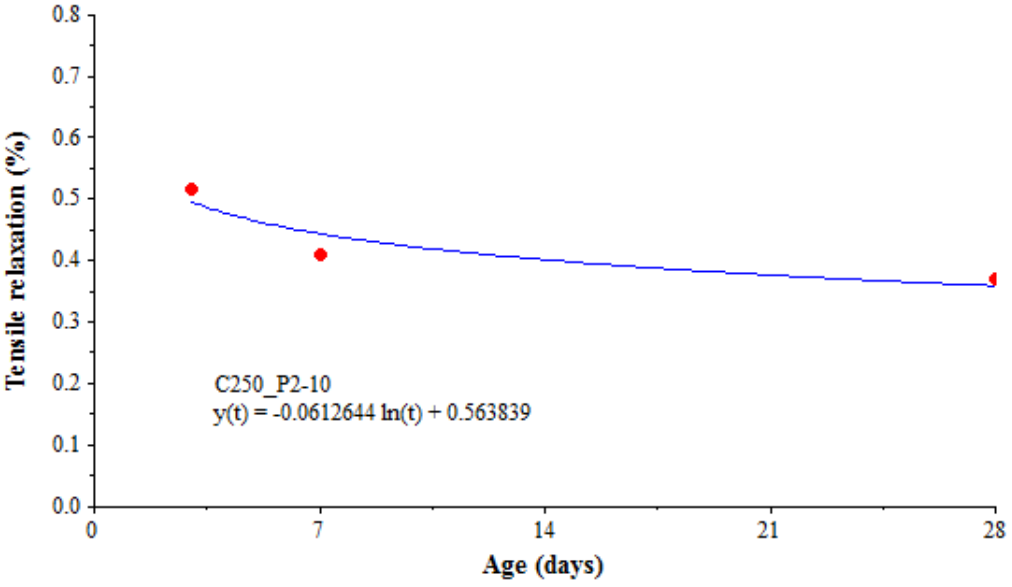

FIGURE E.22: Tensile relaxation regression curve for mix C250_P2-10

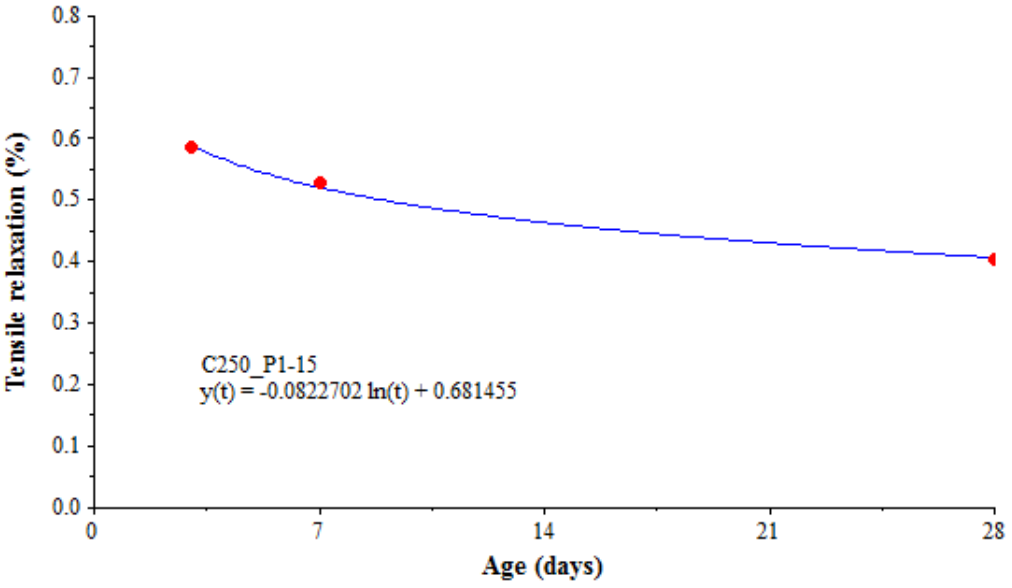

FIGURE E.23: Tensile relaxation regression curve for mix C250_P1-15

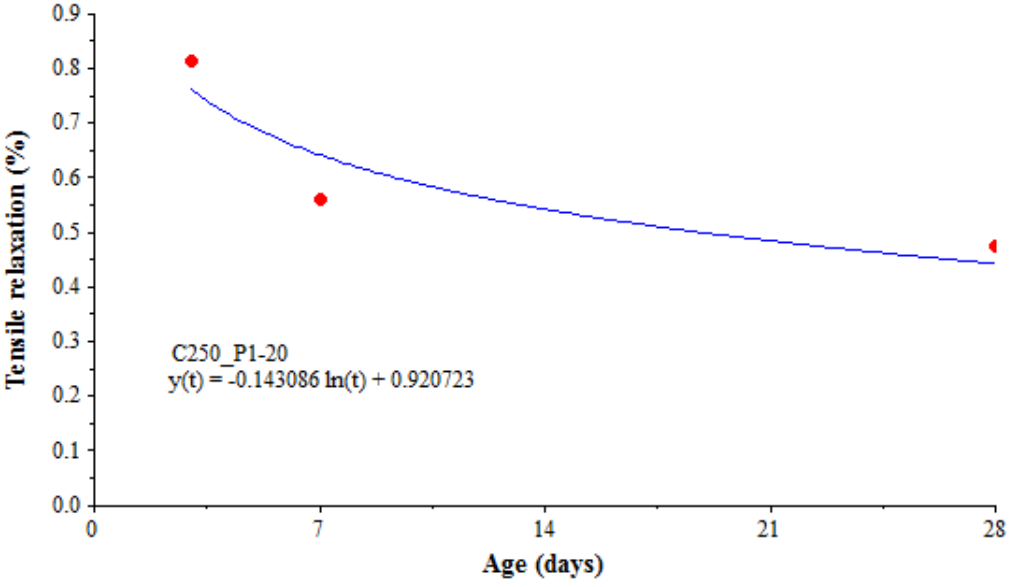

FIGURE E.24: Tensile relaxation regression curve for mix C250_P1-20

E.1.4 Drying shrinkage curves

Comparative graphs of both the actual and the predicted drying shrinkage across the test specimens are hereby presented.

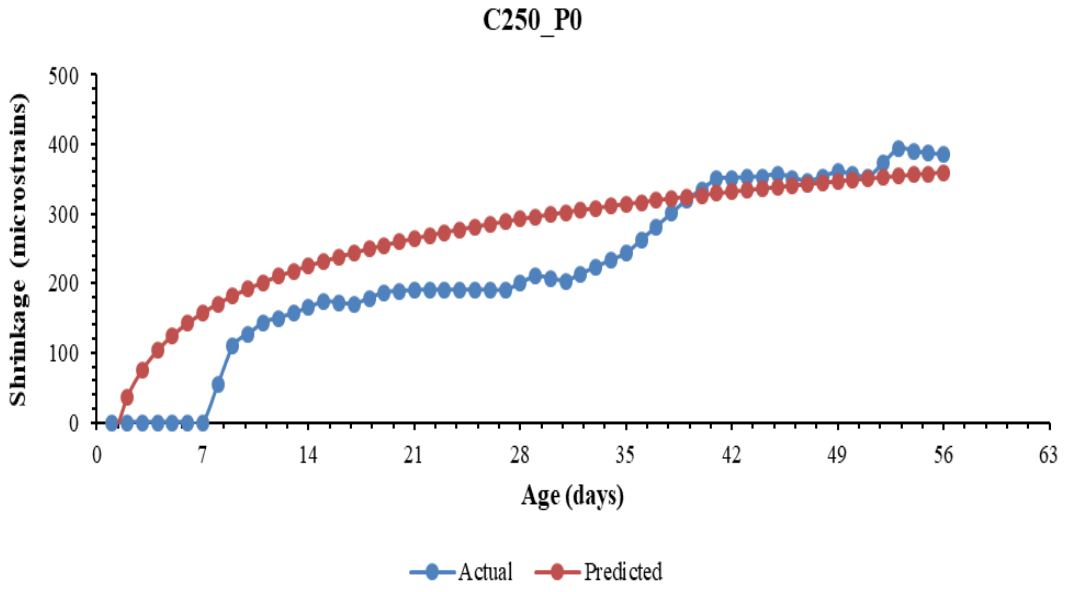

FIGURE E.25: A comparative graph of actual and predicted drying shrinkage for mix C250_P0

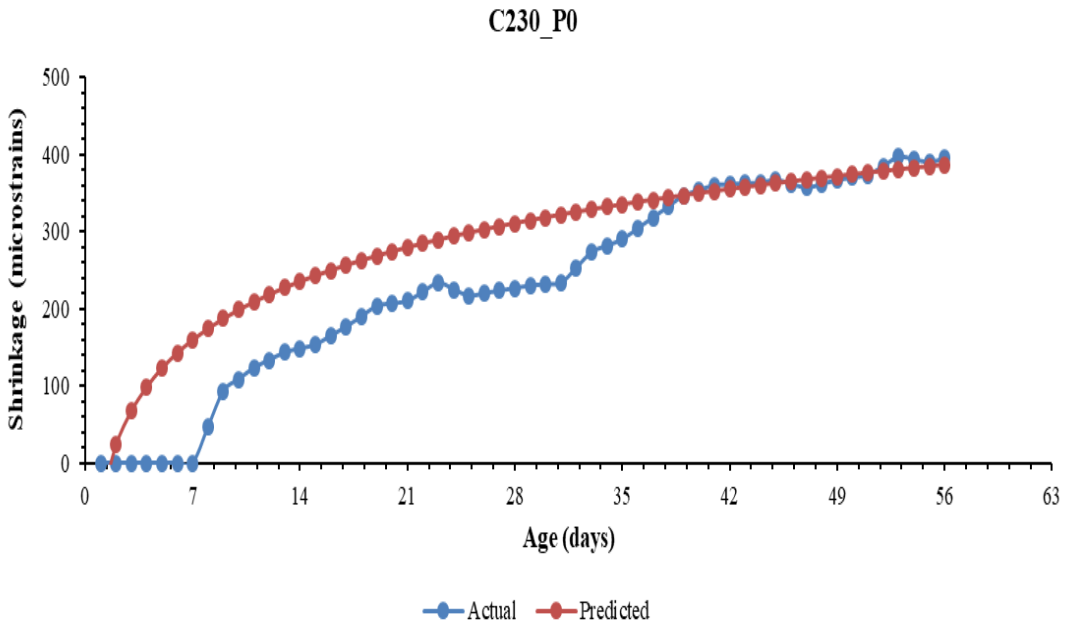

FIGURE E.26: A comparative graph of actual and predicted drying shrinkage for mix C230_P0

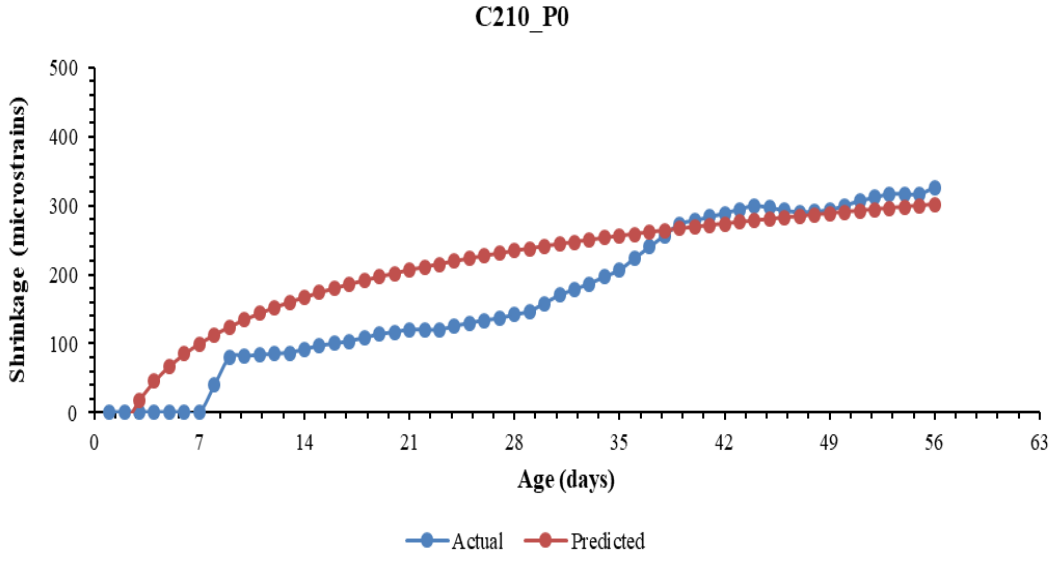

FIGURE E.27: A comparative graph of actual and predicted drying shrinkage for mix C210_P0

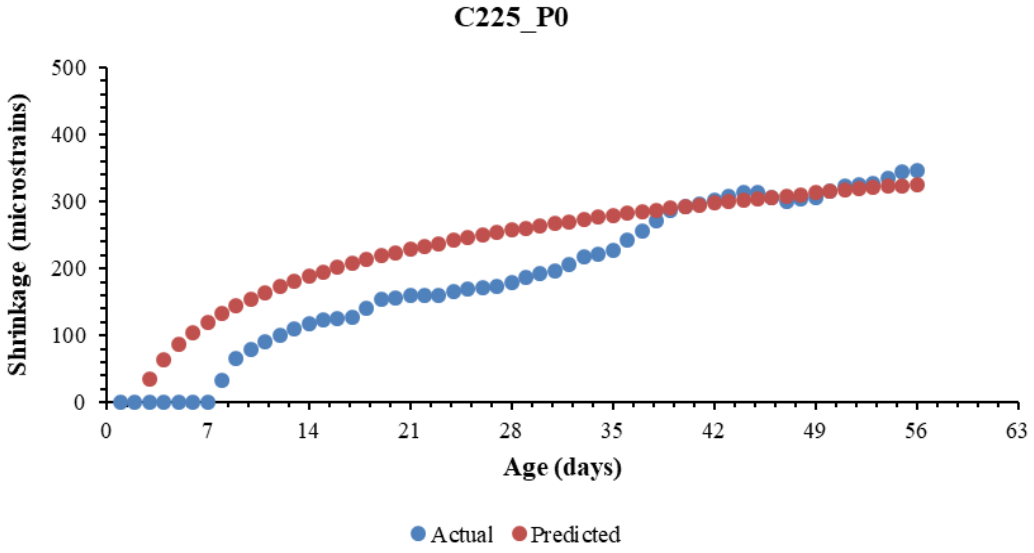

FIGURE E.28: A comparative graph of actual and predicted drying shrinkage for mix C225_P0

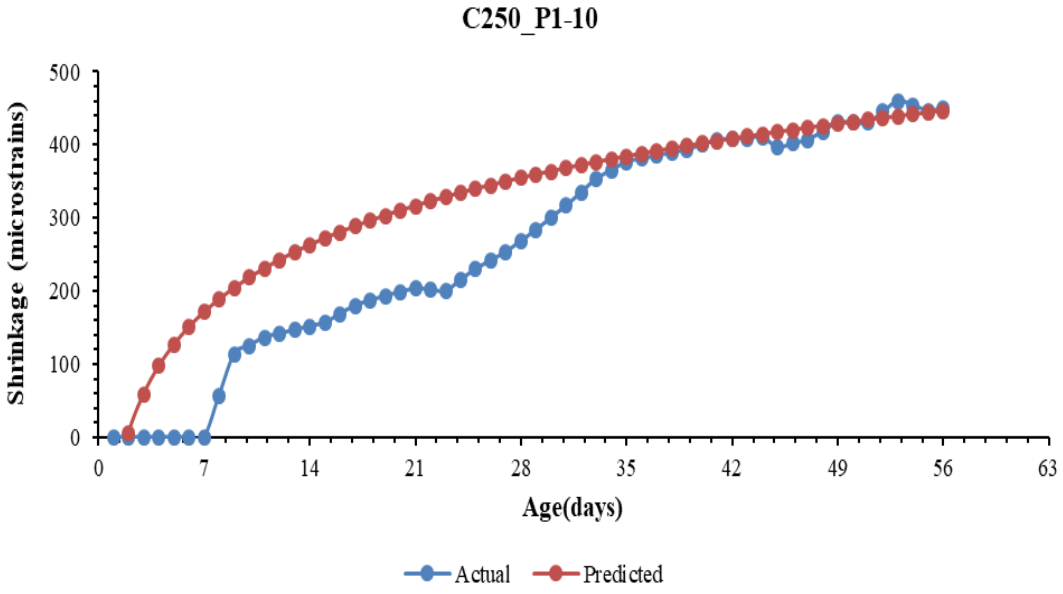

FIGURE E.29: A comparative graph of actual and predicted drying shrinkage for mix C250_P1-10

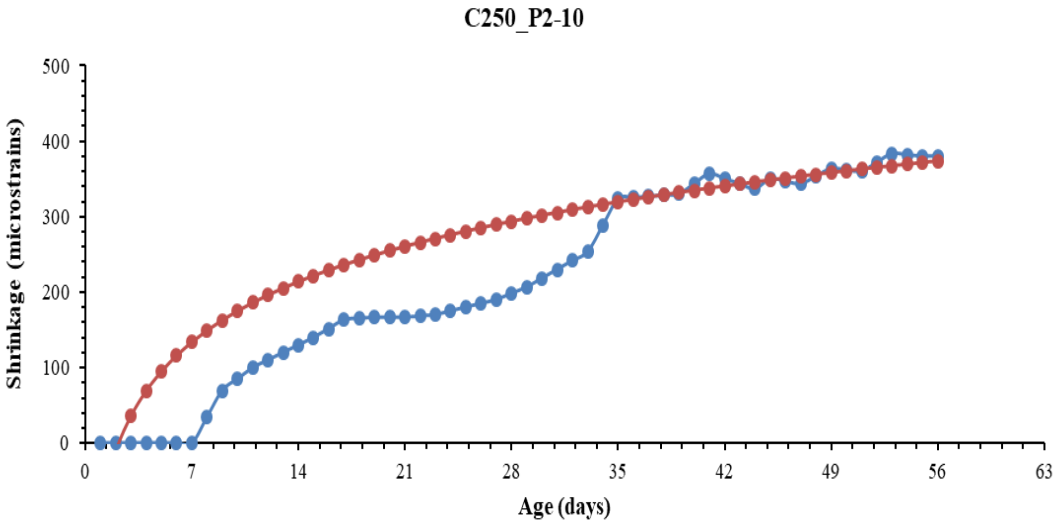

FIGURE E.30: A comparative graph of actual and predicted drying shrinkage for mix C250_P2-10

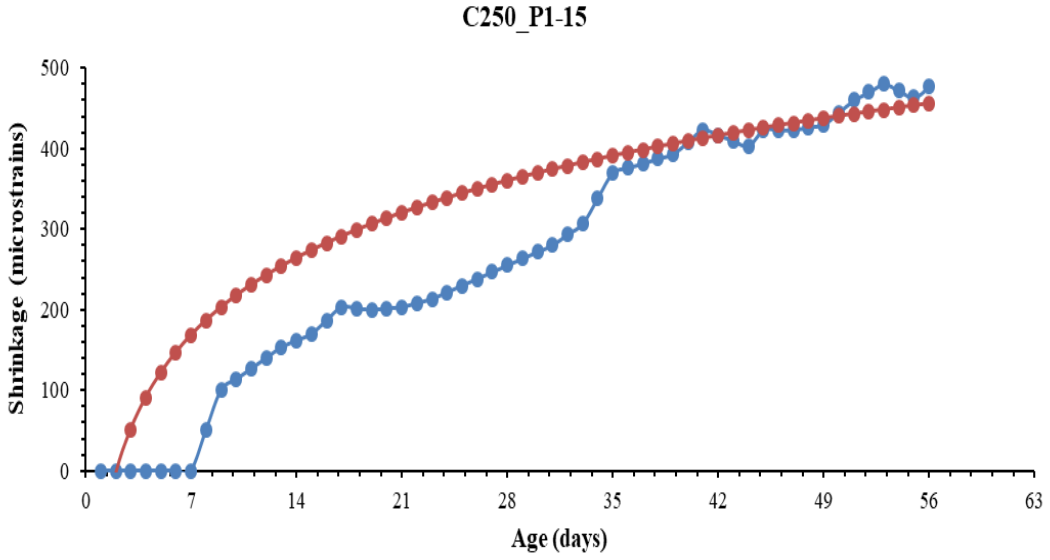

FIGURE E.31: A comparative graph of actual and predicted drying shrinkage for mix C250_P1-15

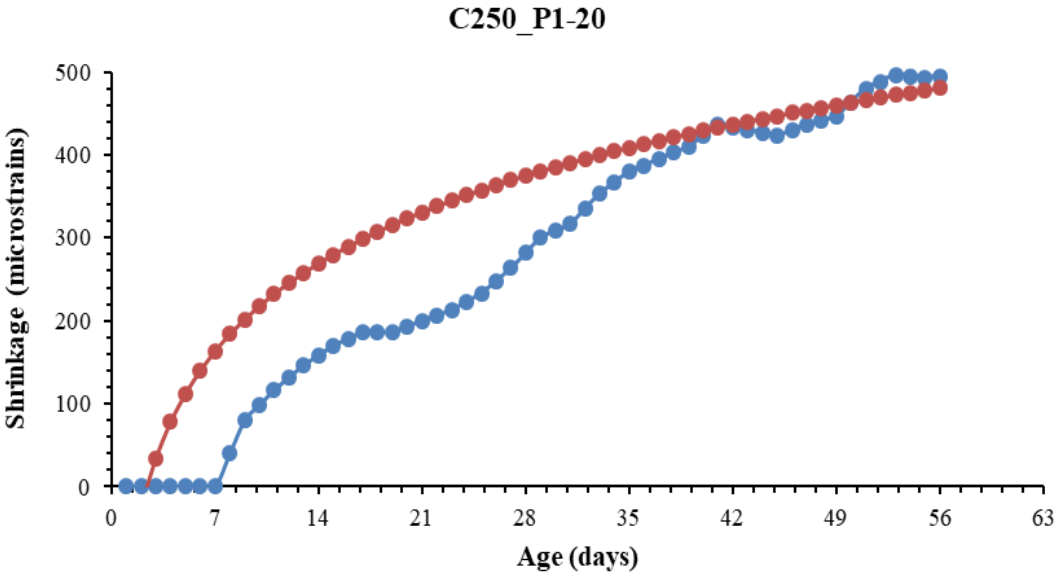

FIGURE E.32: A comparative graph of actual and predicted drying shrinkage for mix C250_P1-20

E.2 Degree of restraint estimation curves

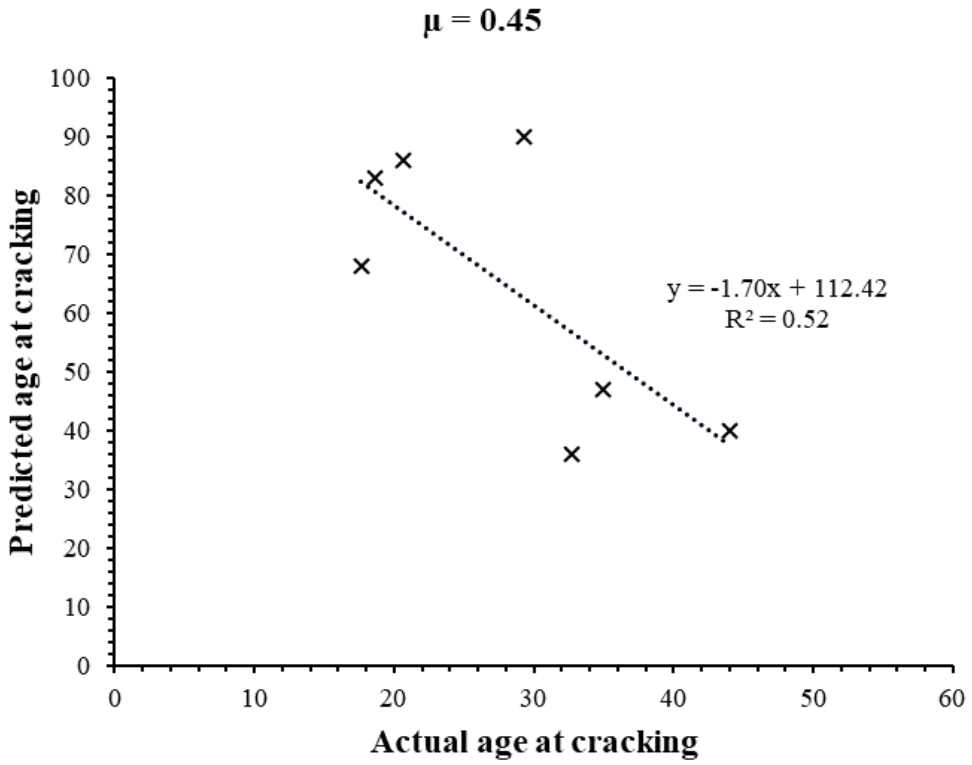

FIGURE E.33: Scatter plot of predicted vs. actual age at cracking ($\mu = 0.45$)

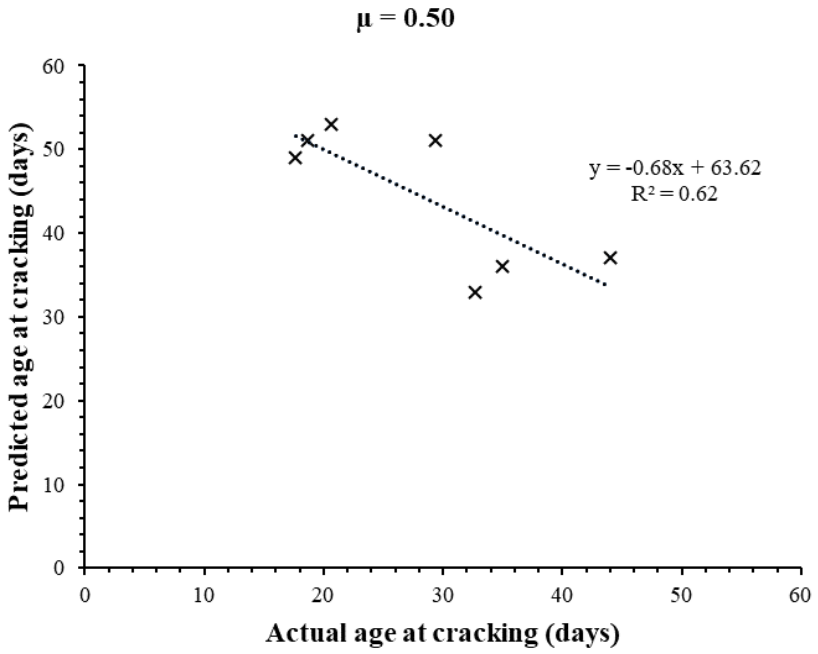

FIGURE E.34: Scatter plot of predicted vs. actual age at cracking ($\mu = 0.50$)

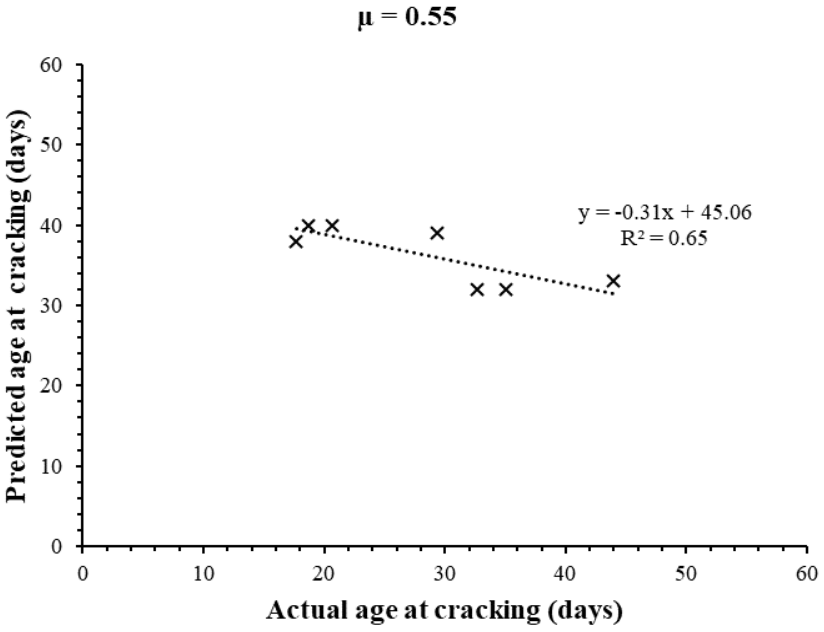

FIGURE E.35: Scatter plot of predicted vs. actual age at cracking ($\mu = 0.55$)

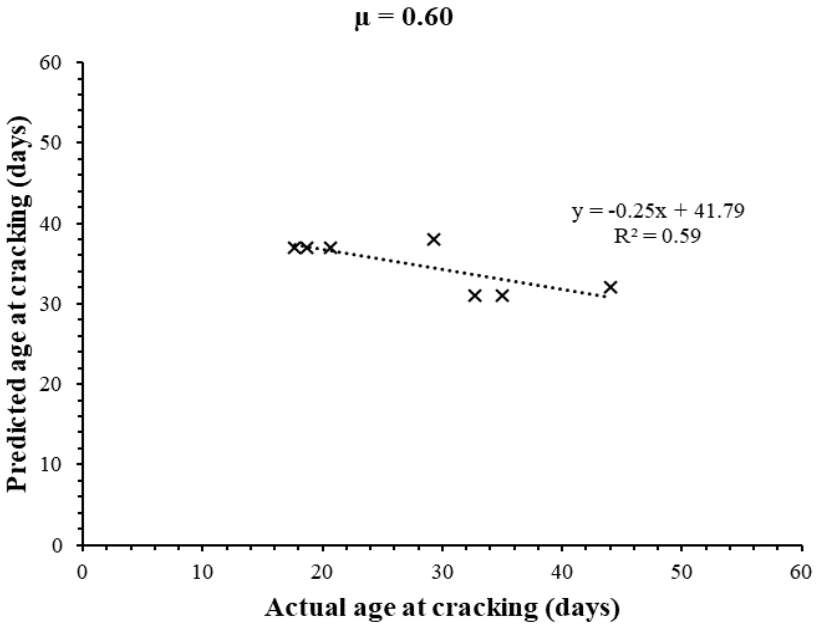

FIGURE E.36: Scatter plot of predicted vs. actual age at cracking ($\mu = 0.60$)

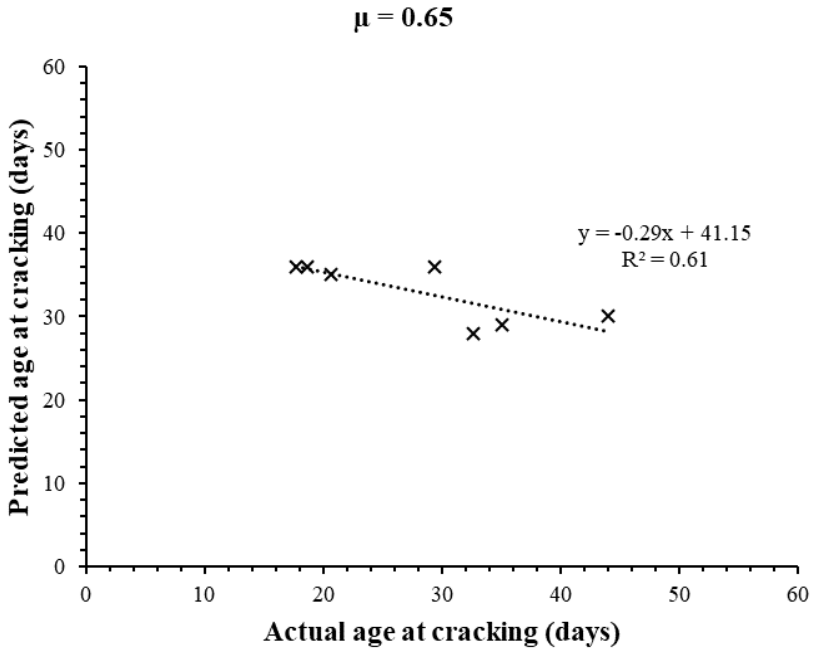

FIGURE E.37: Scatter plot of predicted vs. actual age at cracking ($\mu = 0.65$)

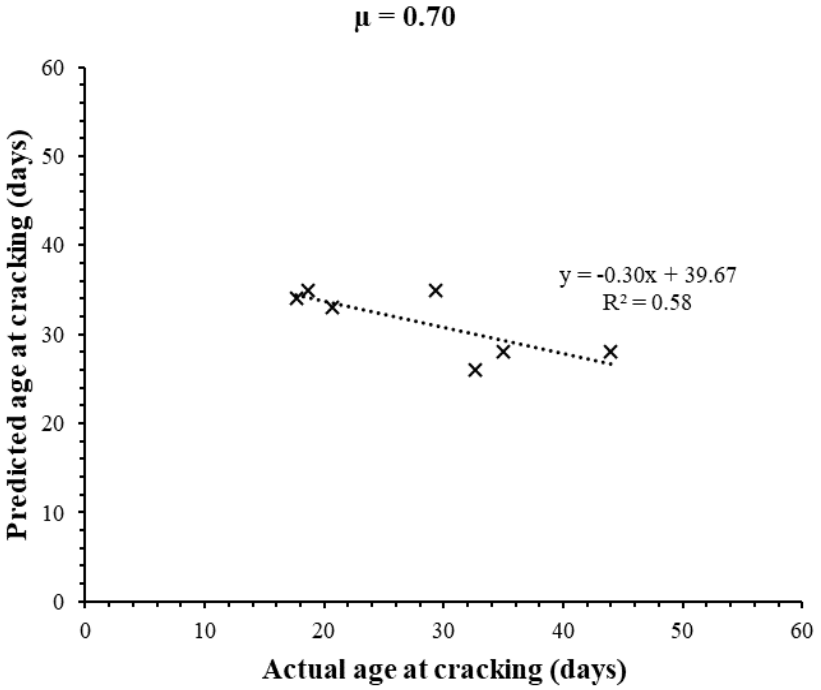

FIGURE E.38: Scatter plot of predicted vs. actual age at cracking ($\mu = 0.70$)

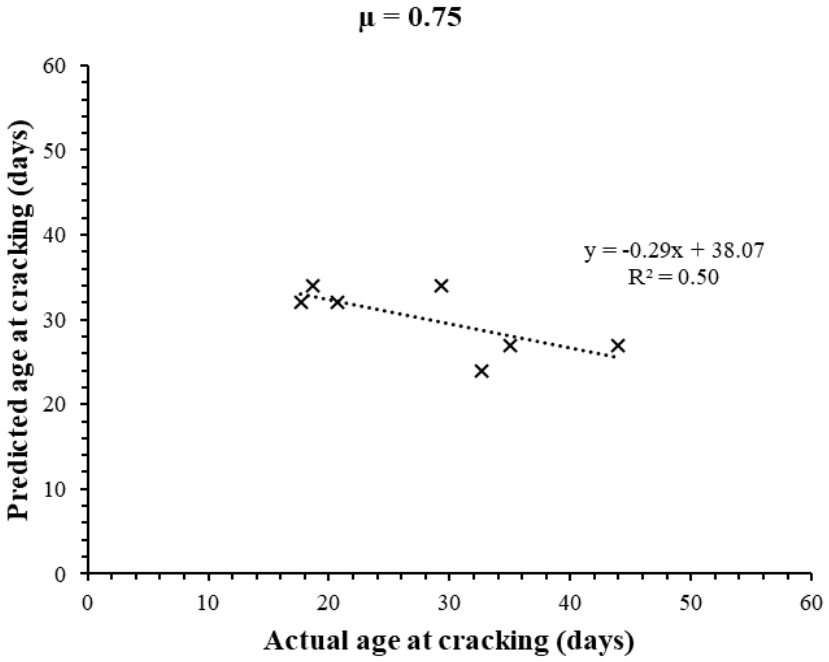

FIGURE E.39: Scatter plot of predicted vs. actual age at cracking ($\mu = 0.75$)

E.3 Stress development curves

The tensile stress prediction curves using the existing deterministic empirical analytical model and proposed deterministic analytical model are hereby presented.

E.3.1 Stress development curves using the existing empirical analytical model

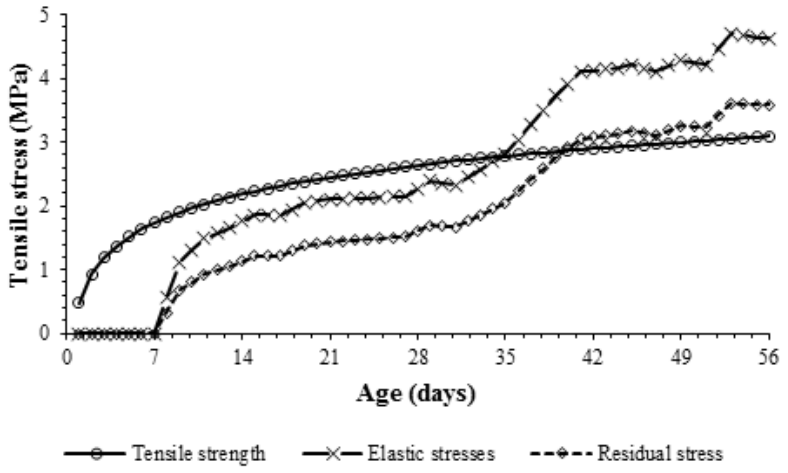

FIGURE E.40: Stress development in mix C250_P0

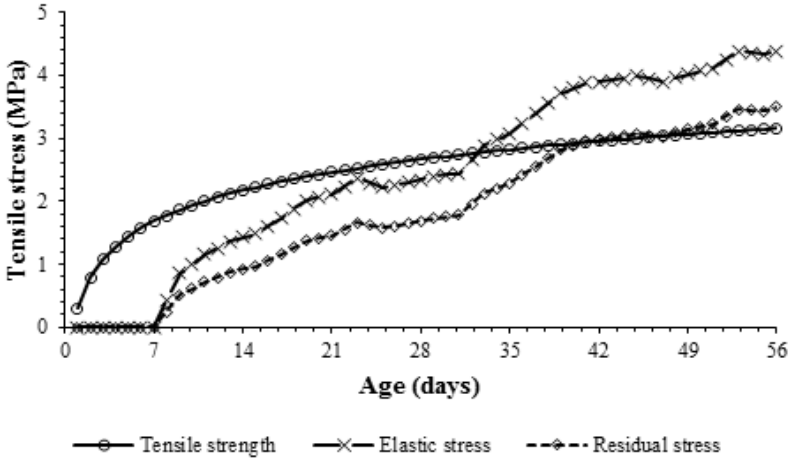

FIGURE E.41: Stress development in mix C230_P0

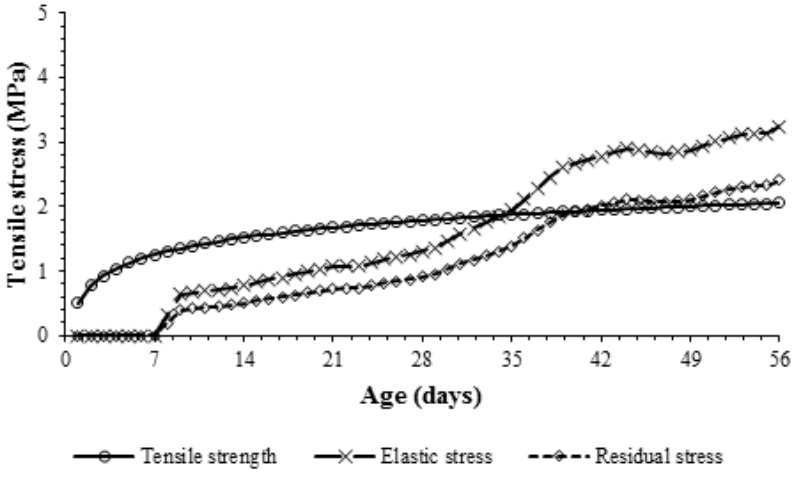

FIGURE E.42: Stress development in mix C210_P0

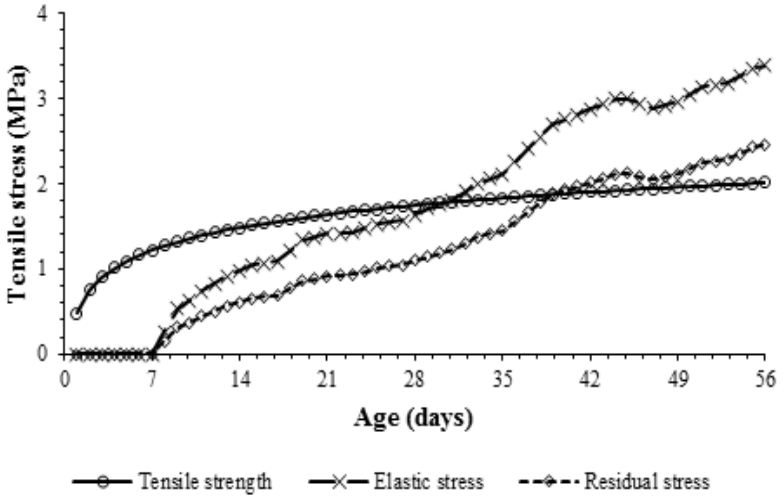

FIGURE E.43: Stress development in mix C225_P0

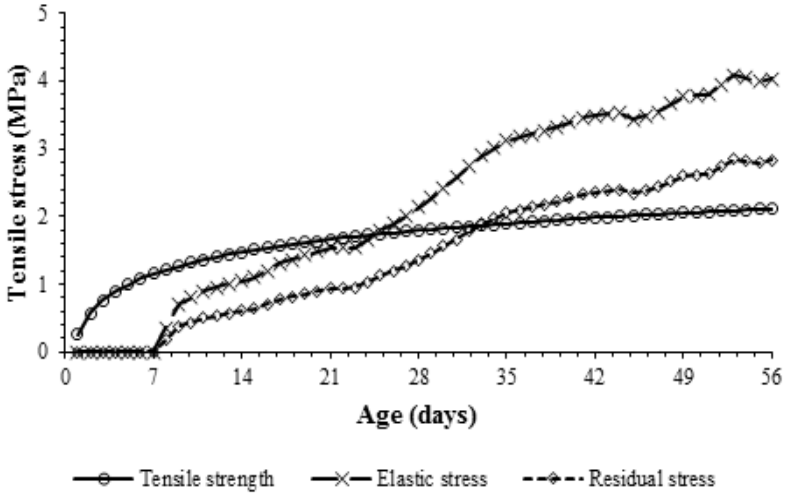

FIGURE E.44: Stress development in mix C250_P1-10

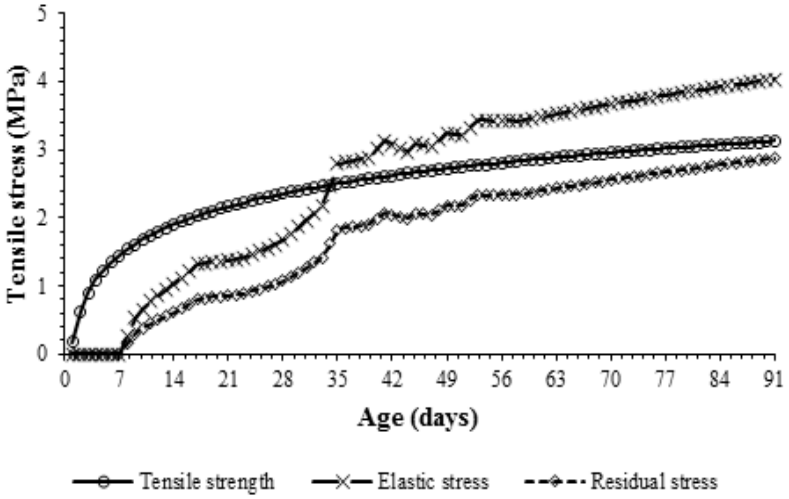

FIGURE E.45: Stress development in mix C250_P2-10

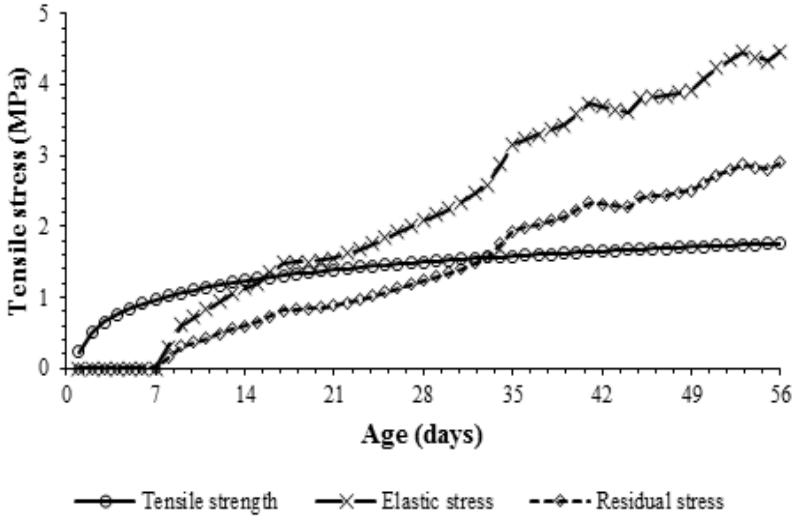

FIGURE E.46: Stress development in mix C250_P1-15

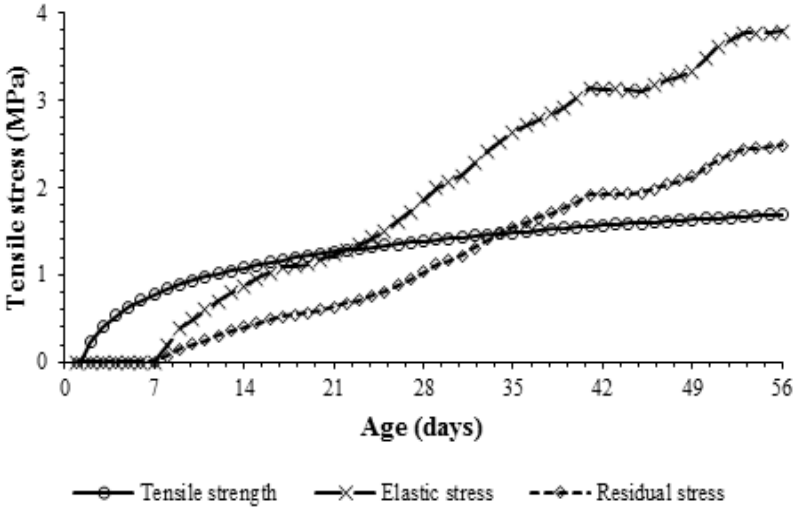

FIGURE E.47: Stress development in mix C250_P2-20

E.3.2 Stress development using the proposed empirical analytical model

The stress development curves in the PRM mixes using the proposed empirical deterministic analytical model are hereby presented.

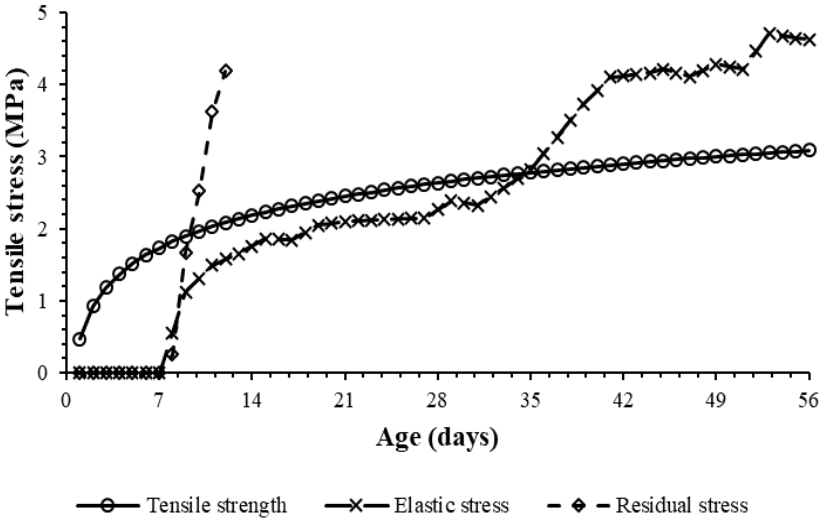

FIGURE E.48: Stress development in mix C250_P0

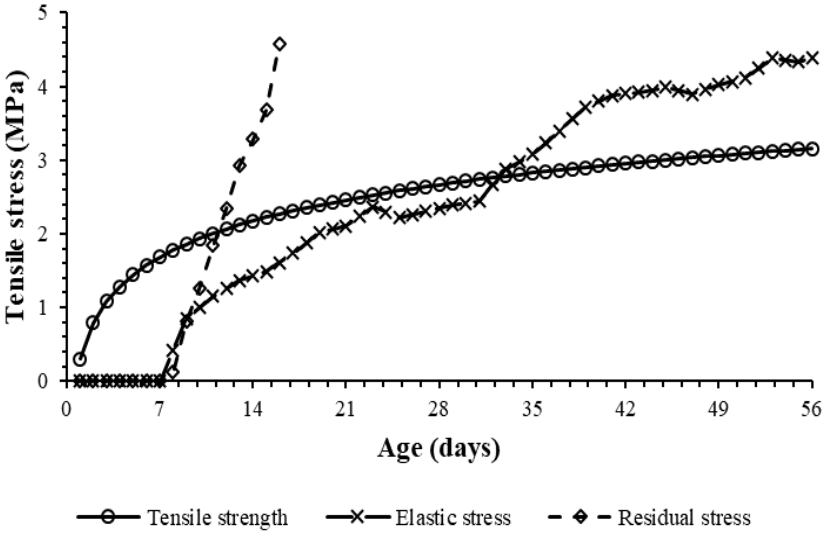

FIGURE E.49: Stress development in mix C230_P0

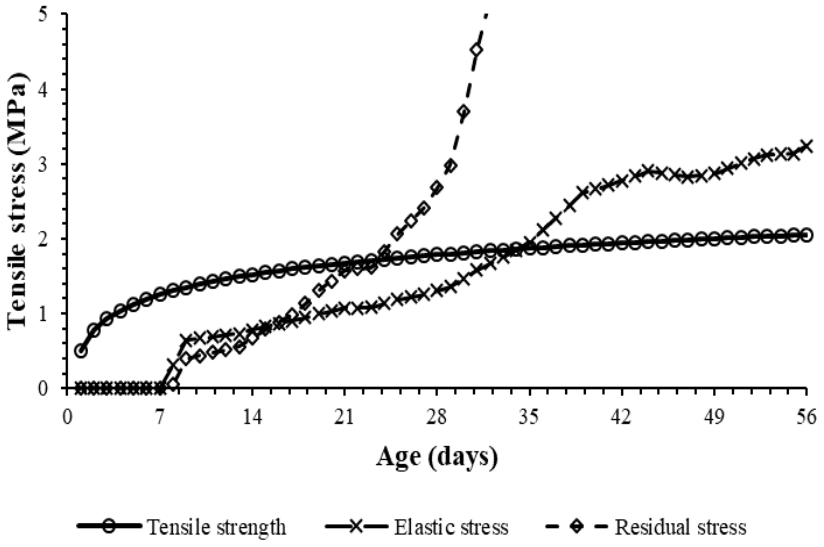

FIGURE E.50: Stress development in mix C210_P0

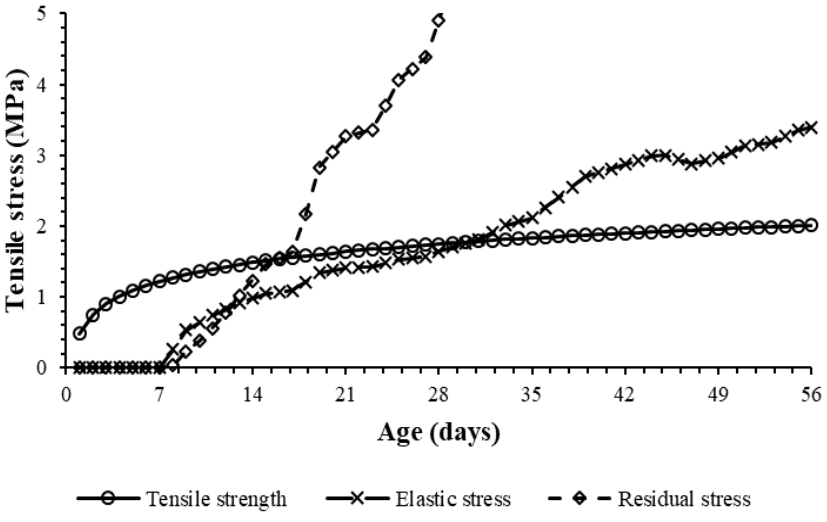

FIGURE E.51: Stress development in mix C225_P0

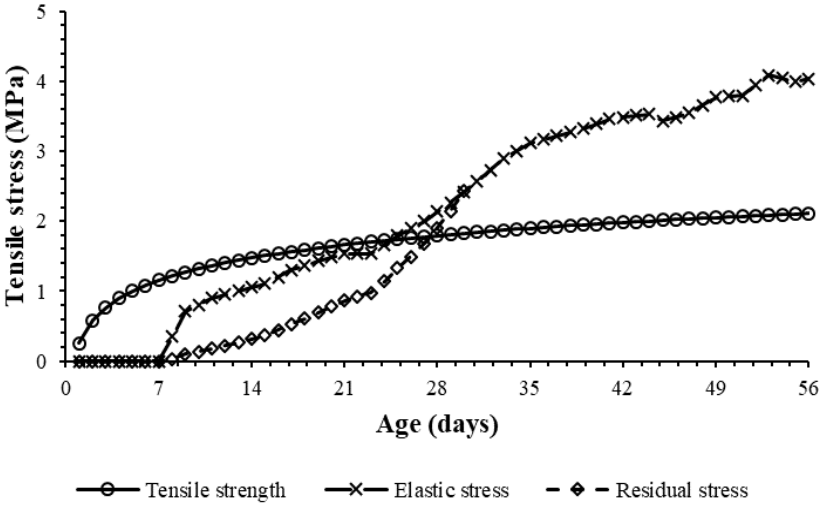

FIGURE E.52: Stress development in mix C250_P1-10

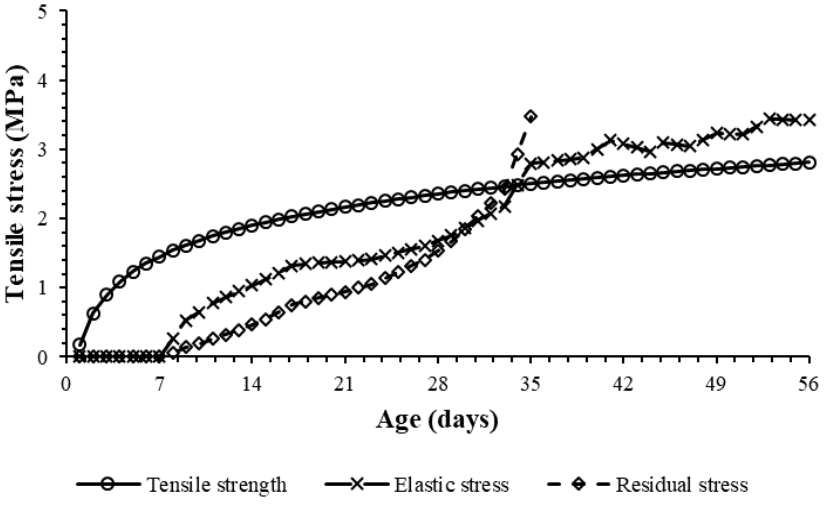

FIGURE E.53: Stress development in mix C250_P2-10

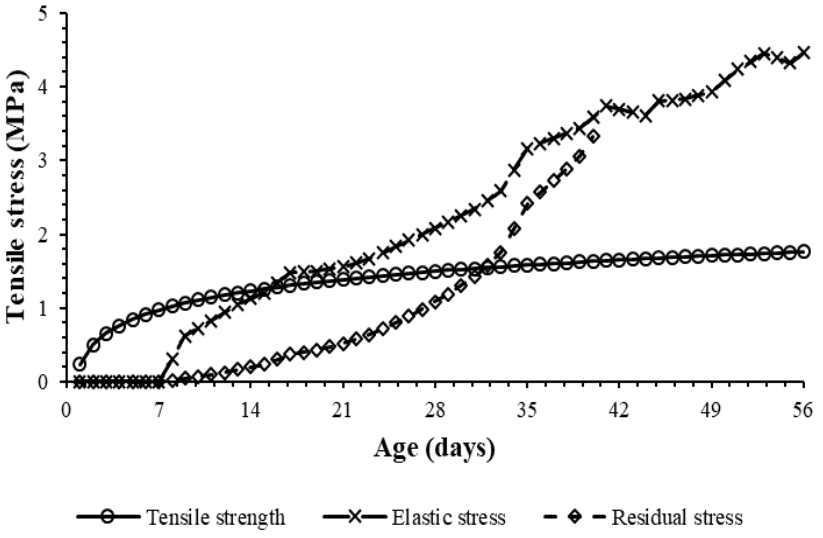

FIGURE E.54: Stress development in mix C250_P1-15

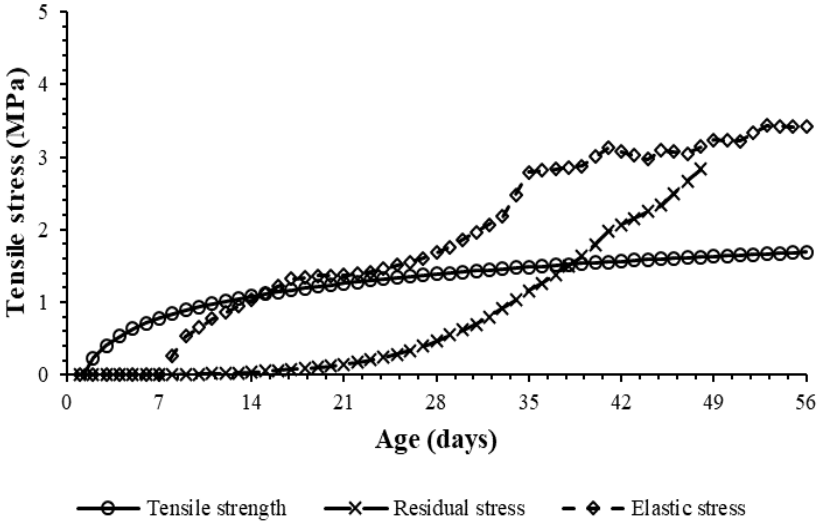

FIGURE E.55: Stress development in mix C250_P1-20